UNIVERSITY OF CALIFORNIA, SAN DIEGO

Degrading Proteases and Organ Failure during Physiological Shock

A dissertation submitted in partial satisfaction of the requirements for the degree Doctor of Philosophy

in

Bioengineering

by

Angelina E. Altshuler

Committee in Charge:

Professor Geert W. Schmid-Schönbein, Chair
Professor Shu Chien, Co-Chair
Professor Pedro Cabrales
Professor Yeshaiahu Fainman
Professor Alison Marsden
Professor John Watson

2013

The Dissertation of Angelina E. Altshuler is approved, and it is acceptable in quality and form for publication on microfilm and electronically:

_____

_____

_____

_____

_____
Co-Chair

_____
Chair

University of California, San Diego

2013

DEDICATION

I dedicate this thesis to my family for their encouragement and support.

TABLE OF CONTENTS

LIST OF ABBREVIATIONS

ANGD	Nafamostat mesilate
ANOVA	Analysis of variance
BALF	Bronchoalveolar lavage fluid
DOX	Doxycycline
ECL	Enhanced chemiluminescence
EDTA	Ethylenediaminetetraacetic acid
GLUC	Glucose
HS	Hemorrhagic shock
IM	Intramuscular
IP	Intraperitoneal
IV	Intravenous
MAP	Mean arterial pressure
MMP	Matrix metalloproteinase
MPO	Myeloperoxidase
RFU	Relative fluorescent units
RIU	Relative intensity units
RU	Relative units
SAO	Splanchnic arterial occlusion
TA	Tranexamic acid
TIMP	Tissue inhibitor of metalloproteinase
TLCK	Tosyllysine Chloromethyl Ketone Hydrochloride
VEGF	Vascular endothelial growth factor
VEGFR-2	Vascular endothelial growth factor receptor 2

LIST OF FIGURES

LIST OF TABLES

ACKNOWLEDGEMENTS

I would like to thank many individuals who have supported me throughout my PhD studies. First, I would like to thank my advisor, Professor Geert Schmid-Schönbein, for his inspiration, guidance, support, and countless hours of discussions regarding my research. He has shared his passion for bioengineering thinking to understanding human diseases and has allowed me to pursue many interesting research topics throughout my studies. I also would like to thank Professor Shu Chien for his time and valuable guidance both in the lab and in life. Professor Pedro Cabrales, Professor Yeshaiahu Fainman, Professor Alison Marsden, and Professor John Watson served on my committee, and I appreciate their time and suggestions to my work.

The members of Professor Schmid-Schönbein's laboratory have been extremely influential in helping me through this journey, and for that I am extremely grateful. I would like to thank Dr. Alexander Penn, who taught me how to perform surgeries, discussed projects with me, and offered advice. I would like to recognize and thank Dr. Erik Kistler for reviewing my work and providing a clinical perspective. Michael Richter also participated in many valuable discussions and graciously helped me during surgeries. I am appreciative to the many discussions and useful suggestions over the years with Dr. Rafi Mazor and Tom Aslaigh. I thank Dr. Marisol Chang for answering my many technical questions. I thank Frank Delano for his general support in the lab and for the help with printing posters. I am appreciative of Dr. Angela Chen's ever-present positive outlook on research as it inspired me to never give up. I would like to thank Amy Chan,

Sharon Wu, Shakti Valdez, Jason Chow, Noi Plongthongkum and Dr. Edward Tran for their help in the lab during the early stages of my PhD.

I would also like to recognize my outstanding undergraduate students that I had the opportunity to train and mentor during my graduate studies: Mary Morgan (2009-10), Parth Chokshi (2010-12), Jessica Yang (2010-11), Ga-Ram Kim (Cox) (2010-11), Itze Lamadrid (2011-12), Stephanie Ma (2011-13), Leena Kurre (2011-13), Diana Li (2011-13), Jason Chou (2012-13), Lynn Han (2011-13), Param Bhatter (2013-), and Diana Muñoz (2013-). Training these students inspired me to keep a fresh prospective on my research, and I am extremely thankful for their countless hours of dedication, consistency, and loyalty.

I am very extremely grateful for the many individuals that assisted me in the laboratory with cell culture experiments, although these experiments were not included is this thesis. I would like to acknowledge Jerry Norwich, Suli Yuan, Dr. Julie Li, Dr. Dayu Teng, Dr. Jing Zhao and Phu Nguyen for answering numerous questions and contributing to my scientific understanding.

I would like to thank Chris (Seh-Hong) Lim from the National Health Research Institutes (NHRI) in Taiwan for teaching me how to be a better surgeon. I would also like to thank Dr. Yi Ting Yeh for her help during the summer I spent at NHRI and Dr. Jeng-Jiann Chiu for allowing me to be a guest in their lab.

Most importantly, I would like to thank my family. They supported my scientific interests from the beginning, and without their continuous support and encouragement, I would not have made it this far.

Chapter 2, in full, is currently being prepared for submission for publication entitled “Transmural intestinal wall permeability in severe ischemia after enteral protease inhibition” by Angelina E. Altshuler, Itze Lamadrid, Diana Li, Stephanie Ma, Leena Kurre, Geert W. Schmid-Schönbein, and Alexander H. Penn. Table 2.4 was contributed by Alexander H. Penn. The dissertation author is the primary author of this manuscript.

Chapter 3 was published in PLoS ONE with the title “Protease activity increases in plasma, peritoneal fluid, and vital organs after hemorrhagic shock in rats” by Angelina E. Altshuler, Alexander H. Penn, Jessica A. Yang, Ga-Ram Kim, and Geert W. Schmid-Schönbein. The dissertation author is co-first author of this manuscript. Figures 3.3 and 3.4 were contributed by Alexander H. Penn. Figure 3.8 was contributed by Mr. Michael Richter.

Chapters 5, 6 and 7, in full, are currently being prepared for submission for publication entitled “Strategies to minimize organ injury by proteolytic enzymes in hemorrhagic shock” by Angelina E. Altshuler, Michael Richter, Jason Chou, Diana Li, Leena Kurre, Alexander H. Penn, and Geert W. Schmid-Schönbein. The dissertation author is the primary author of this manuscript.

VITA AND PUBLICATIONS

2008 Bachelor of Science, University of California, San Diego

2010 Master of Science, University of California, San Diego

2013 Doctor of Philosophy, University of California, San Diego

PUBLICATIONS:

Altshuler AE, Richter M, Chou J, Li D, Kurre, L, Penn AH, Schmid-Schönbein G.W. Strategies to minimize organ injury by proteolytic enzymes in hemorrhagic shock, In Preparation.

Altshuler AE, Lamadrid I, Li D, Ma S, Kurre L, Schmid-Schönbein GW, Penn, AH. Transmural Intestinal Wall Permeability in Severe Ischemia after Enteral Protease Inhibition, In Preparation.

Friese RS, Altshuler AE, Salem RM, Gayen JR, Mahapatra NR, Biswas N, Cale M, Kim HS, Courel M, Taupenot L, Mahata SK, Schmid-Schönbein GW, O'Connor DT. (2013) Micro-RNA-22 motif polymorphism of the Chga transcript in genetic hypertension: Functional and therapeutic implications for gene expression and the pathogenesis of hypertension. Human Molecular Genetics (in press).

Mazor R, Alsaigh T, Shaked H, Altshuler AE, Pocock ES, Kistler EB, Karin M, Schmid-Schönbein GW. (2013) Matrix metalloproteinase-1-mediated up-regulation of vascular endothelial growth factor-2 in endothelial cells. J Biol Chem 288: 598-607.

Altshuler AE, Morgan MJ, Chien S, Schmid-Schönbein GW. (2012) Proteolytic activity attenuates the response of endothelial cells to fluid shear stress. Cell Mol Bioeng 5: 82-91.

Altshuler AE, Penn AH, Yang JA, Kim GR, Schmid-Schönbein GW. (2012) Protease activity increases in plasma, peritoneal fluid, and vital organs after hemorrhagic shock in rats. PLoS One 7: e32672.

Penn AH, Altshuler AE, Small JW, Taylor SF, Dobkins KR, Schmid-Schönbein GW. (2012) Digested formula but not digested fresh human milk causes death of intestinal cells in vitro: Implications for necrotizing enterocolitis. Pediatr Res. 72(6):560-7.

Doern A, Cao X, Sereno A, Reyes CL, Altshuler A, Huang F, Hession C, Flavier A, Favis M, Tran H, Ailor E, Levesque M, Murphy T, Berquist L, Tamraz S, Snipas T, Garber E, Shestowsky WS, Rennard R, Graff CP, Wu X, Snyder W, Cole L, Gregson D, Shields M, Ho SN, Reff ME, Glaser SM, Dong J, Demarest SJ, Hariharan K. (2009) Characterization of inhibitory anti-insulin-like growth factor receptor antibodies with different epitope specificity and ligand-blocking properties: Implications for mechanism of action in vivo. J Biol Chem 284: 10254-10267.

ABSTRACTS:

Altshuler AE, Penn AH, Schmid-Schönbein GW. "Luminal contents from the intestine contribute to gut injury after hemorrhagic shock." UC Systemwide Bioengineering Symposium, La Jolla, CA (19-21 June 2013)

Altshuler AE, Penn AH, Lamadrid I, Li D, Ma S, Kurre L, Schmid-Schönbein GW. "Development of strategies to prevent autodigestion and death: methods to preserve the barrier of an ischemic intestine." UC Systemwide Bioengineering Symposium, La Jolla, CA (19-21 June 2013)

Altshuler AE, Richter M, Schmid-Schönbein GW. "Pancreatic proteases are transported through mesenteric lymph to systemic circulation' Shock Society Annual Meeting; San Diego, CA (June 2 2013)

Altshuler AE, Chou J, Li D, Penn AH, Schmid-Schönbein GW. "Enteral tranexamic acid attenuates lung endothelial protein damage following hemorrhagic shock" Shock Society Annual Meeting; San Diego, CA (2 June 2013)

Altshuler AE, Penn AH, Lamadrid I, Li D, Ma S, Kurre L, Schmid-Schönbein GW. "Development of strategies to prevent autodigestion and death: methods to preserve the barrier of an ischemic intestine." UCSD Jacobs Research Expo (18 April 2013)

Altshuler AE, Yang JY, Kim G, Schmid-Schönbein GW. **"**Trypsin and MMP-9 levels increase in plasma and lung after hemorrhagic shock: potential mechanism for membrane receptor damage" Shock Society Annual Meeting; Miami, FL (12 June 2012)

Altshuler AE, Penn AH, Lamadrid I, Li D, Ma S, Yang JA, Kurre L, Han L. "Intestinal permeability increase during ischemia is reduced by enteral serine protease inhibitors ANGD and cyclokapron", Shock Society Annual Meeting; Miami FL (12 June 2012)

Altshuler AE, Penn AH, Yang JY, Kim G, Schmid-Schönbein GW. "Trypsin and MMP-9 Levels and Activity Increase in Plasma, Peritoneal Space, and Vital Organs during Hemorrhagic Shock", FASEB; San Diego, CA (25 April 2012)

Altshuler AE, Yang JY, Kim G, Schmid-Schönbein GW. **"**Trypsin and MMP-9 levels increase in plasma and lung after hemorrhagic shock: potential mechanism for membrane receptor damage" UCSD Jacob's Research Expo La Jolla, CA (12 April 2012) (*Honorable Mention*)

Penn AH, Altshuler AE, Schmid-Schönbein GW. Plasma Protease Activity Increases after Hemorrhagic Shock in Rats, When Measured with Peptidic Substrates. Washington DC (April 2011)

Altshuler AE, Schmid-Schönbein GW. "Proteolytic Activity Disturbs the Endothelial Cell's Response to Fluid Shear", Biomedical Engineering Society Conference; Austin, TX (6 Oct 2010)

Altshuler AE, Schmid-Schönbein GW. "Proteolytic Activity Reduces the Endothelial Cell's Response to Fluid Shear," U.C. Systemwide Bioengineering Symposium. Davis, CA (19 June 2010)

Altshuler AE, Michailova A, Abramson D "Cardiac modeling using Nimrod: stabilizing myocyte subcell calcium transient and action potential calculations", Supercomputing Conference; Tampa Bay, FL (14 Nov 2006)

ABSTRACT OF THE DISSERTATION

Degrading Proteases and Organ Failure during Physiological Shock

by

Angelina E. Altshuler

Doctor of Philosophy Science in Bioengineering

University of California, San Diego, 2013

Professor Geert W. Schmid-Schönbein, Chair

Circulatory shock is a frequent cause of death and one of the most important unresolved medical problems. Reduction of blood supply to the small intestine during ischemia disrupts the mucosal epithelial barrier, allowing inflammatory materials in the lumen of the intestine, including digestive enzymes, to cross into the intestinal wall. If digestive enzymes are transported into the periphery, they can activate other proteases and degrade extracellular structures. Understanding the contribution of degrading proteases to circulatory shock may be essential to interfere with its lethal course.

My objective is to determine which proteases are involved in the progression of shock and their contribution to intestinal degradation and peripheral organ failure. I hypothesize that during shock, the intestine is proteolytically degraded, accelerating leakage of proteases into the plasma, lymphatics, and peritoneal space, which may cause subsequent activation of proteases in peripheral organs and degradation of extracellular structures on endothelial and epithelial cells.

To determine degradative mechanisms inherent to the intestinal wall and independent of luminal contents, I will use a model of severe intestinal ischemia to study barrier failure, digestive and wall proteases, and epithelial protein degradation. I will study the activities and transport of digestive proteases from the lumen of the intestine during hemorrhagic shock. I will determine the contribution of luminal contents to intestine and lung injury after hemorrhagic shock. Lastly, I will test methods to prevent breakdown of the intestinal barrier to reduce penetration of luminal contents past the mucosal barrier and reduce peripheral organ injury.

I obtained evidence that the intestinal tissue degrades in severe ischemia even without luminal digestive enzymes. In hemorrhagic shock, I show that luminal contents are responsible for intestinal injury but not lung injury as determined by neutrophil accumulation and endothelial protein degradation. Protease activity and levels are elevated in the peritoneal space, lymph, blood, and vital organs after hemorrhagic shock. Protease inhibition to the gut reduces intestinal injury and protein degradation in the lung. These results suggest that proteases play a critical role in the pathophysiology of shock and may be important targets to reduce organ injury.

Chapter 1

Introduction

1.1 Physiological Shock

In the past century, advances in many areas of medicine have improved quality of life and life expectancy. However, less progress has been made in the area of *circulatory shock*, which accounts for 70% of deaths in intensive care units and is the leading cause of death for individuals under 44 years of age [1].

During shock, the normal physiological state is severely disrupted. In several forms of shock, including shock caused by excessive blood loss, the central blood pressure is reduced, which results in inadequate cardiac output and reduced oxygen delivery to the tissues. After a systemic blood pressure drop, perfusion to peripheral organs is reduced and the limited blood supply is redirected to maintain vital organs such as the heart and brain [2]. As a result, there is reduced flow to organs supplied by the splanchnic circulation, including the small and large intestine, causing these organs to become ischemic from inadequate oxygen and nutrient supply [3]. The ultimate mortality of shock follows a succession of failing organs [4]. This is phenomenon to as *multiple organ system dysfunction.*

Many hypotheses have been tested to try to explain the mechanism of multiple organ system dysfunction in shock. These include inappropriate neutrophil activation and adhesion [5,6], release of oxygen free radicals [7,8], and translocation of bacteria from the intestine [1,9,10]. However, these events occur in later stages of organ failure and are not the underlying mechanism that initiates organ dysfunction. Shock can occur at any age, race, or sex and is less likely caused by genetics [11,12].

The decline of cell and organ function during multiple organ dysfunction has long been attributed to the small intestine [13-15]. The response to shock is not species specific and has been observed in all mammalian animals studied, suggesting a commonality in the mechanisms that lead to organ failure. Among all organs that fail in shock, investigators pioneering the field of shock observed that intestinal failure occurred early and consistently in experimental shock models [14,16,17]. It has been found that peripheral organ injury is less severe in organs distant from the intestine if the intestine is excised prior to hemorrhagic shock [18]. Since the intestine is easily injured, we will begin our discussion on the current perspectives of the gut in shock.

1.2 The Role of the Intestine in Shock

Early shock studies attributed the intestine as a major contributor to the progression of organ failure during shock [14]. Reducing blood flow to the intestine is sufficient to induce shock without removal of systemic blood volume [16] and serves as a model for initiating shock. Since the intestine is a complex organ and may fail via a

variety of mechanisms, we will start by discussing the barriers and transport routes from the intestine to the peripheral organs.

1.2.1 The Mucus Layer and Epithelial Barrier

The fundamental function of the intestine is to absorb nutrients from ingested food. Food begins its journey through the digestive track by being chewed in the mouth and swallowed, then conducted via the esophagus by parasympathetic peristalsis into the stomach. The chyme, a mixture of food, saliva and stomach secretions, is secreted by the stomach and enters the lumen of the small intestine (duodenum where it is mixed with digestive enzymes secreted from the pancreas and bile salts from the liver which are stored in the gall bladder) so that it can be broken down into absorbable elemental components. The mixture is transported through the jejunum and ileum portions of the small intestine by means of peristaltic contractions generated by smooth muscle in the intestinal wall.

The luminal contents inside the intestine interface with the mucus layer on the surface of the epithelial cells. Mucins are carbohydrate rich glycoproteins that compose a major part of the mucus layer [19]. There are several mucin isoforms in the small intestine that are secreted from goblet cells and anchored to the epithelial barrier [20-22]. The mucus layer protrudes about 150-300 μm over the epithelial membrane [23] containing integrated antimicrobial agents and ultimately preventing penetration of particles that are unable to be absorbed [24].

Mucins also protect the epithelial cells from apoptosis [25]. The intestinal epithelial barrier is sensitive to ischemia. Enhancement of epithelial apoptosis has been observed as early as 15 minutes after ischemia [26]. Disruption of the mucins occurs early in intestinal ischemia and the mucin barrier becomes severely disrupted in less than 30 minutes of ischemia [27-29]. Mucosal lesions may be accompanied by damage to the submucosa and take days and weeks to heal [30].

Enterocytes, the epithelial cells that line the intestinal villi, form a tight barrier beneath the mucus layer [31]. These epithelial cells are continuously generated by progenitor cells in the crypts and enter apoptosis when they are expelled off the tip of the villi into the lumen [32,33]. The epithelial layer in the gut has one of the most rapid cell turnover rates in the body [34]. The epithelial cells are tightly held together by a plethora of tight and adheren junctional proteins [31]. On the epithelial surface, there are many transporters that move the monomeric compounds across to the blood [35,36]. Enterocytes rely on glucose diffusion through the mucus layer that can be internalized by the GLUT2 receptor for metabolic support and consequently maintain a high intracellular glucose concentration [37].

The high metabolic demand of epithelial cells makes them sensitive to ischemic conditions that accompany shock. Intestinal ischemia accelerates the natural apoptotic process of the epithelial cells [26]. In fact, the detachment of epithelial cells from the villi, termed anoikis, was discovered under ischemic conditions in the intestine [26]. Metabolic support by enteral glucose administration during intestinal ischemia has been able to reduce apoptotic shedding [38-41]. However, there are still many unanswered

questions regarding the status of these cells and which proteins, if any, are degraded during the ischemic state and whether luminal contents affect protein degradation.

1.2.2 The Intestinal Microvascular Network

One major route of nutrition absorption by the mucosal epithelium is the portal venous system. The circulation carries absorbed micronutrients such as carbohydrates and small peptides through the intestinal venules that protrude into the microvilli.

Escape of erythrocytes from microvessels is an early marker for macroscopic lesions. In the intestine, these lesions occur frequently at the tip of the villi during prolonged ischemia and can eventually propagate into the deeper tissue layers of the intestinal wall [15,41,42]. The phenomenon of diffuse bleeding into the lumen of the intestine may be a result of intestinal necrosis and has been repeatedly observed in different mammalian species [41,43]. Even a low flow state is sufficient to cause microvessels to rupture and allow hemorrhage into the lumen of the intestine [13]. The lack of oxygen as a consequence of reduced intestinal perfusion may be a major contributor to the degradation of these microvessels [44]. Irreversible organ failure is postulated to correlate with the severity of intestinal regions with hemorrhagic necrosis [44].

1.2.3 The Intestinal Lymphatic Network

The lymphatics are involved in fluid, protein, lipid absorption and immune cell transport from the tissues, a process that is intimately linked to regulating immunity [45]. The mesenteric lymph duct is a large lymphatic vessel that is a collecting point for lymph generated by the intestine and pancreas.

Since intestinal ischemia leads to destruction of villi, the lymphatic channels responsible for draining lymph fluid from the villi may collect intestinal extracellular fluid [46]. Furthermore, lymph fluid from animals that undergo intestinal ischemia is toxic [47,48] and may contain food particles like free fatty acids [49]. Cross transfusions of post-shock mesenteric lymph from an animal that has been subjected to hemorrhagic shock to a naïve animal is sufficient to generate organ damage in the lung [50].

1.2.4 The Muscularis

The primary function of intestinal muscularis is to aid in gastric motility [51] and is the least sensitive component of the intestinal villi to ischemic conditions [52]. If this layer is damaged, the gastric motility transiently increases followed by paralysis [53]. During ischemia, neutrophils accumulate in the muscularis [6], which has been linked to a reduction in motility [52]. Following ischemic injury, the muscularis displays morphological changes including contraction and cell lysis [54].

Intestinal components that penetrate the muscularis may enter into the peritoneal cavity. Evidence for this possibility is supported from the observation that after intestinal

ischemia-reperfusion injury, the peritoneal fluid contains components from the lumen of the intestine, along with inflammatory mediators [55].

1.3 The Autodigestion Hypothesis

Recently, a hypothesis has been advanced, referred to collectively as the *autodigestion hypothesis*, to explain the dramatic breakdown of the intestinal wall during ischemia as well as the destruction of cellular and molecular elements in the systemic circulation and peripheral organs. The autodigestion hypothesis states that digestive enzymes escape from the lumen of the intestine during intestinal ischemia due to breakdown of the mucosal barrier. The hypothesis is based on the idea that the primary source of the enzymatic activity necessary for nonselective degradation of food is derived from pancreatic digestive enzymes and is located in the lumen of the intestine where proteins, lipids, and carbohydrates are naturally degraded into absorbable components. In shock, the mucosal barrier of the intestine is damaged, allowing normally compartmentalized pancreatic proteases to break down the intestinal wall [13,27,28]. As the epithelial barrier breaks open during intestinal ischemia, the proteases that traditionally are contained in the lumen of the intestine may appear in the intestinal wall and may damage extracellular components of cells and tissues, thereby compromising homeostasis [46]. As digestive enzymes escape further into the systemic circulation, cells in the circulation (e.g. blood cells, endothelial and parenchymal cells) may be exposed to their proteolytic activity and be subject to possible structural degradation [56].

Several studies have established a correlation between the ability of an animal to recover from shock and blockage of the digestive enzymes [57-62]. If the enzymes in the intestine are inhibited during shock, cell and tissue injury are reduced. As a result, there are fewer activated leukocytes, fewer rolling leukocytes in venules, reduced endothelial apoptosis, in addition to a higher incidence of survival [63,64]. Despite the potential importance of proteolytic degradation in shock, the types of proteases involved in these degrading processes and their concentrations have not been determined.

1.4 Proteases Involved In Shock

1.4.1 Serine Proteases

The pancreas is a major source of serine proteases (chymotrypsin, trypsin, and elastase); these are produced in the acinar cells of the exocrine pancreas in the zymogen form. The zymogens are secreted into the small intestine through pancreatic ducts and are activated by enterokinases and able to activate other zymogens [65]. Once activated, serine proteases are powerful enzymes (i.e. concentrated, relatively unspecific and fully activated) cleaving the carboxyl side after specific individual amino acids (i.e. trypsin cleaves after lysine and arginine amino acid residues). The high concentration and activity of these enzymes in the intestine is an essential requirement for food digestion and generation of monomeric components that can be absorbed by membrane transporters in the epithelium. Digestive proteases are usually compartmentalized in the lumen of the small intestine by the mucosal barrier, which prevents larger molecules from

entering the wall of the intestine under normal physiological conditions [66]. However, in the case of intestinal ischemia when the enhanced apoptosis of the villi and the intestinal mucus layer disintegrate [26,33], digestive enzymes are able to penetrate into the wall [27,67].

As a result of a longstanding interest to block the digestive enzymes in conditions like pancreatitis, inhibitors against pancreatic digestive enzymes have been developed. Synthetic protease inhibitors, such as nafamostat mesilate (ANGD) and gabexate mesilate (FOY), have been shown to be effective at blocking luminal serine proteases and reducing peripheral inflammation during shock [13,68].

Besides pancreatic digestive proteases, the serine protease elastase can be released by neutrophils, which has been shown to damage the microcirculation during ischemia/reperfusion injury [69]. Early studies have hypothesized that activated neutrophils in ischemia can damage endothelial cells [70].

Serine proteases are also present in the clotting cascade and include enzymes like plasmin, thrombin, complement factor and Factors XI, IX, VII, X [71]. Some of these proteases interact with the surface of endothelial cells. For example, thrombin can activate protease-activated receptor 1 (PAR-1) on endothelial cells [72], so the possibility of protease-cell interaction exists and has been studied in limited circumstances outside of the shock community.

The plasma contains a plethora of serine protease inhibitors (serpins) including α-1-anti-trypsin and α-2 macroglobulin [73-77]. Deficiency of these protease inhibitors may be a lethal progression of shock [78].

1.4.2 MATRIX METALLOPROTEINASES

Matrix metalloproteinases (MMPs) are a class of proteases that degrade the extracellular matrix. They are synthesized in pro-enzyme forms and can be activated by serine proteases [79-81]. MMP-1, MMP-2 and MMP-9 are synthesized by endothelial cells [82-84]. Endothelial cells shed MMP-2 and MMP-9 from protease-containing vesicles during angiogenesis within a four-hour period [85], which may be important in the repair process after shock injury. Neutrophils are another source of MMP-9 [81,86].

MMPs have a specific class of inhibitors called tissue inhibitors of metalloproteinases (TIMPs). The balance between MMPs and TIMPs is critical to regulating their activity [87]. Several synthetic drugs such as statins and doxycycline are capable of inhibiting MMPs [84]. Administration of doxycycline has been shown to reduce injury and MMP-2 and 9 levels in the brain, lung, and kidney after ischemia injury [88-90].

There are several studies that have examined the levels of MMPs during ischemia; however, there are few studies that investigated their activity in hemorrhagic shock models. In hemorrhagic shock, cDNA levels of MMP-2,7,9 are unchanged while the TIMP mRNA levels increase after 3 hr of resuscitation [91]. One study using a model for hemorrhagic shock detected increased MMP-9 levels after hemorrhage and resuscitation [92]. However, these results in hemorrhagic shock models do not match results observed in localized organ ischemia where MMP-2/9 has been found to be elevated in renal, brain, lung, and cardiac ischemia compared to normally perfused animals [93-96]. In the family of MMPs, MMP-9 has been specifically attributed to disrupting endothelial barrier

integrity [97]. In-vitro studies demonstrate an increase in shear stress is sufficient to increase MMP-9 activity [98,99], and thus it may be sensitive to mechanical stimulation.

MMP-9 can cleave multiple surface components including ICAM-1, IL-2Rα, pro-IL-1β, KIT-l, pro-TGF-β, VE-cadherin, occludin, syndecan-1, syndecan-4, and NG2 proteoglycan [100]. MMP-9 can also cleave pro-TNF and increase levels of TNF-α after resuscitation [101,102].

1.4.3 Plasma Protease Activity

There is limited evidence for elevated pancreatic enzyme activity in the plasma of shock animals. Amylase and lipase activity levels have been found to be elevated in shock patients and are a measure for the state of shock and progression of organ failure [103]. Direct exposure of post-shock plasma to cultured endothelial cell monolayers increases endothelial permeability, although the mechanism or the particular proteases potentially involved is not well established [104]. Digestive enzymes may be involved in generating inflammatory mediators in the circulation [13,105]. Pancreatic proteases may activate MMP-9 in rats subjected to intestinal ischemia [81]. Since serine proteases activate other proteases, the cascade can result in a systemic amplification of degrading protease activity in the circulation and possibly in various other tissues.

1.5 Peripheral Organ Injury and the Gut

The severity of peripheral organ injury is linked to the quality of the gut after shock. If the proteases are inhibited in the gut before the onset of shock with the serine protease inhibitor ANGD, lung injury is attenuated as measured by myeloperoxidase (MPO) secretion as a marker for neutrophil accumulation [62,106]. Furthermore, evidence supports that gut derived inflammatory mediators, potentially containing these proteases, are transported through the mesenteric lymph [47,48]. All of the pro-inflammatory products that eventually enter into the circulation can activate neutrophils [63]. Activated neutrophils can propagate the damage by entrapment in the microcirculation and by rupturing the basement membrane of endothelial cells through secretion of neutrophil elastase [107,108]. Neutrophils also secrete MMPs, which can digest extracellular matrix proteins during transmigration and tissue repair [109,110]. These local protease secretions stimulated by luminal factors may be important in the progression of organ injury and endothelial dysfunction.

1.6 Endothelial Dysfunction in Shock: Potential Connection with Proteolytic Activity

To date, there has been limited exploration of how serine proteases or MMPs may damage extracellular surface components of endothelial and other cells in-vivo following shock.

One of the key events arising from proteolytic activity is a shift in vascular permeability. Vascular permeability can be increased proteolytically by direct injection of collagenases into the circulation [111], and therefore may be in part a protease dependent process. Vascular permeability can increase if tight junction proteins, e.g. occludin, beta catenin, and VE-cadherin are fragmented rather than the creation of transcellular holes [112,113]. Endothelial apoptosis correlates with the level of permeability of the endothelium [114,115]. After hemorrhagic shock, endothelial cells exhibit hyperpermeability and an increased rate of apoptosis [116,117].

The extent of damage to the endothelial surface proteins resulting from protease activation and/or gut injury has yet to be explored in the case of hemorrhagic shock.

1.7 Overview of Dissertation

There is increasing evidence that the intestine is the driving force for the irreversible outcomes that follow an initial insult in shock and that it may initiate a dramatic sequence of proteolytic events in sites distant from the intestine. The objective of this thesis is to determine which families of proteases are involved in the progression of shock and how they contribute to intestinal degradation and peripheral organ failure.

I hypothesize that in hemorrhagic shock, the reduction of blood flow in the intestine results in a proteolytic breakdown of the mucosal barrier, allowing leakage of the digestive proteases into in the wall of the intestine followed by further transport into plasma, lymphatics, and peritoneal space, which may cause subsequent activation of other proteases in peripheral organs. The up-regulated proteolytic activity causes damage

by digesting extracellular membrane components on epithelial and endothelial cells such as cadherins, tight junction proteins, and functional proteins like vascular endothelial growth factor receptor 2 (VEGFR-2), resulting in cellular dysfunction (including increases in permeability and apoptosis).

To test this hypothesis, I propose the following Specific Aims:

Aim 1: Determine during complete intestinal ischemia the role of proteases in intestinal tissue damage as the ischemic intestine barrier fails. The breakdown of the intestinal wall will be studied and interventions against key classes of proteases will be tested. The types of protease activities present, epithelial protein degradation, and apoptosis levels will be examined to build a foundation for understanding the mechanisms of gut breakdown during ischemia.

Aim 2: Investigate the activities and transport of proteases to peripheral organs during hemorrhagic shock. The pancreatic protease activities and levels will be determined in the blood, peritoneal space, and organs distant from the intestine (lung, liver, heart and brain). Protease activation in peripheral organs will also be investigated.

Aim 3: Examine in hemorrhagic shock the differences in protease activation and organ damage between a flushed and unflushed intestinal lumen. The role of luminal digestive proteases in protease activation, intestinal and peripheral organ damage following hemorrhagic shock will be elucidated.

Aim 4: Identify whether protection of the gut mucosal barrier and/or protease inhibition during hemorrhagic shock has an effect on endothelial surface receptors in selected systemic organs. Previous inhibition studies during shock were directed solely on blocking pancreatic proteases in the lumen of the intestine. In this aim, we will explore the effectiveness of individual and combinatorial therapeutics to reduce the transport, activity, and destruction caused by proteases. Endothelial surface receptors degradation will also be examined.

1.8 REFERENCES

1. Swank GM, Deitch EA. (1996) Role of the gut in multiple organ failure: Bacterial translocation and permeability changes. World J Surg 20: 411-417.

2. Strunin L. (1975) Organ perfusion during controlled hypotension. Br J Anaesth 47: 793-798.

3. Carter EA, Tompkins RG, Yarmush ML, Walker WA, Burke JF. (1988) Redistribution of blood flow after thermal injury and hemorrhagic shock. J Appl Physiol 65: 1782-1788.

4. Barie PS, Hydo LJ, Pieracci FM, Shou J, Eachempati SR. (2009) Multiple organ dysfunction syndrome in critical surgical illness. Surg Infect (Larchmt) 10: 369-377.

5. Xu DZ, Lu Q, Adams CA, Issekutz AC, Deitch EA. (2004) Trauma-hemorrhagic shock-induced up-regulation of endothelial cell adhesion molecules is blunted by mesenteric lymph duct ligation. Crit Care Med 32: 760-765.

6. Kalff JC, Hierholzer C, Tsukada K, Billiar TR, Bauer AJ. (1999) Hemorrhagic shock results in intestinal muscularis intercellular adhesion molecule (ICAM-1) expression, neutrophil infiltration, and smooth muscle dysfunction. Arch Orthop Trauma Surg 119: 89-93.

7. Itoh M, Guth PH. (1985) Role of oxygen-derived free radicals in hemorrhagic shock-induced gastric lesions in the rat. Gastroenterology 88: 1162-1167.

8. Zollei I, Karacsony G, Baltas B, Nagy S. (1989) Role of oxygen-derived free radicals in hemorrhagic shock-induced gastric lesions of rats. Acta Physiol Hung 73: 357-362.

9. Deitch EA, Specian RD, Berg RD. (1991) Endotoxin-induced bacterial translocation and mucosal permeability: Role of xanthine oxidase, complement activation, and macrophage products. Crit Care Med 19: 785-791.

10. Huang CY, Hsiao JK, Lu YZ, Lee TC, Yu LC. (2011) Anti-apoptotic PI3K/Akt signaling by sodium/glucose transporter 1 reduces epithelial barrier damage and bacterial translocation in intestinal ischemia. Lab Invest 91: 294-309.

11. Sperry JL, Minei JP. (2008) Gender dimorphism following injury: Making the connection from bench to bedside. J Leukoc Biol 83: 499-506.

12. Fry DE. (2000) Multiple organ dysfunction syndrome: Past, present and future. Surg Infect (Larchmt) 1: 155-61; discussion 161-3.

13. Mitsuoka H, Schmid-Schönbein GW. (2000) Mechanisms for blockade of in vivo activator production in the ischemic intestine and multi-organ failure. Shock 14: 522-527.

14. Lillehei RC. (1957) The intestinal factor in irreversible hemorrhagic shock. Surgery 42: 1043-1054.

15. Ahren C, Haglund U. (1973) Mucosal lesions in the small intestine of the cat during low flow. Acta Physiol Scand 88: 541-550.

16. Shapiro PB, Bronsther B, Frank NK ED, Fine J. (1958) Host resistance to hemorrhagic shock. XI. role of deficient flow through intestine in development of irreversibility. Proc Soc Exp Biol Med 97: 372-376.

17. Robinson JW, Antonioli JA, Mirkovitch V. (1966) The intestinal response to ischaemia. Naunyn Schmiedebergs Arch Pharmakol Exp Pathol 255: 178-191.

18. Evans WE, Shore RT, Carey LC, Darin JC. (1967) Effect of intestinal exclusion in escherichia coli endotoxin shock. Arch Surg 95: 511-516.

19. Johansson ME, Ambort D, Pelaseyed T, Schutte A, Gustafsson JK, Ermund A, Subramani DB, Holmen-Larsson JM, Thomsson KA, Bergstrom JH, van der Post S, Rodriguez-Pineiro AM, Sjovall H, Backstrom M, Hansson GC. (2011) Composition and functional role of the mucus layers in the intestine. Cell Mol Life Sci 68: 3635-3641.

20. Allen A, Hutton DA, Pearson JP. (1998) The MUC2 gene product: A human intestinal mucin. Int J Biochem Cell Biol 30: 797-801.

21. Williams SJ, Wreschner DH, Tran M, Eyre HJ, Sutherland GR, McGuckin MA. (2001) Muc13, a novel human cell surface mucin expressed by epithelial and hemopoietic cells. J Biol Chem 276: 18327-18336.

22. McAuley JL, Linden SK, Png CW, King RM, Pennington HL, Gendler SJ, Florin TH, Hill GR, Korolik V, McGuckin MA. (2007) MUC1 cell surface mucin is a critical element of the mucosal barrier to infection. J Clin Invest 117: 2313-2324.

23. Atuma C, Strugala V, Allen A, Holm L. (2001) The adherent gastrointestinal mucus gel layer: Thickness and physical state in vivo. Am J Physiol Gastrointest Liver Physiol 280: G922-9.

24. McGuckin MA, Linden SK, Sutton P, Florin TH. (2011) Mucin dynamics and enteric pathogens. Nat Rev Microbiol 9: 265-278.

25. Sheng YH, Lourie R, Linden SK, Jeffery PL, Roche D, Tran TV, Png CW, Waterhouse N, Sutton P, Florin TH, McGuckin MA. (2011) The MUC13 cell-surface mucin protects against intestinal inflammation by inhibiting epithelial cell apoptosis. Gut 60: 1661-1670.

26. Ikeda H, Suzuki Y, Suzuki M, Koike M, Tamura J, Tong J, Nomura M, Itoh G. (1998) Apoptosis is a major mode of cell death caused by ischaemia and ischaemia/reperfusion injury to the rat intestinal epithelium. Gut 42: 530-537.

27. Chang M, Kistler EB, Schmid-Schönbein GW. (2012) Disruption of the mucosal barrier during gut ischemia allows entry of digestive enzymes into the intestinal wall. Shock 37: 297-305.

28. Chang M, Alsaigh T, Kistler EB, Schmid-Schönbein GW. (2012) Breakdown of mucin as barrier to digestive enzymes in the ischemic rat small intestine. PLoS One 7: e40087.

29. Sheth SU, Lu Q, Twelker K, Sharpe SM, Qin X, Reino DC, Lee MA, Xu DZ, Deitch EA. (2010) Intestinal mucus layer preservation in female rats attenuates gut injury after trauma-hemorrhagic shock. J Trauma 68: 279-288.

30. Ming SC, Bonakdarpour A. (1977) Evolution of lesions in intestinal ischemia. Arch Pathol Lab Med 101: 40-43.

31. Ballard ST, Hunter JH, Taylor AE. (1995) Regulation of tight-junction permeability during nutrient absorption across the intestinal epithelium. Annu Rev Nutr 15: 35-55.

32. Grossmann J, Walther K, Artinger M, Rummele P, Woenckhaus M, Scholmerich J. (2002) Induction of apoptosis before shedding of human intestinal epithelial cells. Am J Gastroenterol 97: 1421-1428.

33. Grossmann J. (2002) Molecular mechanisms of "detachment-induced apoptosis--anoikis". Apoptosis 7: 247-260.

34. Jones BA, Gores GJ. (1997) Physiology and pathophysiology of apoptosis in epithelial cells of the liver, pancreas, and intestine. Am J Physiol 273: G1174-88.

35. Thorens B. (1993) Facilitated glucose transporters in epithelial cells. Annu Rev Physiol 55: 591-608.

36. Daniel H. (2004) Molecular and integrative physiology of intestinal peptide transport. Annu Rev Physiol 66: 361-384.

37. Newsholme EA, Carrie AL. (1994) Quantitative aspects of glucose and glutamine metabolism by intestinal cells. Gut 35: S13-7.

38. McArdle AH, Chiu CJ, Gurd FN. (1972) Intraluminal glucose: Substrate for ischemic intestine. Arch Surg 105: 441-445.

39. Kozar RA, Schultz SG, Bick RJ, Poindexter BJ, DeSoignie R, Moore FA. (2004) Enteral glutamine but not alanine maintains small bowel barrier function after ischemia/reperfusion injury in rats. Shock 21: 433-437.

40. Kozar RA, Hu S, Hassoun HT, DeSoignie R, Moore FA. (2002) Specific intraluminal nutrients alter mucosal blood flow during gut ischemia/reperfusion. JPEN J Parenter Enteral Nutr 26: 226-229.

41. Chiu CJ, McArdle AH, Brown R, Scott HJ, Gurd FN. (1970) Intestinal mucosal lesion in low-flow states. I. A morphological, hemodynamic, and metabolic reappraisal. Arch Surg 101: 478-483.

42. Haglund U, Hulten L, Ahren C, Lundgren O. (1975) Mucosal lesions in the human small intestine in shock. Gut 16: 979-984.

43. Lillehei RC, Dietzman RH, Movsas S. (1967) The visceral circulation in shock. Gastroenterology 52: 468-471.

44. Lillehei RC, Longerbeam JK, Bloch JH, Manax WG. (1964) The nature of experimental irreversible shock with its clinical application. Int Anesthesiol Clin 2: 297-363.

45. Miller MJ, McDole JR, Newberry RD. (2010) Microanatomy of the intestinal lymphatic system. Ann N Y Acad Sci 1207 Suppl 1: E21-8.

46. Schmid-Schönbein GW. (2009) 2008 landis award lecture. inflammation and the autodigestion hypothesis. Microcirculation 16: 289-306.

47. Deitch EA. (2010) Gut lymph and lymphatics: A source of factors leading to organ injury and dysfunction. Ann N Y Acad Sci 1207 Suppl 1: E103-11.

48. Lu Q, Xu DZ, Davidson MT, Hasko G, Deitch EA. (2004) Hemorrhagic shock induces endothelial cell apoptosis, which is mediated by factors contained in mesenteric lymph. Crit Care Med 32: 2464-2470.

49. Qin X, Dong W, Sharpe SM, Sheth SU, Palange DC, Rider T, Jandacek R, Tso P, Deitch EA. (2012) Role of lipase-generated free fatty acids in converting mesenteric lymph from a noncytotoxic to a cytotoxic fluid. Am J Physiol Gastrointest Liver Physiol 303: G969-78.

50. Wohlauer MV, Moore EE, Harr J, Eun J, Fragoso M, Banerjee A, Silliman CC. (2011) Cross-transfusion of postshock mesenteric lymph provokes acute lung injury. J Surg Res 170: 314-318.

51. Hierholzer C, Kalff JC, Audolfsson G, Billiar TR, Tweardy DJ, Bauer AJ. (1999) Molecular and functional contractile sequelae of rat intestinal ischemia/reperfusion injury. Transplantation 68: 1244-1254.

52. Hierholzer C, Kalff JC, Audolfsson G, Billiar TR, Tweardy DJ, Bauer AJ. (1999) Molecular and functional contractile sequelae of rat intestinal ischemia/reperfusion injury. Transplantation 68: 1244-1254.

53. Chou CC, Gallavan RH. (1982) Blood flow and intestinal motility. Fed Proc 41: 2090-2095.

54. Ming SC, McNiff J. (1976) Acute ischemic changes in intestinal muscularis. Am J Pathol 82: 315-326.

55. Ishimaru K, Mitsuoka H, Unno N, Inuzuka K, Nakamura S, Schmid-Schönbein GW. (2004) Pancreatic proteases and inflammatory mediators in peritoneal fluid during splanchnic arterial occlusion and reperfusion. Shock 22: 467-471.

56. Sun Z, Wang X, Lasson A, Bojesson A, Annborn M, Andersson R. (2001) Effects of inhibition of PAF, ICAM-1 and PECAM-1 on gut barrier failure caused by intestinal ischemia and reperfusion. Scand J Gastroenterol 36: 55-65.

57. Mitsuoka H, Kistler EB, Schmid-Schönbein GW. (2000) Generation of in vivo activating factors in the ischemic intestine by pancreatic enzymes. Proc Natl Acad Sci U S A 97: 1772-1777.

58. Ohnishi H, Suzuki K, Niho T, Ito C, Yamaguchi K. (1985) Protective effects of urinary trypsin inhibitor in experimental shock. Jpn J Pharmacol 39: 137-144.

59. Doucet JJ, Hoyt DB, Coimbra R, Schmid-Schönbein GW, Junger WG, Paul LW, Loomis WH, Hugli TE. (2004) Inhibition of enteral enzymes by enteroclysis with nafamostat mesilate reduces neutrophil activation and transfusion requirements after hemorrhagic shock. J Trauma 56: 501-10; discussion 510-1.

60. Fitzal F, DeLano FA, Young C, Schmid-Schönbein GW. (2004) Improvement in early symptoms of shock by delayed intestinal protease inhibition. Arch Surg 139: 1008-1016.

61. Allport JR, Lim YC, Shipley JM, Senior RM, Shapiro SD, Matsuyoshi N, Vestweber D, Luscinskas FW. (2002) Neutrophils from MMP-9- or neutrophil elastase-

deficient mice show no defect in transendothelial migration under flow in vitro. J Leukoc Biol 71: 821-828.

62. Deitch EA, Shi HP, Lu Q, Feketeova E, Xu DZ. (2003) Serine proteases are involved in the pathogenesis of trauma-hemorrhagic shock-induced gut and lung injury. Shock 19: 452-456.

63. Fitzal F, DeLano FA, Young C, Rosario HS, Schmid-Schönbein GW. (2002) Pancreatic protease inhibition during shock attenuates cell activation and peripheral inflammation. J Vasc Res 39: 320-329.

64. DeLano FA, Hoyt DB, Schmid-Schönbein GW. (2013) Pancreatic digestive enzyme blockade in the intestine increases survival after experimental shock. Sci Transl Med 5: 169ra11.

65. Kitamoto Y, Yuan X, Wu Q, McCourt DW, Sadler JE. (1994) Enterokinase, the initiator of intestinal digestion, is a mosaic protease composed of a distinctive assortment of domains. Proc Natl Acad Sci U S A 91: 7588-7592.

66. Wang J, Boerma M, Fu Q, Hauer-Jensen M. (2007) Significance of endothelial dysfunction in the pathogenesis of early and delayed radiation enteropathy. World J Gastroenterol 13: 3047-3055.

67. Kistler EB, Alsaigh T, Chang M, Schmid-Schönbein GW. (2012) Impaired small-bowel barrier integrity in the presence of lumenal pancreatic digestive enzymes leads to circulatory shock. Shock 38: 262-267.

68. Harada N, Okajima K, Kushimoto S. (1999) Gabexate mesilate, a synthetic protease inhibitor, reduces ischemia/reperfusion injury of rat liver by inhibiting leukocyte activation. Crit Care Med 27: 1958-1964.

69. Carden DL, Korthuis RJ. (1996) Protease inhibition attenuates microvascular dysfunction in postischemic skeletal muscle. Am J Physiol 271: H1947-52.

70. Chung AW, Booth AD, Rose C, Thompson CR, Levin A, van Breemen C. (2008) Increased matrix metalloproteinase 2 activity in the human internal mammary artery is associated with ageing, hypertension, diabetes and kidney dysfunction. J Vasc Res 45: 357-362.

71. Davie EW, Fujikawa K, Kisiel W. (1991) The coagulation cascade: Initiation, maintenance, and regulation. Biochemistry 30: 10363-10370.

72. Coughlin SR. (1999) How the protease thrombin talks to cells. Proc Natl Acad Sci U S A 96: 11023-11027.

73. Hubbard RC, Crystal RG. (1988) Alpha-1-antitrypsin augmentation therapy for alpha-1-antitrypsin deficiency. Am J Med 84: 52-62.

74. Borgstrom A, Lasson A. (1984) Trypsin-alpha 1-protease inhibitor complexes in serum and clinical course of acute pancreatitis. Scand J Gastroenterol 19: 1119-1122.

75. Kuroiwa K, Nakatsuyama S, Katayama K, Nagasawa T. (1989) Determination of alpha 2-macroglobulin-trypsin complex with a new synthetic substrate. Clin Chem 35: 2169-2172.

76. Largman C, Reidelberger RD, Tsukamoto H. (1986) Correlation of trypsin-plasma inhibitor complexes with mortality in experimental pancreatitis in rats. Dig Dis Sci 31: 961-969.

77. Aubry M, Bieth J. (1976) A kinetic study of the inhibition of human and bovine trypsins and chymotrypsins by the inter-alpha-inhibitor from human plasma. Biochim Biophys Acta 438: 221-230.

78. Nakade O, Kasai K, Satoh M, Yamamura M, Kakiuchi H, Kaku T, Mori M. (1999) Alpha1-antitrypsin deficiency and toxic shock: A japanese autopsy case. Pathol Int 49: 79-84.

79. Lindstad RI, Sylte I, Mikalsen SO, Seglen PO, Berg E, Winberg JO. (2005) Pancreatic trypsin activates human promatrix metalloproteinase-2. J Mol Biol 350: 682-698.

80. Kistler EB, Hugli TE, Schmid-Schönbein GW. (2000) The pancreas as a source of cardiovascular cell activating factors. Microcirculation 7: 183-192.

81. Rosario HS, Waldo SW, Becker SA, Schmid-Schönbein GW. (2004) Pancreatic trypsin increases matrix metalloproteinase-9 accumulation and activation during acute intestinal ischemia-reperfusion in the rat. Am J Pathol 164: 1707-1716.

82. Arenas IA, Xu Y, Lopez-Jaramillo P, Davidge ST. (2004) Angiotensin II-induced MMP-2 release from endothelial cells is mediated by TNF-alpha. Am J Physiol Cell Physiol 286: C779-84.

83. Genersch E, Hayess K, Neuenfeld Y, Haller H. (2000) Sustained ERK phosphorylation is necessary but not sufficient for MMP-9 regulation in endothelial cells: Involvement of ras-dependent and -independent pathways. J Cell Sci 113 Pt 23: 4319-4330.

84. Hanemaaijer R, Visser H, Koolwijk P, Sorsa T, Salo T, Golub LM, van Hinsbergh VW. (1998) Inhibition of MMP synthesis by doxycycline and chemically modified tetracyclines (CMTs) in human endothelial cells. Adv Dent Res 12: 114-118.

85. Taraboletti G, D'Ascenzo S, Borsotti P, Giavazzi R, Pavan A, Dolo V. (2002) Shedding of the matrix metalloproteinases MMP-2, MMP-9, and MT1-MMP as membrane vesicle-associated components by endothelial cells. Am J Pathol 160: 673-680.

86. Hibbs MS. (1992) Expression of 92 kDa phagocyte gelatinase by inflammatory and connective tissue cells. Matrix Suppl 1: 51-57.

87. Verma RP, Hansch C. (2007) Matrix metalloproteinases (MMPs): Chemical-biological functions and (Q)SARs. Bioorg Med Chem 15: 2223-2268.

88. Reyes R, Guo M, Swann K, Shetgeri SU, Sprague SM, Jimenez DF, Barone CM, Ding Y. (2009) Role of tumor necrosis factor-alpha and matrix metalloproteinase-9 in blood-brain barrier disruption after peripheral thermal injury in rats. J Neurosurg 110: 1218-1226.

89. Ihtiyar E, Yasar NF, Erkasap N, Koken T, Tosun M, Oner S, Erkasap S. (2011) Effects of doxycycline on renal ischemia reperfusion injury induced by abdominal compartment syndrome. J Surg Res 167: 113-120.

90. Palei AC, Zaneti RA, Fortuna GM, Gerlach RF, Tanus-Santos JE. (2005) Hemodynamic benefits of matrix metalloproteinase-9 inhibition by doxycycline during experimental acute pulmonary embolism. Angiology 56: 611-617.

91. Chen H, Inocencio R, Alam HB, Rhee P, Koustova E. (2005) Differential expression of extracellular matrix remodeling genes in rat model of hemorrhagic shock and resuscitation. J Surg Res 123: 235-244.

92. Maitra SR, Bhaduri S, El-Maghrabi MR, Shapiro MJ. (2005) Inhibition of matrix metalloproteinase on hepatic transforming growth factor beta1 and caspase-3 activation in hemorrhage. Acad Emerg Med 12: 797-803.

93. Caron A, Desrosiers RR, Beliveau R. (2005) Ischemia injury alters endothelial cell properties of kidney cortex: Stimulation of MMP-9. Exp Cell Res 310: 105-116.

94. van der Kaaij NP, Kluin J, Haitsma JJ, den Bakker MA, Lambrecht BN, Lachmann B, de Bruin RW, Bogers AJ. (2008) Ischemia of the lung causes extensive long-term pulmonary injury: An experimental study. Respir Res 9: 28.

95. Bauer AT, Burgers HF, Rabie T, Marti HH. (2010) Matrix metalloproteinase-9 mediates hypoxia-induced vascular leakage in the brain via tight junction rearrangement. J Cereb Blood Flow Metab 30: 837-848.

96. Sutton TA, Kelly KJ, Mang HE, Plotkin Z, Sandoval RM, Dagher PC. (2005) Minocycline reduces renal microvascular leakage in a rat model of ischemic renal injury. Am J Physiol Renal Physiol 288: F91-7.

97. Thanabalasundaram G, Pieper C, Lischper M, Galla HJ. (2010) Regulation of the blood-brain barrier integrity by pericytes via matrix metalloproteinases mediated activation of vascular endothelial growth factor in vitro. Brain Res 1347: 1-10.

98. Sho E, Sho M, Singh TM, Nanjo H, Komatsu M, Xu C, Masuda H, Zarins CK. (2002) Arterial enlargement in response to high flow requires early expression of matrix metalloproteinases to degrade extracellular matrix. Exp Mol Pathol 73: 142-153.

99. Chen L, Sun X, Tang J, Ding Y, Li J, Li W, Gong J, Wang H. (2010) Effect of laminar shear stress on the expression of matrix metalloproteinases-9 in rat bone marrow-derived mesenchymal stem cells. Sheng Wu Yi Xue Gong Cheng Xue Za Zhi 27: 1261-1265.

100. Cauwe B, Van den Steen PE, Opdenakker G. (2007) The biochemical, biological, and pathological kaleidoscope of cell surface substrates processed by matrix metalloproteinases. Crit Rev Biochem Mol Biol 42: 113-185.

101. Gearing AJ, Beckett P, Christodoulou M, Churchill M, Clements JM, Crimmin M, Davidson AH, Drummond AH, Galloway WA, Gilbert R. (1995) Matrix metalloproteinases and processing of pro-TNF-alpha. J Leukoc Biol 57: 774-777.

102. Yao YM, Bahrami S, Leichtfried G, Redl H, Schlag G. (1996) Significance of NO in hemorrhage-induced hemodynamic alterations, organ injury, and mortality in rats. Am J Physiol 270: H1616-23.

103. Malinoski DJ, Hadjizacharia P, Salim A, Kim H, Dolich MO, Cinat M, Barrios C, Lekawa ME, Hoyt DB. (2009) Elevated serum pancreatic enzyme levels after hemorrhagic shock predict organ failure and death. J Trauma 67: 445-449.

104. Magnotti LJ, Upperman JS, Xu DZ, Lu Q, Deitch EA. (1998) Gut-derived mesenteric lymph but not portal blood increases endothelial cell permeability and promotes lung injury after hemorrhagic shock. Ann Surg 228: 518-527.

105. Penn AH, Hugli TE, Schmid-Schönbein GW. (2007) Pancreatic enzymes generate cytotoxic mediators in the intestine. Shock 27: 296-304.

106. Shi HP, Liu ZJ, Wen Y. (2004) Pancreatic enzymes in the gut contributing to lung injury after trauma/hemorrhagic shock. Chin J Traumatol 7: 36-41.

107. Tomizawa N, Ohwada S, Ohya T, Takeyoshi I, Ogawa T, Kawashima Y, Adachi M, Morishita Y. (1999) The effects of a neutrophil elastase inhibitor (ONO-5046.na) and neutrophil depletion using a granulotrap (G-1) column on lung reperfusion injury in dogs. J Heart Lung Transplant 18: 637-645.

108. Ishikawa N, Oda M, Kawaguchi M, Tsunezuka Y, Watanabe G. (2003) The effects of a specific neutrophil elastase inhibitor (ONO-5046) in pulmonary ischemia-reperfusion injury. Transpl Int 16: 341-346.

109. Ardi VC, Kupriyanova TA, Deryugina EI, Quigley JP. (2007) Human neutrophils uniquely release TIMP-free MMP-9 to provide a potent catalytic stimulator of angiogenesis. Proc Natl Acad Sci U S A 104: 20262-20267.

110. Girard TD, Ware LB, Bernard GR, Pandharipande PP, Thompson JL, Shintani AK, Jackson JC, Dittus RS, Ely EW. (2012) Associations of markers of inflammation and coagulation with delirium during critical illness. Intensive Care Med .

111. Volkl KP, Dierichs R. (1986) Effect of intravenously injected collagenase on the concentration of circulating platelets in rats. Thromb Res 42: 11-20.

112. Krizbai IA, Lenzser G, Szatmari E, Farkas AE, Wilhelm I, Fekete Z, Erdos B, Bauer H, Bauer HC, Sandor P, Komjati K. (2005) Blood-brain barrier changes during compensated and decompensated hemorrhagic shock. Shock 24: 428-433.

113. McDonald DM, Thurston G, Baluk P. (1999) Endothelial gaps as sites for plasma leakage in inflammation. Microcirculation 6: 7-22.

114. Grunenfelder J, Miniati DN, Murata S, Falk V, Hoyt EG, Kown M, Koransky ML, Robbins RC. (2001) Upregulation of bcl-2 through caspase-3 inhibition ameliorates ischemia/reperfusion injury in rat cardiac allografts. Circulation 104: I202-6.

115. Senthil M, Brown M, Xu DZ, Lu Q, Feketeova E, Deitch EA. (2006) Gut-lymph hypothesis of systemic inflammatory response syndrome/multiple-organ dysfunction syndrome: Validating studies in a porcine model. J Trauma 60: 958-65; discussion 965-7.

116. Matsuda N, Teramae H, Yamamoto S, Takano K, Takano Y, Hattori Y. (2010) Increased death receptor pathway of apoptotic signaling in septic mouse aorta: Effect of systemic delivery of FADD siRNA. Am J Physiol Heart Circ Physiol 298: H92-101.

117. Masini E, Cuzzocrea S, Mazzon E, Muia C, Vannacci A, Fabrizi F, Bani D. (2006) Protective effects of relaxin in ischemia/reperfusion-induced intestinal injury due to splanchnic artery occlusion. Br J Pharmacol 148: 1124-1132.

Chapter 2

Breakdown of the Intestinal Wall during Ischemia and Interventions to Maintain Barrier Integrity

2.1 INTRODUCTION

Intestinal ischemia is an important problem in critical care that can be caused by trauma or sepsis and is accompanied by an increase in small intestine permeability [1-4]. The reduced perfusion to the intestine results in damage to the intestinal villi and other components of the intestinal wall [5,6]. The permeability increases so that intestinal contents may leak across the mucosal barrier [7,8]. After escape from the intestinal lumen, intestinal contents can be transported through the venous intestinal vasculature [9,10], lymphatics [11], or if they pass completely through the intestinal wall, via the peritoneum into the systemic circulation [12,13], and may be responsible for distant organ injury [11,14]. Enteral blockade of digestive enzymes attenuates these processes [9,15], but the mechanisms by which these inhibitors provide protection and the initial

mechanisms in ischemia that leads to a permeable intestinal wall permitting entry of luminal contents are not well defined.

In ischemia, there are many potential sources of enzymes present in the intestinal tissue that may contribute to the breakdown of the intestinal wall. There are, of course, the digestive enzymes in the lumen. These enzymes may persist in the lumen even after the passage of food as shown by the detection of digestive proteases such as trypsin in the mucus layer of the epithelium despite flushing out all solid content [16]. In addition, epithelial cells and the wall of the intestine are characteristically rich in matrix metalloproteinases (MMPs), capable of digesting the extracellular matrix [17,18]. Endothelial cells, in the rich network of microvessels, and extravasated leukocytes are also potential sources of MMPs [19,20]. If activated or released during ischemia, these enzymes could degrade the intestinal wall, enabling leakage of pancreatic-derived digestive enzymes and/or small cytotoxic mediators such as free fatty acids [13,21,22] from the lumen, across the wall of the intestine, into the peritoneum.

In a severe ischemic state, there may also be other mechanisms for breakdown of the intestine, e.g. by depletion of ATP, including cell apoptotic processes [5]. However, the contribution of a proteolytic versus an apoptotic mechanism to the increased permeability and breakdown of the intestinal wall in severe ischemia in the absence of luminal contents is not well understood.

2.2 CHAPTER AIMS

The objective of this chapter is to investigate in a severe model of intestinal ischemia which degrading processes (cell death, proteases, and/or lipase) contribute to the transmural permeability of a low molecular weight tracer and breakdown of the intestinal wall. This is done in the absence of luminal contents to distinguish the mechanisms inherent to the intestinal wall from those that may result from mediators in the luminal content (discussed in Chapter 5). I hypothesize that metabolic support will preserve the epithelial barrier while proteolytic inhibition will prevent tissue breakdown during complete intestinal ischemia (Figure 2.1). To test this hypothesis, glucose, which can be directly metabolized by enterocytes and has documented positive effects during intestinal ischemia [23-26], will be placed into the lumen to provide a source of metabolic energy to the epithelium during severe ischemia. In order to study whether proteases contribute to intestinal wall breakdown, several classes of inhibitors will be placed into the intestinal lumen to assess whether degrading enzymes (e.g. serine proteases, lipase, MMPs) contribute to the rise in wall permeability and tissue destruction. Morphological damage, the level of protease activity in the tissue, and junctional protein integrity are examined. Understanding the breakdown process of the intestinal wall may help in the design and implementation of new interventions against escape of luminal contents into the peritoneum during intestinal ischemia.

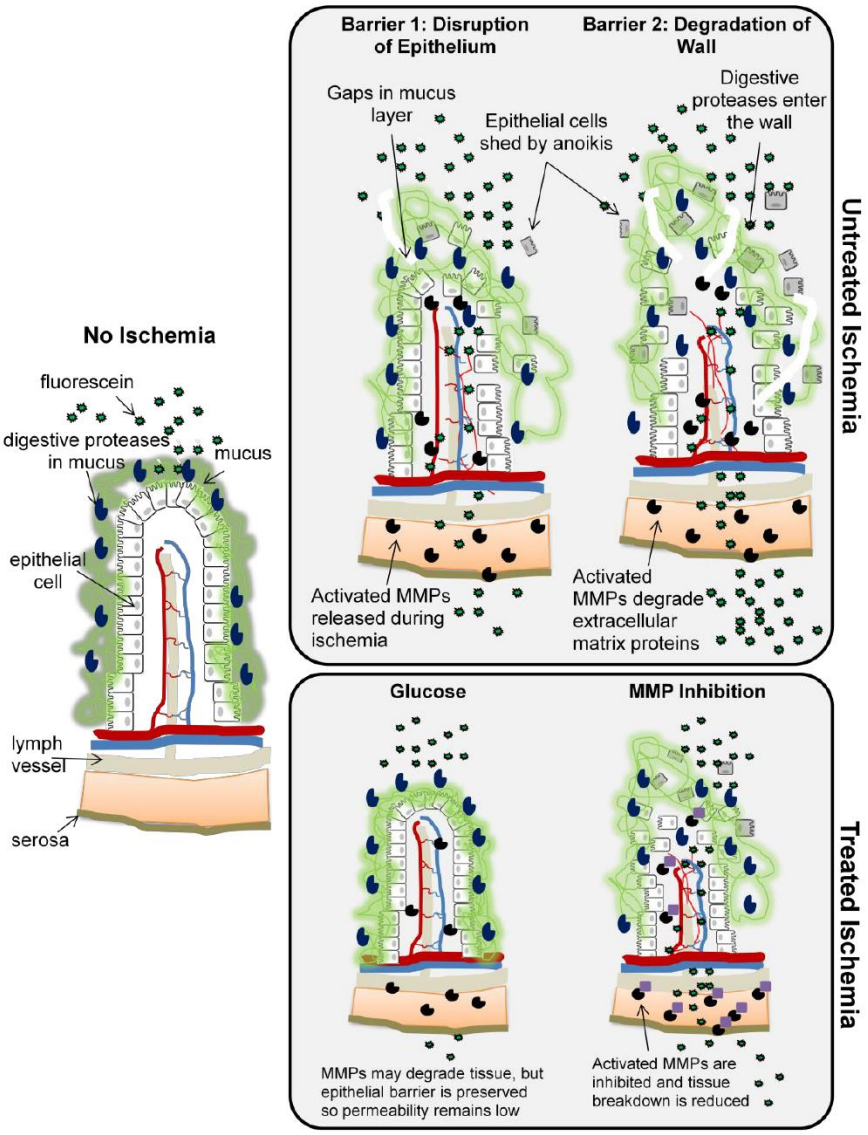

Figure 2.1 Hypothesis summary for intestinal wall breakdown during iscehmia. In a vascularized non-ischemic intestine, the epithelium is intact and is the primary barrier preventing transmural fluorescein penetration. During ishemia with no intervention, the epithelial barrier breaks down and the cells shed into the lumen by anoikis (grey epithelial cells) (Barrier 1). Activated MMPs released during ischemia create gaps large enough for fluorescein transport in the wall (Barrier 2). Disruption of the primary barrier allows fluorescein to penetrate past the muscularis and serosa. Serine proteases found in the mucus layer also may degrade the internal structure of the villi. If nutritional support in administered to the lumen as a source of ATP from glucose metabolism to the epithelial cells, the epithelial barrier remains intact (Glucose). Alternatively, MMP inhibition prevents degradation of the tissue past the epithelial barrier so that fluorescein penetrates to the abluminal side (MMP Inhibition).

2.3 METHODS

2.3.1 ANIMALS

The animal protocol was reviewed and approved by the University of California, San Diego Institutional Animal Care and Use Committee. Male Wistar rats (body weight between 250-400 g, Harlan, Indianapolis, IN) were allowed food and water *ad libitum* prior to surgery. Rats were administered general anesthesia (xylazine, 4 mg/kg; ketamine 75 mg/kg IM) and euthanized with B-Euthanasia (120 mg/kg).

2.3.1.1 INTESTINAL ISCHEMIA

Since intestinal properties are non-homogenous, the transmural permeability over the entire length of the jejunum and ileum was investigated. Due to physical constraints of the small intestine anatomy, it is not feasible to simultaneously analyze permeability from multiple segments in-vivo. Therefore, an ex-vivo approach was designed to measure permeability along the entire length of the small intestine.

A midline incision was made to expose the intestine. The proximal end of the jejunum (approximately 5 cm distal from the ligament of Treitz) was cannulated with a female luer to barb tube connector (1/8" inner diameter). The intestine was removed and placed in saline immediately before euthanasia. The lumen of the intestine was flushed with 40 ml saline using pulsatile pressure. Removal of all solid content was verified by visual inspection. Next, the intestine was cut into eight equal length segments (~8 cm)

sequentially ordered from the proximal jejunum (position 1) to the distal ileum (position 8). Both ends of each segment were cannulated with Female Luer to Barb tube connectors (thus allowing entry and exit points from the intestinal lumen to be sealed completely), secured with 4-0 suture, and the exterior portion of one adaptor on each segment sealed with clay.

To determine the permeability of the intestine, all 8 segments from one animal were filled with fluorescein (332 Daltons, 20 µg/ml from 5 mg/ml stock in ethanol; Sigma-Aldrich, St. Louis, MO) as small molecular weight tracer mixed with saline, glucose (100 mg/ml in saline; Sigma-Aldrich), the non-metabolizing glucose analog mannitol (100 mg/ml in saline) the broad-spectrum protease and lipase inhibitor ANGD (2 mg/ml in 100 mg/ml D-glucose in saline; *nafamostat mesilate*, Torii Pharmaceutical, Chiba, Japan), the lipase inhibitor orlistat (0.25 mg/ml in saline from 100 mg/ml stock in ethanol; Sigma-Aldrich), the serine protease inhibitor aprotinin (Trasylol, $1x10^4$ kallikrein inhibitor units/ml; Bayer Health Care, Pittsburgh, PA), the serine protease inhibitor tranexamic acid (31 mg/ml in saline; Sigma-Aldrich), the MMP inhibitor doxycycline hyclate [27] (1 mg/ml in saline; Sigma-Aldrich), or the MMP inhibitor GM 6001 [28] (1 µg/ml in saline from 1 mg/ml stock in DMSO, Millipore, Billerica, MD). These inhibitors were chosen because enteral tranexamic acid, ANGD+glucose, and aprotinin+orlistat have previously been shown to mitigate mortality after experimental shock [6,10,12,15,21,29]. Whether these improvements were from the effects of the inhibitors on luminal content or from maintaining the intestinal barrier needed to be determined.

Table 2.1 Molarity and osmolarity of enteral solutions.

	Concentration (moles/L)	Total Osmolarity (osm/L)
Saline	0.154	0.308
Glucose	0.555	0.863
Mannitol	0.555	0.863
ANGD+Glucose	$3.7x10^{-3}$	0.867
Orlistat	$5x10^{-4}$	0.308
Aprotinin	$1x10^{4}$ (kallikrein inhibitor units/ml)	0.308
Orlistat+Aprotinin	$5x10^{-4}/1x10^{4}$ (kallikrein inhibitor units/ml)	0.308
Tranexamic Acid	0.200	0.508
Doxycycline	$1.95x10^{-3}$	0.310
GM 6001	$2.57x10^{-6}$	0.308
Tranexamic Acid+Glucose	0.200/0.555	1.063
GM 6001+Glucose	$2.57x10^{-6}$/0.555	0.863

Table 2.2 Inhibitor molecular weight and target enzymes.

	Molecular Weight (Da)	Trypsin Inhibitor	Chymotrypsin Inhibitor	Elastase Inhibitor	Lipase Inhibitor	MMP Inhibitor
ANGD	542	yes	yes	yes	yes	no
Orlistat	498	no	no	no	yes	no
Aprotinin	6540	yes	yes	yes	no	no
Tranexamic Acid	158	weak	no	no	no	Yes and inhibits plasmin, an MMP activator
Doxycycline	444	no	no	no	no	yes
GM 6001	388	no	no	no	no	yes

300 µl of sample were added to each intestinal segment (not enough to fully inflate the intestinal tissue) through the open tubing adaptor before sealing with clay. Sealed segments were rinsed in saline, individually placed in 15 ml conical tubes containing 6 ml saline, and incubated at 37 ºC for 2 hours. The exterior solution for each position was sampled at 0, 30, 60, 90, and 120 minutes and loaded in duplicate (75 µl/well) into a 96 well plate (black-sided flat bottom polystyrene, Corning, New York, NY). Plates were read in a plate reader (FilterMax F-5 Multi-mode, Molecular Devices, Sunnyvale, CA) for concentration of fluorescein (excitation 494/emission 521) to quantify leakage across the wall of the intestine.

After the two-hour incubation, intestinal pieces from segments 2 and 7 were embedded in O.C.T. (Tissue Tek, Torrance, CA) and snap frozen in t-methyl butane in

liquid nitrogen. Tissue pieces from segments 5 (for enzyme analysis) and segment 7 (for immunoblots) were snap frozen and stored for subsequent homogenization.

The small intestines of a separate group of animals were used as *Pre-Ischemic Controls* for morphology and the corresponding regions of tissue were embedded in O.C.T. and frozen. As a non-ischemic control for permeability, a segment of distal ileum (approximating segment 7 which had the greatest permeability in the ex-vivo ischemic case) from a separate group of animals was cannulated, flushed, filled with saline with fluorescent markers as described above, and immersed in a small saline bath, but the blood supply to the segment was left intact. The animals were maintained under general anesthesia for 2 hours and the samples of exterior fluid from the saline bath were measured and adjusted for the volume dilution of the bath.

2.3.2 Permeability Analysis

To determine the fluorescein transport across the intestinal wall, the velocity at time 0 was subtracted from velocity values at later time points to correct for background, and fluorescence values were corrected to account for the volume reduction due to sampling during the experiment. The relative fluorescent unit (RFU) measurements were converted to equivalent moles by using the linear relationship between concentration and fluorescein fluorescence (not shown, R^2=0.999). The transport of fluorescein across the wall (measured in moles, per time) was calculated as the change in fluorescence over a 30 min interval divided by 30 min. Individual positions were excluded if the fluorescence measured at time 0 exceeded a pre-selected threshold, suggesting a torn specimen or a

specimen with improperly sealed ends (this occurred 9 times out of a total of 408 intestinal segments).

2.3.3 Morphological Analysis and TUNEL Labeling

Intestinal segments frozen in O.C.T. were cut into 5 µm sections. Sections were fixed using ice-cold methanol (8 min at -20 ºC) and immediately washed four times in distilled water. Nuclei were stained by incubating sections in freshly mixed Weigert's Iron Hematoxylin A and B (Electron Microscopy Science, Hatfield, PA) (10 min) followed by rinsing thoroughly with water. Collagen fibers were labeled by incubating (2 min) in Van Gieson's Solution (Electron Microscopy Science).

To assess the level of apoptosis after ischemia, in-situ terminal transferase dUTP nick end labeling (TUNEL) labeling was completed using a kit (Trevigen, Gaithersburg, MD) according to manufacturer's instructions. Sections were counterstained with 0.05% toluidine blue in 1% boric acid to contrast 3,3'-diaminobenzidine **(**DAB) positive nuclei (brown) from negatively stained nuclei (blue).

Prior to mounting, all slides were dehydrated (70, 95, 100% ethanol) and cleaned with xylene. After air-drying overnight, sections were mounted using Hard Set Mounting Media (Vector Laboratories, Burlingame, CA). Digital images were captured with a 20x objective (numerical aperture 0.5) and digitally montaged together after background subtraction.

2.3.4 Enzyme Activity

To examine protease activation in ischemic intestines, I used plate zymography with a casein substrate as well as gel zymography with gelatin or casein substrates. Segments of intestine were homogenized (0.1 g tissue/ml homogenization buffer; PBS pH 7.4 with 0.5% hexadecyltrimethyl bromide) and centrifuged at $1.4x10^4$ g for 20 minutes. Supernatants were stored at -80 ºC until samples were processed.

2.3.4.1 Casein Plate Zymography

Small amounts of pancreatic digestive enzymes are potentially present in the intestinal wall under physiological conditions (15). Therefore, to determine the *in-vitro* capabilities of each inhibitor, we combined pure trypsin (100 µg/ml), chymotrypsin (1 mg/ml), elastase (1 mg/ml), or lipase (1 mg/ml) with ANGD, orlistat, aprotinin, or tranexamic acid in the same concentrations used in the intestinal lumen and evaluated protease activity using the casein substrate (Enzchek, Invitrogen, Carlsbad, CA) for protease activity (180 µl substrate with 20 µl sample for 1 hour; Ex/Em: 589/617 nm) or C-POM (Invitrogen) hydrolysis for lipase activity (150 mM C-POM mixed 2:1 with sample for 2 hours; Ex/Em: 360/460 nm). Results are presented as the percent inhibition relative to the caseinolytic or lipase activity of pure enzymes.

To determine the total protease activity of the flushed intestine including the effects of any inhibitors (native or exogenous) that might be present in the tissue or lumen, 20 µg of intestinal homogenate protein (determined by the BCA protein assay kit;

ThermoScientific, Waltham, MA) were diluted to a total volume of 20 µl and loaded in duplicate. Either 180 µl of casein substrate or a known concentration of the substrate's fluorophore, Texas Red, in assay buffer (to correct for auto-fluorescence or fluorescence absorbance by the sample) was added to the samples. Fluorescence was measured at 0 and 120 min of incubation at 37 ºC and is expressed as: Normalized Activity = $(F_{Sample+Casein@120})*(F_{Tx+Buffer@0}/F_{Tx+Sample@0})$.

2.3.4.2 GELATIN AND CASEIN GEL ZYMOGRAPHY

To assess the proteolytic activities of individual proteases in intestinal tissue samples, sample volumes of 1 µl (with 2 µg of protein) or 8 µl (with 16 µg total protein) were separated by gel electrophoresis in SDS-PAGE gels containing 80 µg/ml gelatin or 100 µg/ml casein, respectively. Gels were renatured by four 15 min washes with 2.5% Triton X-100 and incubated overnight at 37 ºC in developing buffer (0.05 M Tris base, 0.2 M NaCl, 4 µM $ZnCl_2$, 5 mM $CaCl_2 \cdot 2H_2O$). After incubation, gels were fixed and stained (50% methanol, 10% acetic acid, 40% water, and 0.25% Coomassie blue solution) for three hours before destaining in water. The molecular weights of the proteases were estimated by use of a standard protein ladder (Invitrogen). Gels were digitized and bands were analyzed by densitometry in ImageJ (http://rsbweb.nih.gov/ij/)). Gel zymography activates the zymogen forms of MMPs, and thus both the pro- and active bands are visible.

2.3.4 IMMUNOBLOTTING

To determine whether select epithelial barrier proteins were degraded during ischemia, we analyzed pre- and post-ischemic tissue homogenates for relative levels of mucin 13, claudin-1, occludin, and E-cadherin.

Tissues were homogenized for immunoblot analysis in buffer (CelLytic, Sigma-Aldrich) with protease inhibitor cocktail (HALT, Thermo Scientific, 1:100 dilution) and centrifuged ($1x10^4$ g, 20 min). To separate proteins by gel electrophoresis, 30 µg of protein/well were loaded in 8 or 12% resolving gels with 4% stacking gels and transferred to nitrocellulose membranes (Bio-Rad, Hercules, CA). Membranes were blocked for one hour with either 5% bovine serum albumin (BSA) or 5% nonfat milk in tris-buffered saline with 0.5% Tween-20 (TBS-T). Primary antibodies diluted in 1% BSA or 1% nonfat milk against mucin 13 (1:1000, extracellular domain, sc-66973 Santa Cruz Biotechnology, Santa Cruz, CA), E-cadherin (1:1000, intracellular domain, 33-4000, Invitrogen), claudin-1 (1:1000, intracellular domain, 51-9000, Invitrogen), occludin (1:1000, intracellular domain, 33-1500, Invitrogen), pancreatic trypsin (1:1000, sc-137077 Santa Cruz Biotechnology), or β-actin (1:1000, sc-130301, Santa Cruz Biotechnology) were incubated overnight at 4 ºC. After incubation, membranes were washed with TBS-T (3x, 10 min) before addition of goat anti-rabbit or rabbit anti-mouse secondary antibodies (Santa Cruz Biotechnology) diluted 1:000 in TBS-T. Following secondary antibody incubation (60 min), the membranes were washed with TBS-T (3x) and developed.

2.3.5 Statistical Analysis

Results are presented as mean ± standard error of mean (N=6/group) for figure clarity. Two factor ANOVA was used to compare between positions (1-8) over time within each treatment group followed by Tukey post hoc test analysis to compare each position over time and each position to position 2 (which typically showed the least permeability). To compare the saline group to the treatment groups, the data were fit with polynomial equations (third order polynomials gave the best data representation). Inhibitors' equations were compared to saline's equation by the F-test. Single factor ANOVA analysis followed by Tukey post hoc test was used for protease activity measurements and immunoblot comparisons. Statistical analysis was performed using OriginLabs software (Northampton, MA).

2.4 Results

2.4.1 Intestinal Permeability and Morphology

In the in-vivo non-ischemic control intestines, there was negligible fluorescein transport across the intestinal ileum into the ambient saline bath compared to the corresponding position subject to total ischemia (Table 2.3). However, the intestine absorbed saline from the bath, making reservoir convection a potential confounding factor. In contrast, during ischemia, fluorescein transport across the intestinal wall was positive with increasing fluorescence at all locations along the intestine for every group

and time interval (Figure 2.1A). The average fluorescein transport from ischemic intestines increased with position along the length of the intestine from the jejunum to the ileum (except for position 1 at the proximal jejunum which generally had a higher transport than position 2) (Figure 2.2A and 2.3A).

Table 2.3 Rate of outward fluorescein* penetration through the intestine wall.

	0-30 Min	90-120 Min
No Ischemia	0.119±0.004	-0.053±0.065
Ischemia	1.255±0.236*	4.883±0.360**

*Fluorescein transport (nmol/min) across the wall of the intestine (distal ileum, equivalent to position 7) filled with saline after 2 hours. N=3 rats/group for No Ischemia group and N=6 rats/group for the Ischemia group.

Glucose administration into the lumen of the intestine drastically reduced the fluorescein transport across the wall of the intestine (Figure 2.2A). Ischemic conditions in the presence of saline resulted in a major destruction of the intestinal villi and wall both in the jejunum and the ileum that was attenuated in the presence of glucose (Figure 2.3B).

Multiple serine and lipase inhibitors were tested that had previously been shown to improve shock outcome [6,10,21,30-32]. Ischemic intestines containing ANGD+glucose maintained low transmural permeability and had intact villi after 2 hours of ischemia, similar to glucose alone (Figure 2.2B). Tranexamic acid reduced fluorescein transport over a period of about 90 min. Orlistat and aprotinin alone or in combination did not reduce the fluorescein transport across the intestinal wall. After 2 hours of

ischemia, the villi structures in both the jejunum and ileum were notably disrupted with all inhibitor treatments, except ANGD+glucose (Figure 2.3B). Direct comparison of the fluorescein transport between saline, ANGD+glucose, and glucose groups showed that the ANGD+glucose and glucose groups had a significantly decreased rate of transmural fluorescein transport compared to saline (Figure 2.4). Despite the low transmural permeability of the glucose and ANGD+glucose groups, evidence of internal degradation beneath the epithelial layer was visible in the jejunum regions after ischemia in both groups (Figure 2.3B and Figure 2.4B), suggesting that this separation of epithelium from the lamina propria was not mediated by pancreatic serine proteases or lipase activity.

To confirm the beneficial effects of the metabolic and proteolytic enteral treatments were not a consequence of increased osmolarity of the solution, mannitol, a non-metabolizable monosaccharide, was substituted for glucose and neither prevented fluorescein penetration nor preserved villi structure (Figure 2.5A) [26,33], though its maximum permeability at the 90-120 time point was improved compared to saline (equivalent to saline's 30-60 minute time point (Figure 2.4)). Additionally, the structure of the villi was substantially degraded similar to other interventions that showed an increase in permeability by the two hour time point (Figure 2.2 and Figure 2.3).

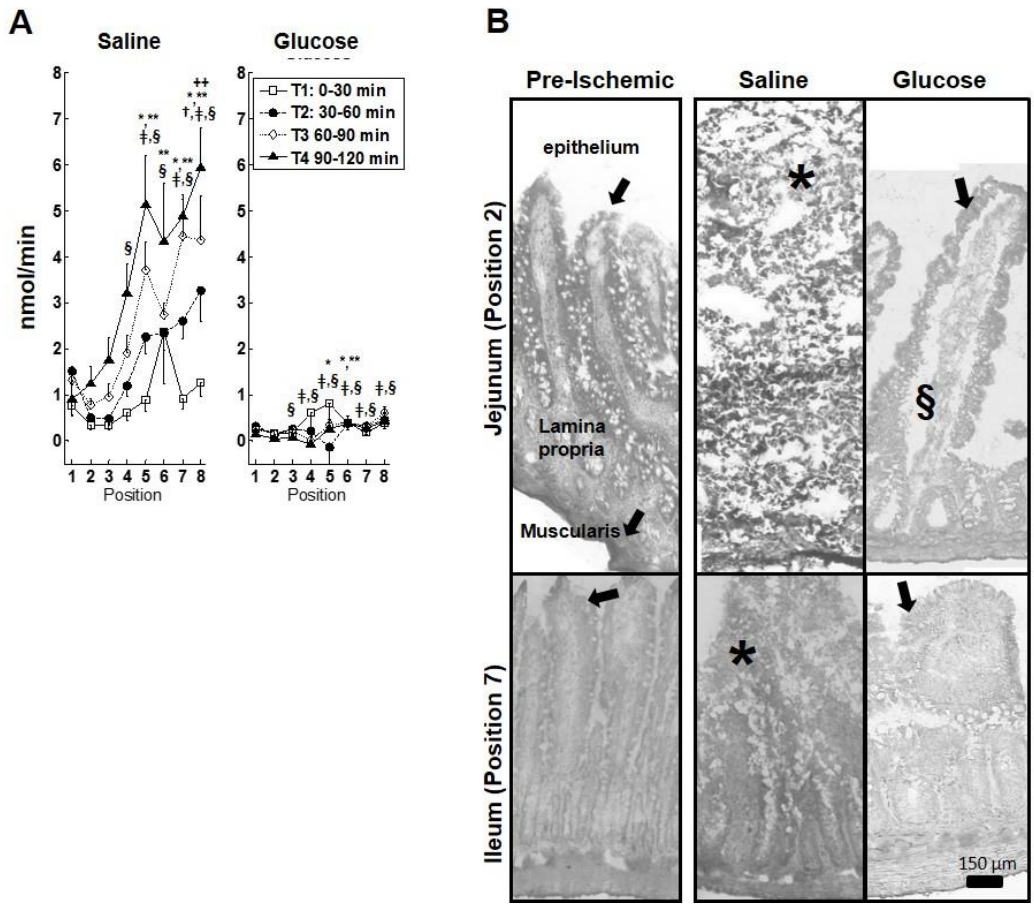

Figure 2.2 Fluorescein transport in saline and glucose treated ischemic intestines. (A) Fluorescent tracer rates (computed as amount of nanomoles of fluorescein penetrating the outside the intestinal wall over 30 min time intervals) across the wall of ischemic intestinal segments along the length of the small intestine from the proximal jejunum (position 1) to the distal ileum (position 8). The intestinal segments were enterally filled with saline or glucose. $p<0.05$ by two way ANOVA followed by Tukey post hoc analysis compared to Position 2 marked by ++ (during time interval T2), * (T3), ** (T4). $p<0.05$ by Tukey post hoc analysis compared to T1 shown by † (T2), ǂ (T3) and § (T4). N=6 rats/group for saline and N=5 rats/group for glucose. (B) Intestinal wall morphology in the jejunum (top) and ileum (bottom) as seen on frozen sections after Van Gieson and hematoxylin labeling. Arrows indicate intact villi structure that best matched the structure of the pre-ischemic tissue and (*) indicates a sites of damaged villi, and (§) specifies internal damage to the villi.

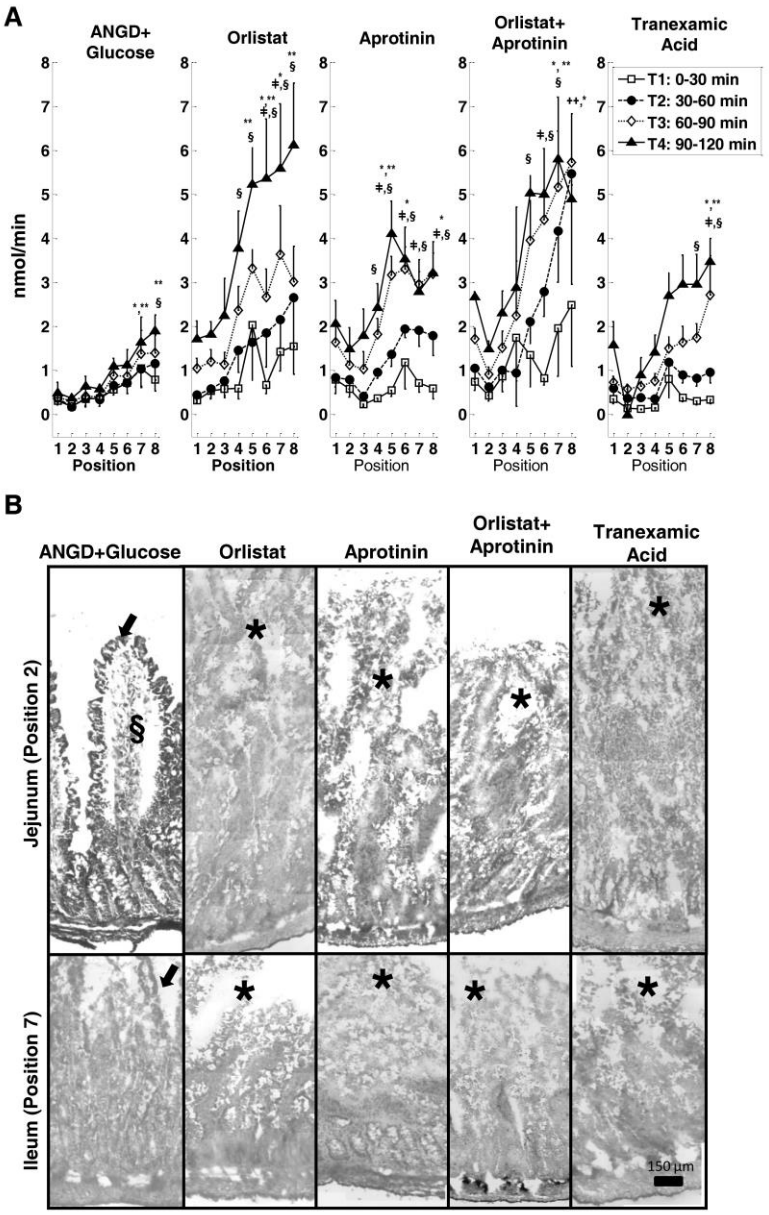

Figure 2.3 Fluorescein transport with serine protease or lipase inhibition. (A) Fluorescent tracer rates across the wall of ischemic intestinal segments filled with ANGD+glucose, orlistat, aprotinin, orlistat+aprotinin, and tranexamic acid. $p<0.05$ by Tukey post hoc test compared to Position 2 shown by ++ (during time interval T2), * (T3), ** (T4). $p<0.05$ by two way ANOVA followed by Tukey post hoc test in compared to T1 shown by ǂ (during T3) and § (during T4). N=6 rats/group except for orlistat+aprotinin groups where N=3 rats/group. (B) Representative micrographs of intestinal villi after ischemia. Arrows indicate intact villi structure that best matched the structure of the pre-ischemic tissue, (*) indicates a sites of damaged villi, and (§) specifies internal damage to the villi.

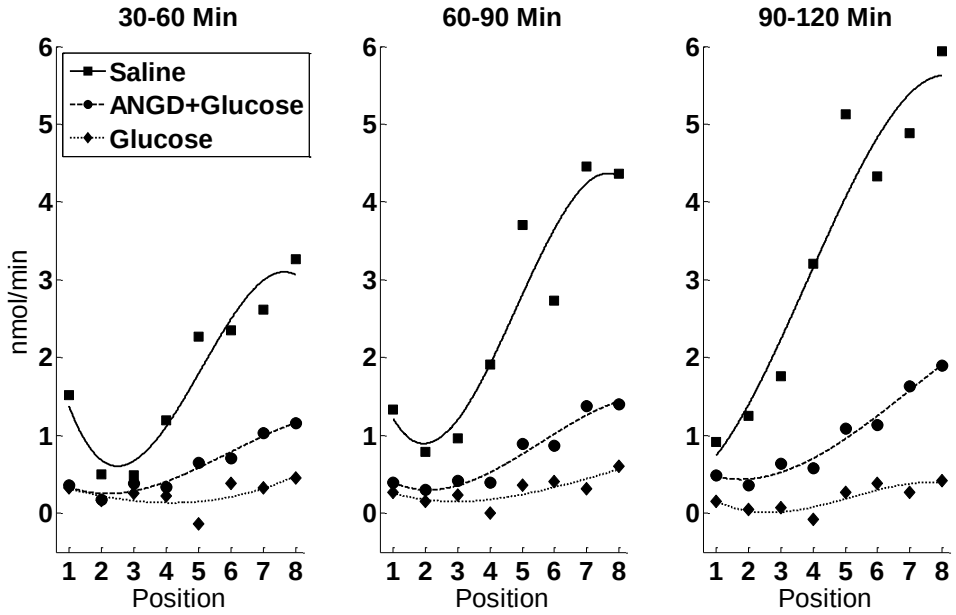

Figure 2.4 Comparison between glucose interventions with saline. Nanomoles/min of fluorescein penetration across the wall of the small intestine during ischemia as a function of the position along its position (see Figure 1 legend). Measurements points are fit (using a third order polynomial) for the cases of saline, ANGD+glucose, and glucose placed into the lumen of the intestine. Adjusted R^2 values are 0.87, 0.93, -0.02 for 30-60 min; 0.80, 0.90, and 0.46 for 60-90 min; 0.86, 0.94, 0.68 for 90-120 min for saline, ANGD+glucose, and glucose curves, respectively. Comparing best fit curves of ANGD+glucose or glucose to saline by F-test, $p=1.4\times10^{-4}$ and 3.19×10^{-5} for 30-60 min; $p=5\times10^{-4}$ and 9.8×10^{-5} for 60-90 min; $p=8.6\times10^{-4}$ and 1.1×10^{-5} for 90-120 min.

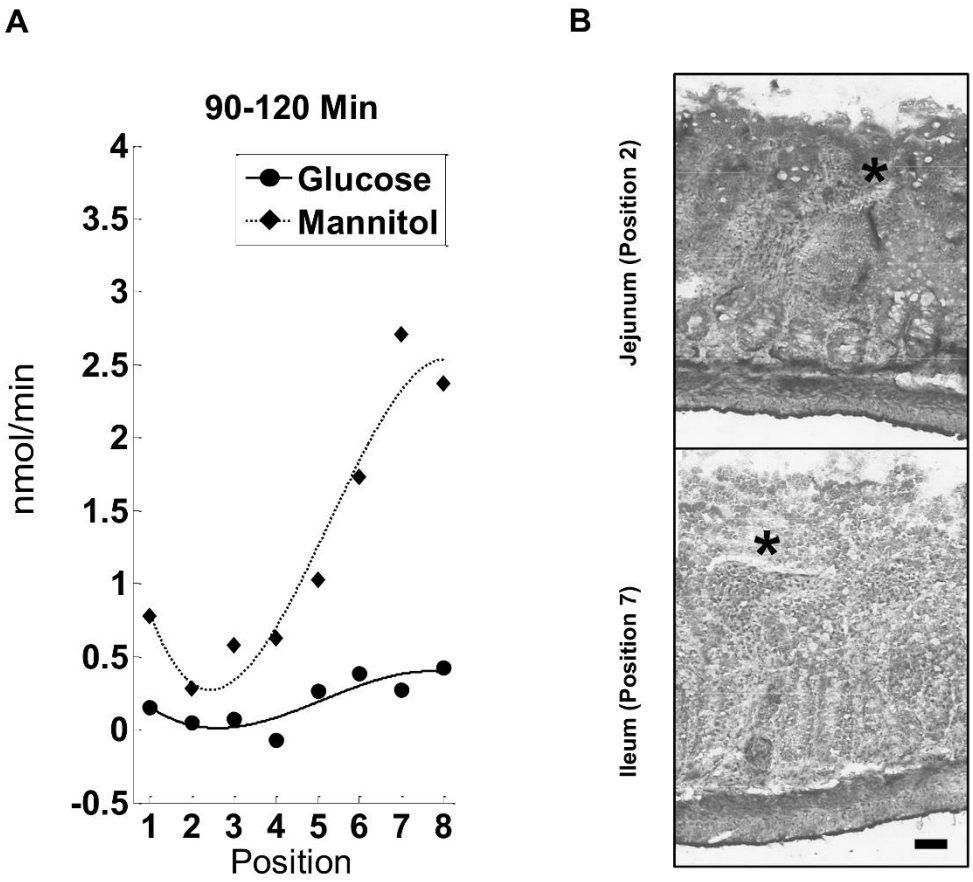

Figure 2.5 Comparison between glucose and mannitol interventions. (A) Nanomoles/min of fluorescein penetration across the wall of the small intestine at the 90-120 minute time during ischemia as a function of the position along its position (see Figure 2.3 legend). Measurements points are fit (using a third order polynomial) for the cases of glucose and mannitol placed into the lumen of the intestine. Adjusted R^2 values for glucose and mannitol are 0.68 and 0.91, respectively. The probability between the two curves is $p=3.8x10^{-5}$. (B) Representative micrographs of intestinal villi with mannitol after ischemia. Asterisks indicate destroyed villi structure that best matched the structure of the saline tissue (Figure 2.2).

2.4.2 PROTEASE ACTIVITY

At the concentrations used in our experiments, ANGD and aprotinin inhibited purified trypsin, chymotrypsin, and elastase (Table 2.4). ANGD, along with orlistat, inhibited lipase activity. Tranexamic acid, in contrast, had little effect on chymotrypsin, elastase, or lipase activity and blocked about a third of the trypsin activity compared to ANGD or aprotinin.

Table 2.4 Percent inhibition of casein proteolysis or C-POM hydrolysis*.

	Trypsin	Chymotrypsin	Elastase	Lipase
ANGD (542 Da)	88	84	82	43
Orlistat (498 Da)	7	8	-2	56
Aprotinin (6540 Da)	96	90	82	8
Tranexamic acid (158 Da)	30	0	1	14

*Percent inhibition of 0.1 mg/ml trypsin, 1 mg/ml lipase, chymotrypsin, or elastase with casein or C-POM substrates. Negative values indicate activation.

Caseinolytic activity values measured by plate zymography in homogenates of intestinal tissue segments with aprotinin or tranexamic acid in their lumen were reduced compared to the saline group (Figure 2.6). In contrast, ANGD+glucose did not significantly decrease caseinolytic activity suggesting that the protease activity in the ischemic intestine may not arise from serine proteases inhibited by ANGD (e.g. the pancreatic proteases). Pre-ischemic intestines exhibited higher activity than their ischemic saline counterparts (not significant).

The proteolytic activity profile between the jejunum and ileum differed drastically (Figure 2.7). Many of these proteases were eliminated or reduced by addition of ANGD (inhibits pancreatic enzymes and plasmin) or tranexamic acid to the renaturing and developing solutions (Figure 2.7), including a direct inhibition of MMPs by tranexamic acid that is not mentioned in most literature on the subject. Passage of material from the jejunum during flushing did not affect proteases in the ileum as there were no differences in protease activity bands in the ileum between intestines that were flushed from jejunum to ileum or intestines that had only the ileum (segment 7) flushed (not shown).

Gelatin and casein gel zymography revealed proteases in tissue homogenates, even in the pre-ischemic case, capable of cleaving both substrates (Figure 2.8A&B), including MMP-2, MMP-9 and bands associated with serine proteases. Aprotinin treatment significantly reduced total protease activity in both gelatin and casein gels (Figures 2.7A&B). Additionally, quantification of individual bands showed that aprotinin significantly reduced activity in a 50 kDa gelatinase and the 20 kDa serine proteases bands ($p<0.05$). The serine protease bands were also significantly decreased by ANGD+glucose and tranexamic acid ($p<0.05$). However, aprotinin, unlike the other

inhibitors, was able to irreversibly block serine proteases when applied to pure trypsin, chymotrypsin or elastase (Figure 2.8) despite electrophoretic separation, suggesting it could have bound irreversibly to proteases after homogenization as opposed to decreasing activity by preventing activation of enzymes.

Because our previous findings by immunohistochemistry and in-situ zymography show that a small amount of pancreatic-derived digestive enzymes are naturally present in the wall of the intestine (15), we measured trypsin levels by immunoblot analysis. Trypsin was detected in every sample; however, we saw no significant difference in trypsin levels measured between groups in segment 7 (Figure 2.9). As trypsin *levels* are not likely to change after removal of a segment of intestine from the body, this suggests that starting levels of trypsin adhered to intestinal tissue were also similar between groups, as would be expected.

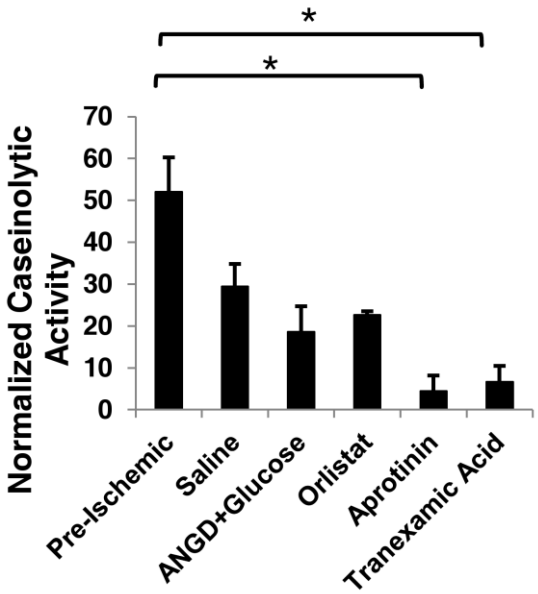

Figure 2.6 Caseinolytic activity of intestinal wall homogenates. Caseinolytic activity of intestinal homogenates wall from plate zymography of segment 5. N=10 for pre-ischemic group and N=6 for all other groups. *, $p<0.05$ by Tukey post hoc test.

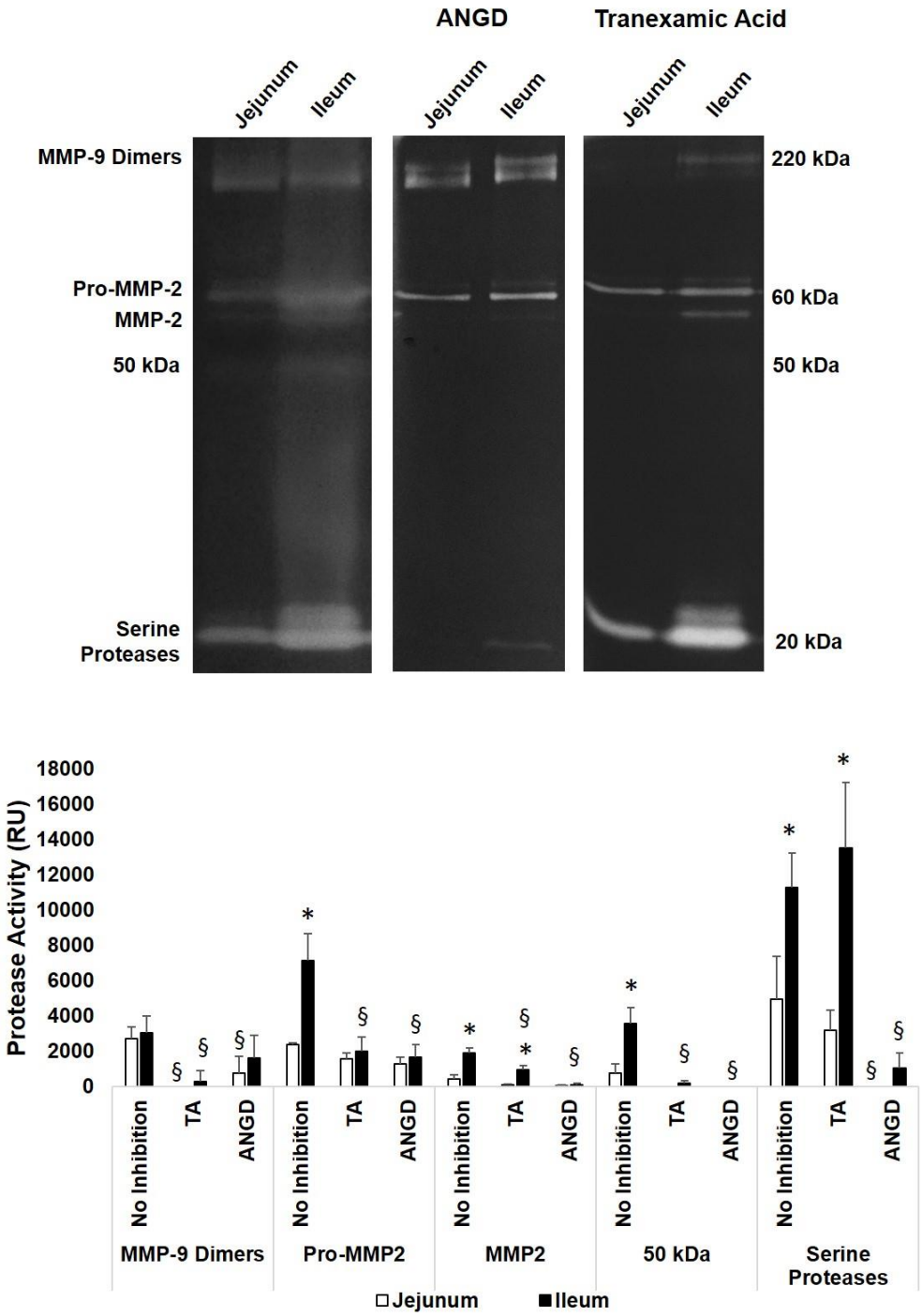

Figure 2.7 Jejunum compared to ileum protease activity. Protease activity in the jejunum (segment 2) and ileum (segment 7) had distinct bands for MMPs and serine proteases that were enhanced in the ileum. Renaturation with ANGD eradicated all serine protease bands at the bottom of the gel and reduced the prominent band at 50 kDa. *, $p<0.05$ by paired t-test compared to the jejunum. §, $p<0.01$ by t-test with Bonferroni correction compared to No Inhibition. N=4 rats/group.

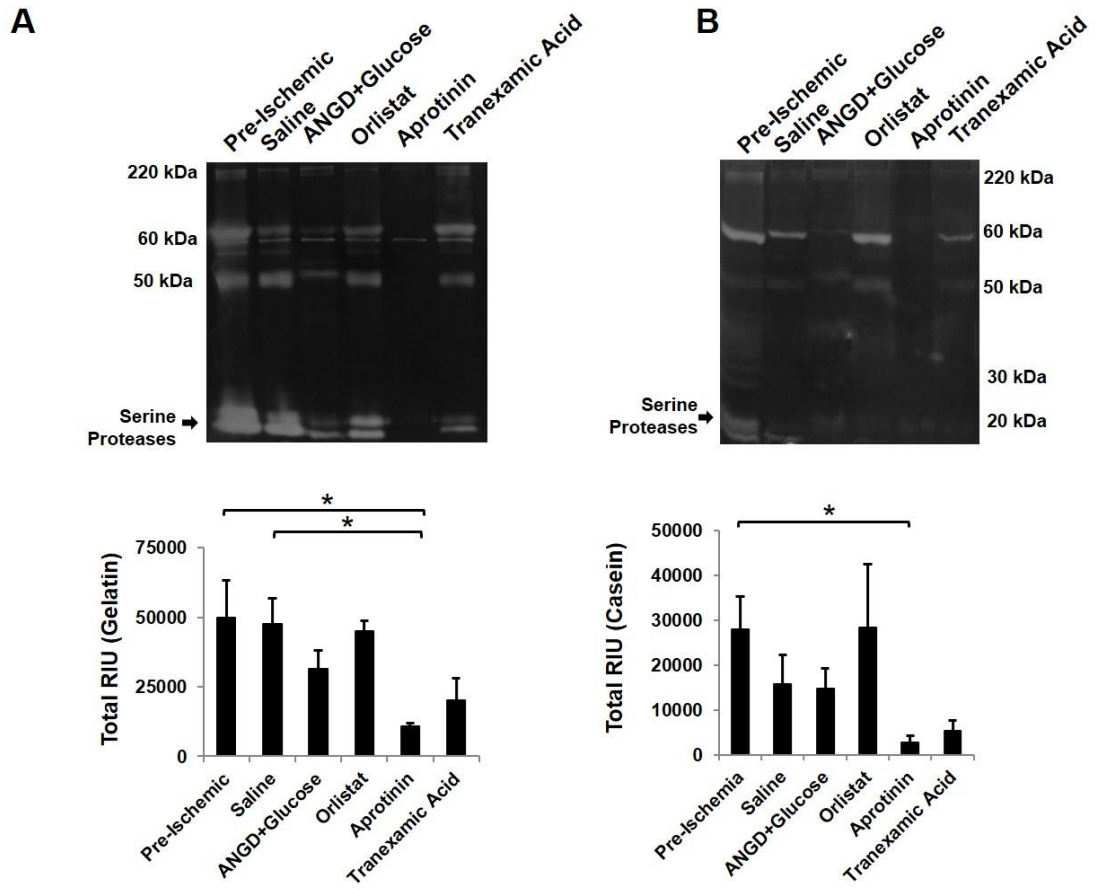

Figure 2.8 Gelatin and casein gel zymographies of intestinal wall homogenates. Representative images of gelatin (A) and casein (B) gel zymographies. (A&B Lower) Quantification of total activity in each lane by total area under the intensity curve reported in relative intensity units (RIU). N=5 rats/group for pre-ischemic group and N=6 rats/group for all other groups. * $p<0.05$ by Tukey post hoc test.

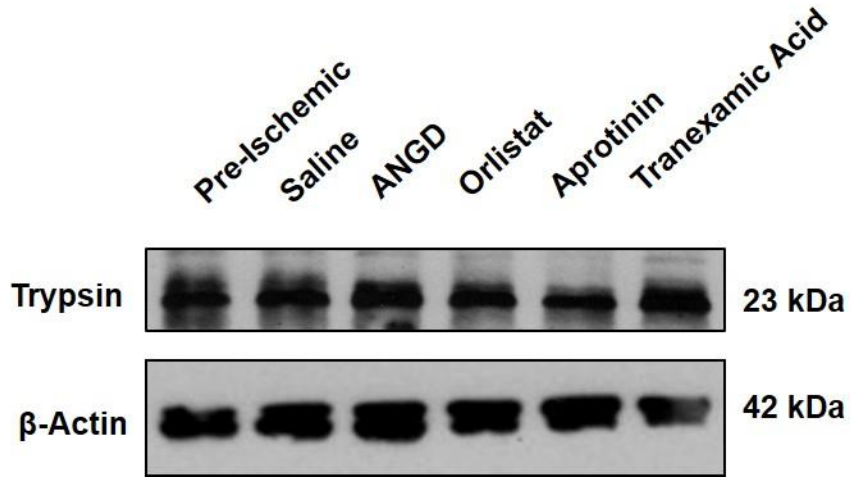

Figure 2.9 Pancreatic trypsin levels in the wall of a homogenized intestine. Pancreatic trypsin was detected in the homogenized wall of the flushed intestine by the femto ECL substrate.

2.4.3 MMP INHIBITION

Tranexamic acid reduced casein plate zymography protease activity and permeability, despite weak inhibition of pancreatic serine proteases. Since tranexamic acid inhibits plasmin, an MMP activator, and to some extent MMPs directly (Figure 2.7), we next investigated whether permeability increases through an MMP-derived mechanism.

Inhibition with the broad-spectrum MMP inhibitors doxycycline or GM 6001 prevented significant increases in fluorescein transport at early time points (Figure 2.10A). However, the villi in the jejunum and ileum were not intact after 2 hrs of ischemia (Figure 2.10B). The doxycycline and GM 6001 transport curves closely

matched the tranexamic acid curve in the 30-60 min and 60-90 min periods and were significantly decreased compared to the saline treated intestines (Figure 2.11). However, in the 90-120 min period, GM 6001 was more effective at reducing the transmural permeability compared to either doxycycline or tranexamic acid. Caseinolytic activity was not significantly decreased compared to pre-ischemic homogenates by doxycycline and GM 6001 (Figure 2.12).

The combination of tranexamic acid+glucose and GM 6001+glucose (Figure 2.13A) maintained low permeability throughout the two hour ischemic period and did not behave differently than glucose alone. Because of the glucose, the intestine villi also remained intact following ischemia (Figure 2.13B).

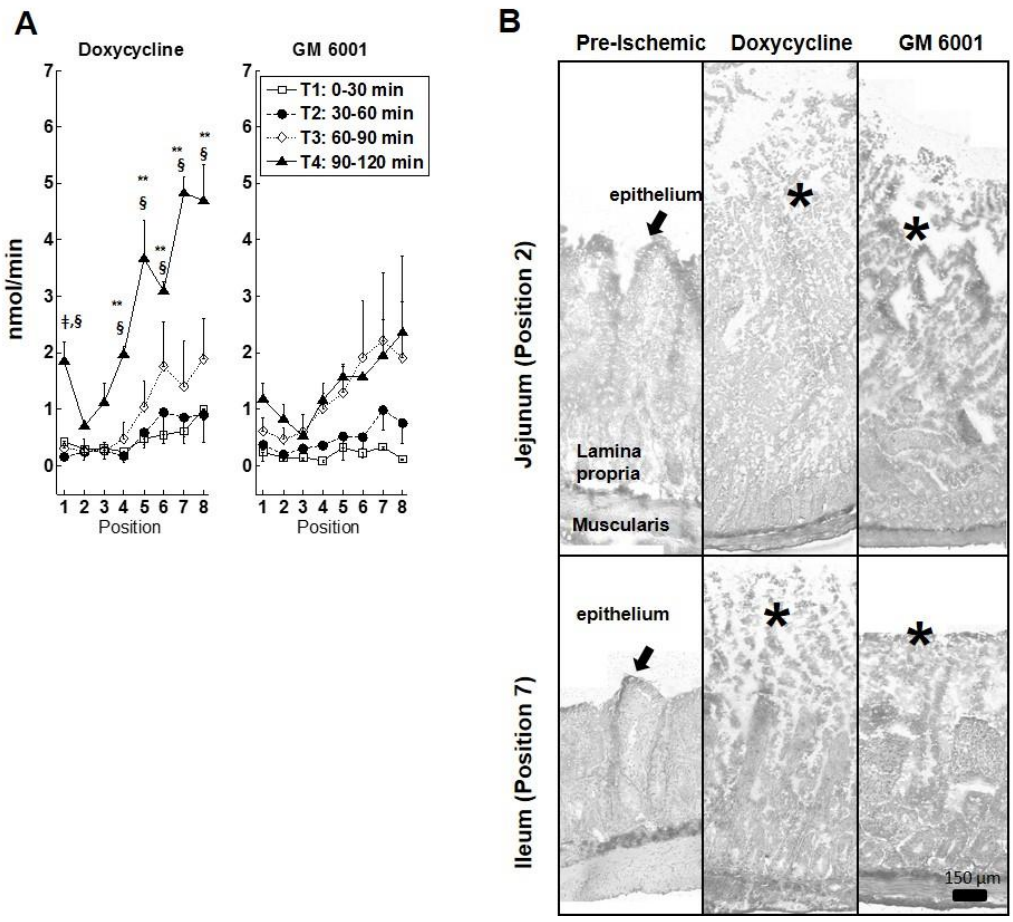

Figure 2.10 Fluorescein transport with MMP inhibition. (A) Fluorescein transport across the wall of ischemic intestinal segments filled with doxycycline and GM 6001. $p<0.05$ by Tukey post hoc test compared to Position 2 shown by ** (during T4). Significant changes ($p<0.05$ by Tukey post hoc test) compared to T1 shown by ǂ (T3) and § (T4). N=3 rats/group. (B) Representative images of the intestinal villi. Arrows indicate intact villi structure and (*) indicates a sites of damaged villi after ischemia.

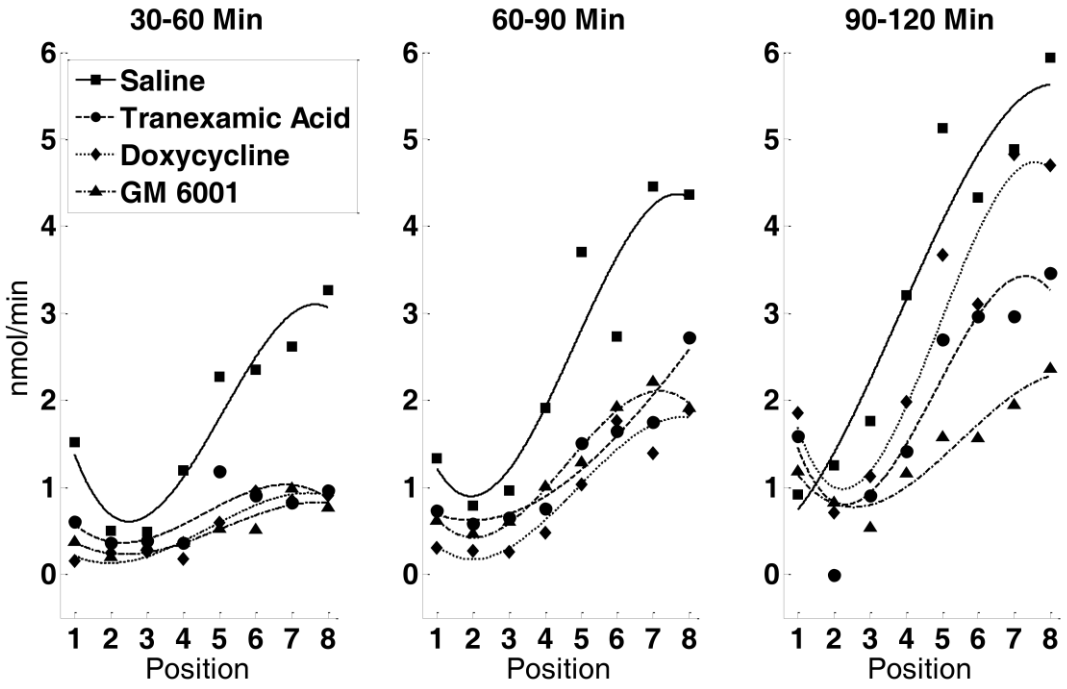

Figure 2.11 Comparison between MMP and tranexamic acid interventions. Comparison of fluorescein rate across the wall of ischemic intestines between doxycycline, GM 6001 and saline groups. Tranexamic acid is presented to demonstrate the similarities in permeability profile with the MMP specific inhibitors. Adjusted R^2 values are 0.87, 0.37, 0.81, and 0.71 for 30-60 min; 0.80, 0.89, 0.97, and 0.86 for 60-90 min; 0.86, 0.89, 0.86, and 0.86 for 90-120 min for saline, tranexamic acid, doxycycline and GM 6001 curves, respectively. Comparing best fit curves of doxycycline or GM 6001 to saline by F-test, $p=1.3\times10^{-4}$ and 9.1×10^{-5} for 30-60 min; $p=1.8\times10^{-3}$ and 4.3×10^{-3} for 60-90 min; non-significant and 2.8×10^{-4} for 90-120 min.

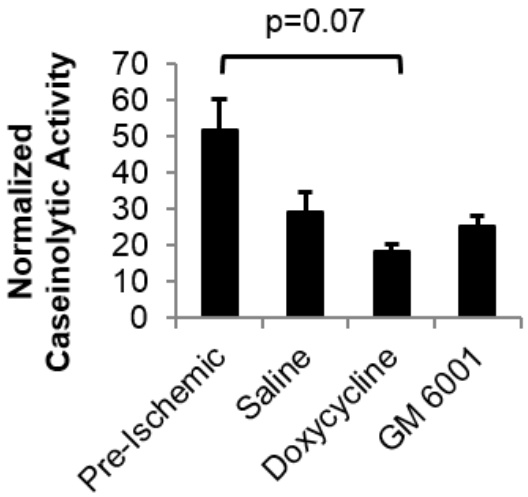

Figure 2.12 Caseionlytic activity of intestinal wall homogenates treated with MMP inhibitors. Caseinolytic activity in ischemic intestine homogenates. N=6/group for pre-ischemic; N=3/group for doxycycline and GM 6001.

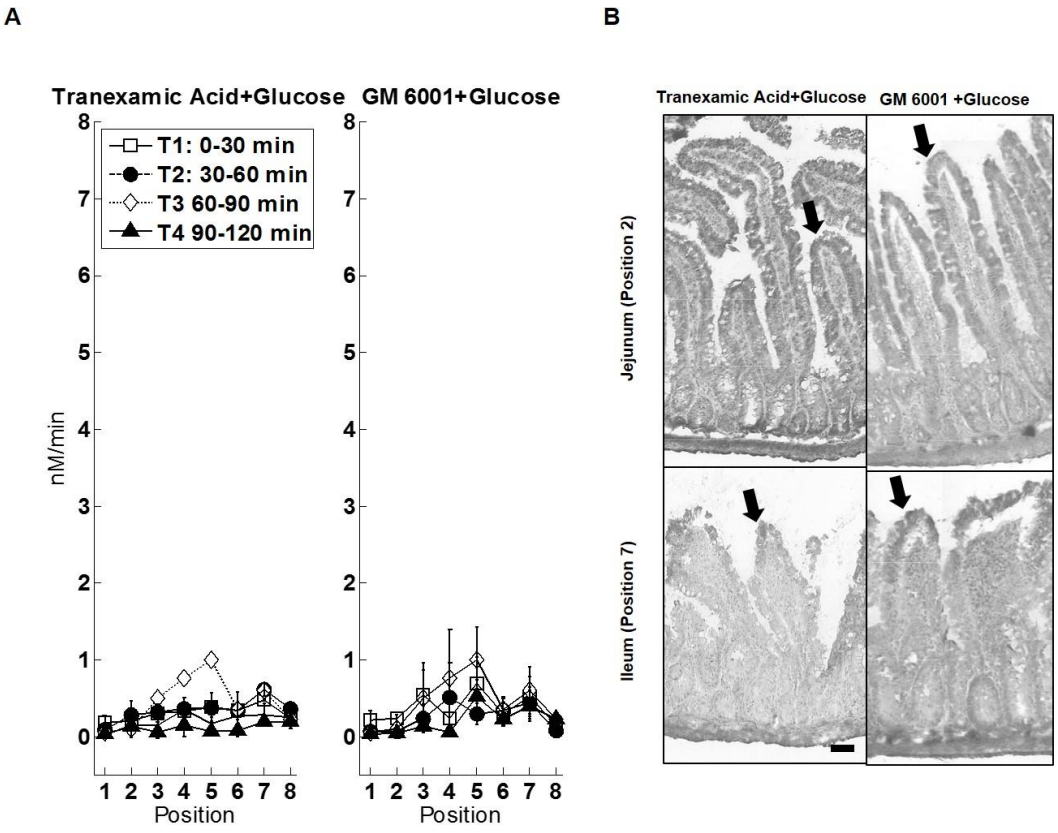

Figure 2.13 Fluorescein transport for tranexamic acid+glucose and GM 6001+glucose treatments. (A) Fluorescent tracer rates across the wall of ischemic intestinal segments filled with tranexamic acid+glucose or GM 6001+glucose. N=3 rats/group (B) Representative micrographs of intestinal villi with tranexamic acid+glucose or GM 6001+glucose after ischemia. Arrows indicate intact villi structure that best matched the structure of the pre-ischemic tissue (Figure 2.2).

2.4.4 APOPTOSIS

Pre-ischemic intestines had little apoptosis except near the tips of the villi (Figure 2.14) while saline-treated ischemic intestines showed extensive apoptosis in both cells in the villi and cells detached from the villi (nuclei are visible despite loss of villi structure). Enteral glucose treated intestines had little apoptosis in the villi, though TUNEL labeling similar to that in the saline group was present in the muscle layer (Figure 2.14).

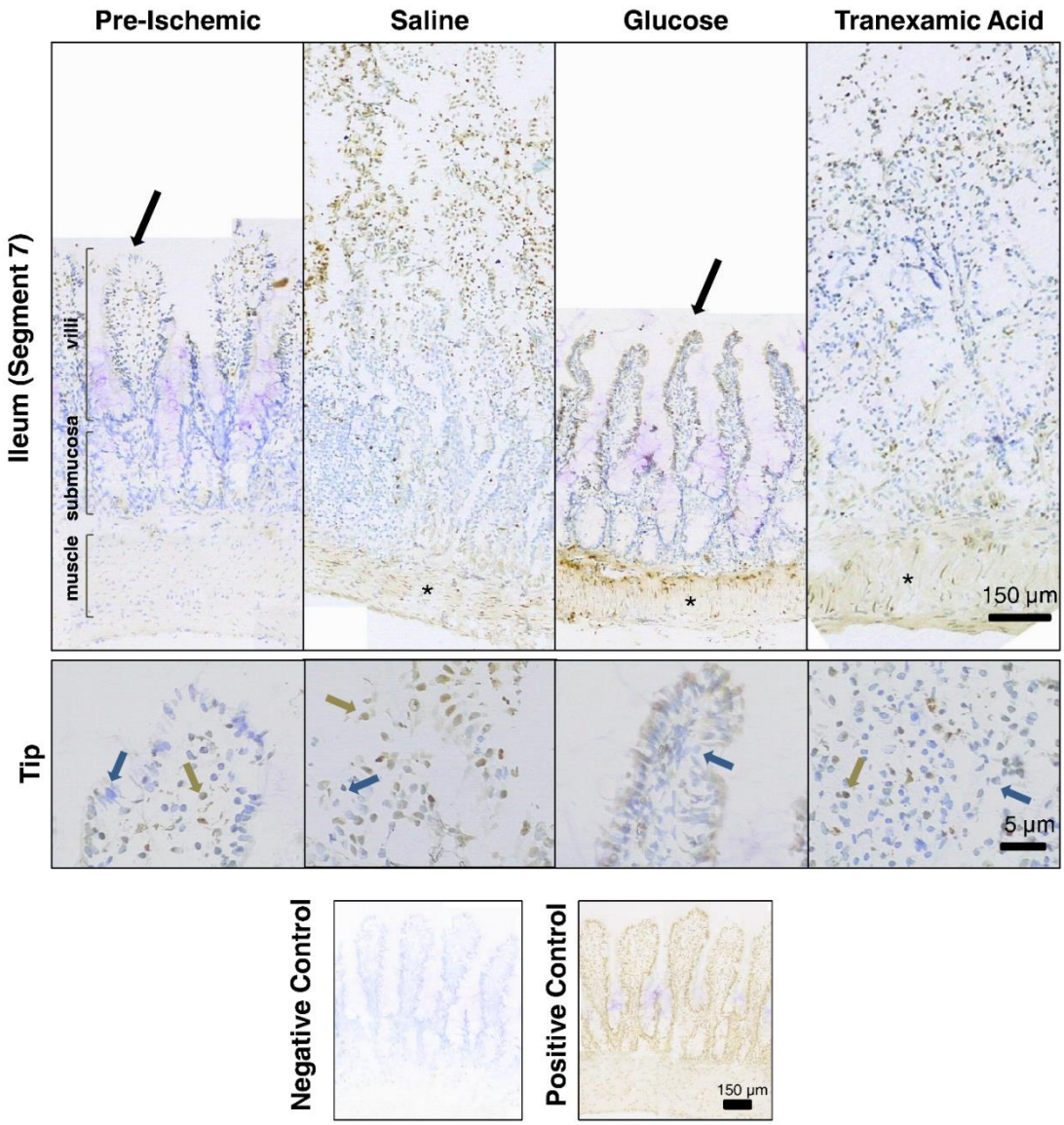

Figure 2.14 TUNEL labeling of intestinal segments. TUNEL labeling of pre-ischemic control intestines and the tips. Black arrows point to intact villi. **Brown** stained nuclei indicate positive TUNEL labeling while **blue** labeled nuclei indicate negative labeling as indicated by the brown and blue arrows respectively. * indicates muscle TUNEL positive cells.

2.4.5 Epithelial Barrier Proteins

To investigate the ability of protease inhibition to preserve barrier proteins after ischemia, we measured mucin 13 (the membrane-bound component of the mucin layer), occludin and claudin-1 (tight junction proteins), and E-cadherin (adheren junction protein), in intestinal homogenates before and after ischemia. Mucin 13 levels were decreased with saline, orlistat, and aprotinin treatments compared to pre-ischemic levels but were preserved significantly with glucose and tranexamic acid treated intestines (in 5 out of 6 tranexamic acid cases there was nearly complete preservation) compared to saline (Figure 2.15A&B). Mucin 13 levels in the ANGD+glucose group were not significantly reduced compared to the pre-ischemic group, but neither were they significantly elevated compared to saline. Occludin levels decreased in all cases except for glucose and tranexamic acid treatment groups (Figure 2.15A&B). E-cadherin levels decreased significantly after ischemia regardless of treatment (Figure 2.15A&B). In contrast, there was no significant change in claudin-1 protein levels from ischemia or inhibitor treatment (Figure 2.15B). The MMP inhibitors doxycycline and GM 6001 did not preserve mucin 13, occludin, or E-cadherin compared to saline-treated animals (Figure 2.15C).

Additionally, distinct patterns of mucin 13 fragmentation bands have been shown to form during ischemia in starved animals prior to SAO [6,29]. In contrast, in this study where food was not restricted from these animals prior to the experiments, the mucin 13 fragmentation patterns were completely random, even occurring consistently in pre-ischemic intestine segments (Figure 16). Fragmentation patterns varied greatly even

within each treatment, suggesting that the fragmentation may be related to the last time the animal ate rather than the unrelated to ischemia.

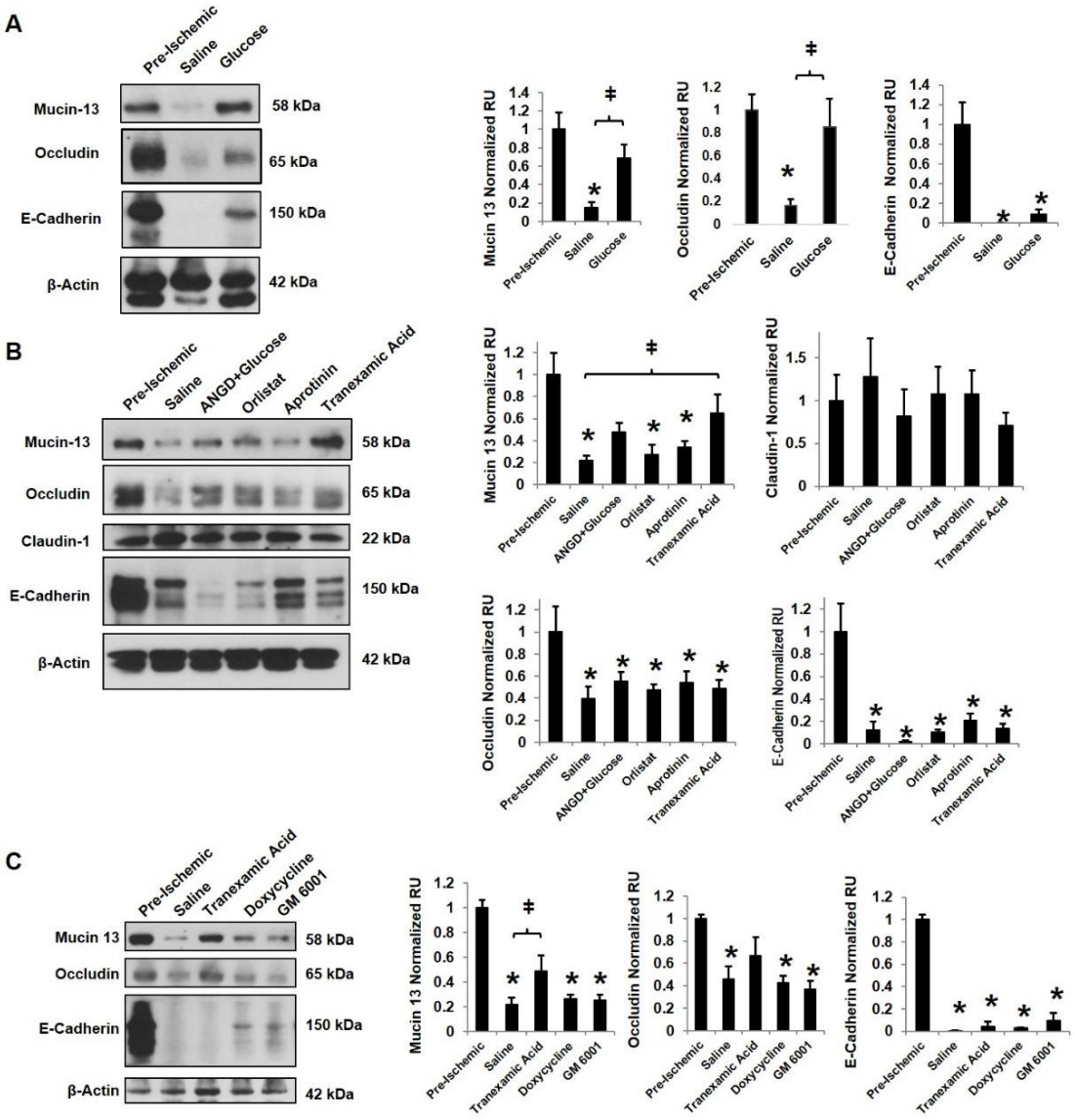

Figure 2.15 Immunoblots of epithelial proteins. (A) Immunoblots (left) and quantification (right) for mucin 13 and E-cadherin. N=4/group. There was a significant difference between groups by ANOVA for mucin 13 and E-cadherin. (B) Immunoblots and quantification for mucin 13, occludin, claudin-1, and E-cadherin. There was a significant difference between groups by ANOVA for mucin 13, E-cadherin, and occludin. N=4 for pre-ischemic groups, N=6 for all other groups. (C) Comparison of Doxycycline and GM 6001 treatments with pre-ischemic, saline and tranexamic acid groups for mucin 13, occludin, and E-cadherin. N=6/group for pre-ischemic control, saline, and Tranexamic acid and N=3/group for doxycycline and GM 6001. *, $p<0.05$ compared to pre-ischemic control and ǂ, $p<0.05$ compared to saline by Tukey post hoc analysis.

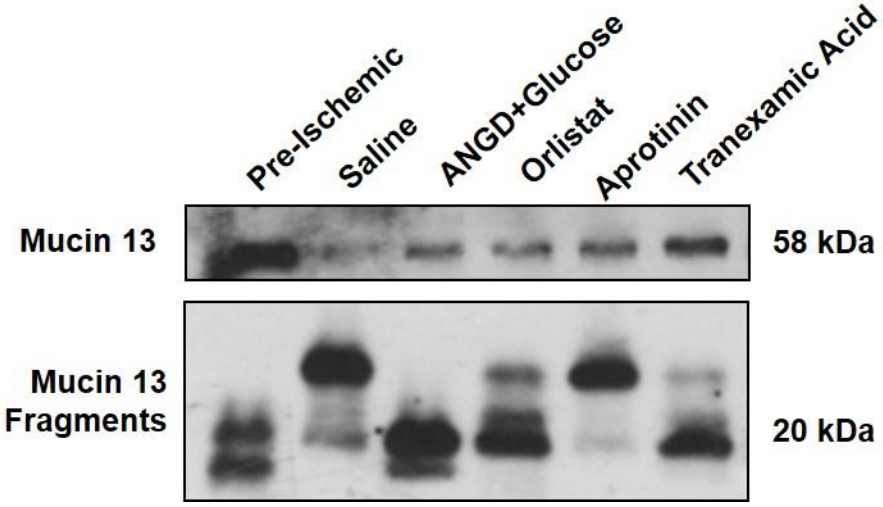

Figure 2.16 Mucin fragmentation. Mucin 13 fragmentation in the different groups did not demonstrate any pattern in the fragments formed both before and after ischemia.

2.5 DISCUSSION

2.5.1 SUMMARY

The current results indicate that the transmural transport of a low molecular weight tracer from the lumen across the rat intestinal wall was undetectable in a non-ischemic state but increases after ischemia in the absence of luminal contents. The permeability increased consistently from the jejunum to the ileum in all cases and may be a result of the increased protease activity in the ileum tissue. Placement of glucose into the lumen of the small intestine abrogated the permeability increase, reduced apoptosis, and served to maintain the epithelial barrier but not necessarily the underlying intestinal wall (Figure 2.2B, also reported by Derikx, et al.) [34]. In the absence of glucose, only the MMP inhibitors doxycycline and GM 6001 and the protease inhibitor tranexamic acid reduced the transmural permeability, but they did not prevent the villi destruction or apoptosis of the epithelium at 2 hrs. The evidence suggests that both the epithelium and the tissue under the epithelium act as barriers to the transmural passage of a low molecular weight tracer, though they appear to fail by different, though likely interdependent, mechanisms during severe intestinal ischemia (Figure 2.1).

2.5.2 Glucose Preserves the Epithelial Barrier by Preventing Epithelial Cell Shedding

Glucose administration curtailed the transmural permeability increase in the ischemic intestine, likely by maintaining the epithelial barrier, in agreement with previous results showing preservation of the mucosal epithelial barrier during ischemia in the presence of luminal glucose [24-26]. Despite blood flow cessation, glucose provides epithelial cells a direct source of metabolic energy to produce ATP [23] which has been shown to maintain the barrier in-vitro [35]. ATP supply, which could be achieved by glucose supplementation, is required for epithelial cells to maintain attachments and prevent excessive apoptosis [25,36-38] and anoikis, the shedding of apoptotic epithelial cells into the lumen [5]. Elevated levels of apoptosis in epithelial cells can occur within 15 minutes of ischemia [5] which illustrates the sensitivity of the intestine to ischemic conditions. The presence of glucose in the lumen during ischemia prevented the cells from undergoing apoptosis (Figure 2.14) and loss of the tight junction protein occludin, which may explain why permeability and a connected layer of epithelial cells were maintained even when they were separated from the underlying lamina propria.

In the current model, the epithelium was intact at the start of the experiment and remained intact with glucose treatment, or any combination of inhibitors with glucose (Figure 2.2, Figure 2.3, and Figure 2.13). Epithelial shedding during initial stages of ischemia may result in gaps that are incapable of timely repair and result in an intestine that inadequately absorbs nutrients [34]. Likewise, the transition from reversible to irreversible shock may be related to the severity of the epithelial barrier destruction and

the extent to which full physiological gut barrier/digestive features can be restored [39]. Patients undergoing elective surgery that anticipate intestinal ischemia may therefore benefit from intraluminal glucose supplementation in order to reduce epithelial damage [24,40].

2.5.3 Serine Protease or Lipase Inhibition was not as Effective without Glucose

Since ANGD is solubilized in glucose, and glucose alone was sufficient to attenuate a transmural permeability increase over the course of a period of 2 hours, further experiments are required to determine the effects of ANGD, independent of glucose, under conditions when no luminal digestive protease are present. The presence of visible gaps that formed between the epithelial layer and the interior portions of the villi in the jejunum (Figure 3B, also reported by Derikx, et al.) [34] suggests that ANGD may not be able to prevent the degradation of the wall under the epithelium. These gaps were reduced when glucose was mixed with tranexamic acid or GM 6001 (Figure 2.13).

Aprotinin, unlike ANGD, was able to inhibit proteases in the intestinal wall (Figures 2.6 and Figure 2.8) but did not protect the morphology or prevent the permeability increase. As a 6540 Da protein (over 10x the size of the other inhibitors used in this study), aprotinin may not be able to diffuse into the intestinal wall in time to provide protection against degrading proteases in an ischemic state because of its low bioavailability [41]. For example, inhibition occurred but possibly only after the intestinal wall was degraded and/or after homogenization.

ANGD has been shown to attenuate gut and lung injury in hemorrhagic shock, even in the absence of the glucose solvent [15]. In a *non-flushed* intestine, a small opening in the mucosal barrier may allow penetration of luminal content and amplify intestinal damage by increasing proteolytic breakdown of the extracellular matrix and accumulation of neutrophils [20]. By inhibiting luminal enzymes, ANGD reduces intestinal damage and may prevent shock mediators from passing the mucosal barrier [21,22,42,43] that contribute to multi-organ failure, making it more applicable as a treatment for the more physiologic, non-flushed cases of shock [9,15].

Aprotinin in combination with orlistat is a powerful inhibitor of the main luminal digestive enzymes, comparable to ANGD (Table 4). Similar to ANGD+glucose, aprotinin+orlistat can provide protection against shock and intestinal hemorrhage following intestinal ischemia in-vivo and generation of shock mediators from the lumen of the intestine [21]. The protection provided by aprotinin and ANGD in non-flushed intestines may be due to inhibition of luminal enzymes that generate pro-inflammatory mediators in the gut. Another possibility is that ischemia may open the mucus layer and expose the epithelial cells to protease activity or cytotoxic intestinal products which may open the epithelial barrier just enough to allow aprotinin to penetrate and prevent further breakdown of the intestinal wall underneath the epithelium.

2.5.4 Tranexamic Acid Works by a Mechanism Similar to MMP Inhibition

While less capable of inhibiting luminal digestive enzymes than either ANGD or aprotinin (Table 2), tranexamic acid is more bioavailable than aprotinin and is able to

significantly lower the activity of the proteases in the intestinal wall (Figures 2.6, Figure 2.7, Figure 2.8). It also was able to preserve mucin 13, which could improve epithelial survival in non-flushed intestines [6,29]. In addition, tranexamic acid was able to maintain low transmural permeability through the first 90 minutes of ischemia. It is currently unclear how much of this preservation was due to protection of the wall extracellular matrix versus reduced apoptosis of the epithelial barrier (Figure 2.14), since both the extracellular matrix and epithelial layer were damaged by the 120 min collection time.

Tranexamic acid, as a lysine analog, inhibits plasmin and conversion of plasminogen to plasmin. Plasmin is a trypsin-like enzyme that is a potent activator of MMPs [44,45] and ADAMs ("a disintegrin and metalloproteinase"), which are expressed on epithelial cells and activated during ischemia [45]. Therefore, inhibiting plasmin, plus the direct inhibition of MMPs by tranexamic acid that we observed (Figure 2.7) which also prevents the consequent downstream activation of metallo- or other proteases, could explain the reduction of caseinolytic activity detected by plate zymography relative to the pre-ischemic controls (Figure 2.6). Inhibition of plasmin and/or metalloproteinases could protect extracellular matrix proteins from degradation, and therefore, minimize the creation of pores that fluorescein could penetrate through to pass the serosa [17]. Tranexamic acid may also help the preservation of epithelial attachments to the basement membrane, which may reduce anoikis (Figure 2.14).

The intestine is rich in MMPs, and we detected gelatinase activities at approximately 50 kDa (MMP-1 or MMP-3), 60 kDa (MMP-2), and 220 kDa (MMP-9 dimer) which are similar to previous findings [18,46]. Doxycycline and GM 6001 are

both broad-spectrum MMP inhibitors [47] (GM 6001 also inhibits ADAMs [28]). Like tranexamic acid, over the first 90 minutes they reduced, but did not prevent, a permeability increase. By 120 minutes, the permeability increased and the epithelium was dismantled with either doxycycline or GM 6001 treatments (Figure 2.10B). This suggests that metalloproteinases may be responsible for tissue destruction that increases transmural permeability, but that the epithelial barrier is the dominant barrier that controls permeability.

2.5.5 Epithelial Proteins Degrade during Ischemia

We studied several candidate proteins that contribute to epithelial barrier integrity. Mucin 13, which is bound to the epithelial cell membrane, was reduced with ischemia and restored when the lumen was treated with glucose or tranexamic acid (Figure 2.15). However, since MMP inhibition was unable to prevent mucin 13 degradation, tranexamic acid appears to be acting through a different mechanism. There were no changes in claudin-1 levels, but there was a severe reduction in the tight junction protein occludin and the adheren junction protein E-cadherin following ischemia irrespective of treatment or protease activity levels in the intestinal tissue. Lactic acid build up in the cells after 2 hours of ischemia could reduce the intracellular pH and aid in E-cadherin degradation.

Occludin and E-cadherin can be degraded by MMPs [48-50]. However, MMP inhibition did not curtail occludin or E-cadherin destruction implying they are not responsible for their reduction following ischemia. Alternatively, as the epithelium

becomes apoptotic, occludin, E-cadherin, and mucin 13 may be internalized and internally degraded [29,51]. It should be noted that E-cadherin and mucin 13 also degrade in the presence of luminal proteases [6,29]. The breakdown of mucin 13, E-cadherin, and occludin may occur sequentially as the intestinal barrier fails and future studies need to investigate the kinetics of the degradation of these molecules in a less severe form of intestinal ischemia.

2.5.6 JEJUNUM AND ILEUM HAVE DIFFERENT PERMEABILITY PROFILES

In all cases, the transmural permeability for fluorescein increased from the jejunum to the ileum (with the exception of a non-significant increased permeability in position 1 compared to position 2). The major transition from an impermeable to a permeable state occurred after 1 hour in positions 5 and higher, corresponding to the ileum. The ileum, often described as the most permeable region of the intestine [52,53], is associated with the most damage after trauma and/or shock, and is where the majority of microhemorrhages occur in experimental shock animals and necrotizing enterocolitis [54-57]. We were surprised that the morphology of the untreated ischemic jejunum appeared as disrupted as that of the untreated ischemic ileum, despite its lower transmural permeability. Since the epithelial layer, which when intact serves as the most effective barrier to fluorescein, was destroyed in both cases, the differences between the jejunum and ileum lie beneath the epithelium.

When we measured the proteolytic activity by gelatin gel zymography, the ileum had a much higher density of serine proteases and MMPs compared to the jejunum in

pre-ischemic tissue (Figure 2.7). These proteases could degrade the extracellular matrix structure of the villi, muscularis, and/or serosa more rapidly in the ileum than in the jejunum allowing fluorescein to pass through with less resistance, even in the absence of a visible difference. If this is the case, then given more time the jejunum would be expected to reach the same high levels of permeability as the ileum. Alternatively, the enhanced presence of proteases in the ileum could cleave integrin attachments between cells and the extracellular matrix which may enhance cell apoptosis in the wall of the ileum at a greater rate than the jejunum [58]. Detachment of cells from the extracellular matrix would provide another route for fluorescein to penetrate across the barrier. Although the transmural permeability of the jejunum is lower than the ileum, it would not necessarily prevent egress through the blood or lymph.

2.5.7 LIMITATIONS

Flushing the lumen was a great tool to uncover which factors inherent to the intestinal wall are responsible for degradation of the wall of the intestine. However, if there are luminal proteases present, the breakdown process may become more complex. Additionally, when the intestine is not excised from the animal, there may be additional transport routes via the blood and lymph for luminal content that may or may not be prevented by the mechanisms that were effective at reducing transmural permeability.

2.6 CONCLUSIONS

The increase in transmural permeability to small molecules during total ischemia of the small intestine occurs by a combination of epithelial shedding and MMP-derived proteolysis of the intestinal wall, both of which occur in the absence of luminal contents. The increased transmural permeability was reduced by placement of glucose into the lumen of the intestine, as well as by administration of MMP inhibitors or tranexamic acid. Our results suggest that prophylactic treatment with enteral glucose and/or MMP inhibition for patients at high risk for intestinal ischemia may reduce intestinal permeability and transmural passage of luminal content.

Chapter 2, in full, is currently being prepared for submission for publication entitled "Transmural intestinal wall permeability in severe ischemia after enteral protease inhibition" by Angelina E. Altshuler, Itze Lamadrid, Diana Li, Stephanie Ma, Leena Kurre, Geert W. Schmid-Schönbein, and Alexander H. Penn. Table 2.4 was contributed by Alexander H. Penn. The dissertation author is the primary author of this manuscript.

2.7 REFERENCES

1. Haglund U. (1993) Systemic mediators released from the gut in critical illness. Crit Care Med 21: S15-8.

2. Haglund U. (1994) Gut ischaemia. Gut 35: S73-6.

3. Hebra A, Brown MF, McGeehin K, Broussard D, Ross AJ,3rd. (1993) The effects of ischemia and reperfusion on intestinal motility. J Pediatr Surg 28: 362-5; discussion 365-6.

4. Dauterive AH, Flancbaum L, Cox EF. (1985) Blunt intestinal trauma. A modern-day review. Ann Surg 201: 198-203.

5. Ikeda H, Suzuki Y, Suzuki M, Koike M, Tamura J, Tong J, Nomura M, Itoh G. (1998) Apoptosis is a major mode of cell death caused by ischaemia and ischaemia/reperfusion injury to the rat intestinal epithelium. Gut 42: 530-537.

6. Chang M, Kistler EB, Schmid-Schönbein GW. (2012) Disruption of the mucosal barrier during gut ischemia allows entry of digestive enzymes into the intestinal wall. Shock 37: 297-305.

7. Sun Z, Wang X, Deng X, Lasson A, Wallen R, Hallberg E, Andersson R. (1998) The influence of intestinal ischemia and reperfusion on bidirectional intestinal barrier permeability, cellular membrane integrity, proteinase inhibitors, and cell death in rats. Shock 10: 203-212.

8. Langer JC, Sohal SS. (1992) Increased mucosal permeability after intestinal ischemia-reperfusion injury is mediated by local tissue factors. J Pediatr Surg 27: 329-31; discussion 331-2.

9. Mitsuoka H, Kistler EB, Schmid-Schönbein GW. (2000) Generation of in vivo activating factors in the ischemic intestine by pancreatic enzymes. Proc Natl Acad Sci U S A 97: 1772-1777.

10. Mitsuoka H, Schmid-Schönbein GW. (2000) Mechanisms for blockade of in vivo activator production in the ischemic intestine and multi-organ failure. Shock 14: 522-527.

11. Deitch EA. (2010) Gut lymph and lymphatics: A source of factors leading to organ injury and dysfunction. Ann N Y Acad Sci 1207 Suppl 1: E103-11.

12. Altshuler AE, Penn AH, Yang JA, Kim GR, Schmid-Schönbein GW. (2012) Protease activity increases in plasma, peritoneal fluid, and vital organs after hemorrhagic shock in rats. PLoS One 7: e32672.

13. Ishimaru K, Mitsuoka H, Unno N, Inuzuka K, Nakamura S, Schmid-Schönbein GW. (2004) Pancreatic proteases and inflammatory mediators in peritoneal fluid during splanchnic arterial occlusion and reperfusion. Shock 22: 467-471.

14. Schmid-Schönbein GW. (2007) A journey with tony hugli up the inflammatory cascade towards the auto-digestion hypothesis. Int Immunopharmacol 7: 1845-1851.

15. Deitch EA, Shi HP, Lu Q, Feketeova E, Xu DZ. (2003) Serine proteases are involved in the pathogenesis of trauma-hemorrhagic shock-induced gut and lung injury. Shock 19: 452-456.

16. Kistler EB, Alsaigh T, Chang M, Schmid-Schönbein GW. (2012) Impaired small-bowel barrier integrity in the presence of lumenal pancreatic digestive enzymes leads to circulatory shock. Shock 38: 262-267.

17. Medina C, Radomski MW. (2006) Role of matrix metalloproteinases in intestinal inflammation. J Pharmacol Exp Ther 318: 933-938.

18. Seifert WF, Wobbes T, Hendriks T. (1996) Divergent patterns of matrix metalloproteinase activity during wound healing in ileum and colon of rats. Gut 39: 114-119.

19. Taraboletti G, D'Ascenzo S, Borsotti P, Giavazzi R, Pavan A, Dolo V. (2002) Shedding of the matrix metalloproteinases MMP-2, MMP-9, and MT1-MMP as membrane vesicle-associated components by endothelial cells. Am J Pathol 160: 673-680.

20. Rosario HS, Waldo SW, Becker SA, Schmid-Schönbein GW. (2004) Pancreatic trypsin increases matrix metalloproteinase-9 accumulation and activation during acute intestinal ischemia-reperfusion in the rat. Am J Pathol 164: 1707-1716.

21. Penn AH, Schmid-Schönbein GW. (2008) The intestine as source of cytotoxic mediators in shock: Free fatty acids and degradation of lipid-binding proteins. Am J Physiol Heart Circ Physiol 294: H1779-92.

22. Qin X, Dong W, Sharpe SM, Sheth SU, Palange DC, Rider T, Jandacek R, Tso P, Deitch EA. (2012) Role of lipase-generated free fatty acids in converting mesenteric lymph from a noncytotoxic to a cytotoxic fluid. Am J Physiol Gastrointest Liver Physiol 303: G969-78.

23. Thorens B. (1993) Facilitated glucose transporters in epithelial cells. Annu Rev Physiol 55: 591-608.

24. McArdle AH, Chiu CJ, Gurd FN. (1972) Intraluminal glucose: Substrate for ischemic intestine. Arch Surg 105: 441-445.

25. Robinson JW, Mirkovitch V. (1977) The roles on intraluminal oxygen and glucose in the protection of the rat intestinal mucosa from the effects of ischaemia. Biomedicine 27: 60-62.

26. Chiu CJ, Scott HJ, Gurd FN. (1970) Intestinal mucosal lesion in low-flow states. II. the protective effect of intraluminal glucose as energy substrate. Arch Surg 101: 484-488.

27. Golub LM, Ramamurthy NS, McNamara TF, Greenwald RA, Rifkin BR. (1991) Tetracyclines inhibit connective tissue breakdown: New therapeutic implications for an old family of drugs. Crit Rev Oral Biol Med 2: 297-321.

28. Moss ML, Rasmussen FH. (2007) Fluorescent substrates for the proteinases ADAM17, ADAM10, ADAM8, and ADAM12 useful for high-throughput inhibitor screening. Anal Biochem 366: 144-148.

29. Chang M, Alsaigh T, Kistler EB, Schmid-Schönbein GW. (2012) Breakdown of mucin as barrier to digestive enzymes in the ischemic rat small intestine. PLoS One 7: e40087.

30. Shi HP, Liu ZJ, Wen Y. (2004) Pancreatic enzymes in the gut contributing to lung injury after trauma/hemorrhagic shock. Chin J Traumatol 7: 36-41.

31. Doucet JJ, Hoyt DB, Coimbra R, Schmid-Schönbein GW, Junger WG, Paul LW, Loomis WH, Hugli TE. (2004) Inhibition of enteral enzymes by enteroclysis with nafamostat mesilate reduces neutrophil activation and transfusion requirements after hemorrhagic shock. J Trauma 56: 501-10; discussion 510-1.

32. DeLano FA, Hoyt DB, Schmid-Schönbein GW. (2013) Pancreatic digestive enzyme blockade in the intestine increases survival after experimental shock. Sci Transl Med 5: 169ra11.

33. Mirkovitch V, Menge H, Robinson JW. (1975) Protection of the intestinal mucosa during ischaemia by intraluminal perfusion. Res Exp Med (Berl) 166: 183-191.

34. Derikx JP, Matthijsen RA, de Bruine AP, van Bijnen AA, Heineman E, van Dam RM, Dejong CH, Buurman WA. (2008) Rapid reversal of human intestinal ischemia-reperfusion induced damage by shedding of injured enterocytes and reepithelialisation. PLoS One 3: e3428.

35. Unno N, Baba S, Fink MP. (1998) Cytosolic ionized Ca2+ modulates chemical hypoxia-induced hyperpermeability in intestinal epithelial monolayers. Am J Physiol 274: G700-8.

36. Honda K, Kato K, Dairaku N, Iijima K, Koike T, Imatani A, Sekine H, Ohara S, Matsui H, Shimosegawa T. (2003) High levels of intracellular ATP prevent nitric oxide-induced apoptosis in rat gastric mucosal cells. Int J Exp Pathol 84: 281-288.

37. Vakonyi T, Wittmann T, Varro V. (1977) Effect of local circulatory arrest on the structure of the enterocytes of the isolated intestinal loop. Digestion 15: 295-302.

38. Flynn WJ,Jr, Gosche JR, Garrison RN. (1992) Intestinal blood flow is restored with glutamine or glucose suffusion after hemorrhage. J Surg Res 52: 499-504.

39. Grootjans J, Hameeteman W, Masclee AA, van Dam RM, Buurman WA, Dejong CH. (2012) Real-time in vivo imaging of early mucosal changes during ischemia-reperfusion in human jejunum. PLoS One 7: e39638.

40. Kozar RA, Hu S, Hassoun HT, DeSoignie R, Moore FA. (2002) Specific intraluminal nutrients alter mucosal blood flow during gut ischemia/reperfusion. JPEN J Parenter Enteral Nutr 26: 226-229.

41. Beath SM, Nuttall GA, Fass DN, Oliver WC,Jr, Ereth MH, Oyen LJ. (2000) Plasma aprotinin concentrations during cardiac surgery: Full- versus half-dose regimens. Anesth Analg 91: 257-264.

42. Zhang Q, Itagaki K, Hauser CJ. (2010) Mitochondrial DNA is released by shock and activates neutrophils via p38 map kinase. Shock 34: 55-59.

43. Davis GE. (2010) Matricryptic sites control tissue injury responses in the cardiovascular system: Relationships to pattern recognition receptor regulated events. J Mol Cell Cardiol 48: 454-460.

44. Lijnen HR. (2001) Plasmin and matrix metalloproteinases in vascular remodeling. Thromb Haemost 86: 324-333.

45. Hakulinen J, Keski-Oja J. (2006) ADAM10-mediated release of complement membrane cofactor protein during apoptosis of epithelial cells. J Biol Chem 281: 21369-21376.

46. Moore BA, Manthey CL, Johnson DL, Bauer AJ. (2011) Matrix metalloproteinase-9 inhibition reduces inflammation and improves motility in murine models of postoperative ileus. Gastroenterology 141: 1283-92, 1292.e1-4.

47. Golub LM, Ramamurthy NS, McNamara TF, Greenwald RA, Rifkin BR. (1991) Tetracyclines inhibit connective tissue breakdown: New therapeutic implications for an old family of drugs. Crit Rev Oral Biol Med 2: 297-321.

48. Cummins PM. (2012) Occludin: One protein, many forms. Mol Cell Biol 32: 242-250.

49. Liu W, Hendren J, Qin XJ, Shen J, Liu KJ. (2009) Normobaric hyperoxia attenuates early blood-brain barrier disruption by inhibiting MMP-9-mediated occludin degradation in focal cerebral ischemia. J Neurochem 108: 811-820.

50. Steck N, Hoffmann M, Sava IG, Kim SC, Hahne H, Tonkonogy SL, Mair K, Krueger D, Pruteanu M, Shanahan F, Vogelmann R, Schemann M, Kuster B, Sartor RB, Haller D. (2011) Enterococcus faecalis metalloprotease compromises epithelial barrier and contributes to intestinal inflammation. Gastroenterology 141: 959-971.

51. Bojarski C, Weiske J, Schoneberg T, Schroder W, Mankertz J, Schulzke JD, Florian P, Fromm M, Tauber R, Huber O. (2004) The specific fates of tight junction proteins in apoptotic epithelial cells. J Cell Sci 117: 2097-2107.

52. Deitch EA, Specian RD, Berg RD. (1991) Endotoxin-induced bacterial translocation and mucosal permeability: Role of xanthine oxidase, complement activation, and macrophage products. Crit Care Med 19: 785-791.

53. Cui N, Madsen KL, Friend DR, Stevenson BR, Fedorak RN. (1996) Increased permeability occurs in rat ileum following induction of pan-colitis. Dig Dis Sci 41: 405-411.

54. Wani I, Parray FQ, Sheikh T, Wani RA, Amin A, Gul I, Nazir M. (2009) Spectrum of abdominal organ injury in a primary blast type. World J Emerg Surg 4: 46.

55. Bounous G, Cronin RF, Gurd FN. (1967) Dietary prevention of experimental shock lesions. Arch Surg 94: 46-60.

56. Israel EJ. (1994) Neonatal necrotizing enterocolitis, a disease of the immature intestinal mucosal barrier. Acta Paediatr Suppl 396: 27-32.

57. Kosloske AM, Musemeche CA. (1989) Necrotizing enterocolitis of the neonate. Clin Perinatol 16: 97-111.

58. Chen CS, Mrksich M, Huang S, Whitesides GM, Ingber DE. (1997) Geometric control of cell life and death. Science 276: 1425-1428.

Chapter 3

Transport and Activities of Proteases after Hemorrhagic Shock

3.1 INTRODUCTION

Trauma is associated with high mortality [1]. One major cause of death in trauma patients is hemorrhagic shock [2], during which the intestine is underperfused [2,3]. As a result of ischemia the intestinal permeability increases [4], allowing luminal content, including pancreatic digestive enzymes, to escape from the lumen into the wall of the intestine [5,6]. Proteases that have penetrated the barrier can further increase the overall proteolytic activity in the intestinal wall by activating MMPs [6,7]. Pretreatment in the intestinal lumen with a broad spectrum serine protease and lipase inhibitor (nafamostat mesilate, ANGD), reduces circulating neutrophil activation [8] and delays or prevents mortality in experimental shock models indicating the intestine as a key organ to preserve during shock [8-10]. One of the possible effects of ANGD in the lumen of the intestine may be to prevent active pancreatic proteases from entering the circulation, by helping to preserve the mucosal barrier and/or by inhibiting proteases that enter the intestinal wall.

Shock mediators entering or formed in the wall of the intestine may be transported out of the intestine via the portal venous system, the intestinal lymph, or by passive transport through the intestinal wall into the peritoneum [11-13]. It is unknown whether digestive enzymes are among the mediators transported out of the intestine into the systemic circulation and other organs during hemorrhagic shock. Should this occur, uncontrolled proteolytic activity in compartments outside the lumen of the intestine could lead to cleavage of important plasma proteins and/or cell surface receptors contributing to the morbidity and possible mortality of the animal [14].

However, there are documented cases where serine proteases enter into the periphery. In pancreatitis, which has similarities to shock and may also result in multi-organ failure, plasma trypsin levels have been correlated with mortality [15]. In shock, pancreatic amylase and lipase have been measured in plasma and predict mortality [16], but the presence and activity of pancreatic *proteases* remains to be determined. It has been hypothesized that, if released into the systemic circulation, pancreatic proteases will not be active due to binding to plasma protease inhibitors (serpins; e.g. α_2-macroglobulin, α_1-antitrypsin, etc.) [17]. However, the blocking ability of serpins is limited. They may be saturated, and it has been shown that while binding to these inhibitors prevents proteases like trypsin from digesting large proteins, smaller peptides are still cleavable [18]. Thus, proteins with exposed loops or terminal ends may still be at risk for proteolytic degradation [14].

Due to possible binding to circulating antiproteases, measurements of the potential for proteolysis in shock plasma or lymph may be underestimated if the selected test substrate is a large globular protein such as casein, a substrate commonly used to

measure non-specific protease activity. Additionally, our group has observed that serine protease activity in plasma samples decreases with increasing storage time (-20 ºC) and/or freeze-thaw cycles, further increasing the difficulty of obtaining a complete spectrum of the proteolytic potential in shock plasma [19]. Therefore, we will test plasma samples fresh and using a variety of substrates.

3.2 CHAPTER AIMS

Since the intestinal barrier is compromised during shock, the immediate testing of the activity and transport of serine proteases potentially derived from the intestine can open up many possible implications for the role of these proteases in the pathophysiology of shock. The objectives for this chapter are to determine in experimental hemorrhagic shock (1) select protease activities and concentrations outside of the intestine (plasma, peritoneal fluid, lymph fluid, and vital organs) by plate zymography, gel zymography, and immunoblotting and (2) whether the mechanism by which serine protease inhibition in the intestinal lumen provides protection in hemorrhagic shock is due to reduction of protease activity in the systemic circulation. I hypothesize that luminal serine proteases can escape via three routes: (1) portal venous blood, (2) peritoneal space, and (3) mesenteric lymph (Figure 3.1).

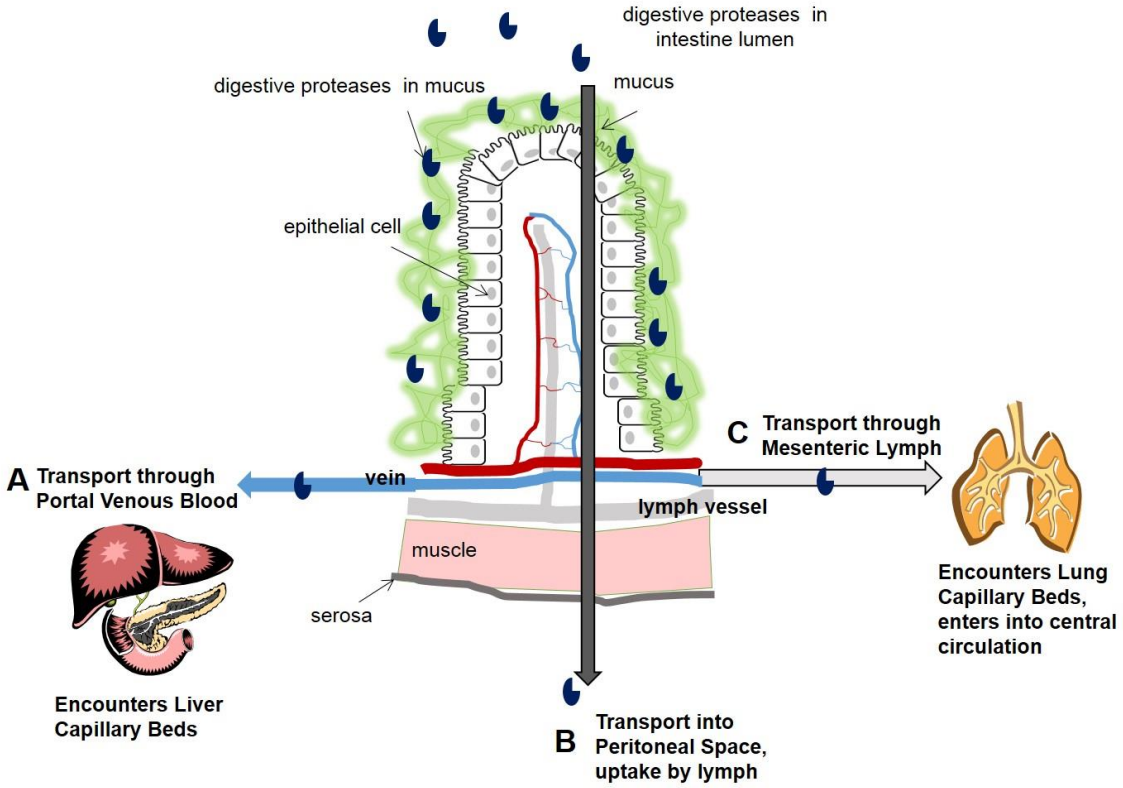

Figure 3.1 Hypothesis for serine protease transport from the intestine. Serine proteases may enter into the periphery by three routes. (A) Proteases may directly enter into portal venous blood and encounter the liver first. (B) Proteases may be transported directly across the wall of the intestine into the peritoneal space where they may be transported into the lymph. (C) Proteases enter through mesenteric lymph and encounter the lung capillary beds and into the central circulation.

3.3 METHODS

3.3.1 ANIMAL PROTOCOL AND TISSUE COLLECTION

The animal protocols were reviewed and approved by the University of California, San Diego Animal Subjects committee (Protocol Number S01113). Male Wistar rats (body weight between 270 and 460g; 347±49g [mean±sd], Harlan, Indianapolis, IN) were administered general anesthesia (xylazine, 20 mg/kg IM, followed 20 minutes later by sodium pentobarbital, 50 mg/kg IM). After laparotomy, 2 ml saline were injected into the peritoneal space then drained after 2 minutes. The lavage fluid was collected in a tube containing 20 µl heparin and centrifuged (1000 g, 5 min) to remove any accumulated cells. Next, the left femoral vein and artery were cannulated. Saline (*HS+SAL* group) or a serine protease inhibitor (6-amidino-2-naphtyl *p*-guanidinobenzoate dimethanesulfate, ANGD, *nafamostat mesilate*, Torii Pharmaceutical, Chiba, Japan; *HS+ANGD* group; 2 mg/ml [3.7 mM] ANGD in 100 mg/ml D-glucose in saline) was injected into the lumen of the small intestine (7-10 ml at two to three injection sites to fill the small intestine but avoid circumferential stretching). To prevent clotting in catheters and shed blood, animals were heparinized (10 U/ml IV, assuming 6% blood volume per body weight) prior to inducing hemorrhagic shock.

Mean arterial blood pressure (MAP) was reduced to 35 mmHg by withdrawing blood through the venous catheter (0.2 ml/min). This pressure was maintained by further withdrawal/return of blood over a 2-hour ischemic period. The first two milliliters of shed blood were collected, centrifuged (1000 g, 5 min), and stored at 4º C as pre-

hemorrhagic shock *(Pre-HS)* plasma. After 2 hours, the remaining shed blood plus 2 ml of heparinized saline (to replace the 2 ml of pre-ischemic blood) was reinfused (0.5 ml/min IV), and the animal observed for 2 hours. At the end of this reperfusion period, 4 ml of post-hemorrhagic shock (*Post-HS*) blood was collected, centrifuged (1000 g, 5 min) and plasma aliquots were either immediately measured for protease activity or frozen (-20º C). An aliquot of post-HS plasma received an extra 10 U/ml heparin before centrifugation.

Post-peritoneal lavage fluid was collected in the same manner as described above. The brain, heart, liver, and lung were collected immediately after euthanasia (120 mg/kg sodium pentobarbital IV) and snap frozen for later protease assays, gelatin zymography, and immunoblot analysis. Separate animals (*No-HS* group) were euthanized immediately after femoral catheterization for control brain, heart, liver, and lung tissue samples. Given the limited availability of Pre-HS plasma, some assays were performed using remaining unpaired Pre-HS plasma (i.e. Pre-HS plasma drawn from animals in both the HS+SAL and HS+ANGD groups).

Brain, heart, liver, and lung were homogenized (0.1 g tissue/ml) in phosphate buffered saline (PBS) (pH 6) containing 0.5% hexadecyltrimethyl bromide (HTAB) for myeloperoxidase (MPO) assays, MMP-1/9 assays, and gelatin gel zymography. Tissues were homogenized for immunoblot analysis in CelLytic buffer (Sigma-Aldrich, St. Louis, MO) with protease inhibitor cocktail (Sigma-Aldrich). Homogenates were centrifuged ($1.4x10^4$ g, 4 ºC, 30 min) and the supernatants collected, aliquoted, and stored at -80 º C. After removal from -80º C, protein concentrations were measured (BCA protein assay kit, ThermoScientific, Waltham, MA) prior to use of samples in subsequent experiments.

3.3.2 Microplate Assays

All microplate assays were performed in triplicate in 96 well black-sided flat bottom polystyrene plates (Corning, New York, NY) using a microplate reader (FilterMax F-5 Multi-mode, Molecular Devices, Sunnyvale, CA).

Since shed blood was held outside the body for 2 hours during the ischemic period, a pilot study was performed to confirm that any increased protease activity after reperfusion was not due to increases in-vitro in the shed whole blood. In a set of pilot studies, freshly drawn blood was compared to blood that had been stored for 2 hours for all protease activity measurements. No significant differences were detected.

3.3.2.1 Myeloperoxidase (MPO) Activity Assay

As a measure of the degree of inflammation after shock, myeloperoxidase activity was determined as a measure for neutrophil infiltration/accumulation in lung, liver, heart, and brain. 20 µl of 1 mg/ml brain, heart, liver, or lung homogenate, were added to 180 µl of 0.167 mg/ml o-dianisidine dihydrochloride (Sigma-Aldrich) and 0.005% H_2O_2 in PBS (pH 6). Absorbance was measured at 450 nm every 5 minutes for 1 hour at 37º C. MPO activity is presented as the change in absorbance per minute per milligram of protein.

3.3.2.2 Trypsin-, Chymotrypsin-, and Elastase-like Activity Measurements

The ability of shock plasma and peritoneal lavage fluid to digest small peptides was determined using benzoylarginyl-p-nitroanilide hydrochloride (BAPNA, Sigma-Aldrich), N-succinyl-L-phenylalanine-p-nitroanilide (SPNA, Sigma-Aldrich), N-succinyl-alanine-alanine-proline-leucine-p-nitroanilide;L-leucinamide, N-(3-carboxy-1-oxopropyl)-L-alanyl-L-alanyl-L-prolyl-N-(4-nitrophenyl) (SAAPLPNA, Sigma-Aldrich), which are substrates for trypsin-like, chymotrypsin-like, and elastase-like enzyme activity, respectively. Stock solutions were prepared in dimethylsulfoxide (DMSO) (BAPNA-20 mM, SPNA-100 mM, and SAAPLPNA-84.7 mM). Stock solutions were then diluted in PBS to their working solution concentrations (0.5 mM for BAPNA, 5 mM for SPNA, and 0.5 mM for SAAPLPNA). 20 µl of fresh plasma, peritoneal fluid, or PBS as control were added to either 180 µl of PBS (containing the same percentage of DMSO as substrates) for control or working solution of BAPNA, SPNA, or SAAPLPNA, respectively. Light absorbance readings (at 405 nm) were made at time=0 hr and 24 hrs (resulting measurements were below the maximum absorbance for each substrate). Post hemorrhagic shock plasma samples were susceptible to light diffraction due to colloid material (opacity) if allowed to evaporate. Therefore, plates were kept covered at room temperature. Opacity was also minimized in post shock blood by treatment with additional heparin, hypothesizing that clotting was a reason for the opacity in the samples. A normalized absorbance was computed as:

$$A_n=\Delta A_{Sa+Sub} - \Delta A_{Sa} - \Delta A_{Sub} \text{ where } \Delta A_{Sa+Sub}$$

is the change in absorbance of the sample+substrate, ΔA_{Sa} is the change in absorbance of the sample+PBS w/ DMSO, and ΔA_{Sub} is the change in absorbance of the substrate+PBS.

To convert trypsin-, chymotrypsin-, and elastase-like activities into equivalent uninhibited concentrations of each enzyme, purified bovine trypsin (Sigma-Aldrich), chymotrypsin (Sigma-Aldrich), and elastase (Worthington Biochemical Corporation, Lakewood, NJ) were serially diluted (in the micromolar to femtomolar range) and added to their respective substrates. The plates were read at 24 hours and a calibration curve generated to estimate the equivalent uninhibited concentration, based on proteolytic activity, in the samples. 24 hours of incubation was necessary to achieve adequate signal to noise ratios with these substrates even when using pure enzymes.

3.3.2.3 CASEIN PROTEASE ACTIVITY MEASUREMENT

To assess the ability of proteases in plasma and peritoneal lavage fluid to digest large globular proteins, Enzchek protease assay kit (Invitrogen, Carlsbad, CA) was utilized, which consists of casein internally quenched with Texas Red fluorophores (Ex/Em: 589/617 nm) reconstituted in a digestion buffer. One part fresh plasma or peritoneal fluid was added to four parts digestion buffer and five parts casein substrate ($F_{Sample+Casein}$). To determine how much of the measured activity was due to serine proteases, a second aliquot of each sample received 1 mM (final concentration) phenylmethylsulfonyl fluoride (PMSF), a serine protease inhibitor. To correct for absorption or auto-fluorescence of the sample at 617 nm, a known quantity of Texas Red

(Vector Laboratories, Burlingame, CA) was mixed in digestion buffer 9:1 with sample ($F_{Tx+Sample}$) or digestion buffer ($F_{Tx+Buffer}$). Samples were incubated for 100 min at 37 ºC in a microcentrifuge tube before pipetting the reaction mixture to the microplate and reading fluorescence. Caseinolytic activity (Relative Fluorescent Units; RFU) was determined as:

$$(F_{Tx+Buffer}/F_{Tx+Sample})*(F_{Sample+Casein}).$$

3.3.2.4 MMP-1/9 Activity Measurements

Pilot studies revealed that, unlike other protease activities examined, MMP-1/9 activity was not diminished by storage at -20 ºC, which permitted the use of stored plasma and peritoneal fluid. Plasma (100-fold final dilution) or peritoneal fluid (50-fold final dilution) samples were loaded into a 96 well plate with fluorescent MMP-1/9 substrate (American Peptide Company, Sunnyvale, CA) diluted to a final concentration of 10 µM in digestion buffer (100 mmol NaCl, 23 mmol Tris HCl, 2.4 mmol $CaCl_2$, 5 µM $ZnCl_2$, 0.01% Brj 35, pH 7.6, with 1 mM PMSF to inhibit any residual serine protease activity). Samples with digestion buffer only (no substrate) served as control for autofluorescence. Sample fluorescence was measured every 5 minutes for 30 minutes (Ex/Em: 365/450 nm). Activity was reported as the initial change of substrate fluorescence per unit time (relative fluorescent units per minute).

3.3.3 GELATIN GEL ZYMOGRAPHY

As a first step towards identification, gelatin gel zymography was used to determine molecular weights of prominent proteases appearing in tissue homogenates, stored plasma, and stored peritoneal fluid after hemorrhagic shock. It should be noted that gel zymography characteristically separates all proteases from non-covalently bound inhibitors (pilot studies revealed this includes the binding of ANGD to trypsin, chymotrypsin, or elastase) and can also activate some pro-enzymes to become able to cleave gelatin substrate.

For tissue homogenates, 30 µg of protein was added to equal volume of Laemmli sample loading buffer (Bio-Rad, Hercules, CA). Either 0.5 µl of plasma or 2 µl of peritoneal fluid were diluted in 8 µl sample loading buffer before loading the gel. Samples were separated by gel electrophoresis on a 4% stacking gel and 10% SDS-PAGE resolving gel containing 80 µg/ml porcine gelatin (Sigma-Aldrich) as the protease substrate. After protein separation, proteins in the gels were renatured in four 15-minute washes of 2.5% Triton X-100 solution. Gels were incubated overnight at 37º C in developing buffer (0.05 M Tris base, 0.2 M NaCl, 4 µM $ZnCl_2$, 5 mM $CaCl_2 \cdot 2H_2O$). Following incubation, gels were stained (50% methanol, 10% acetic acid, 40% water, and 0.25% Coomassie blue solution) for three hours. Gels were destained (50% methanol, 10% acetic acid, and 40% water solution) until the first appearance of bands, then transferred to water for rehydration before acquiring images.

To confirm that the low molecular weight bands (20-30 kDa) were serine proteases, gels were run in duplicate. One gel was renatured as described above. The

second gel was renatured and developed in buffers containing 200 µg/ml of the serine protease inhibitor, ANGD. Pilot studies with pure trypsin, chymotrypsin, or elastase, with and without ANGD, confirmed that ANGD can inhibit each enzyme as measured by plate zymography.

To determine trypsin-specific activity of lower bands, select gels were also renatured and developed in 100 µM tosyl-lysine chloromethyl ketone hydrochloride (TLCK) (Sigma-Aldrich), a specific inhibitor of trypsin-like enzymes.

The gel analysis function in ImageJ (http://rsbweb.nih.gov/ij/) was used to quantify protease activity bands by densitometry. Values are reported in Relative Intensity Units (RIU).

3.3.4 IMMUNOBLOTTING

Based on results from our lab suggesting that trypsin may more readily penetrate into the wall of an ischemic intestine than chymotrypsin or elastase [20], and on preliminary results from this study suggesting MMP-9 activity is increased in HS, the immunoblot studies were focused on those two proteases.

To determine the relative concentrations of MMP-9 and pancreatic trypsin in plasma, peritoneal fluid, and tissue homogenates, each fluid was first denatured by mixing 1:1 with 2x sample loading buffer (Bio-Rad) containing the reducing agent β-mercaptoethanol (0.05% by volume) before boiling for 10 minutes. 2 µl (MMP-9 assays) or 4 µl (trypsin assays) of denatured plasma solution or 10 µl denatured peritoneal fluid solution was loaded per well into an SDS-PAGE gel (8% resolving, 4% stacking for

MMP-9; 12% or precast 4-20% gels from Bio-Rad for trypsin). For detection of MMP-9 and trypsin in tissue homogenates, 40 µg and 80 µg of protein per well, respectively were loaded into the gel. After separation, proteins were transferred onto a nitrocellulose membrane (Bio-Rad). Membranes were blocked with 5% bovine serum albumin in tris-buffered saline with 0.5% Tween-20 (TBS-T). Primary antibodies against MMP-9 (1:1000, ab-76003, Abcam, Cambridge, MA), pancreatic trypsin (1:1000, sc-137077, Santa Cruz Biotechnology, Santa Cruz, CA), GAPDH (1:2000; sc-48167) and β-actin (1:2000, sc-130301, Santa Cruz Biotechnology) were diluted in 1% BSA in TBS-T and incubated with membranes overnight at 4º C on a rotary shaker (60 cycles/minute). Primary antibodies were washed with TBS-T (3x, 10 min) before application of anti-goat, -rabbit, or -mouse secondary antibodies (1:3000; Santa Cruz Biotechnology). Secondary antibodies were also washed in TBS-T (3x, 10 min). Bands were detected using enhanced chemiluminescence (ECL) pico substrate (Thermo Scientific) for all proteins except for plasma and lung pancreatic trypsin and brain MMP-9, which were detected using the femto substrate (Thermo Scientific). Bands were quantified by densitometry (ImageJ) and expressed as pico Relative Units (RU) or femto RU based on the type of ECL detection utilized.

3.3.5 Statistical Analysis

Results are presented as mean ± standard deviation (n=5 or 6 rats/group). Paired t-tests or Mann-Whitney tests were used to compare plasma and peritoneal fluid values before versus after hemorrhagic shock (in individual animals) and unpaired t-tests to

compare HS+SAL versus HS+ANGD groups. Unpaired t-tests or Mann-Whitney tests were used to compare tissue samples of the No-HS group with HS+SAL or HS+ANGD shock groups or when insufficient Pre-HS plasma remained to perform a paired assay. $P<0.05$ was considered statistically significant.

3.4 Results

3.4.1 Inflammation and Intestinal Damage in Hemorrhagic Shock

ANGD treatment after shock reduced MPO activity (i.e. neutrophil infiltration) in brain, heart, and lung tissues, but not significantly in liver homogenates at two hours after reperfusion ($p=0.18$) (Figure 3.2). ANGD treated animals also had fewer macroscopic lesions on the intestine in the form of visible red cell microhemorrhages into the interstitium after hemorrhagic shock compared to saline treated animals (not shown).

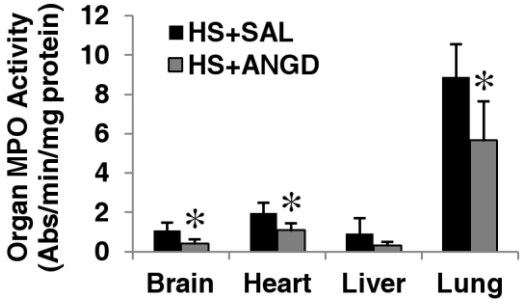

Figure 3.2 Myeloperoxidase activity. MPO activity in tissue homogenates at 2 hours after hemorrhagic shock. N=5 rats per group. *, $p<0.05$ by t-test vs. HS+SAL.

3.4.2 Protease Activity Detected by Small Peptide Substrates but not Casein Substrate

When using the small peptide substrates BAPNA, SPNA, and SAAPLPNA to assess protease activity, post-shock plasma trypsin-, chymotrypsin-, and elastase-like activities were all elevated after shock compared to low activity levels in pre-shock controls (Figure 3.3A). Trypsin-, chymotrypsin-, and elastase-like activities in peritoneal fluid were also significantly elevated after shock, though variability was enhanced in the HS+SAL group due to individual cases with high protease activity (Figure 3.3B). Overall, trypsin and elastase activity levels were higher in the peritoneal fluid compared to plasma, though this elastase activity could be due in part to elastase released from neutrophils. ANGD had no significant effect on peritoneal fluid protease activity or on plasma protease activity other than to increase post-shock trypsin activity.

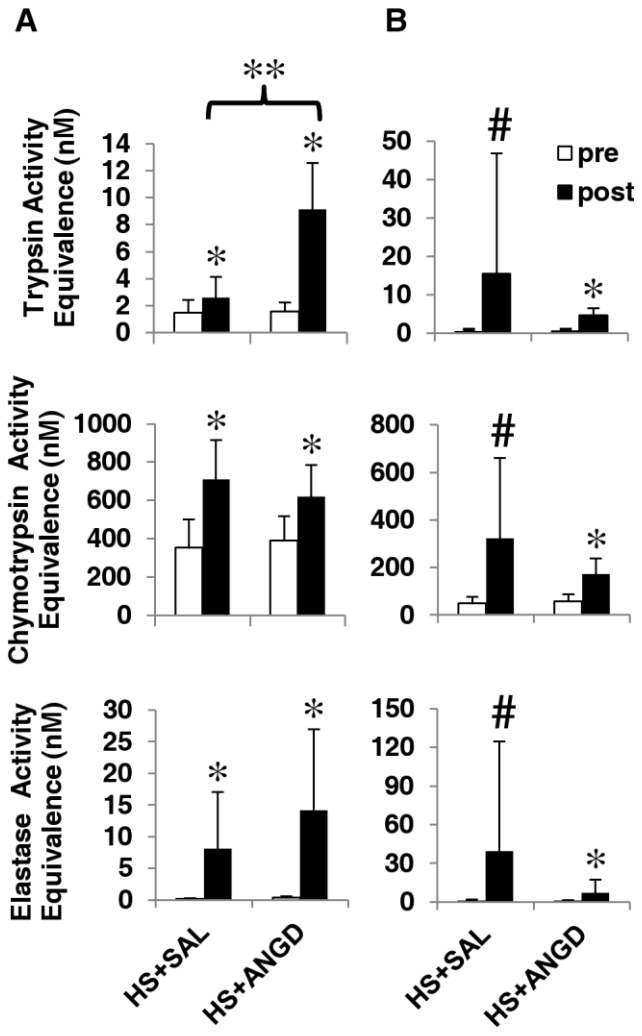

Figure 3.3 Plasma and peritoneal fluid serine protease activity. Trypsin-, chymotrypsin-, and elastase-like activities in (A) plasma and (B) peritoneal fluid expressed as equivalent activity to concentrations of pure trypsin, chymotrypsin, and elastase. Note the difference in scales of the ordinate. N=6 rats per group. *, $p<0.05$, paired t-test comparing pre vs. post HS+SAL or HS+ANGD; **, $p<0.05$ by t-test vs. post HS+SAL; #, $p<0.05$, paired Mann-Whitney test comparing pre vs. post HS+SAL or HS+ANGD.

When general protease activity was measured using a casein substrate, there was no significant difference in plasma protease activity two hours after HS compared to before HS (with or without ANGD) (Figure 3.4A). There was a significant increase in protease activity after shock in peritoneal fluid (Figure 3.4B), and the caseinolytic activity in post-shock peritoneal fluid correlated well with MAP at 2 hours post-HS (Figure 3.5). ANGD treatment did not significantly reduce protease activity in peritoneal fluid compared to saline-treated animals. Interestingly, PMSF significantly lowered the remaining protease activity in nearly all cases, suggesting a portion was of serine protease origin. There was an increase in PMSF-resistant protease activity over the pre- to post-shock time period in the plasma of the HS+SAL group, but not the plasma of the HS+ANGD group, in which activity levels did not noticeably increase after shock (Figure 3.4A).

Given the tendency of post-shock plasma to clot if the small-peptide zymography plates were not covered during digestion (see Methods), we sought to determine whether some of the measured increase in protease activity could be due to activation of proteases in the clotting cascade. Supplemental heparin added to the post-shock blood only affected chymotrypsin-like activity measured with SPNA (from 0.17 to 0.13 normalized absorbance, $P<0.04$). Similarly, there was a tendency for post-shock plasma (only) to cause a gel to form during the casein digestion. This gel was easily disrupted and did not form if the post-shock blood was supplemented with heparin, which prevented coagulation. Supplemental heparin gave similar results to disrupted gels (not shown).

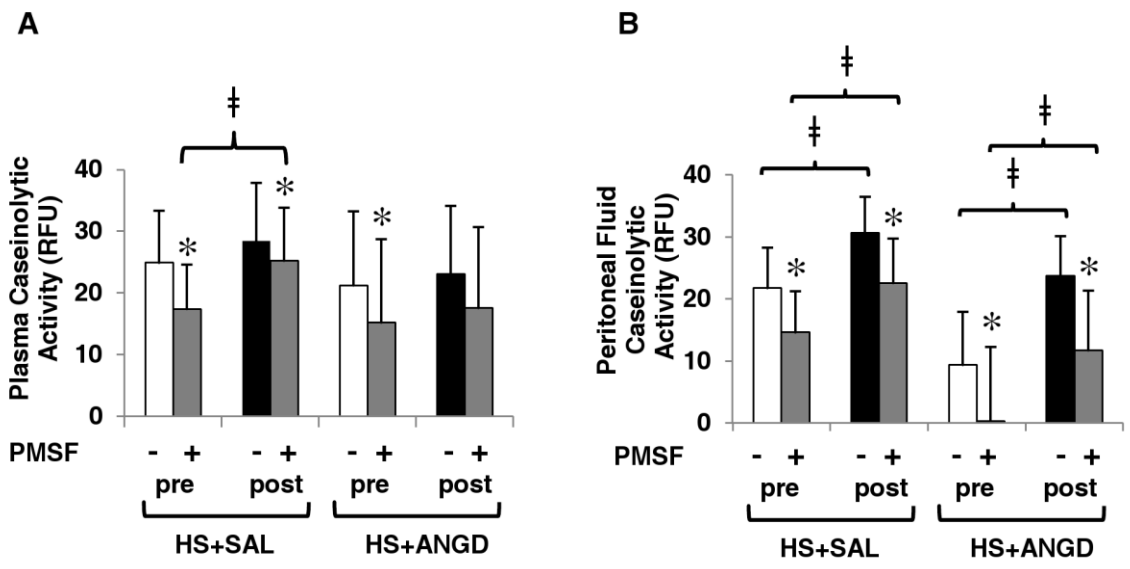

Figure 3.4 Plasma and peritoneal fluid caseinolytic activity. Caseinolytic activity with and without addition of a serine protease inhibitor, 1 mM PMSF, of (A) plasma and (B) peritoneal fluid pre/post shock with saline or ANGD pre-treatment in the intestinal lumen. Protease activity was detectable, but low with this substrate. N=5 rats per group. *, $p<0.05$ by paired t-test vs. without PMSF; ǂ, $p<0.05$ by paired t-test comparing pre vs. post plasma or peritoneal fluid from HS+SAL or HS+ANGD animals.

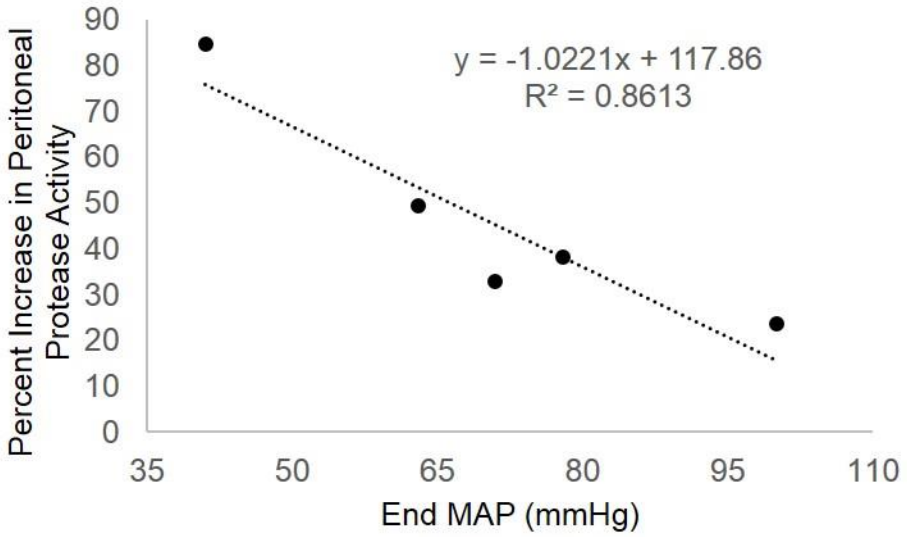

Figure 3.5 MAP correlation with peritoneal lavage protease activity. The percent change of peritoneal protease activity for HS+SAL animals correlates with the MAP at the end of the reperfusion observation period 2 hours after hemorrhagic shock.

3.4.3 PERIPHERAL TRYPSIN DETECTION

Low molecular weight bands around 20 kDa (the approximate molecular weight of pancreatic serine proteases) were also detected in the plasma and peritoneal fluid by gelatin gel zymography (Figure 3.5A). These low molecular weight bands did not appear when the gels were renatured and developed in buffer containing ANGD, suggesting they could potentially be trypsin, chymotrypsin, and elastase. In further support of this hypothesis, renaturing and developing in buffer containing TLCK, a trypsin-like enzyme inhibitor, also caused a substantial reduction in the appearance of the bands (Figure 3.7). Interestingly, ANGD treated animals had significantly higher levels of this band in the plasma suggesting the band corresponds primarily to trypsin activity, given our trypsin results in Figure 3.3A.

Two isoforms of pancreatic trypsin were detected in plasma by immunoblot at 23 and 26 kDa. Variability was great for the 23 kDa band, which required femto ECL to detect. There was a non-significant trend for increased presence of this band after HS ($P=0.07$ for HS+SAL and $P=0.11$ for HS+ANGD by Mann-Whitney test). No trend was observed for the 26 kDa band in plasma. The 26 kDa isoform of trypsin in the peritoneal fluid was significantly increased in the HS+SAL group and to a lesser, though still significant, extent in the HS+ANGD group (Figure 3.6B right; $P=0.15$ for HS+SAL vs. HS+ANGD post-shock peritoneal fluid by Mann-Whitney test). TLCK inhibition reduced the appearance of serine protease bands in the post-HS peritoneal fluid (Figure 3.7), suggesting they are of serine origin.

Both trypsin and chymotrypsin activity was detected in the lymph fluid collected after 1 hour of intestinal ischemia by SAO (Figure 3.8; adapted from Michael Richter's thesis [21]). The protein levels of trypsin and chymotrypsin did not change after intestinal ischemia (Figure 3.8C).

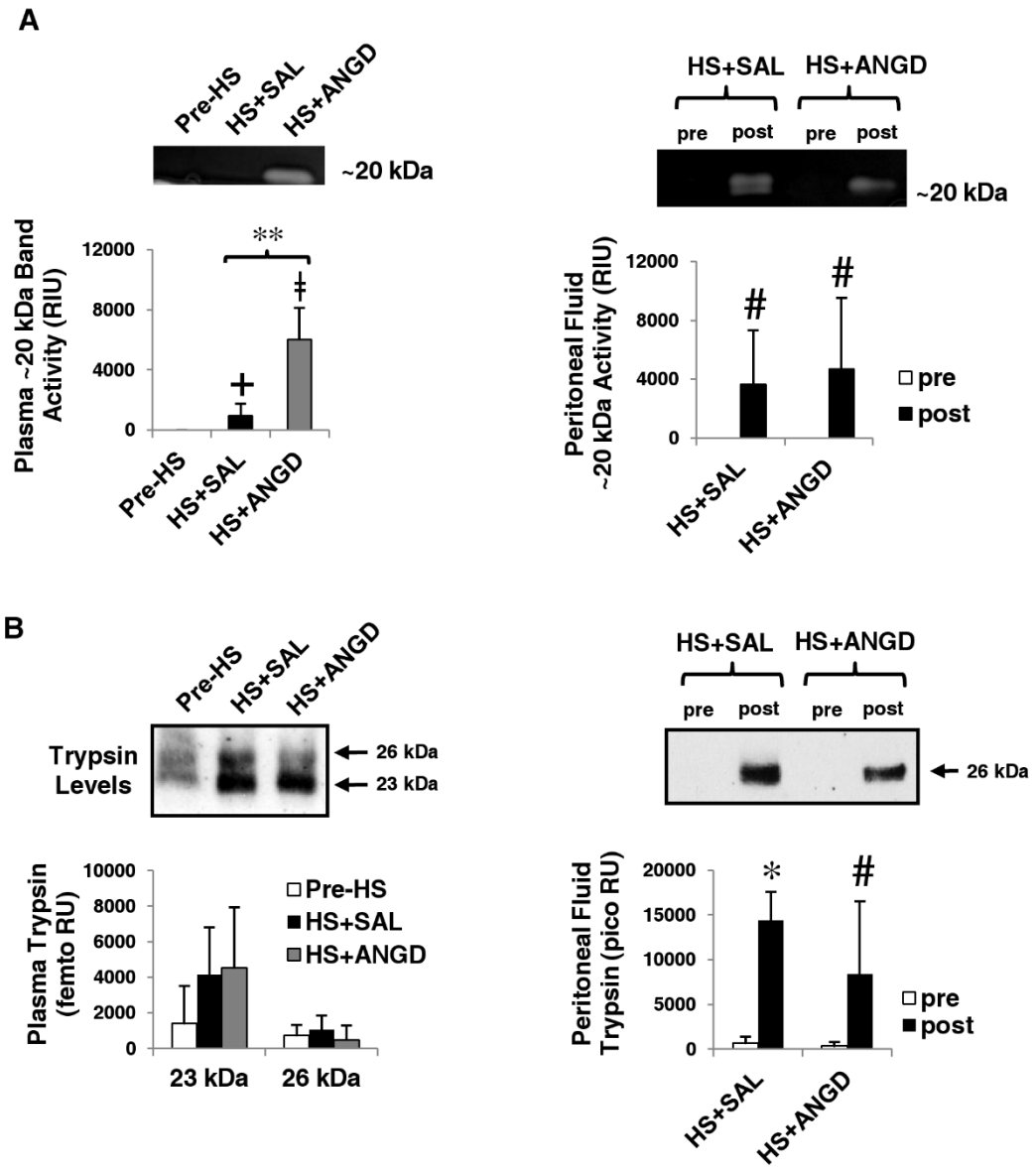

Figure 3.6 Plasma and peritoneal fluid gel zymography and trypsin levels. (A) Gelatin gel zymography detection and quantification in Relative Intensity Units (RIU; bar graph beneath) of ~20 kDa bands for plasma (right; N=6, 6, 5 rats/group) and peritoneal fluid (left; N=5 rats per group). (B) Immunoblot detection and quantification (bar graph beneath) of trypsin in plasma (left) and peritoneal fluid (right), revealing the 26 and 23 kDa isoforms of trypsin that are present. +$p<0.05$ by Mann-Whitney test vs. Pre-HS; ǂ, $p<0.05$ by t-test vs. Pre-HS; **, $p<0.05$ by t-test HS+ANGD vs. HS+SAL; #, $p<0.05$ pre vs. post HS+SAL or HS+ANGD by paired Mann-Whitney test; *, $p<0.05$ by paired t-test comparing pre vs. post HS+SAL.

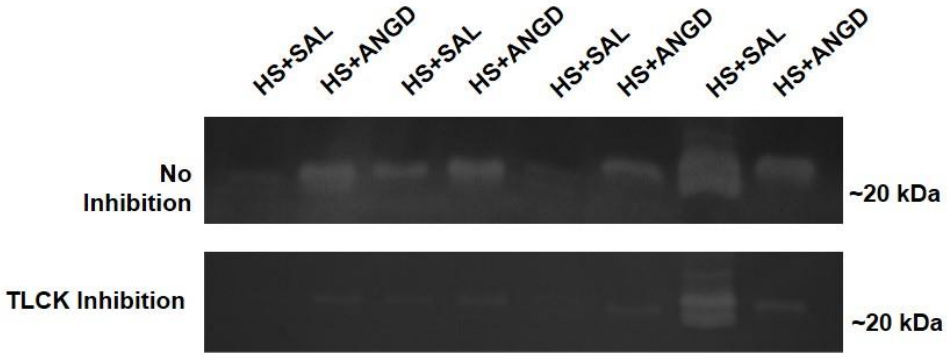

Figure 3.7 TLCK inhibition of trypsin-like proteases in peritoneal fluid. Post-HS peritoneal fluid samples' low molecular weight bands with or without ANGD treatment were diminished after incubation with TLCK, a trypsin inhibitor, following overnight digestion. Each lane represents a separate animal.

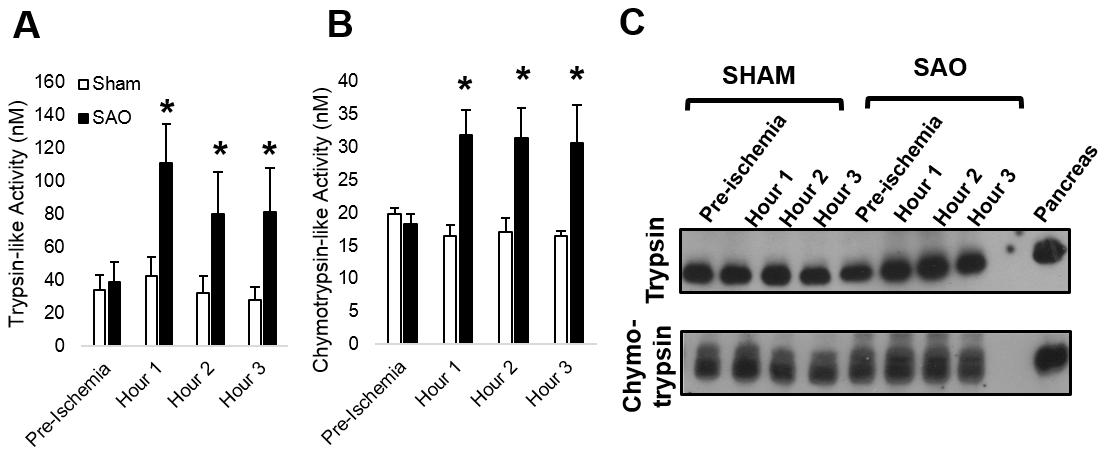

Figure 3.8 Lymph fluid protease activity and levels after SAO (adapted from Michael Richter's thesis [21]). Serine protease activity in the mesenteric lymph fluid of (A) trypsin and (B) chymotrypsin by cleavage of charge separating substrates was elevated after 1 hour of intestinal ischemia during each hour of reperfusion. (C) Immunoblots confirm the presence of trypsin and chymotrypsin protein levels in the lymph, although they were not significantly different between before and after intestinal ischemia. *, $p<0.05$ by t-test for each time point.

Lung tissue homogenates also had two distinct bands of low molecular weight protease activity observed by gelatin zymography that were inhibited by renaturing in ANGD (Figure 3.9A). The proteases were confirmed to be at least trypsin-like in specificity by the failure of the bands to appear strongly after renaturing and developing the gels in buffers containing TLCK (Figure 3.10). The upper band was significantly elevated after shock. There was considerable variability in the presence of the lower band in the HS+SAL group, but no significant differences between the groups. Three isoforms (23, 26, and 32 kDa) of pancreatic trypsin were detected by immunoblotting (Figure 3.9B) with the 32 kDa band likely corresponding to trypsinogen-3, the zymogen form of trypsin-3 from the pancreas (according to the antibody manufacturer's datasheet).

These 23 and 32 kDa isoforms were significantly elevated after hemorrhagic shock in the HS+SAL group. The 26 kDa isoform of pancreatic trypsin was present in all HS+SAL animals but only detected in one lung homogenate from the HS+ANGD group. No isoforms of trypsin were detected in heart or liver tissues by immunoblot.

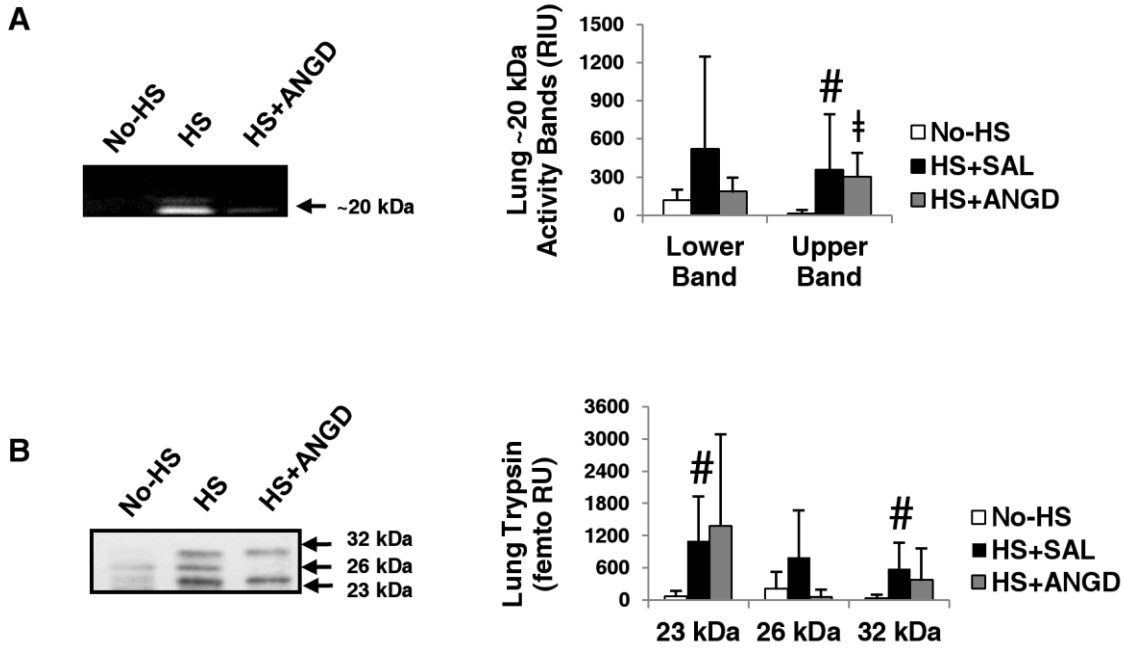

Figure 3.9 Pancreatic trypsin levels in lung tissue. (A) Two activity bands around 20 kDa were detected in lung homogenate by gel zymography. (B) Three isoforms of trypsin were detected in lung tissue homogenate using the femto ECL substrate. The 32 kDa band corresponds to the molecular weight of the trypsin precursor, trypsinogen, whereas the 23 and 26 kDa bands probably correspond to active forms of trypsin. N=5, 6, 6 rats per group for No-HS, HS+SAL, and HS+ANGD, respectively. #, $p<0.05$ vs. No-HS by Mann-Whitney test; ǂ, $p<0.05$ vs. No-HS by t-test.

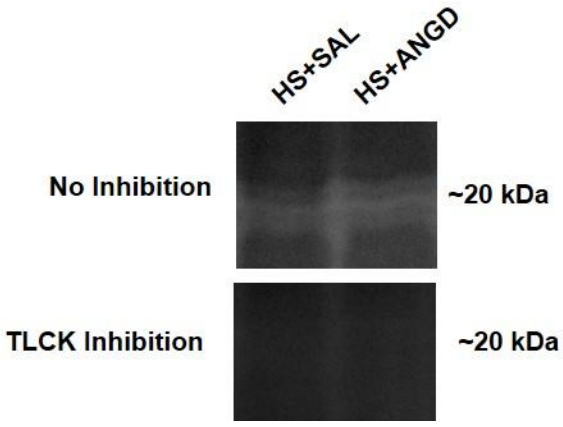

Figure 3.10 TLCK eliminates low molecular weight bands in lung. Low molecular weight bands in lung homogenates corresponding to serine proteases were undetectable after TLCK incubation during digestion of the gel.

3.4.4 MMP-9 Activity and Concentration

MMP-9 activity was significantly elevated after shock compared to pre-shock levels as detected by plate zymography with the MMP-1/9 specific substrate (Figure 3.11A). Gelatin gel zymography also revealed elevated MMP-9 bands in hemorrhagic shock that were undetectable in pre-shock plasma and peritoneal fluid (Figure 3.11B). Immunoblot results for total protein confirmed the presence of MMP-9 in post-HS plasma and peritoneal fluid regardless of pre-treatment with ANGD, but little to no MMP-9 before shock (Figure 3.11C). On average, activity of MMP-9 dimers was increased in the plasma of ANGD treated animals (undetectable in HS+SAL group).

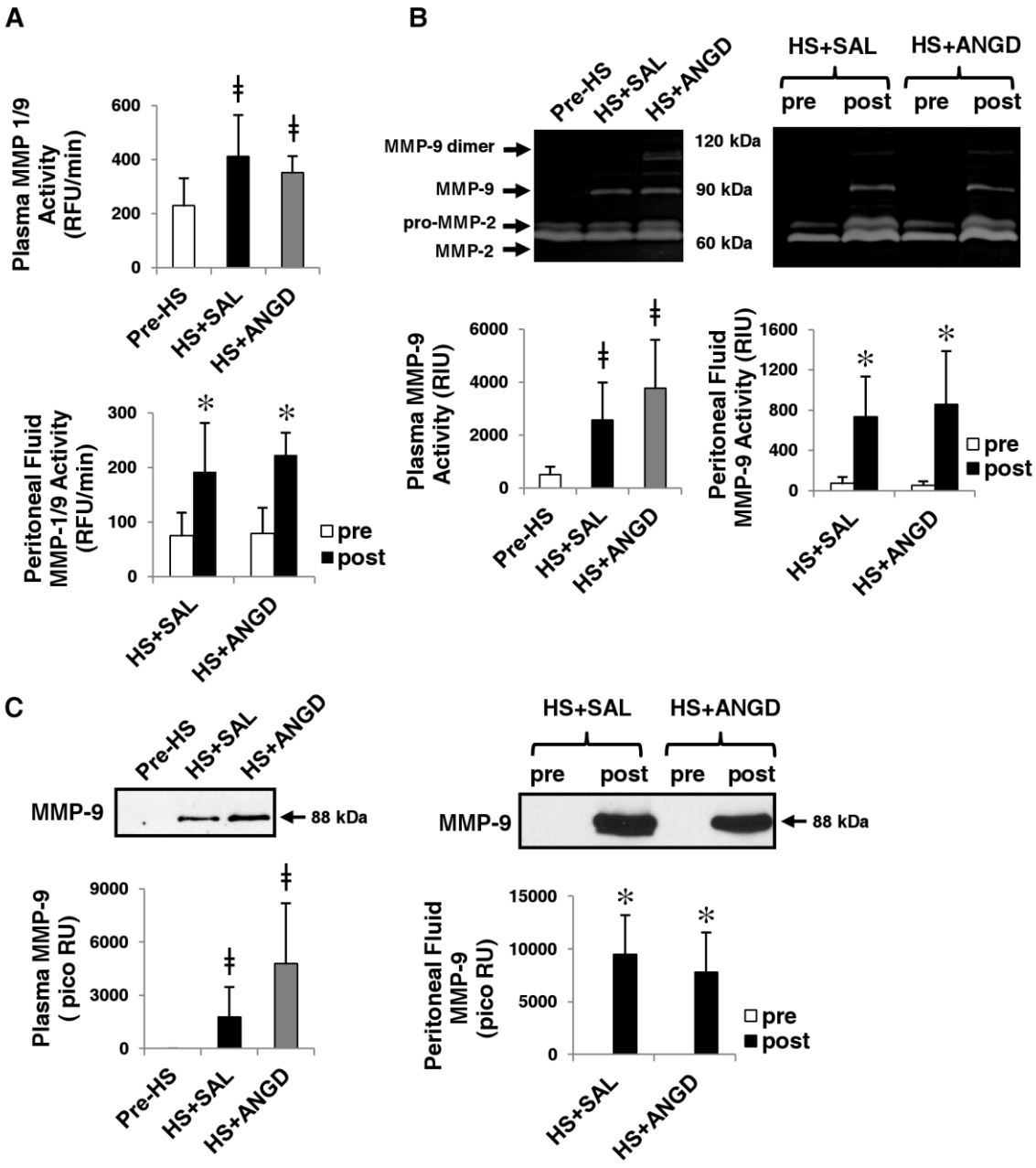

Figure 3.11 MMP-9 activity and levels in plasma and peritoneal fluid. (A) Plate zymography with MMP-1/9 substrate, (B) gelatin gel zymography, and (C) immunoblots for MMP-9 in plasma (left) and peritoneal fluid (right)**.** MMP-9 activity was elevated by both plate and gelatin gel zymography. There was no change in MMP-2. N=6, 5, 5 rats per group for plasma and N=6 rats per group for peritoneal fluid. Immunoblots were quantified in RU with the pico ECL substrates. ǂ, $p<0.05$ vs. Pre-HS group by t-test; *, $p<0.05$ by paired t-test comparing pre vs. post HS+SAL or HS+ANGD.

Lung, liver, and heart homogenates also had elevated MMP-9 activity levels after shock measured by gelatin gel zymography (Figure 3.12A). Immunoblot analysis revealed detectable MMP-9 in all organs after shock, although they were low and femto chemiluminescent detection of MMP-9 protein levels was necessary to visualize bands in the brain homogenate (Figure 3.12B).

Both pro-MMP-2 and MMP-2 were detected by gel zymography in all samples, but there were no differences between the groups after quantification (not shown).

Since MMP-9 can be directly activated by serine proteases, blood was collected every 15 minutes during the first hour of ischemia of HS+SAL animals to determine the order of appearance of MMP-9 and serine proteases in the plasma as measured by gelatin gel zymography and immunoblots. In all animals (N=3), bands at the molecular weight of active MMP-9 appeared in gelatin gel zymography and immunoblots by 15 minutes, whereas serine protease bands in the zymography or trypsin levels measured in the immunoblot did not distinctively appear during the first hour of ischemia, suggesting MMP release and initial activation in HS did not depend on entry of serine proteases into the circulation.

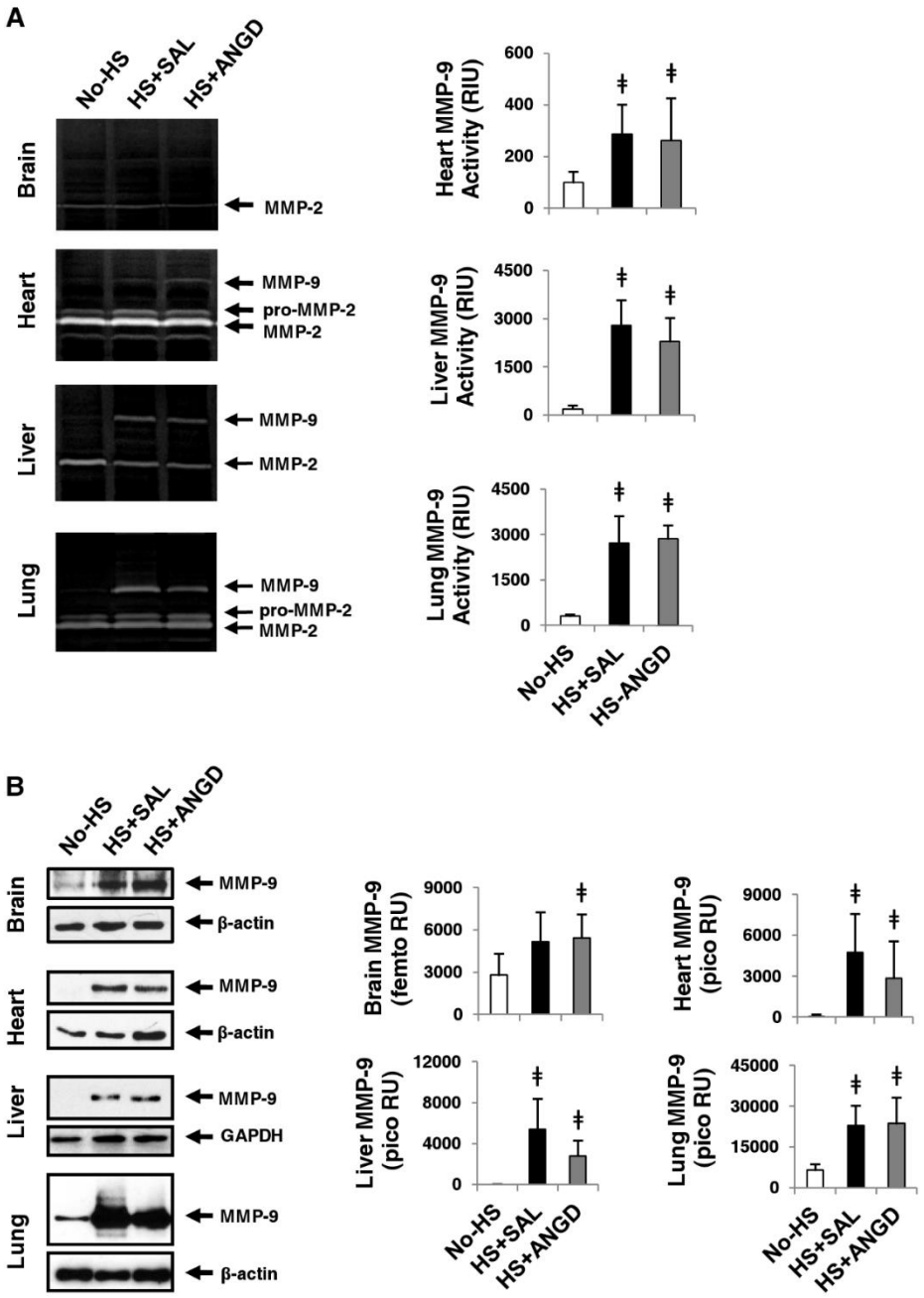

Figure 3.12 MMP-9 activity and levels in vital organs. (A) Gelatin gel zymography revealed increased levels of MMP-9 activity in the heart, liver, and lung (quantifications to the right) after hemorrhagic shock. There was no change in MMP-2. (B) Immunoblot detection of MMP-9 was upregulated in brain (bands detected with femto ECL substrate), heart, liver, and lung (bands detectable by pico ECL substrate). N=5 rats per group, ǂ, $p<0.05$ by t-test vs. No-HS.

3.5 DISCUSSION

3.5.1 SUMMARY

Following hemorrhagic shock, protease activities by trypsin-, chymotrypsin-, elastase-like enzymes, and MMP-9 were significantly elevated in plasma and peritoneal fluid when measured by specific small substrates and gelatin gel zymography. However, a general substrate, casein, served to detect elevated activity in peritoneal fluid but not in plasma. Immunoblotting confirmed the transport of pancreatic trypsin and the presence of increased levels of MMP-9 activity after hemorrhagic shock in the plasma, peritoneal fluid, and peripheral organs.

3.5.2 TRANSPORT OF SERINE PROTEASES INTO THE PERIPHERY

An active form of trypsin was detected in peritoneal fluid only after shock, indicating a direct penetration of trypsin into the peritoneal fluid from the intestinal lumen or pancreas. This evidence suggests that after hemorrhagic shock not only the intestinal mucosal barrier but also the entire intestinal wall in the rat may become permeable to shock mediators and to digestive enzymes [22]. Increased permeability could explain the presence of inflammatory mediators in the peritoneal fluid after shock [11].

Serine proteases may also be transported by the mesenteric lymph fluid and enter into the circulation via the thoracic duct (Figure 3.8). The lymph fluid mixes with the

blood before entering the capillary bed in the lung, one of the first organs to fail in shock [12,23]. While the increase in *plasma* trypsin levels after shock as measured by immunoblotting was moderate and non-significant (femto ECL substrate was necessary to visualize the bands by immunoblotting), three isoforms of pancreatic trypsin were detected in the lung homogenate and two of the three were significantly elevated in hemorrhagic shock (Figure 3.9). Thus, it is possible that pancreatic intestinal proteases are being transported through the lymphatic fluid and become entrapped in lung tissue, which is susceptible to increased vascular permeability allowing collection of plasma proteins in the tissue [24]. The inability to detect pancreatic trypsin in the liver may indicate that transport of intestinal proteases at this early stage of hemorrhagic shock predominantly is through the lymph fluid and peritoneal fluid rather than via the portal venous blood.

3.5.3 MMP Activities and Levels

Active MMP-9 was elevated in all samples after hemorrhagic shock, in line with reported events during ischemia-reperfusion in organs, including non-intestinal organs [25-28]. *De-novo* transcription of MMP-9 requires several hours and is less likely a major source at the two-hour reperfusion collection in the current study, than release of existing MMP-9. Given that endothelial cells, neutrophils, and monocytes are all sources of MMP-9 [29,30] and MMP-9 levels were all increased after the ischemia/reperfusion induced by hemorrhagic shock, MMP-9 may be activated by the ischemia associated with hemorrhagic shock rather than only by specific events in the intestine. This hypothesis is

supported by our finding that MMP levels are increased in plasma at 15 minutes of ischemia, while pancreatic proteases remain undetectable with current techniques in the plasma through the first hour of ischemia. Transport of the serine proteases may occur predominately during reperfusion, when the majority of injury during shock occurs, rather than during ischemia [31]. Since MMP-9 was not detected in the zymogen form in the plasma during the first hour of ischemia, it is less likely that serine proteases entering upon reperfusion would convert appreciable amounts of zymogen MMP-9 into its active form, though serine proteases may stimulate further MMP release. Our group has previously shown that MMPs in the ischemic intestinal wall are activated by trypsin entering from the intestinal lumen [6], so it is also possible that *additional* active MMP-9 from the intestine or pancreas could enter the circulation during reperfusion.

3.5.4 ANGD Reduces Neutrophil Accumulation but Not Protease Activity

ANGD in the intestinal lumen reduces protease activity in an ischemic intestine, morphological damage to the villi and systemic inflammation [8]. Other serine protease inhibitors with similar structure give similar protective effects when enterally administered [32]. Our results also show that gross morphological damage to the intestine and neutrophil infiltration in peripheral organs as measured by organ MPO levels are decreased with ANGD treatment.

However, at 2 hours after hemorrhagic shock ANGD had little effect on protease activities measured in compartments distant from the intestine (plasma, as well as lung, liver, heart, and brain homogenates). The limited effect may be due in part to the

ischemic pancreas acting as a source of plasma proteases that would not be affected by ANGD in the lumen of the intestine. This hypothesis is supported by the presence of a trypsinogen band in the lung and by the fact that the 26 kDa band of trypsin, the only band of trypsin detected in peritoneal fluid, was absent from all but one of the lung homogenates in the HS+ANGD group, while 23 kDa and 32 kDa (trypsinogen) bands were unaffected by intestinal ANGD treatment.

Enterally administered ANGD prevented organ neutrophil infiltration, but did not significantly lower protease activities. This evidence suggests that neutrophil infiltration is facilitated by the low flow state in conjunction with shock mediators other than circulating proteases. This hypothesis is supported by the limited efficacy in *acute* shock of ANGD given IV as opposed to administration into the intestinal lumen [33]. We hypothesize that there are multiple categories of shock mediators derived from digestive enzymes or their byproducts, which may enter into the intestinal wall and may be affected by enzyme inhibitor treatment in the lumen of the intestine. These mediators may cause distant organ injury after transport from the ischemic intestine via the circulation. Besides the digestive enzymes focused here, they include: 1) bioactive peptides formed by proteolytic cleavage of extracellular proteins in the intestine [34], 2) free fatty acids formed by digestive lipases acting on intestinal cells and/or dietary fat in the intestinal lumen, which may damage cells directly via a detergent mechanism [5,35], and 3) damage associated molecular pattern molecules (DAMPs) released from dead cells in the intestine (e.g. after free fatty acid-induced necrosis) [34]. It is possible that these latter mediator types may be involved in neutrophil infiltration into organs distant from the intestine in hemorrhagic shock.

ANGD in the lumen of the intestine also had the surprising effect of increasing plasma trypsin-like activity, as well as gelatinolytic activity in a band at the molecular weight of trypsin. Plasma trypsin protein concentration, however, as determined by immunoblot after HS was not different with saline versus with ANGD, suggesting that the presence of ANGD may have caused the trypsin that was crossing into the blood to become modified to a more active form or activate other trypsin-like enzymes of a similar molecular weight, rather than increasing the actual trypsin present.

3.5.5 Size of Protease Substrate Influences Digestion Potential

Both large and small protease substrates were tested in this study to compare their efficacies in detecting protease activity in plasma. Casein is a large globular substrate that can be collectively cleaved by multiple protease classes (serine proteases, MMPs, sulfhydryl, and acid proteases, etc.), making it a useful substrate for general detection of proteolytic activity. Though it is possible that, given a longer digestion time, plasma digested casein may yield an improved fluorescent signal, at 2 hours reperfusion only low levels, barely above those measured by buffer alone were observed. Despite this, differences could be detected between pre- and post-HS plasma when PMSF was used to block serine proteases. The remaining activity could be from MMPs such as MMP-9, which is increased after HS (Figure 3.11). However, casein was not able to detect a significant increase in overall activity in plasma after shock that was observed using smaller, more specific substrates.

Casein substrate may not be the optimal choice for detection of protease activity in shock plasma. The small peptide substrates were significantly cleaved despite levels of activity of only nanomolar concentrations of trypsin, chymotrypsin, and elastase, whereas casein was not able to detect differences before and after HS. These findings support the evidence that plasma protease inhibitors such as α_2-macroglobulin, α_1-antitrypsin, etc., only prevent pancreatic proteases from hydrolyzing larger globular proteins such as casein, but do not inhibit their activity on smaller substrates [18]. Instead, either the actual protein of interest should be used as a substrate, or in lieu of that, small peptide substrates alone or in combination with the hypothesized substrate may be better able to reveal the proteolytic potential in a given plasma sample.

The intestine is a key organ in the etiology of shock. If the release of mediators from the intestine is limited by ligation of the major mesenteric lymph vessels, both lung injury and mortality are reduced [12]. Several intestine-derived shock mediators have been proposed, but because of the presence of plasma protease inhibitors, digestive enzymes have mostly been discounted as potential shock mediators distant from the intestine itself. However, active proteases are capable of degrading surface receptors such as the insulin receptor or activating receptors such as the protease-activated receptors [14,36]. Furthermore, MMP-9 cleaves vascular endothelial cadherin, which is important to maintain endothelial permeability, and is disrupted during shock [37,38]. Cytokines pro-IL-1β and pro-TNFα are converted into their active form by MMP-9 and are involved in vascular inflammation during shock [39-42]. Though early neutrophil infiltration into organs distant from the intestine may not be affected by plasma, peritoneal, and organ protease activities, it is likely that later events in shock, such as

insulin resistance, may be linked to the action of proteases. Thus circulating proteases may represent a distinct damage mechanism. Organ failure in shock may be the result of the synergy of multiple damage mechanisms.

3.6 CONCLUSIONS

This investigation has shown that both serine and MMP proteolytic activity is increased early (2 hr ischemia/2 hr reperfusion) after shock in plasma, peritoneal fluid, and organs distant from the intestine, especially the lung, which is particularly vulnerable to damage during shock. The increase in protease presence and activities may contribute to the lethal progression of shock and may be a target for therapeutics.

Chapter 3 was published in PLoS ONE with the title "Protease activity increases in plasma, peritoneal fluid, and vital organs after hemorrhagic shock in rats" by Angelina E. Altshuler, Alexander H. Penn, Jessica A. Yang, Ga-Ram Kim, and Geert W. Schmid-Schönbein. The dissertation author is co-first author of this manuscript. Figures 3.3 and 3.4 were contributed by Alexander H. Penn. Figure 3.8 was contributed by Mr. Michael Richter.

3.7 REFERENCES

1. Trunkey DD. (1983) Trauma. accidental and intentional injuries account for more years of life lost in the U.S. than cancer and heart disease. among the prescribed remedies are improved preventive efforts, speedier surgery and further research. Sci Am 249: 28-35.

2. Tien H, Nascimento B,Jr, Callum J, Rizoli S. (2007) An approach to transfusion and hemorrhage in trauma: Current perspectives on restrictive transfusion strategies. Can J Surg 50: 202-209.

3. Bohlen HG, Hutchins PM, Rapela CE, Green HD. (1975) Microvascular control in intestinal mucosa of normal and hemorrhaged rats. Am J Physiol 229: 1159-1164.

4. Roumen RM, Hendriks T, Wevers RA, Goris JA. (1993) Intestinal permeability after severe trauma and hemorrhagic shock is increased without relation to septic complications. Arch Surg 128: 453-457.

5. Penn AH, Hugli TE, Schmid-Schönbein GW. (2007) Pancreatic enzymes generate cytotoxic mediators in the intestine. Shock 27: 296-304.

6. Rosario HS, Waldo SW, Becker SA, Schmid-Schönbein GW. (2004) Pancreatic trypsin increases matrix metalloproteinase-9 accumulation and activation during acute intestinal ischemia-reperfusion in the rat. Am J Pathol 164: 1707-1716.

7. Duncan ME, Richardson JP, Murray GI, Melvin WT, Fothergill JE. (1998) Human matrix metalloproteinase-9: Activation by limited trypsin treatment and generation of monoclonal antibodies specific for the activated form. Eur J Biochem 258: 37-43.

8. Mitsuoka H, Schmid-Schönbein GW. (2000) Mechanisms for blockade of in vivo activator production in the ischemic intestine and multi-organ failure. Shock 14: 522-527.

9. Penn AH, Schmid-Schönbein GW. (2011) Severe intestinal ischemia can trigger cardiovascular collapse and sudden death via a parasympathetic mechanism. Shock .

10. Shi HP, Liu ZJ, Wen Y. (2004) Pancreatic enzymes in the gut contributing to lung injury after trauma/hemorrhagic shock. Chin J Traumatol 7: 36-41.

11. Ishimaru K, Mitsuoka H, Unno N, Inuzuka K, Nakamura S, Schmid-Schönbein GW. (2004) Pancreatic proteases and inflammatory mediators in peritoneal fluid during splanchnic arterial occlusion and reperfusion. Shock 22: 467-471.

12. Deitch EA. (2010) Gut lymph and lymphatics: A source of factors leading to organ injury and dysfunction. Ann N Y Acad Sci 1207 Suppl 1: E103-11.

13. Mitsuoka H, Kistler EB, Schmid-Schönbein GW. (2000) Generation of in vivo activating factors in the ischemic intestine by pancreatic enzymes. Proc Natl Acad Sci U S A 97: 1772-1777.

14. DeLano FA, Schmid-Schönbein GW. (2008) Proteinase activity and receptor cleavage: Mechanism for insulin resistance in the spontaneously hypertensive rat. Hypertension 52: 415-423.

15. Largman C, Reidelberger RD, Tsukamoto H. (1986) Correlation of trypsin-plasma inhibitor complexes with mortality in experimental pancreatitis in rats. Dig Dis Sci 31: 961-969.

16. Malinoski DJ, Hadjizacharia P, Salim A, Kim H, Dolich MO, Cinat M, Barrios C, Lekawa ME, Hoyt DB. (2009) Elevated serum pancreatic enzyme levels after hemorrhagic shock predict organ failure and death. J Trauma 67: 445-449.

17. Aubry M, Bieth J. (1976) A kinetic study of the inhibition of human and bovine trypsins and chymotrypsins by the inter-alpha-inhibitor from human plasma. Biochim Biophys Acta 438: 221-230.

18. Kuroiwa K, Nakatsuyama S, Katayama K, Nagasawa T. (1989) Determination of alpha 2-macroglobulin-trypsin complex with a new synthetic substrate. Clin Chem 35: 2169-2172.

19. Whittam JH, Rosano HL. (1973) Effects of the freeze-thaw process on alpha amylase. Cryobiology 10: 240-243.

20. Chang M, Kistler EB, Schmid-Schönbein GW. (2012) Disruption of the mucosal barrier during gut ischemia allows entry of digestive enzymes into the intestinal wall. Shock 37: 297-305.

21. Richter M. (2012) Protease activity in mesenteric lymph following splanchnic arterial occlusion .

22. Sun Z, Wang X, Deng X, Lasson A, Wallen R, Hallberg E, Andersson R. (1998) The influence of intestinal ischemia and reperfusion on bidirectional intestinal barrier permeability, cellular membrane integrity, proteinase inhibitors, and cell death in rats. Shock 10: 203-212.

23. Watkins AC, Caputo FJ, Badami C, Barlos D, Xu da Z, Lu Q, Feketeova E, Deitch EA. (2008) Mesenteric lymph duct ligation attenuates lung injury and neutrophil activation after intraperitoneal injection of endotoxin in rats. J Trauma 64: 126-130.

24. Staub NC. (1981) Pulmonary edema due to increased microvascular permeability. Annu Rev Med 32: 291-312.

25. Kunugi S, Shimizu A, Kuwahara N, Du X, Takahashi M, Terasaki Y, Fujita E, Mii A, Nagasaka S, Akimoto T, Masuda Y, Fukuda Y. (2010) Inhibition of matrix metalloproteinases reduces ischemia-reperfusion acute kidney injury. Lab Invest .

26. Chen W, Hartman R, Ayer R, Marcantonio S, Kamper J, Tang J, Zhang JH. (2009) Matrix metalloproteinases inhibition provides neuroprotection against hypoxia-ischemia in the developing brain. J Neurochem 111: 726-736.

27. Waldow T, Witt W, Buzin A, Ulmer A, Matschke K. (2009) Prevention of ischemia/reperfusion-induced accumulation of matrix metalloproteinases in rat lung by preconditioning with nitric oxide. J Surg Res 152: 198-208.

28. Lalu MM, Pasini E, Schulze CJ, Ferrari-Vivaldi M, Ferrari-Vivaldi G, Bachetti T, Schulz R. (2005) Ischaemia-reperfusion injury activates matrix metalloproteinases in the human heart. Eur Heart J 26: 27-35.

29. Doerner AM, Chen LY, Ye RD, Yong J, Huang S, Pan ZK. (2011) Cell type-specific release of matrix-metallo-proteinase-9 by bacterial chemoattractant in human blood phagocytic leukocytes. Int J Clin Exp Med 4: 67-73.

30. Taraboletti G, D'Ascenzo S, Borsotti P, Giavazzi R, Pavan A, Dolo V. (2002) Shedding of the matrix metalloproteinases MMP-2, MMP-9, and MT1-MMP as membrane vesicle-associated components by endothelial cells. Am J Pathol 160: 673-680.

31. Rushing GD, Britt LD. (2008) Reperfusion injury after hemorrhage: A collective review. Ann Surg 247: 929-937.

32. Fitzal F, DeLano FA, Young C, Rosario HS, Schmid-Schönbein GW. (2002) Pancreatic protease inhibition during shock attenuates cell activation and peripheral inflammation. J Vasc Res 39: 320-329.

33. Deitch EA, Shi HP, Lu Q, Feketeova E, Xu DZ. (2003) Serine proteases are involved in the pathogenesis of trauma-hemorrhagic shock-induced gut and lung injury. Shock 19: 452-456.

34. Davis GE. (2010) Matricryptic sites control tissue injury responses in the cardiovascular system: Relationships to pattern recognition receptor regulated events. J Mol Cell Cardiol 48: 454-460.

35. Penn AH, Schmid-Schönbein GW. (2008) The intestine as source of cytotoxic mediators in shock: Free fatty acids and degradation of lipid-binding proteins. Am J Physiol Heart Circ Physiol 294: H1779-92.

36. Soh UJ, Dores MR, Chen B, Trejo J. (2010) Signal transduction by protease-activated receptors. Br J Pharmacol 160: 191-203.

37. Navaratna D, McGuire PG, Menicucci G, Das A. (2007) Proteolytic degradation of VE-cadherin alters the blood-retinal barrier in diabetes. Diabetes 56: 2380-2387.

38. Todd TR, Baile E, Hogg JC. (1978) Pulmonary capillary and permeability during hemorrhagic shock. J Appl Physiol 45: 298-306.

39. Schonbeck U, Mach F, Libby P. (1998) Generation of biologically active IL-1 beta by matrix metalloproteinases: A novel caspase-1-independent pathway of IL-1 beta processing. J Immunol 161: 3340-3346.

40. Gearing AJ, Beckett P, Christodoulou M, Churchill M, Clements JM, Crimmin M, Davidson AH, Drummond AH, Galloway WA, Gilbert R. (1995) Matrix metalloproteinases and processing of pro-TNF-alpha. J Leukoc Biol 57: 774-777.

41. Zingarelli B, Squadrito F, Altavilla D, Calapai G, Di Rosa M, Caputi AP. (1994) Role of tumor necrosis factor-alpha in acute hypovolemic hemorrhagic shock in rats. Am J Physiol 266: H1512-5.

42. Sato H, Kasai K, Tanaka T, Kita T, Tanaka N. (2008) Role of tumor necrosis factor-alpha and interleukin-1beta on lung dysfunction following hemorrhagic shock in rats. Med Sci Monit 14: BR79-87.

Chapter 4

Damage to Endothelial Surface Receptors after Hemorrhagic Shock

4.1 Introduction

Surface receptors on the endothelial cells have an essential role in regulating vascular permeability and responding to signals transported through the circulation. Since there is a possibility for proteolytic exposure in the plasma to key extracellular components after shock, we have chosen to study several classes of endothelial extracellular proteins.

4.1.1 Functions of VEGFR-2 and VEGFR-3

The receptor VEGFR-2 is a type III kinase receptor important in vascular endothelial cell survival, permeability, migration, and proliferation [1,2]. The extracellular region contains seven immunoglobulin-like dom0ains connected to a short

transmembrane domain to the intracellular region containing the tyrosine kinase domain [3]. When VEGFR-2 is inhibited, cell survival decreases [4].

In addition, VEGFR-2 regulates inflammatory genes like the transcription factor NFκB, which controls the transcription of DNA in response to shear stress [5]. VEGFR-2 is a mechanosensor important for endothelial cell's response to flow patterns [6]. Shear stress activates the VEGFR-2 receptor by phosphorylation and induces VE-cadherin-β-catenin-VEGFR-2 complex formation [7]. Blocking VEGFR-2 by an inhibitor disrupts the shear-induced translocation of NFκB [8], and endothelial cells do not align to the shear stress when VEGFR-2 is proteolytically cleaved [9]. While the soluble VEGFR-2 receptor has not been detected in critical care patients, the soluble receptor has been identified in obesity and correlated to incidence of diabetes [10].

The agonist VEGF can bind to the VEGFR-2 receptor to induce signaling and proliferation [11]. Under hypoxic conditions, VEGF is released to initiate the formation of new blood vessels to aid in the re-oxygenation of tissues [12]. VEGF stimulation induces phosphorylation of VE-cadherin, which promotes loss of endothelial junctions [13]. Gene microarray studies on pigs after hemorrhage and resuscitation have found that hypoxia inducing factor genes are upregulated which directly stimulate the expression of VEGF [14].

Similar to VEGFR-2 in vascular endothelial cells, lymphatic endothelial cells express VEGFR-3 [15]. Though less work has been completed on this receptor, especially in the context of shock, it may also be susceptible to proteolytic breakdown since there is elevated protease activity in the lymph following intestinal ischemia as presented in Chapter 3.

To date, there have been no studies on the effect of hemorrhagic shock on either the VEGFR-2 or VEGFR-3 receptor in organs that are susceptible to injury such as the lung.

4.1.2 VE-Cadherin in Ischemic Conditions

Vascular endothelial cadherin (VE-cadherin) is important in maintaining vascular stability of the endothelium [16]. The protein forms adhesive trans-dimers between neighboring cells [17]. VE-cadherin is especially important in cell-cell adhesion in the lung endothelium [18]. Furthermore, deletion of VE-cadherin results in an increase in vascular permeability that impairs endothelial cell survival [19].

In ischemia, the junctional properties of VE-cadherin can be degraded by proteases such as neutrophil elastase [20]. Therefore, this protein's integrity may be compromised from an increase in protease activity following hemorrhagic shock.

4.1.3 Insulin Receptor and Insulin Resistance

The insulin receptor is a transmembrane tyrosine kinase composed of two alpha and two beta subunits [21]. The insulin receptor binds the hormone insulin, which activates the glucose transporter-4 to uptake glucose into the cell [22]. Once glucose enters the cell, it can be either stored or broken down. When there is an interference with this pathway, glucose remains in the blood causing hyperglycemia (high plasma glucose).

While the most frequent discussion about insulin resistance is in the context of cardiovascular disease and metabolic syndrome, hyperglycemia also has been documented in shock and the critically ill patients [23-25]. The incidence of diabetes induced in hospitalized patients is between 12 and 25% [26]. Median insulin doses administered to patients is higher in non-survivors [27] due to their lack of response to standard doses. Increasing insulin sensitization is hypothesized to be a more effective way to treat patients [28]. Some previous studies have linked cytokines or free fatty acids to reduced glucose metabolism by impairing the insulin receptor function [29,30].

A variety of ischemic and hypotensive organs have displayed insulin resistance [31-34]. Glucose metabolism has been studied in hypotension where both glucose and amino acids levels increase once the pressure drops below 90 mmHg [35]. Glucose metabolism is influenced by catecholamines and the degree of fasting in the animal [36,37]. After hemorrhage, plasma glucose levels can double rapidly [38].

The insulin receptor signaling pathway is disrupted to a greater degree in liver and muscle tissue of older animals [25]. Ischemic livers have decreased AKT phosphorylation and insulin tyrosine phosphorylation [39]. Of the signaling methods described in hypotension and ischemia, there exists no conclusive mechanism that explains why insulin receptor signaling is impaired. Proteases may be involved in the extracellular degradation of the insulin receptor in shock, like seen in hypertension [40,41].

Soluble insulin receptors in the plasma can be cleaved by a protease upon stimulation by insulin, which may be blocked by administration of plasma protease inhibitors, including anti-alpha trypsin [42,43]. Soluble insulin receptors measured in

human plasma samples were associated with Type II diabetes occurrences [44]. Type II diabetes which can disappear with lifestyle changes, diabetes symptoms in critical care patients can also subside if the patient recovers.

4.2 Chapter Aims

Endothelial dysfunctions in the form of increased vascular permeability and insulin resistance occur in critically ill patients [45,46]; however, the levels of these proteins that regulate these events have not been investigated in the context of hemorrhagic shock. Endothelial cells directly interface with active proteases present in the blood following HS, as demonstrated in Chapter 3. The objective of this Chapter is to present measurements of the receptor levels that influence endothelial permeability and regulate blood glucose levels. I hypothesize that the levels of VEGFR-2, VE-cadherin, and the insulin receptor will change after hemorrhagic shock because they are exposed to non-selective protease activity in the plasma (Figure 4.1).

Due to availability, we had to change the choice of anesthetic in our experiments. This chapter will also discuss the development of a model that matches the outcomes of xylazine/Nembutal anesthesia with ketamine/xylazine anesthesia. This new model will be used in subsequent Chapters.

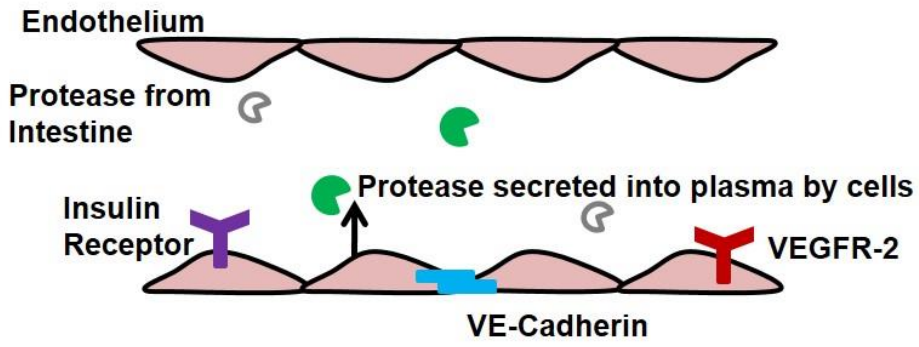

Figure 4.1 Hypothesis summary for receptor degradation by proteases. Protease activity in the plasma increases after shock. The elevated protease activity may attack extracellular protein structures on the surface of the endothelium.

4.3 METHODS

4.3.1 ANIMAL MODELS

The animal protocols were reviewed and approved by the University of California, San Diego Animal Subjects committee (Protocol Number S01113).

4.3.1.1 HEMORRHAGIC SHOCK WITH NEMBUTAL/XYLAZINE

Hemorrhagic shock was performed the same as described in Section 3.3.1.

4.3.1.2 HEMORRHAGIC SHOCK WITH KETAMINE/XYLAZINE

Male Wistar or Sprague Dawley rats were administered general anesthesia (xylazine, 4 mg/kg; ketamine 75 mg/kg IM) and euthanized by infusion of B-Euthanasia IV (120 mg/kg). Following general anesthesia, the femoral artery and vein were cannulated.

Animals were injected with saline into the lumen of their intestine as described in Section 3.3.1. The animals were heparinized to minimize clotting in catheters and in shed blood (1 U/ml calculated blood volume IV assuming 6 ml blood volume per 100 g total body weight) before onset of hemorrhage. MAP was reduced to either 30 mmHg or 35 by withdrawing blood through the venous catheter (0.4 ml/2 min or 0.4 ml/min) with a 5 ml syringe. The initial 1 ml of blood drawn was collected, centrifuged (1000 g, 5 min),

and the plasma was immediately frozen at -80 ºC. The pressure was monitored and adjusted by withdrawal/return of blood over the 90 or 120 minute ischemic period. At the end of ischemia, the shed blood was returned to the animal (0.5 ml/min) plus 1 ml of saline (to replace the 1 ml of blood collected before shock). The animals remained anesthetized and were observed in the reperfusion phase for 2 or 3 hours after the initiation of the return of shed blood. Select animals had 100 µl samples of blood collected hourly during the course of HS.

Gross morphology images of the intestine were captured at the end of the reperfusion period. Post-hemorrhagic shock blood was collected through the arterial catheter, spun (1000 g, 5 min), and the plasma was immediately frozen at -80 ºC. The animals were euthanized and pieces of lung were snap frozen for homogenization.

4.3.2 IMMUNOBLOTTING

Tissues (lung, liver, heart, or brain) were homogenized in lysis buffer containing protease cocktail (1:100, ThermoScientific) diluted to load 40 µg of protein per well and denatured by boiling with the reducing agent β-mercaptoethanol in sample loading buffer (BioRad).

Samples were then separated using an SDS-PAGE gel (8% running, 4% stacking) and transferred onto polyvinylidene fluoride membrane (Biorad). The membrane was blocked with 5% bovine serum albumin in tris-buffered saline tween-20 (TBS-T). Primary antibodies against extracellular VE-Cadherin (C-19, 1:1000; sc-6458), VEGFR-2 (S-20; 1:1000; sc-48161), VEGFR-3 (C-20; 1:1000; sc-321), insulin receptor α-subunit

against the extracellular domain (C-20, 1:1000, sc-710, Santa Cruz Biotechnology, Santa Cruz, CA), insulin receptor β-subunit against the intracellular domain (1:1000, sc-711, Santa Cruz Biotechnology), and β-actin (1:2000, sc-130301, Santa Cruz Biotechnology) were diluted in 1% BSA in TBS-T and incubated overnight at 4º C on a rotary shaker. Primary antibodies were washed three times for ten minutes with TBS-T before application of anti-goat, -rabbit, or -mouse secondary antibodies (Santa Cruz Biotechnology). The bands were detected using chemiluminescence pico substrate (Themo Scientific).

4.3.3 Immunohistochemistry of Insulin Receptor in Tissues

For detection of the insulin receptor subunits, fixed tissues were permeabilized with 0.1% Triton X-100 for 5 minutes and washed twice with TBS-T (0.1%). Peroxidase activity was blocked by incubating with 0.5% hydrogen peroxide for 10 minutes followed by two washes twice with TBS. Tissues were blocked with 5% goat serum for one hour. Primary antibodies were diluted 1:100 in 5% goat serum in TBS-T against insulin receptor α-subunit and β-subunit incubated overnight on a rotary shaker at 4 ºC. Irrelevant normal rabbit antibodies and no primary controls were run simultaneously for each tissue. After incubation, sections were washed three times with TBS-T. HRP conjugated anti-rabbit antibody (Santa Cruz Biotechnology) was diluted in TBS-T with 1% goat serum 1:400 and applied for 1 hour at room temperature. Sections were washed three times in TBS-T before being developed with ImmPact Dab (Vector Labs). Tissues

were washed in water and dehydrated with an ethanol gradient and dried before mounting with hard set mounting media (Vector Labs).

4.3.4 Statistical Analysis

Results are summarized as mean±SEM. For comparisons, a t-test with Bonferroni correction were used and $p<0.025$ was considered significant.

4.4 Results

4.4.1 Protein Degradation after HS with Xylazine/ Nembutal

After hemorrhagic shock, the lung junctional protein VE-cadherin was reduced irrespective of the luminal treatment with ANGD (Figure 4.2). The vascular endothelial survival receptor, VEGFR-2 and the lymphatic endothelial receptor VEGFR-3 were also reduced following shock in lung homogenates (Figure 4.2).

Neither the alpha (extracellular) nor beta (intracellular) insulin receptor subunits were degraded in the lung following hemorrhagic shock (Figure 4.3A). However, the precursor bands which form at higher molecular weights during insulin receptor synthesis were significantly reduced in the HS+SAL and HS+ANGD animals compared to the No-HS animals (Figure 4.3A). Histological sections of a collapsed lung revealed that the labeling for the alpha and beta subunits of the insulin receptor matched the immunoblot

results and were unchanged (Figure 4.3B). The heart, liver, and brain had no changes in the alpha (extracellular) and beta (intracellular) insulin receptor subunits (Figure 4.4)

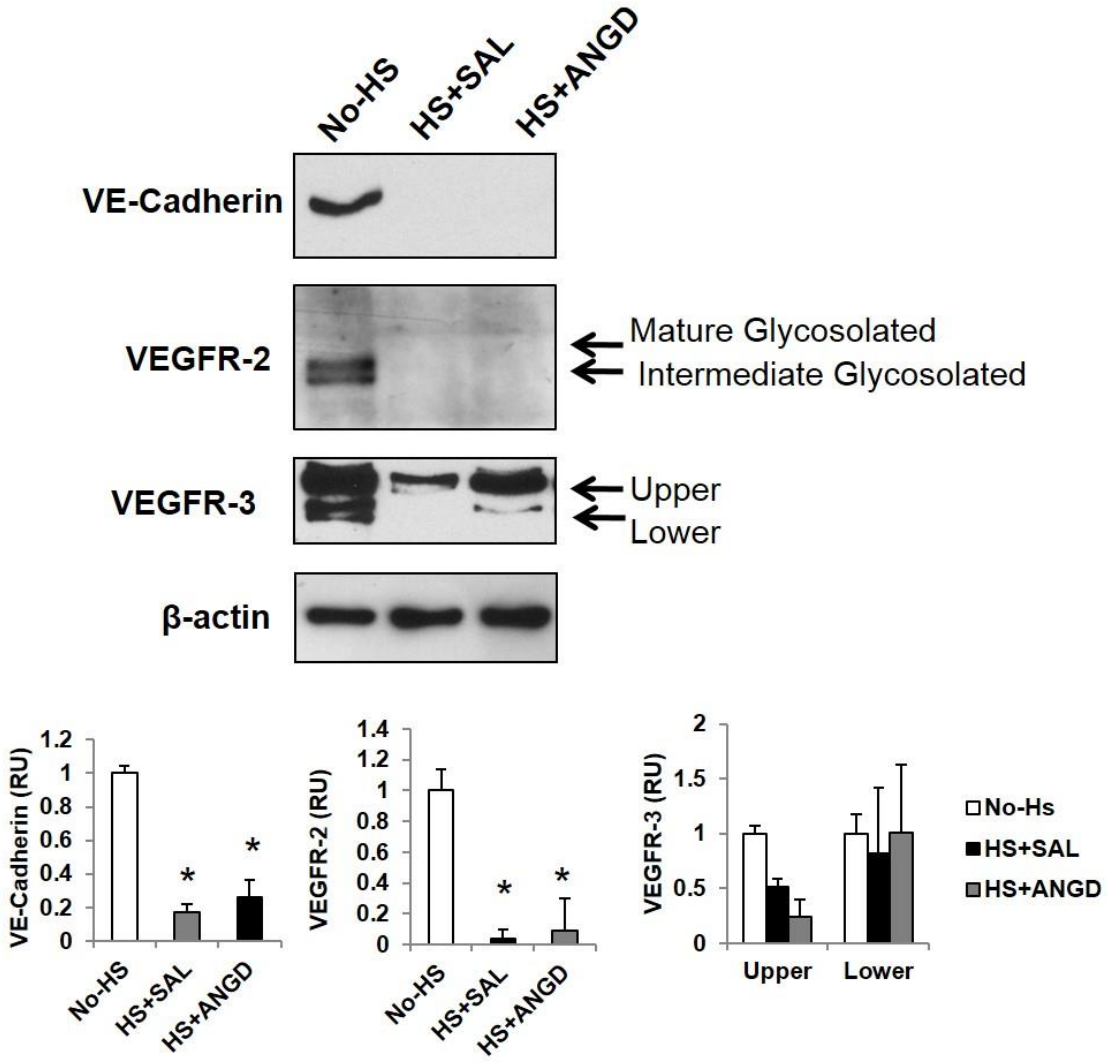

Figure 4.2 Endothelial protein degradation in the lung. VE-cadherin, VEGFR-2, and VEGFR-3 all decreased after HS in the lung regardless of whether ANGD was present in the lumen of the intestine. *, $p<0.025$ by t-test with Bonferroni correction. N=5 rats/group for No-HS and N=6 rats/groups for HS+SAL and HS+ANGD. Bar graphs show mean±SEM.

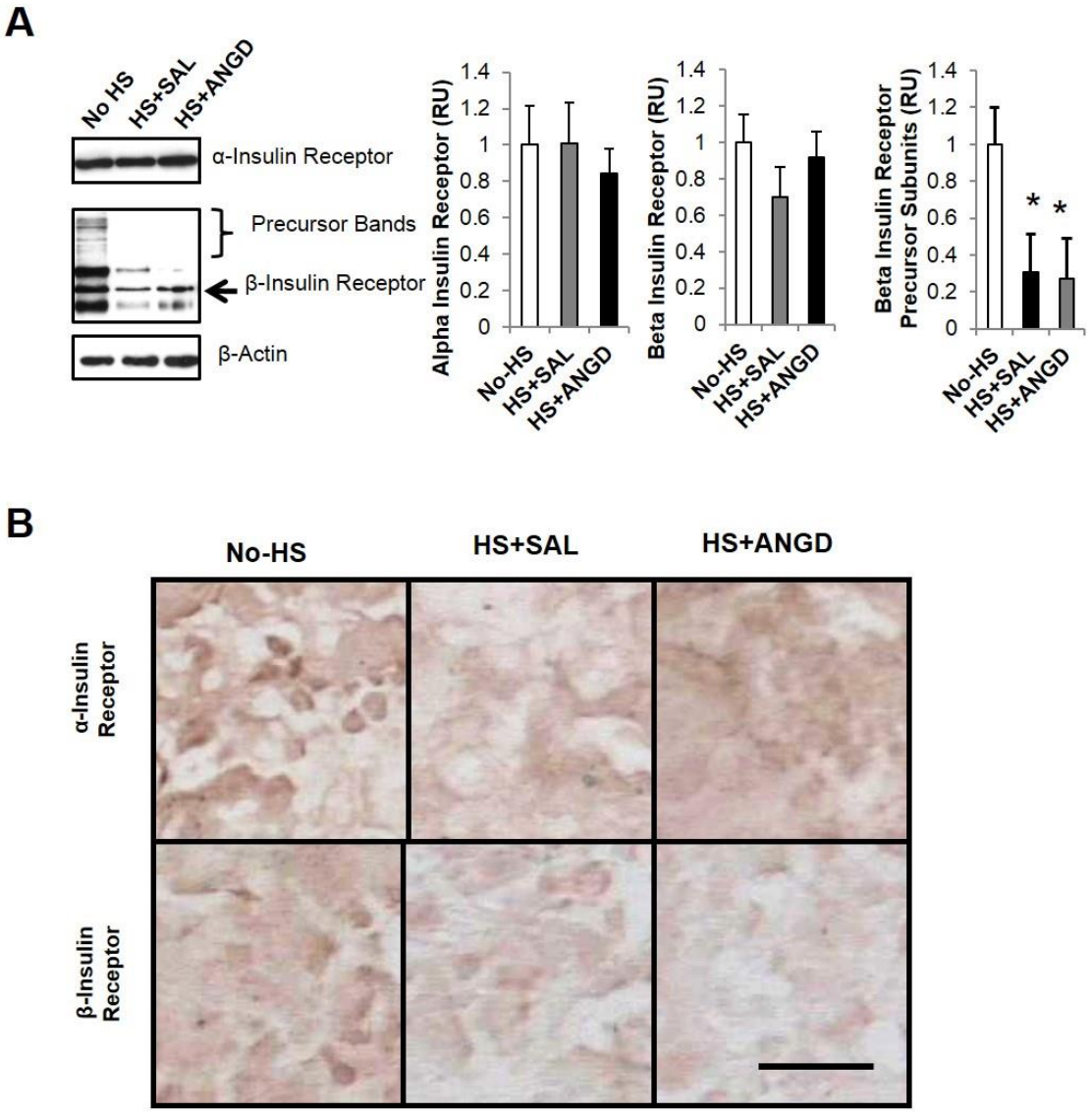

Figure 4.3 Insulin receptor levels before and after shock. (A) The α-insulin receptor subunit (extracellular domain) and the β-insulin receptor subunit (intracellular domain) remained unchanged after hemorrhagic shock. The precursor insulin receptor subunits decreased in both HS+SAL and HS+ANGD animals. *, $p<0.025$ by t-test with Bonferroni correction. N=5 rats/group for No-HS and N=6 rats/groups for HS+SAL and HS+ANGD. Bar graphs show mean±SEM. (C) Representative images of collapsed lung tissue for the insulin receptor subunits. Length bar=5 μm.

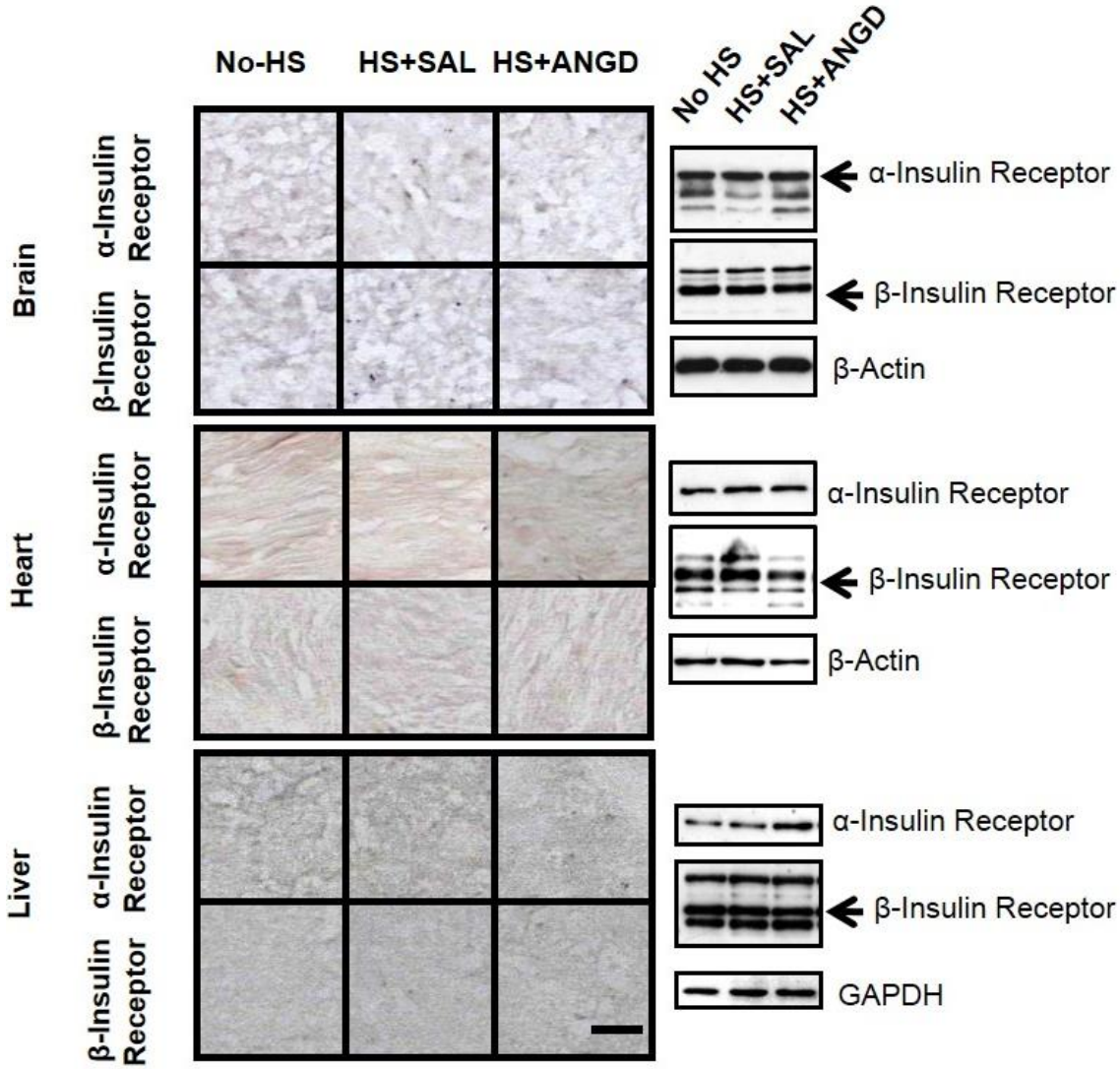

Figure 4.4 Insulin receptor levels in brain, heart and liver. The α-insulin receptor subunit (extracellular domain) and the β-insulin receptor subunit (intracellular domain) remained unchanged after hemorrhagic shock in brain, heart, and liver tissues. Length bar = 5 μm.

4.4.2 Protein Degradation after HS with Ketamine/Xylazine

Due to lack of availability of Nembutal, the anesthetic used for hemorrhagic shock studied was changed from xylazine/Nembutal to xylazine/ketamine. Our first attempt to repeat these previous studies with Nembutal was to replicate the same conditions (remove shed blood at a rate of 0.2 ml/min; 2 hr ischemia at 35 mmHg, 2 hour reperfusion) using male Wistar rats. In the presence of ketamine, there was hardly any intestinal damage after HS (N=2) (Figure 4.5A). Plasma samples were collected each hour of the experiment and like Chapter 3, MMP-9 activity and levels increased by the first hour of ischemia and remained elevated (Figure 4.5B). The levels of VE-cadherin remained unchanged compared to the No-HS animal (Figure 4.5C).

Since organ damage with the xylazine/ketamine did not reach a sufficient extent to determine the benefit or any intervention, we reduced the pressure during ischemia from 35 mmHg to 30 mmHg for two hours followed by a two hour reperfusion period. The final pressure of at the end of the reperfusion period was 50 mmHg. Under these conditions, the intestine was severely damaged after HS as indicated by bleeding into the lumen of the intestine (Figure 4.6A). VE-cadherin and VEGFR-2 were also degraded during ischemia (Figure 4.6B), but not to the same extent as the previous Nembutal studies where the proteins were completely eliminated in the majority of the animals that underwent hemorrhagic shock.

Since different strains of rats can have different outcomes after HS [47], we decided to switch to Sprague Dawley rats so that we could condense the ischemic period while achieving sufficient organ injury to the intestine and lung. Intestinal injury after

hemorrhagic shock was achieved with a 90 min ischemic period at 30 mmHg (remove blood at a rate of 0.4 ml/min) followed by a 3 hour reperfusion period (Figure 4.7A). The levels of VE-cadherin and VEGFR-2 degraded in the lung tissue after hemorrhagic shock with this model (Figure 4.7B).

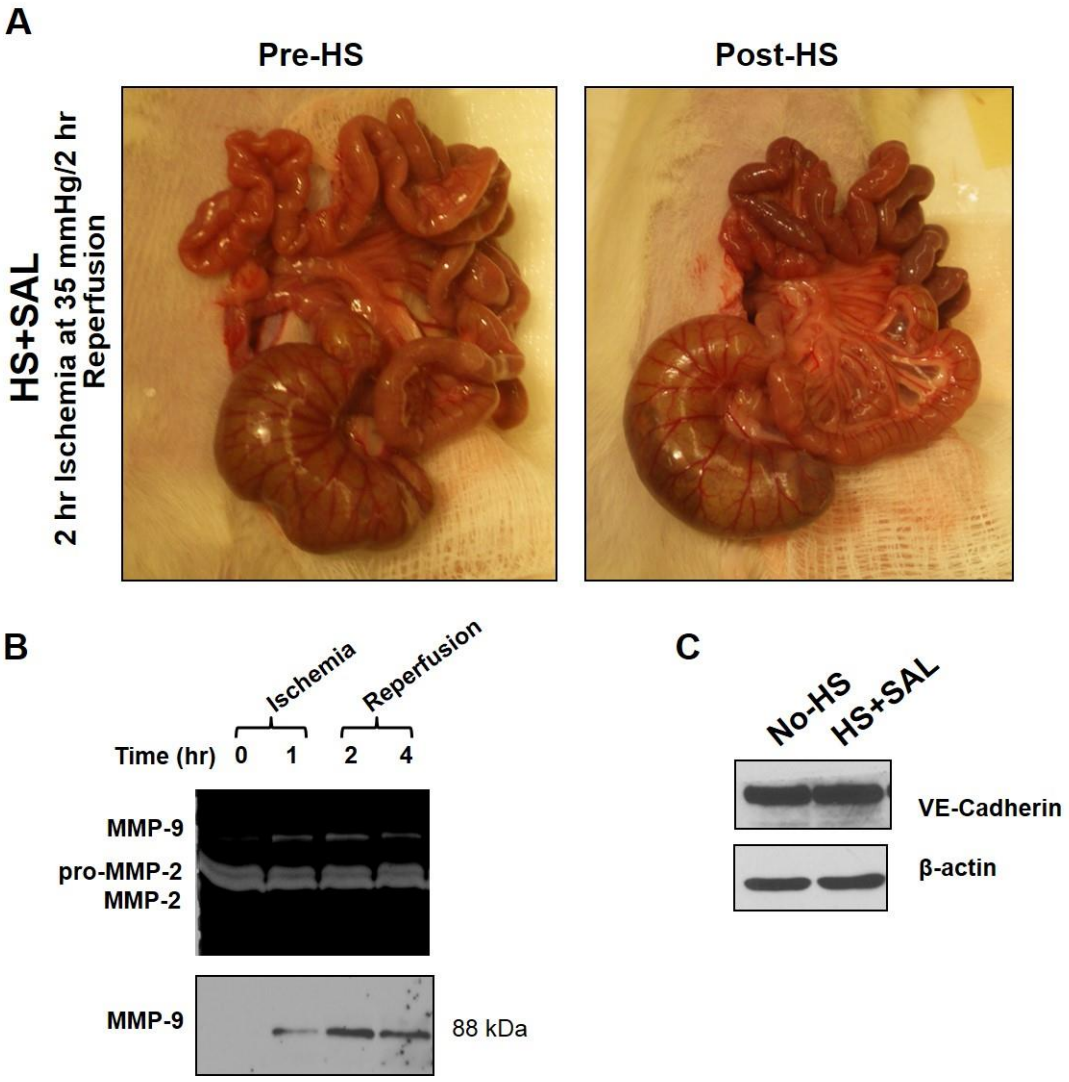

Figure 4.5 Shock parameters with ketamine/xylazine for 2 hr ischemia at 35 mmHg, 2 hr reperfusion model in Wistar rats. (A) Gross morphology of the intestine before and after shock showed little damage or lesions when ketamine/xylazine anesthetic was used. (B) MMP-9 activity increases during the first hour of ischemia and remains elevated throughout shock. (C) VE-cadherin levels remained the same before and after HS+SAL.

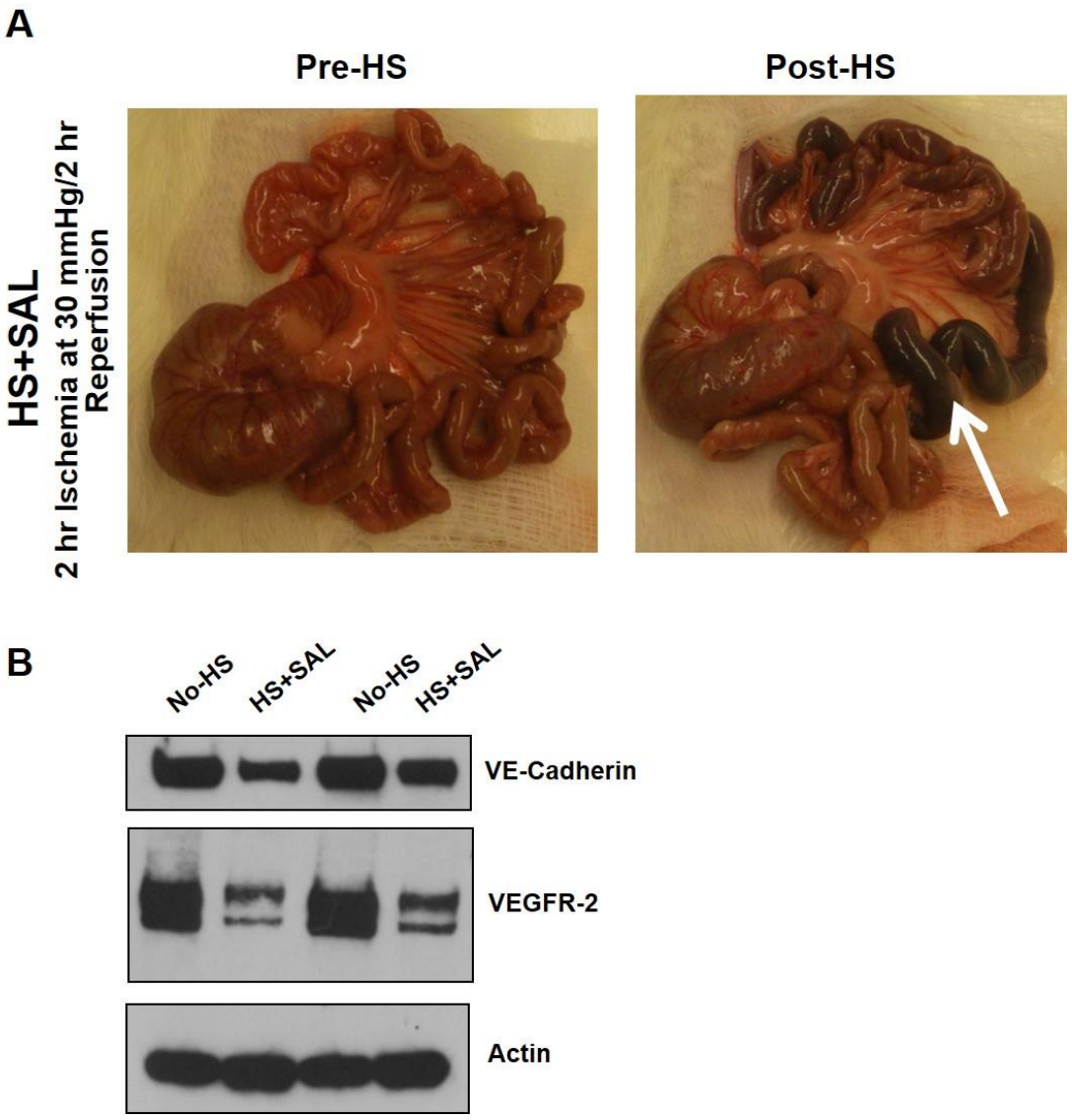

Figure 4.6 Shock parameters with ketamine/xylazine for 2 hr ischemia at 30 mmHg, 2 hr reperfusion model in Wistar rats. (A) Visible signs of hemorrhage (white arrow) developed in the intestine after shock when the ischemia pressure was reduced to 30 mmHg. (B) Both VE-cadherin and VEGFR-2 in the lung degraded after HS.

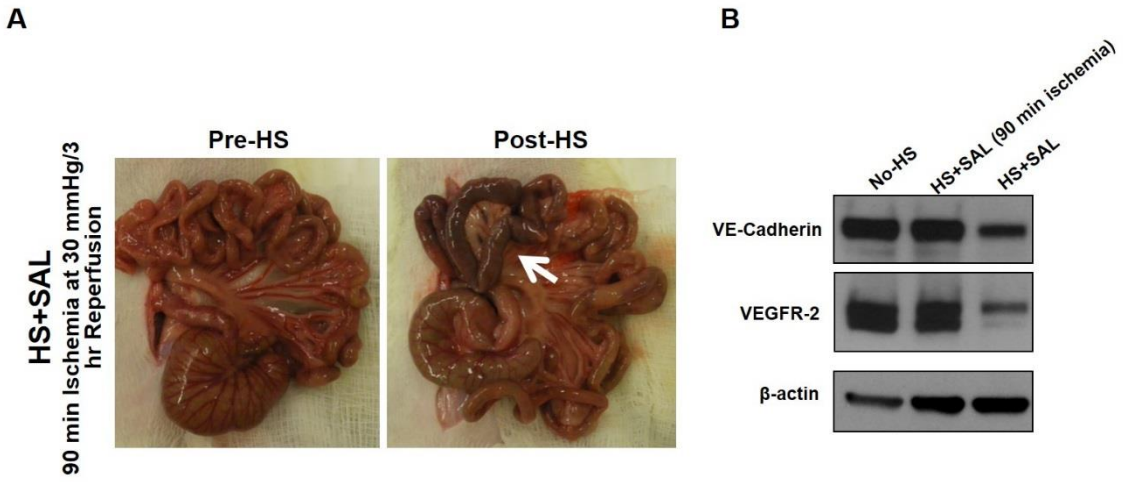

Figure 4.7 Hemorrhagic shock outcomes with ketamine/xylazine for 90 min ischemia at 30 mmHg, 3 hr reperfusion model in Sprague Dawley rats. (A) Visible signs of hemorrhage (white arrow) developed in the intestine after shock. (B) Both VE-cadherin and VEGFR-2 in the lung did not degrade until the full course of reperfusion occurred.

4.5 Discussion

4.5.1 Summary

These studies indicate that key endothelial proteins degrade during hemorrhagic shock including VE-cadherin, VEGFR-2, and VEGFR-3, but not the insulin receptor subunits. The choice of anesthetic influences the severity of shock. Intestinal injury using ketamine/xylazine was not as severe as the previously used xylazine/Nembutal. Lastly, the severity of protein degradation for VE-cadherin and VEGFR-2 is associated with the degree of shock severity.

4.5.2 Degradation of VE-Cadherin

VE-cadherin degraded in hemorrhagic shock regardless of luminal inhibition with ANGD (Figure 4.2). VE-cadherin can be proteolytically degraded by MMPs [48], which remained activated despite the ANGD treatment. The severity of the ischemic conditions also dictates the degree of degradation since animals with little intestinal damage also had preservation of their VE-cadherin levels (Figure 4.5), but once the organ injury surpassed a certain threshold, degradation occurred (Figure 4.6). This suggests that protein degradation is correlated with the severity of shock injury. Reperfusion injury causes the reduction of VE-cadherin. Additionally, proteases may be recycled and internalized by caspases [49,50], which may be stimulated during reperfusion. If the junctional proteins like VE-cadherin disassemble, vascular permeability increases and tissue homeostasis is compromised.

4.5.3 Degradation of VEGFR-2 and VEGFR-3

Both the vascular and lymphatic survival receptors VEGFR-2 and VEGFR-3 were reduced in the lung following hemorrhagic shock (Figure 4.3 and Figure 4.7). Since the VEGFR-2 receptor is essential for tissue repair, permeability regulation and endothelial cell survival [51], the reduction in VEGFR-2 impairs cells signaling. The difference between reversible and irreversible shock could be linked to the ability for this receptor to function and stimulate endothelial growth and repair.

4.5.4 Insulin Receptor Levels

Despite the increase in protease activity in the plasma following hemorrhagic shock, the insulin receptor was not degraded. This deviates from similar situations where there was an increase in protease activity and a decrease in extracellular insulin receptor density [9,40]. The chronic exposure to proteases may differ from the acute situation observed in hemorrhagic shock. The reduction in insulin receptor density may require prolonged exposure to protease activity greater than the two hour reperfusion period in this model.

The insulin receptor is synthesized in the precursor form before it is post processed into separate alpha and beta subunits and linked together by disulfide bonds [42,52]. This form of the receptor decreased after shock in the lung tissue (Figure 4.3). The degradation could be interpreted several ways. First, the protein could be made into the mature form of alpha and beta subunits of the insulin receptor to replace receptors that may be degraded. However, if this were the case, then the beta receptor would be expected to also increase as more alpha subunits are replaced. Alternatively, if the insulin receptor is damaged, the entire protein could be transported from the membrane and recycled. The precursor bands could possibly decrease because the cells are in an ischemic state during shock, and they are conserving their resources rather than synthesizing new proteins and start to degrade nonfunctional proteins. Nevertheless, even if the insulin receptor is still present, it does not necessarily equate to a functional receptor [24,32,53,54].

4.5.5 Choice of Anesthetic

The severity of organ injury measured by intestinal hemorrhage and lung protein degradation drastically differed depending on the type of anesthetic agent administered. Ketamine delays mortality in experimental models for sepsis [55] and mitigates acute lung injury [56]. Since ketamine alleviates some of the shock injury, the mean arterial pressure during ischemia needed to be reduced from 35 to 30 mmHg to replicate the experimental results generated during the use of Nembutal. Lowering the pressure by 5 mmHg substantially increased the organ injury with ketamine, illustrating the sensitivity of rats to small pressure changes during ischemia.

4.6 Conclusions

For the first time, receptors have been shown to degrade in the lung after hemorrhagic shock. This could be of importance for understanding the progression of cell dysfunction and organ failure. The degree of organ injury depends strongly on the model conditions. Since ANGD treatment to the lumen of the intestine did not reduce protein degradation of either VE-cadherin or VEGFR-2 in the lung, other proteases aside from the pancreatic proteases from the lumen of the intestine could potentially be involved in the breakdown process of these proteins. Moreover, the contribution of luminal enzymes compared to peripheral enzymes needs to be established.

4.7 REFERENCES

1. Holmes K, Roberts OL, Thomas AM, Cross MJ. (2007) Vascular endothelial growth factor receptor-2: Structure, function, intracellular signalling and therapeutic inhibition. Cell Signal 19: 2003-2012.

2. Yamamoto K, Sokabe T, Watabe T, Miyazono K, Yamashita JK, Obi S, Ohura N, Matsushita A, Kamiya A, Ando J. (2005) Fluid shear stress induces differentiation of flk-1-positive embryonic stem cells into vascular endothelial cells in vitro. Am J Physiol Heart Circ Physiol 288: H1915-24.

3. Shibuya M. (2002) Vascular endothelial growth factor receptor family genes: When did the three genes phylogenetically segregate? Biol Chem 383: 1573-1579.

4. Shimotake J, Derugin N, Wendland M, Vexler ZS, Ferriero DM. (2010) Vascular endothelial growth factor receptor-2 inhibition promotes cell death and limits endothelial cell proliferation in a neonatal rodent model of stroke. Stroke 41: 343-349.

5. Liu Y, Sweet DT, Irani-Tehrani M, Maeda N, Tzima E. (2008) Shc coordinates signals from intercellular junctions and integrins to regulate flow-induced inflammation. J Cell Biol 182: 185-196.

6. Tzima E, Irani-Tehrani M, Kiosses WB, Dejana E, Schultz DA, Engelhardt B, Cao G, DeLisser H, Schwartz MA. (2005) A mechanosensory complex that mediates the endothelial cell response to fluid shear stress. Nature 437: 426-431.

7. Shay-Salit A, Shushy M, Wolfovitz E, Yahav H, Breviario F, Dejana E, Resnick N. (2002) VEGF receptor 2 and the adherens junction as a mechanical transducer in vascular endothelial cells. Proc Natl Acad Sci U S A 99: 9462-9467.

8. Wang Y, Flores L, Lu S, Miao H, Li YS, Chien S. (2009) Shear stress regulates the flk-1/Cbl/PI3K/NF-kappaB pathway via actin and tyrosine kinases. Cell Mol Bioeng 2: 341-350.

9. Altshuler AE, Morgan MJ, Chien S, Schmid-Schönbein GW. (2012) Proteolytic activity attenuates the response of endothelial cells to fluid shear stress. Cell Mol Bioeng 5: 82-91.

10. Wada H, Satoh N, Kitaoka S, Ono K, Morimoto T, Kawamura T, Nakano T, Fujita M, Kita T, Shimatsu A, Hasegawa K. (2009) Soluble VEGF receptor-2 is increased

in sera of subjects with metabolic syndrome in association with insulin resistance. Atherosclerosis .

11. Holmes K, Roberts OL, Thomas AM, Cross MJ. (2007) Vascular endothelial growth factor receptor-2: Structure, function, intracellular signalling and therapeutic inhibition. Cell Signal 19: 2003-2012.

12. Bergers G, Benjamin LE. (2003) Tumorigenesis and the angiogenic switch. Nat Rev Cancer 3: 401-410.

13. Esser S, Lampugnani MG, Corada M, Dejana E, Risau W. (1998) Vascular endothelial growth factor induces VE-cadherin tyrosine phosphorylation in endothelial cells. J Cell Sci 111 (Pt 13): 1853-1865.

14. Causey MW, Hoffer ZS, Miller SL, Huston LJ, Satterly SA, Martin M, Stallings JD. (2011) Microarray and functional cluster analysis implicates transforming growth factor Beta1 in endothelial cell dysfunction in a swine hemorrhagic shock model. J Surg Res .

15. Makinen T, Veikkola T, Mustjoki S, Karpanen T, Catimel B, Nice EC, Wise L, Mercer A, Kowalski H, Kerjaschki D, Stacker SA, Achen MG, Alitalo K. (2001) Isolated lymphatic endothelial cells transduce growth, survival and migratory signals via the VEGF-C/D receptor VEGFR-3. EMBO J 20: 4762-4773.

16. Dejana E, Giampietro C. (2012) Vascular endothelial-cadherin and vascular stability. Curr Opin Hematol 19: 218-223.

17. Brasch J, Harrison OJ, Ahlsen G, Carnally SM, Henderson RM, Honig B, Shapiro L. (2011) Structure and binding mechanism of vascular endothelial cadherin: A divergent classical cadherin. J Mol Biol 408: 57-73.

18. Shasby DM. (2007) Cell-cell adhesion in lung endothelium. Am J Physiol Lung Cell Mol Physiol 292: L593-607.

19. Carmeliet P, Lampugnani MG, Moons L, Breviario F, Compernolle V, Bono F, Balconi G, Spagnuolo R, Oosthuyse B, Dewerchin M, Zanetti A, Angellilo A, Mattot V, Nuyens D, Lutgens E, Clotman F, de Ruiter MC, Gittenberger-de Groot A, Poelmann R, Lupu F, Herbert JM, Collen D, Dejana E. (1999) Targeted deficiency or cytosolic truncation of the VE-cadherin gene in mice impairs VEGF-mediated endothelial survival and angiogenesis. Cell 98: 147-157.

20. Carden D, Xiao F, Moak C, Willis BH, Robinson-Jackson S, Alexander S. (1998) Neutrophil elastase promotes lung microvascular injury and proteolysis of endothelial cadherins. Am J Physiol 275: H385-92.

21. Blanquart C, Achi J, Issad T. (2008) Characterization of IRA/IRB hybrid insulin receptors using bioluminescence resonance energy transfer. Biochem Pharmacol 76: 873-883.

22. Dugani CB, Randhawa VK, Cheng AW, Patel N, Klip A. (2008) Selective regulation of the perinuclear distribution of glucose transporter 4 (GLUT4) by insulin signals in muscle cells. Eur J Cell Biol 87: 337-351.

23. Fahy BG, Sheehy AM, Coursin DB. (2009) Glucose control in the intensive care unit. Crit Care Med 37: 1769-1776.

24. Xu F, Yang X, Lu Z, Kuang F. (1996) Evaluation of glucose metabolic disorder: Insulin resistance and insulin receptors in critically ill children. Chin Med J (Engl) 109: 807-809.

25. Zhai L, Messina JL. (2009) Age and tissue specific differences in the development of acute insulin resistance following injury. J Endocrinol 203: 365-374.

26. Clement S, Braithwaite SS, Magee MF, Ahmann A, Smith EP, Schafer RG, Hirsch IB, American Diabetes Association Diabetes in Hospitals Writing Committee. (2004) Management of diabetes and hyperglycemia in hospitals. Diabetes Care 27: 553-591.

27. Mowery NT, Carnevale RJ, Gunter OL, Norris PR, Dossett LA, Dortch MJ, Morris JA,Jr, May AK. (2009) Insulin resistance heralds positive cultures after severe injury. Surg Infect (Larchmt) 10: 503-509.

28. Kaneki M, Shinozaki S, Chang K, Shimizu N. (2009) Could insulin sensitization be used as an alternative to intensive insulin therapy to improve the survival of intensive care unit patients with stress-induced hyperglycemia? Crit Care Med 37: 2856-2858.

29. Dhar A, Castillo L. (2011) Insulin resistance in critical illness. Curr Opin Pediatr 23: 269-274.

30. Losser MR, Damoisel C, Payen D. (2010) Bench-to-bedside review: Glucose and stress conditions in the intensive care unit. Crit Care 14: 231.

31. Smit JW, Romijn JA. (2006) Acute insulin resistance in myocardial ischemia: Causes and consequences. Semin Cardiothorac Vasc Anesth 10: 215-219.

32. Kernan WN, Inzucchi SE, Viscoli CM, Brass LM, Bravata DM, Shulman GI, McVeety JC, Horwitz RI. (2003) Impaired insulin sensitivity among nondiabetic patients with a recent TIA or ischemic stroke. Neurology 60: 1447-1451.

33. Raymond RM. (1984) Skeletal muscle metabolism and insulin resistance during endotoxin shock in the dog. Am J Emerg Med 2: 45-59.

34. Ryan NT, George BC, Egdahl DH, Egdahl RH. (1974) Chronic tissue insulin resistance following hemorrhagic shock. Ann Surg 180: 402-407.

35. Engel FL, Winton MG, Long CN. (1943) Biochemical studies on shock : I. the metabolism of amino acids and carbohydrate during hemorrhagic shock in the rat. J Exp Med 77: 397-410.

36. Barth E, Albuszies G, Baumgart K, Matejovic M, Wachter U, Vogt J, Radermacher P, Calzia E. (2007) Glucose metabolism and catecholamines. Crit Care Med 35: S508-18.

37. Menguy R, Masters YF. (1978) Influence of hyperglycemia on survival after hemorrhagic shock. Adv Shock Res 1: 43-54.

38. Torres Filho IP, Torres LN, Pittman RN. (2010) Early physiologic responses to hemorrhagic hypotension. Transl Res 155: 78-88.

39. Cursio R, Miele C, Filippa N, Colosetti P, Auberger P, Van Obberghen E, Gugenheim J. (2009) Tyrosine phosphorylation of insulin receptor substrates during ischemia/reperfusion-induced apoptosis in rat liver. Langenbecks Arch Surg 394: 123-131.

40. DeLano FA, Schmid-Schönbein GW. (2008) Proteinase activity and receptor cleavage: Mechanism for insulin resistance in the spontaneously hypertensive rat. Hypertension 52: 415-423.

41. Delano FA, Zhang H, Tran EE, Zhang C, Schmid-Schönbein GW. (2010) A new hypothesis for insulin resistance in hypertension due to receptor cleavage. Expert Rev Endocrinol Metab 5: 149-158.

42. Lipson KE, Kolhatkar AA, Donner DB. (1989) Insulin stimulates proteolysis of the alpha-subunit, but not the beta-subunit, of its receptor at the cell surface in rat liver. Biochem J 261: 333-340.

43. Sanchez-Casas P, Yusta B, Blazquez E. (1995) Insulin-induced proteolysis of the insulin receptor alpha-subunit from rat liver does not occur in vivo but is prevented in vitro by blood serum proteinase inhibitors. Eur J Biochem 232: 747-754.

44. Soluble Insulin Receptor Study Group. (2007) Soluble insulin receptor ectodomain is elevated in the plasma of patients with diabetes. Diabetes 56: 2028-2035.

45. Engel D, Forrai E. (1943) Capillary permeability in traumatic shock. J Physiol 102: 127-139.

46. Djerassi L, ROY A. (1962) Effects of hemorrhagic shock on vascular permeability to red blood cells. Circ Res 10: 758-762.

47. Badami CD, Senthil M, Caputo FJ, Rupani BJ, Doucet D, Pisarenko V, Xu DZ, Lu Q, Feinman R, Deitch EA. (2008) Mesenteric lymph duct ligation improves survival in a lethal shock model. Shock 30: 680-685.

48. Navaratna D, McGuire PG, Menicucci G, Das A. (2007) Proteolytic degradation of VE-cadherin alters the blood-retinal barrier in diabetes. Diabetes 56: 2380-2387.

49. Ray SK. (2006) Currently evaluated calpain and caspase inhibitors for neuroprotection in experimental brain ischemia. Curr Med Chem 13: 3425-3440.

50. Herren B, Levkau B, Raines EW, Ross R. (1998) Cleavage of beta-catenin and plakoglobin and shedding of VE-cadherin during endothelial apoptosis: Evidence for a role for caspases and metalloproteinases. Mol Biol Cell 9: 1589-1601.

51. Holmes K, Roberts OL, Thomas AM, Cross MJ. (2007) Vascular endothelial growth factor receptor-2: Structure, function, intracellular signalling and therapeutic inhibition. Cell Signal 19: 2003-2012.

52. Fujita-Yamaguchi Y, Kathuria S. (1985) The monomeric alpha beta form of the insulin receptor exhibits much higher insulin-dependent tyrosine-specific protein kinase activity than the intact alpha 2 beta 2 form of the receptor. Proc Natl Acad Sci U S A 82: 6095-6099.

53. Marik PE, Raghavan M. (2004) Stress-hyperglycemia, insulin and immunomodulation in sepsis. Intensive Care Med 30: 748-756.

54. van den Berghe G, Wouters P, Weekers F, Verwaest C, Bruyninckx F, Schetz M, Vlasselaers D, Ferdinande P, Lauwers P, Bouillon R. (2001) Intensive insulin therapy in the critically ill patients. N Engl J Med 345: 1359-1367.

55. Shaked G, Grinberg G, Sufaro Y, Douvdevani A, Shapira Y, Artru A, Czeiger D. (2009) Ketamine delays mortality in an experimental model of hemorrhagic shock and subsequent sepsis. Resuscitation 80: 935-939.

56. Yang CH, Tsai PS, Wang TY, Huang CJ. (2009) Dexmedetomidine-ketamine combination mitigates acute lung injury in haemorrhagic shock rats. Resuscitation 80: 1204-1210.

Chapter 5

Contribution of Luminal Contents to Organ Injury after Hemorrhagic Shock

5.1 Introduction

The intestine has long been associated with the progression of shock and multiple organ dysfunction. The luminal contents in the gut consist of digestive enzymes, food particles, bile, bacteria, etc. that may be non-uniformly distributed along its length. These luminal contents may serve as pro-inflammatory mediators after the onset of intestinal ischemia contributing to the multiple organ system failure that occurs during shock. Some studies in our laboratory have investigated a flushed intestine using an SAO model to study the outcome of the intestine [1,2] but have not thoroughly examined the extent of peripheral organ injury after disruption of the barrier.

Our group and others have provided evidence that the serine protease and lipase inhibitor ANGD reduces intestinal microhemorrhages and improves the outcome after experimental shock [3-6]. However, these experiments largely assume that the damage is attenuated by an inactivation of proteases in the presence of these inhibitors. These

inhibitors may also prevent digestion of intestinal structures, activation of wall proteases, or generation of cytotoxic products in the intestinal lumen. Clarifying these events is required to understand why pancreatic protease inhibitors have been beneficial for recovery and survival after shock [7].

It is also unclear to what degree digestive enzymes are transported into the central circulation from the intestine (as opposed to from the pancreas). As addressed in the previous chapter, pancreatic enzymes can accumulate in the lung, and it has yet to be determined whether luminal contents impact the peripheral protease activation and lung injury following hemorrhagic shock. In addition, the elevation of global protease activity poses a threat to key extracellular components on epithelial cells in the intestine and endothelial cells in the circulation. Lung junctional protein degradation of cadherins after ischemia has been observed [8], but the possibility for receptor degradation has not been fully explored in the case of hemorrhagic shock and few investigations have been completed to determine whether serine proteases are responsible for receptor damage.

5.2 Chapter Aims

The aim of this chapter is to explore the contribution of small intestine's luminal contents to intestinal and peripheral organ injury following hemorrhagic shock. I hypothesize that digestive enzymes enter into the interstitial mucosal wall and subsequently cause microhemorrhages in peripheral organs by the accumulation of proteases and activated neutrophils. These effects will be minimized if the luminal

contents, including the digestive enzymes are flushed out of the lumen of the intestine (Figure 5.1).

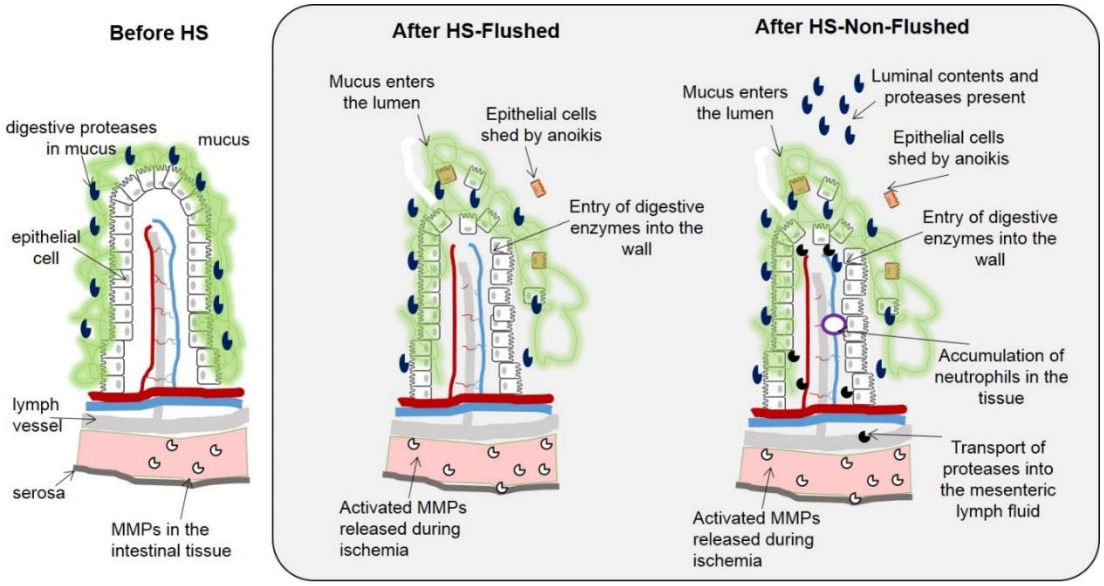

Figure 5.1 Hypothesis summary. Before HS, the intestine and the mucus barrier are intact. In the absence of luminal contents, the mucosal layer and epithelial cells shed into the lumen, but there is minimal destruction of the epithelium since no luminal contents containing cytotoxic mediators (e.g. unbound free fatty acids) enter into the villi. If the intestine is not flushed, digestive enzymes will penetrate into the wall and activate MMPs and be transported to peripheral organs, such as the lung.

5.3 METHODS

5.3.1 ANIMALS

The animal protocol was reviewed and approved by the University of California, San Diego Institutional Animal Care and Use Committee. Male Sprague Dawley (mean body weight 275±18 g, Harlan, Indianapolis, IN) were allowed food and water *ad libitum* prior to surgery. Rats were administered general anesthesia (xylazine, 4 mg/kg; ketamine 75 mg/kg IM) and euthanized by infusion of B-Euthanasia IV (120 mg/kg) at termination of experiments. Following general anesthesia, the femoral artery and vein were cannulated. Systolic, diastolic, heart rate, and mean arterial pressure (MAP) were recorded throughout the procedure using LabChart (AD Instruments, Dunedin, New Zealand).

5.3.1.1 HEMORRHAGIC SHOCK PROCEDURE

Animals were grouped into no hemorrhagic shock (No-HS), hemorrhagic shock with intestinal luminal contents flushed (HS-F), and hemorrhagic shock without intestinal flush (HS-NF). No-HS animals were cannulated and then immediately sacrificed for tissue collection. After femoral vessel cannulation, the HS-F and HS-NF were subject to laparotomy and the intestine was exposed. The proximal jejunum (approximately 5 cm distal from the ligament of Treitz) was carefully cut between intestinal blood vessels and each end was cannulated with Female Luer to Barb tube connectors and secured with 4-0

suture (Figure 5.2). The connector to the duodenum was sealed with clay. Next, the distal ileum located three centimeters from the cecum was cut in order to insert another clay sealed connector into the intestine on the distal side (closest to the cecum) and secured with suture. The proximal end was not cannulated and sealed until after the luminal contents were flushed.

To remove the luminal contents, a syringe filled with 40 ml of saline at 37º C was connected to the adaptor attached to the proximal jejunum and the luminal contents were flushed distally with saline using pulsatile pressure. The contents exiting the intestine through the distal ileum were collected and discarded. Using this technique, all luminal content was visibly removed from the intestine and the last ~15 ml of saline exiting the intestine were clear of color and absent of solid content. Following the intestinal flush, the final connector in the distal ileum was inserted and secured with suture. All connectors were sealed with a small piece of clay. The exterior of the intestine was rinsed with warm saline and placed into the peritoneal cavity. HS-NF animals received the same manipulation to the intestine and placement of connectors, but the luminal contents were not removed. Gross morphology images of pre-HS intestines were recorded immediately after these procedures.

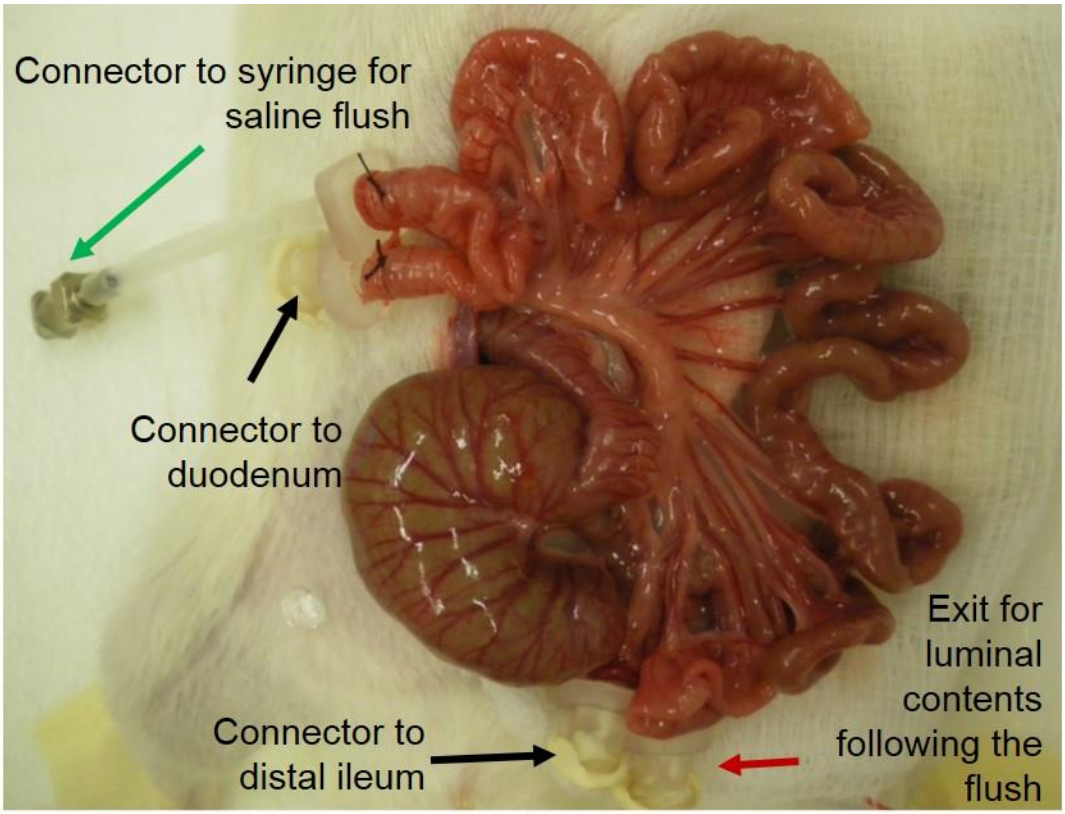

Figure 5.2 Diagram of the surgical preparation before flushing luminal contents. The green arrow indicates the connector to which the syringe will be attached for saline flush. The red arrow indicates the exit point for luminal contents. The other two connectors serve to seal the duodenum and ileum regions (black arrows).

Following these intestinal preparations, the animals were heparinized to minimize clotting in catheters and in shed blood samples (1 U/ml calculated blood volume IV; assuming 6 ml blood volume per 100 g total body weight) before onset of hemorrhage. MAP was reduced to 30 mmHg by withdrawing blood through the venous catheter (0.4 ml/min) with a 5 ml syringe. The initial 1 ml of blood drawn was collected, centrifuged (1000 g, 5 min), and the plasma was immediately frozen at -80º C. The pressure was monitored and adjusted by withdrawal/return of blood over the 90-minute ischemic period. At the end of ischemia, the shed blood was returned to the animals (0.5 ml/min) plus 1 ml of saline (to replace the 1 ml of blood collected before shock). The animals remained anesthetized and were observed in the reperfusion phase for 3 hours after the initiation of the return of shed blood.

Gross morphology images of the intestine were captured at the end of the reperfusion period. Post-hemorrhagic shock blood was collected through the arterial catheter, spun (1000 g, 5 min), and the plasma was immediately frozen at -80º C. The animals were then euthanized and pieces of lung and intestine (jejunum and ileum) were snap frozen for homogenization or embedded in O.C.T. (Tissue Tek).

5.3.1.2 BRONCHOALVEOLAR LAVAGE FLUID

To collect bronchoalveolar lavage fluid (BALF), the left main bronchus leading to the left lung was cannulated with an 18 gauge blunt needle and photographed to assess gross morphological damage after hemorrhagic shock. These gross morphological photographs were later blindly assessed for macroscopic lung damage. Scoring was as

follows: 0, no visible lung damage; 1, mostly pink in color with some lesions starting to form around the central part of the lung near the trachea; 2, some pink color with more lesions forming and spreading throughout the lung; 3, mostly red with lesions through the majority of the lung; 4 complete lung damage.

To collect BALF fluid, saline (approximately 2.0 ml/lavage) was injected and recovered three times before centrifugation (1000 g, 5 min). Following the third wash, the lung was injected with O.C.T., embedded, and frozen. The total volume of recovered BALF fluid was measured and the fraction of saline recovered versus the amount injected was used to normalize measurements.

5.3.2 Tissue Homogenization

In every homogenization procedure, 1 ml of homogenization buffer was added per 0.1 g tissue. Tissues were then mechanically homogenized using a handheld homogenizer for 30 seconds before centrifuging (18,000 g, 20 min). Supernatants were stored at -80 ºC until processed.

5.3.3 Intestinal Hemorrhage

Intestine jejunum segments with intestinal contents still present were homogenized by weight in 0.5% hexadecyltrimethylammonium bromide (HTAB) in PBS (pH 6.0). Samples were read at 405 nm absorbance in duplicate on a plate reader to estimate erythrocyte infiltration by measuring the hemoglobin present in each tissue

homogenate. Intestinal bleeding was also assessed macroscopically by comparing photographs of the intestine before and after hemorrhagic shock.

5.3.4 Enzyme and Protease Activity Measurements

5.3.4.1 Casein Activity in the Intestine

Protease activity was determined by digestion of the globular protein casein hybridized to Texas-red such that fluorescence intensity increases after cleavage (Enzchek protease assay kit). 10 µl of intestinal homogenates (same as 4.3.3) with endogenous luminal contents present were mixed with 90 µl casein substrate and loaded in duplicate. Plates were incubated in a pre-warmed microplate reader and measurements were made every 5 minutes. The change in caseinolytic activity per minute was computed for each sample.

5.3.4.2 Myeloperoxidase (MPO) Activity Assay

In order to assess intestine and lung neutrophil infiltration, myeloperoxidase activity was determined in the intestine (homogenized same as 4.3.3) and lung homogenates (PBS pH 6.0 in 0.5% HTAB). 40 µl of 2 mg/ml intestine homogenate or 20 µl of 1 mg/ml lung homogenate, were added to 180 µl of PBS (pH 6.0) mixed with 0.167 mg/ml o-dianisidine dihydrochloride (Sigma-Aldrich) and 0.001% or 0.0005% H_2O_2 (w/v) for intestine and lung respectively.

To determine neutrophil MPO release into the BALF, 20 µl was loaded into each well before 180 µl of PBS (pH 6.0) mixed with 0.167 mg/ml o-dianisidine dihydrochloride (Sigma-Aldrich) containing 0.001% H_2O_2. BALF protein concentration was also determined. All BALF calculations were normalized to the percent fluid recovered from three lavage collections.

Absorbance was measured kinetically at 450 nm every 5 minutes for 1 hour at 37 ºC. As negative controls, 180 µl of PBS (pH 6.0) was added to 20 µl of sample and the absorbance values of these samples were subtracted from the measurements with the substrate. The change in absorbance was linear within this period and MPO activity is presented as the change in absorbance per minute per milligram of protein.

5.3.4.3 GELATIN GEL ZYMOGRAPHY

Unlike the experiments in 4.3.3-4.3.4, for this study focusing on MMP activity in intestinal tissue, the luminal contents were removed by gently compressing the intestine before homogenizing intestine segments to prevent excess digestion of the gelatin substrate in the gels by luminal proteases. Tissues from shocked animals (flushed and non-flushed) as well as controls were rinsed and blotted dry before weighing. Both intestine and lung tissues were homogenized in PBS (pH 6.0) containing 0.5% HTAB (see Section 4.3.2). Protein concentration was determined using the BCA kit (ThermoScientific) before mixing each sample in a 1:1 ratio with loading dye (containing SDS, but no reducing agent). 2 µg protein/lane of intestine or 20 µg protein/lane of lung

homogenates were loaded. 0.5 µl of plasma was mixed with 2 µl loading dye and loaded into each lane.

Samples were separated by gel electrophoresis in 11% SDS-Page gelatin impregnated gels. Upon separation, gel proteins were renatured in 2.5% Triton-X 100 in water (4x, 15 min) before incubation at 37 ºC overnight in developing buffer (0.05 M Tris base, 0.2 M NaCl, 4 µM $ZnCl_2$, 5 mM $CaCl_2 \cdot 2H_2O$). Gels were then fixed and stained (50% methanol, 10% acetic acid, 40% water, and 0.25% Coomassie blue solution) for three hours. Gels were destained in water to achieve appropriate contrast before photographing and digitally analyzed (ImageJ; http://rsb.info.nih.gov/ij/).

To confirm that the ~20 kDa bands were serine proteases, gels were renatured and developed in the aforementioned buffers with the addition of either 75 µM ANGD or 100 µM TLCK and compared to duplicate gels that received the standard renaturation procedure.

5.3.5 IMMUNOBLOTTING

Before homogenizing intestine samples for immunoblotting, the luminal content was gently pressed out of the intestine for the No-HS and HS-NF samples. The intestines were rinsed in saline and blotted dry before weight determination. Lysis buffer (ThermoScientific) was mixed with a 1:100 dilution of 0.5 M EDTA (ThermoScientific) and a 1:50 dilution of HALT protease inhibitor cocktail. Lungs were homogenized in lysis buffer containng HALT protease inhbitor (1:100).

For organ homogenates, protein concentration was calculated (BCA kit) so that 40 µg protein were loaded per well. Homogenates were mixed 1:1 with sample loading buffer (BioRad) containing β-mercaptoethanol (0.05% by volume). Plasma was mixed in a 1:2 ratio of plasma:sample loading buffer containing β-mercaptoethanol (0.05% w/v), and 3 µl of this solution was loaded per well. Both tissue homogenates and plasma samples were then denatured by boiling for 10 minutes. Proteins were separated on SDS-PAGE gels (8% or 12% resolving, 4% stacking). Following separation, proteins were transferred onto a nitrocellulose membrane (Bio-Rad) and blocked for one hour in 5% bovine serum albumin in tris-buffered saline with 0.5% Tween-20 (TBS-T). Membranes were then incubated overnight with the designated primary antibody (Table 5.1).

Table 5.1 Antibody sources and dilutions.

Target	Product Number	Dilution
β-actin	Santa Cruz Biotechnology sc-8432	1:1000
Chymotrypsin	Abcam ab-35694	1:500
E-cadherin	Invitrogen 33-4000	1:1000
MMP-9	Abcam ab-76003	1:1000
Mucin 13	Santa Cruz Biotechnology sc-66973	1:1000
Occludin (intestine)	Invitrogen 33-1500	1:1000
Occludin (lung)	Invitrogen 71-1500	1:1000
Trypsin	Santa Cruz Biotechnology sc-137077	1:1000
VE-cadherin	Santa Cruz Biotechnology sc-6458	1:1000
VEGFR-2	Santa Cruz Biotechnology sc-48161	1:750

Following incubation, the primary antibody was rinsed (TBS-T, 3x, 10 min). Secondary antibodies against mouse, rabbit, or goat were diluted 1:10,000 in TBS-T and incubated with the membranes for 1 hr. The membranes were washed (TBS-T, 3x, 10 min) and developed using ECL substrate (ThermoScientific).

Membranes were scanned and bands digitally quantified (ImageJ). Lung and intestine bands were standardized by β-actin and normalized by the No-HS controls to determine fold changes in protein levels. Plasma protein levels were not normalized.

5.3.6 HISTOLOGY

All procedures were performed on 8 μm thick frozen sections. Images were acquired using a 20x objective and montaged together.

5.3.6.1 IMMUNOHISTOCHEMISTRY

Mucin distribution was assessed using immunohistochemistry after hemorrhagic shock. Sections were allowed to dry for 20 minutes before fixation in ice-cold acetone at -20 ºC for 10 minutes. Following fixation, slides were washed in PBS (2x, 3 min). Endogenous hydrogen peroxidase activity was quenched in 95% methanol mixed with 3% hydrogen peroxide solution (5 min). Slides were washed again in PBS (2x, 3 min). Individual sections were isolated with a hydrophobic pen (Vector Labs) before blocking with 2.5% normal horse serum (Vector Labs) for 30 minutes. Primary antibodies against MMP-9 (Abcam ab-76003), mucin 2 and mucin 13 (Santa Cruz Biotechnology; sc-15334 and sc-66973 respectively) were diluted 1:200 in 1.25% normal horse serum and incubated with the sections overnight at 4 ºC. The primary antibody was washed with PBS (3x, 5 min) and sections were incubated with anti-rabbit secondary reagent (Immpress Kit, Vector Labs) for 30 minutes. Secondary antibody was removed by washing with PBS (3x, 5 min). Colorimetric labeling was achieved by using DAB (3, 3'-diaminobenzidine) substrate (Vector Labs) for 30 seconds followed by rinsing in water. Sections were finally counterstained with Toluidine blue (0.05% in 1% boric acid) for 5 seconds. Slides were washed with three changes of DI water before dehydrating in an ethanol gradient (70, 95, and 100%) and cleaning with xylene. Slides were allowed to dry overnight before mounting with hard set mounting media (Vector Labs).

5.3.6.2 LUNG HISTOLOGY

Lung sections were allowed to dry for 20 minutes before fixation in ice-cold methanol at -20 ºC. Slides were washed in DI water (4x) and incubated with hematoxylin solution (Vector Labs) for 30 seconds. They were rinsed thoroughly in DI water and incubated in eosin (Fisher) for 30 seconds followed by additional rinses in DI water. The slides were dehydrated in 70%, 95%, and 100% ethanol before cleaning with xylene and were dried overnight before being mounted with hard set mounting media (Vector Labs).

5.3.7 STATISTICAL ANALYSIS

Results are presented as either mean±standard deviation (SD). Paired t-tests were completed for comparisons between groups for MAP during the reperfusion period and between pre- and post-shock plasma samples. Mann-Whitney tests were used for non-normally distributed means. ANOVA followed by Tukey post-hoc analysis was used for normally distributed parametric variables. Statistical analysis was performed in the software OriginLabs (Northampton, MA).

5.4 RESULTS

5.4.1 HEMATOLOGICAL PARAMETERS

HS-F and HS-NF animals had a maximum blood volume loss during ischemia of 42±4% and 42±3%, respectively. MAP was significantly decreased compared to immediately after the completion of reperfusion starting 60 minutes and 45 minutes into reperfusion for HS-F and HS-NF, respectively (Figure 5.3). However, MAP did not significantly differ between the flushed and non-flushed cases. Neither heart rate nor pulse pressure was significantly different between the groups (Table 5.2) but dropped by the end of the third hour or reperfusion compared to the first hour.

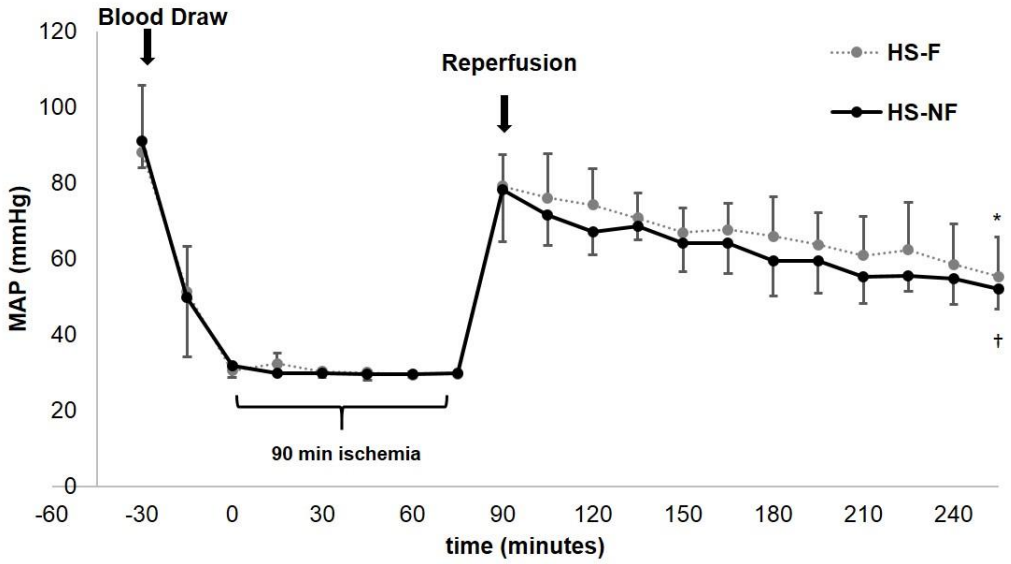

Figure 5.3 Pressure traces. The MAP (mean±SD) during hemorrhagic shock for groups of rats with flushed (HS-F) and non-flushed (HS-NF) intestine. N=6 rats/group. $p<0.001$ by paired t-test compared to MAP at 90 minutes for HS-F (*) and HS-NF (†).

Table 5.2 Heart rate and pulse pressure for HS-F and HS-NF animals.

	Heart Rate‡		Pulse Pressure†	
	HS-NF	**HS-F**	**HS-NF**	**HS-F**
Start	214±17	197±15	47±6	47±4
Draw	160±21	156±14	40±5	33±4
Ischemia	180±40	171±27	30±5.7	31±3
Reperfusion	283±21	264±30	39±5	42±6
Hour 1	278±19	263±29	50±8	50±4
Hour 2	287±18	274±28*	38±4*	43±36
Hour 3	284±29	257±36	31±6*	36±9*

‡, beats/min and †, mmHg. N=6 rats/group. Mean±SD. *, $p<0.025$ by paired t-test compared to Hour 1 reperfusion time.

5.4.2 INTESTINAL DAMAGE

All animals had intestines with a healthy appearance prior to the onset of ischemia/reperfusion injury (Figure 5.4). Following HS, tissue hemorrhage occurred regularly in regions proximal to the surgical sites in the flushed cases. In the no-flush animals, all rats developed visible hemorrhage along the length of the intestine in both the jejunum and ileum regions (Figure 5.4, HS-NF group). These lesions appeared more intense in sites where food appeared to be present. In contrast, among six HS-F animals none had macroscopic lesions in the region where luminal contents had been removed.

Intestinal homogenate absorbance at 405 nm as a quantitative marker for hemoglobin escape was elevated in the HS-NF animals (Figure 5.5), although not significantly. As expected, given the presence of luminal content and proteases, the proteolytic activity as determined by casein substrate digestion in the HS-NF animals was significantly higher compared to flushed animals (Figure 5.6). Interestingly, there was a trend for increased activity in the HS-NF group compared to the No-HS group as well (Figure 5.6). There was a linear correlation among the six HS-NF animals between caseinolytic activity and intestinal hemorrhage (Figure 5.7). MPO activity was also elevated in the HS-NF animals (Figure 5.8). There was a weaker correlation between caseinolytic activity and MPO activity in intestinal homogenates (Figure 5.9).

The villi in both the jejunum and the ileum remained structurally intact after hemorrhagic shock regardless of the presence of luminal content. Mucin 2, derived from goblet cells, entered into the lumen of the intestine after hemorrhagic shock regardless of the state of flushing (Figure 5.10). Epithelial bound mucin 13 was detected along the

villi in all three groups (Figure 5.11A). However, after hemorrhagic shock, mucin 13 and epithelial cells were co-localized in the lumen of the intestine with or without flushing, but more distinguished in the flushed without luminal contents at the beginning of the experiment (Figure 5.11B). There was no difference between the protein levels of mucin 13, and there was no change in the mucin fragmentation pattern (Figure 5.11B).

MMP-9 dimer activity was elevated in the HS-NF group, but there was no change in the band representing the active form of monomer MMP-2 by gelatin gel zymography (Figure 5.12A). Protein levels of MMP-9 detected by immunoblotting (performed under reducing conditions that do not distinguish between monomer and dimer forms) indicated an elevation in the HS-NF animals compared to the No-HS animals (Figure 5.12B). MMP-9 localization was found primarily in the muscularis region and along the epithelial lining of the villi (Figure 5.12C).

The three different E-cadherin bands detected in the intestinal epithelial cells were reduced in the HS-NF animals only (Figure 5.13). The tight junction protein occludin band did not change (Figure 5.13).

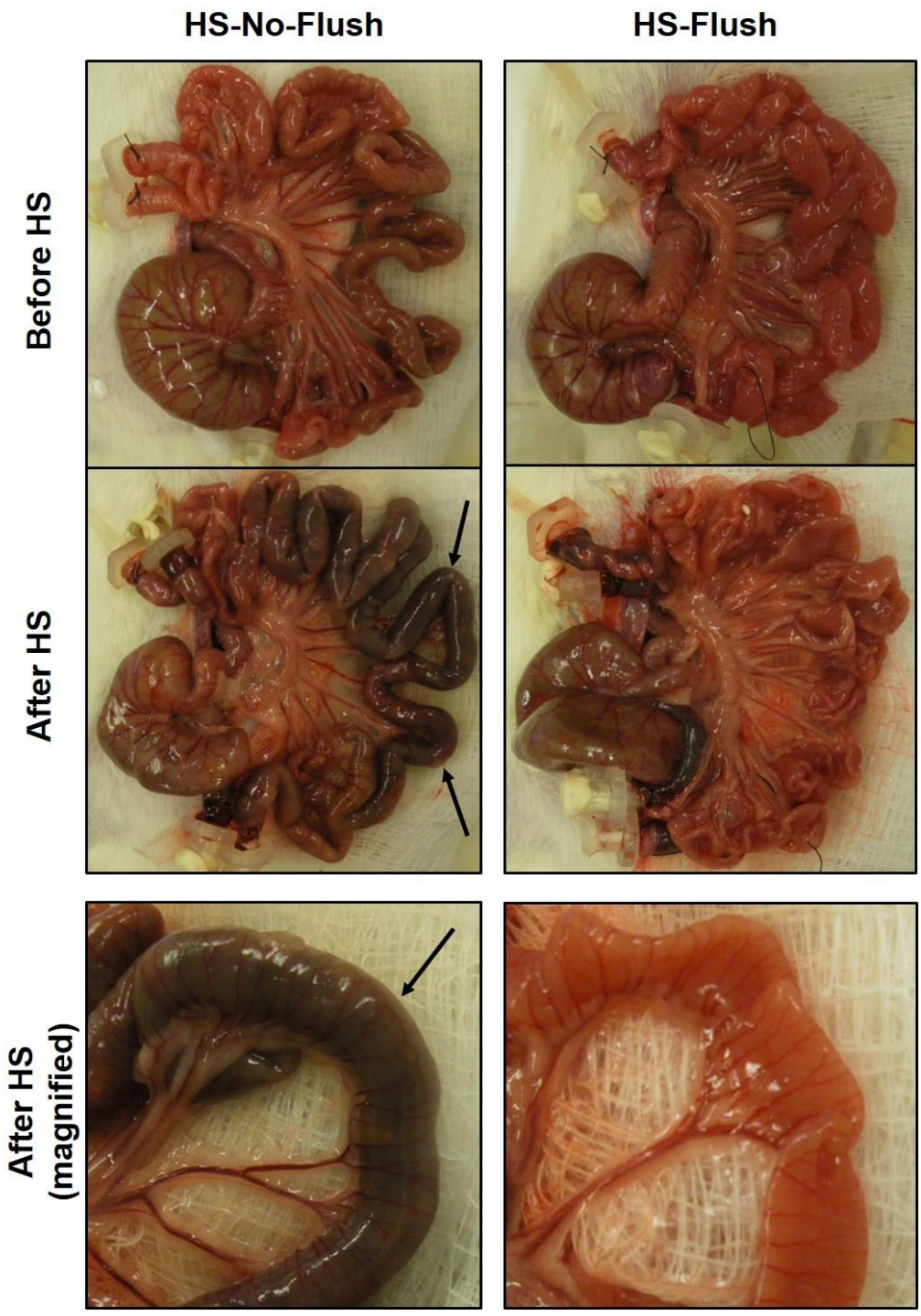

Figure 5.4 Macroscopic intestinal morphology. Gross intestinal morphology following hemorrhagic shock with either a flushed or non-flushed intestine. Black arrows indicate sites of hemorrhagic lesions.

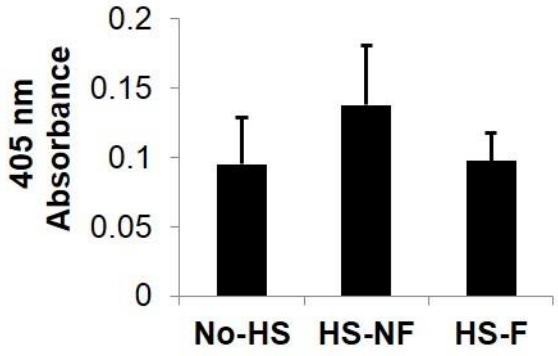

Figure 5.5 Hemorrhage into the intestine. Absorbance values in intestine homogenates at 405 nm for No-HS, HS-F, and HS-NF groups. N=6 rats/group. Data are presented as mean±SD.

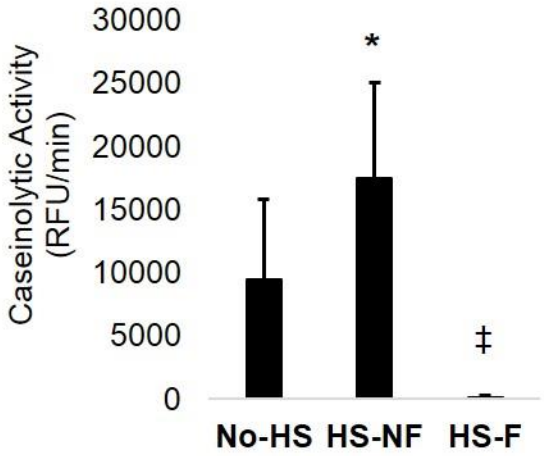

Figure 5.6 Caseinolytic activity of intestinal homogenates. Caseinolytic activity (mean±SD) decreases significantly following flushing luminal contents. Comparison of groups is by ANOVA followed by Tukey post-hoc analysis. *, $p<0.05$ compared to No-HS. ‡, $p<0.0003$ comparing HS-NF and HS-F. N=6 rats/group.

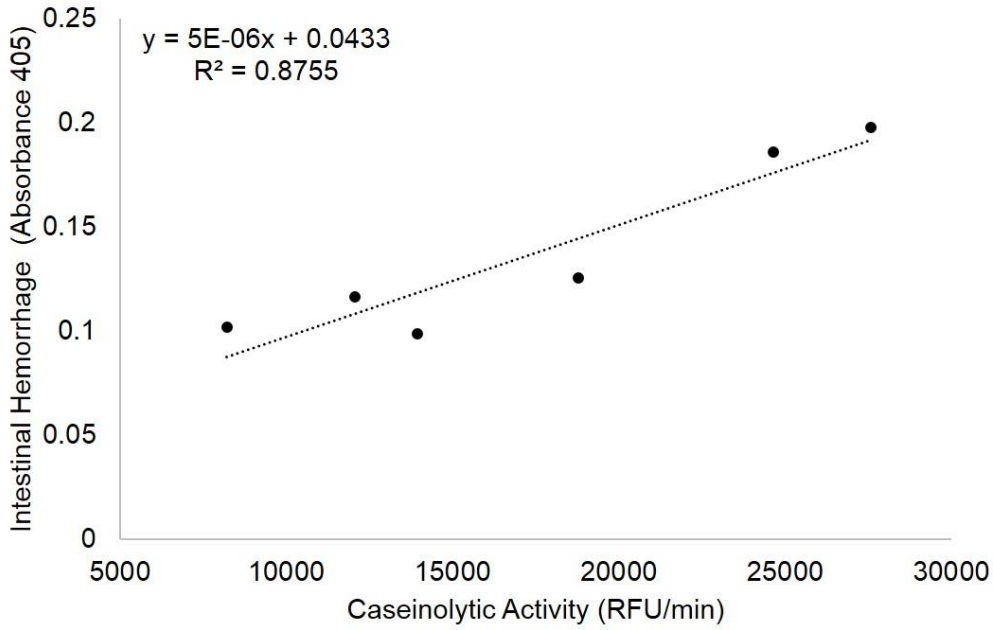

Figure 5.7 Correlation between protease activity and hemorrhage. Data points are from the No-Flush intestinal homogenates. Mean caseinolytic activity of intestinal homogenates correlates linearly with average hemoglobin absorbance at 405 nm.

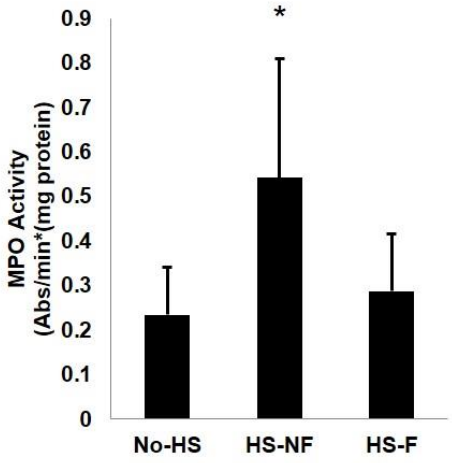

Figure 5.8 MPO activity of intestinal homogenates. MPO activity (mean±SD) of HS-NF intestines was elevated compared to No-HS intestines. *, $p<0.05$ between No-HS and HS-NF by ANOVA followed by Tukey post-hoc. N=6 rats/group.

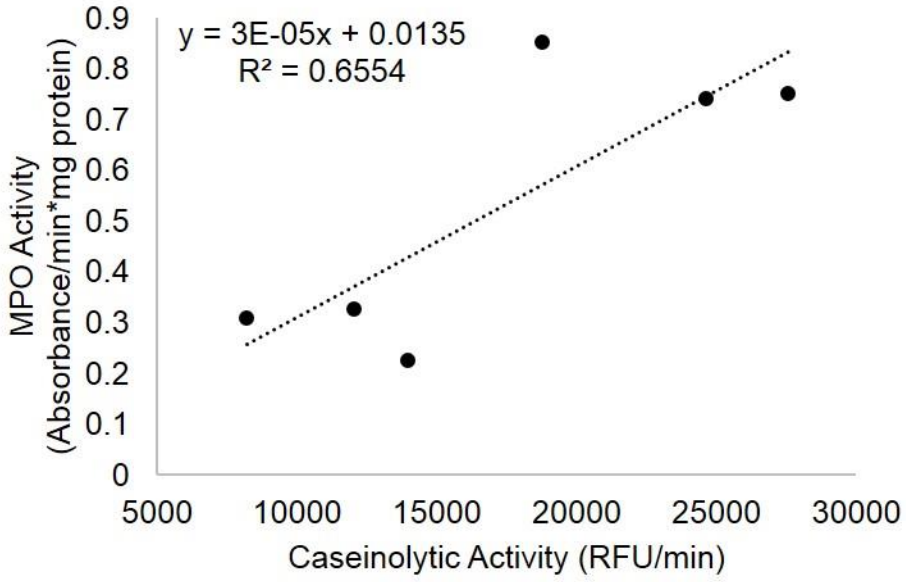

Figure 5.9 Correlation between intestinal homogenate protease activity and MPO activity. Mean MPO activity and mean caseinolytic activity of intestinal homogenates correlate for HS-NF animals.

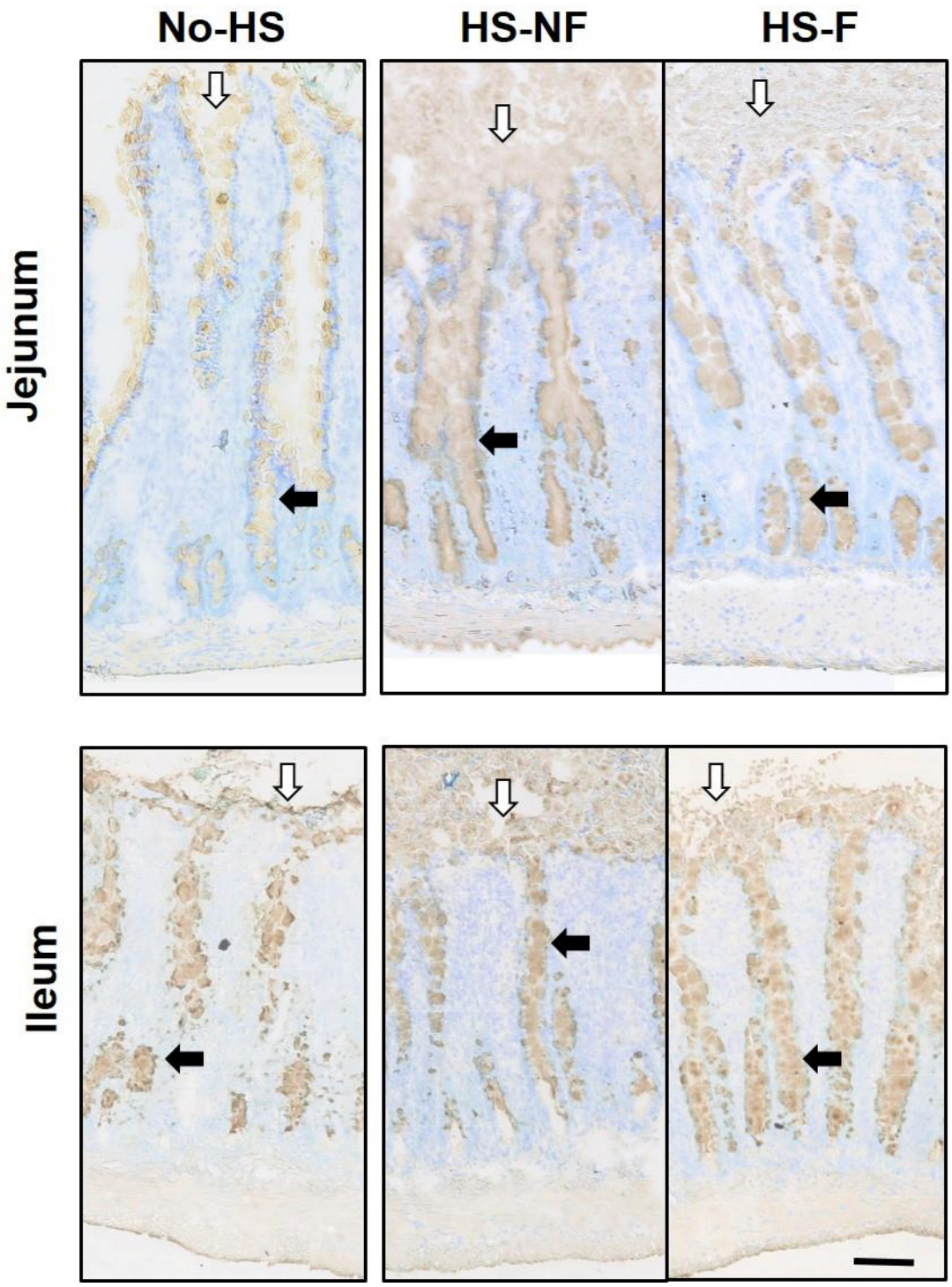

Figure 5.10 Mucin 2 immunohistochemistry. Mucin 2 (**brown**) is detected in both the lumen (white arrows) and the goblet cells (black arrows) in the intestine villi. Counterstain (**blue**) is shows nuclei. After HS, the mucin-2 levels in the lumen of the intestine are enhanced.

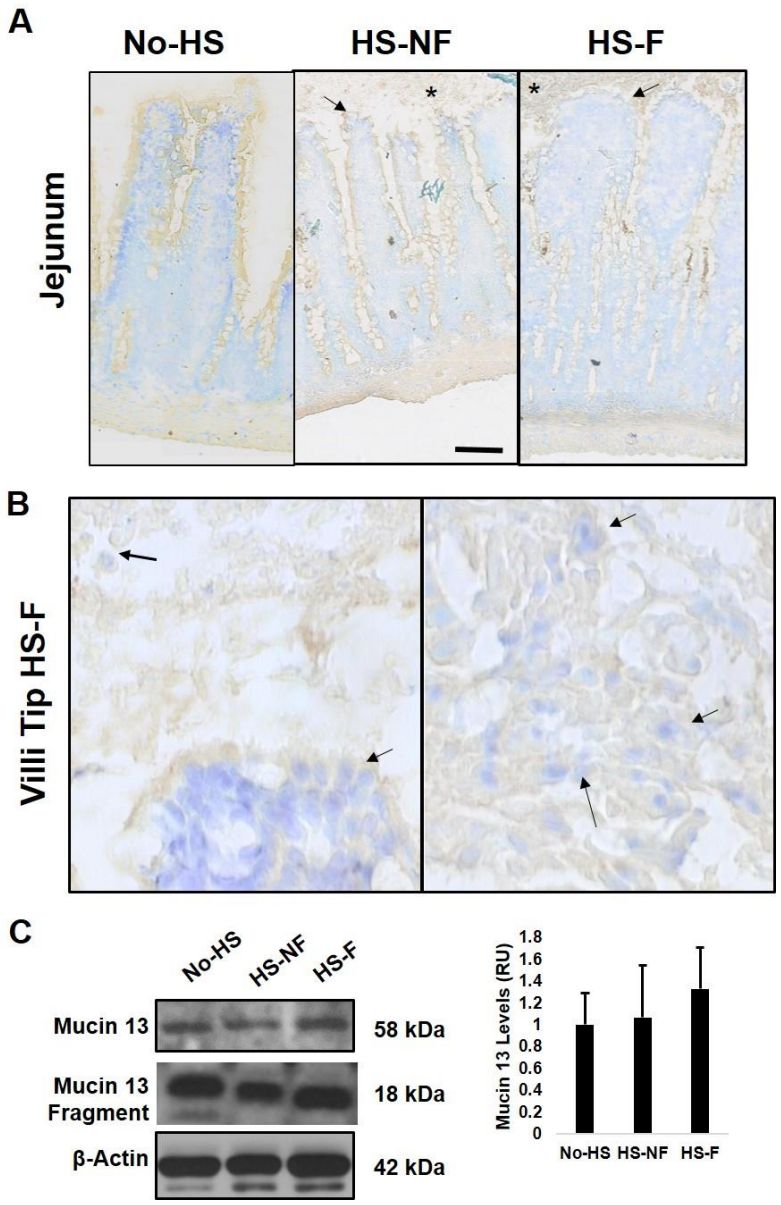

Figure 5.11 Mucin 13 levels in the intestine. (A) Mucin 13 coats the epithelial cells over the villi in all cases (**brown stain**). Arrows indicate the membrane bound mucin 13 and stars (*) indicate the regions in which the mucin 13 is secreted into the lumen. (B) After hemorrhagic shock, mucin 13 bound to shed epithelial cells (**blue**) is observed in the lumen of the intestine in the HS-F animals and the HS-NF animals. Arrows indicate epithelial cells found in the lumen amongst the stained (**brown**) mucin 13. Left panel shows the top of the villi tip and the right panel depicts the cells shed into the lumen of the intestine. (C) There was no change in mucin 13 protein levels by immunoblot analysis of the 58 kDa isoform and no change in the mucin 13 fragments formed. N=6 rats/group. Bar graph shows mean±SD.

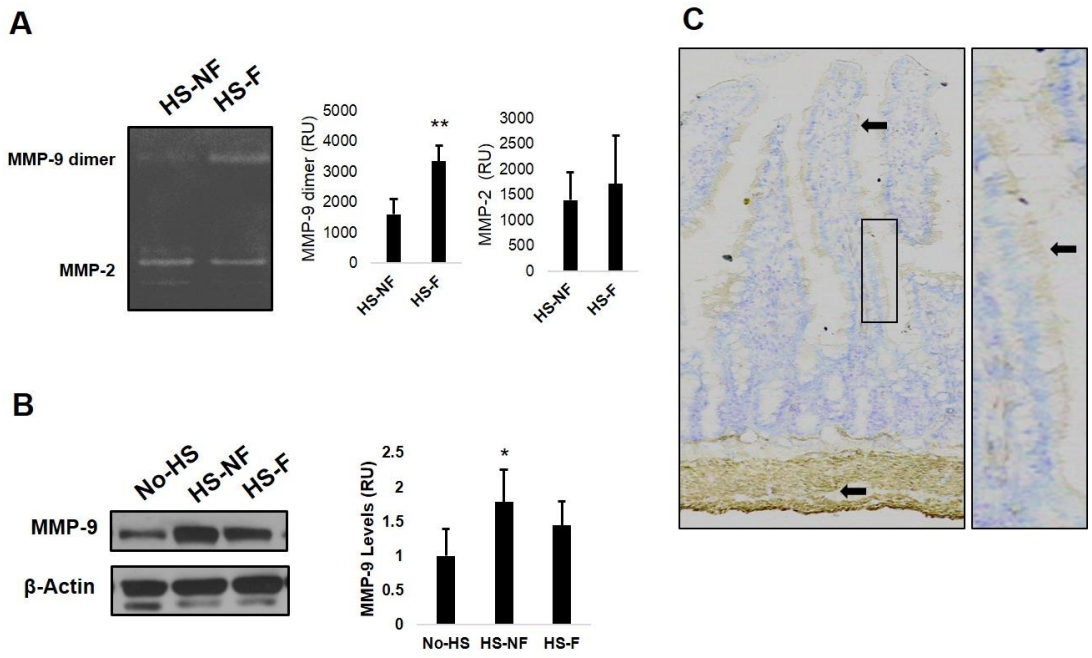

Figure 5.12 MMP-9 activity and levels in intestinal tissue. (A) The density of the MMP-9 dimer activity band is significantly elevated in HS-F intestinal homogenates. **, $p<0.05$ by t-test. There was no change in the activity band corresponding to active monomeric MMP-2. (B) MMP-9 protein levels were elevated by immunoblot in the HS-NF animals compared to the No-HS animals. $P<0.007$ by ANOVA followed by Tukey post-hoc analysis. (C) Immunohistochemistry against MMP-9 indicates the localization of the protein in the muscularis layer and the epithelial cells (magnified in the box to the right) in the jejunum segments. N=6 rats/group. Bar graphs show mean±SD.

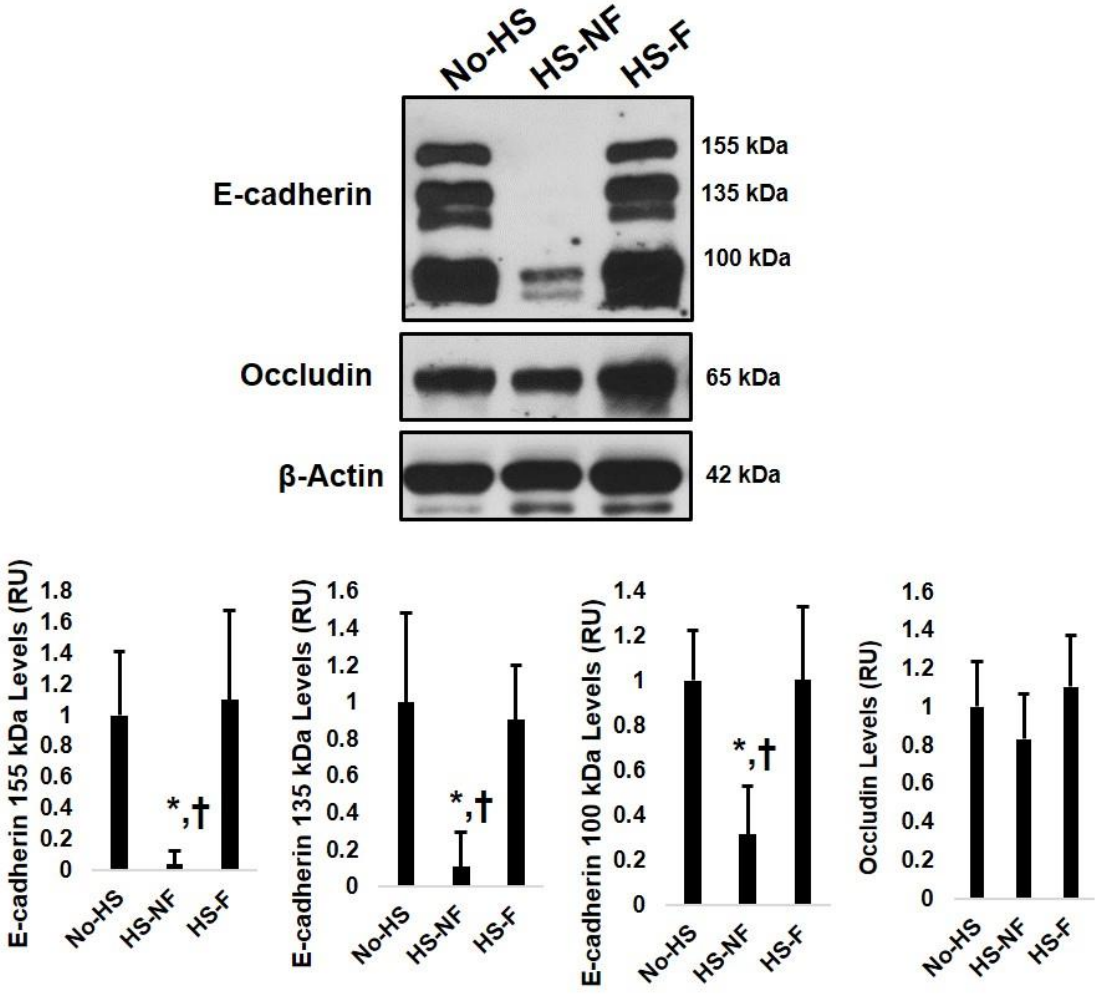

Figure 5.13 Intestinal epithelial junctional proteins. All three E-cadherin bands decreased in the intestine if there was luminal content present. Occludin levels did not significantly change. *, $p < 0.05$ compared to No-HS and †, $p < 0.05$ compared HS-F by ANOVA followed by Tukey post-hoc test. N=6 rats/group. Bar graphs show mean±SD.

5.4.3 Protease Activity and Levels in Plasma

Despite flushing luminal contents, both trypsin and chymotrypsin protein levels in the plasma did not change over the course of the experiment (Figure 5.14). MMP-9 activity in the plasma was elevated after HS in both cases (Figure 5.15A). The MMP-9 protein levels were also elevated after shock and higher in the HS-NF group (Figure 5.15B). There was no change in MMP-2 or pro-MMP-2 levels (not shown).

Homogenates of isolated neutrophils have strong gelatinase activity appearing at molecular weights for active MMP-9, pro-MMP-9 derived from neutrophils, and the MMP-9 dimer (Figure 5.16A). Non-reduced samples also show the same bands for MMP-9 (Figure 5.16B). Note that as little as 156 picograms of *total* neutrophil homogenate produced activity bands that were typically seen with 20 μg of lung homogenate of 0.5 μl of plasma.

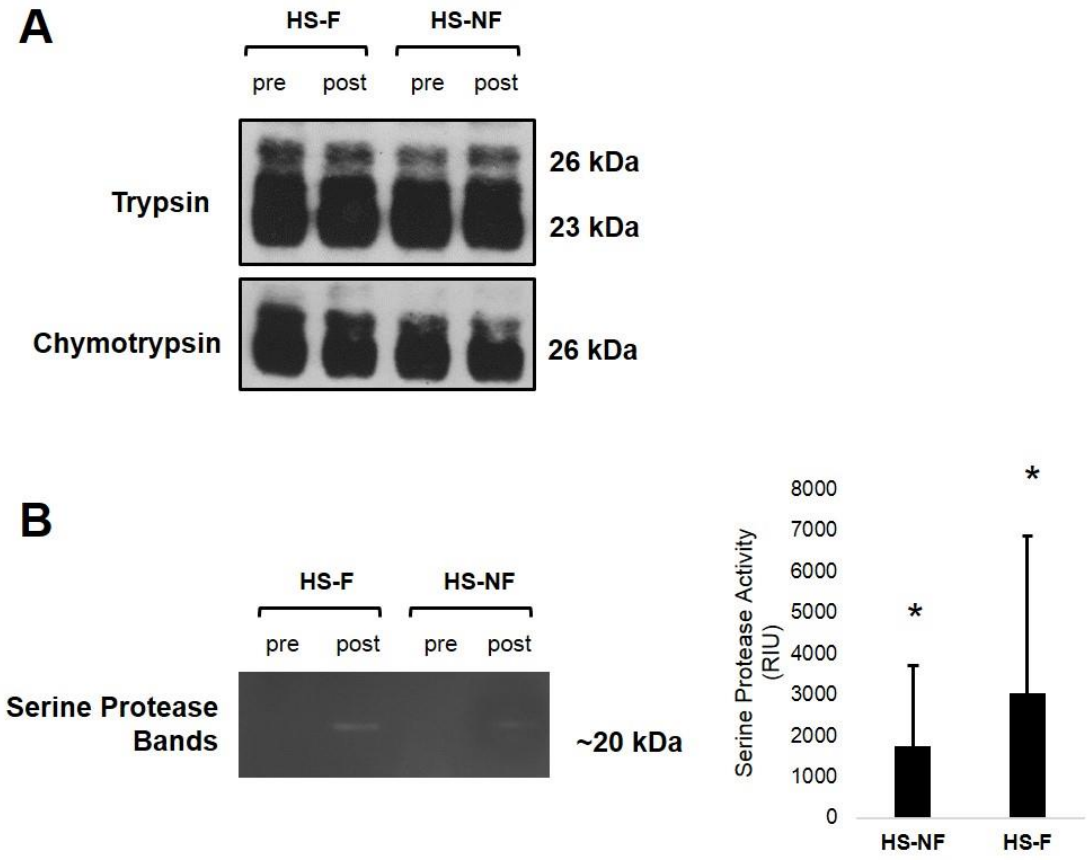

Figure 5.14 Serine proteases in the plasma. (A) Pancreatic trypsin and chymotrypsin were present in pre- and post-plasma samples at equal levels. There was no difference in levels between pre and post HS samples. (B) Activity bands corresponding to the molecular weight of serine proteases (3.7, 3.10, 4.20) formed by gelatin gel zymography of plasma samples after HS (bar graph, mean±SD). *, $p<0.05$ by Mann Whitney paired t-test compared to pre-plasma (undetectable in all Pre-plasma samples. N=6 rats/group.

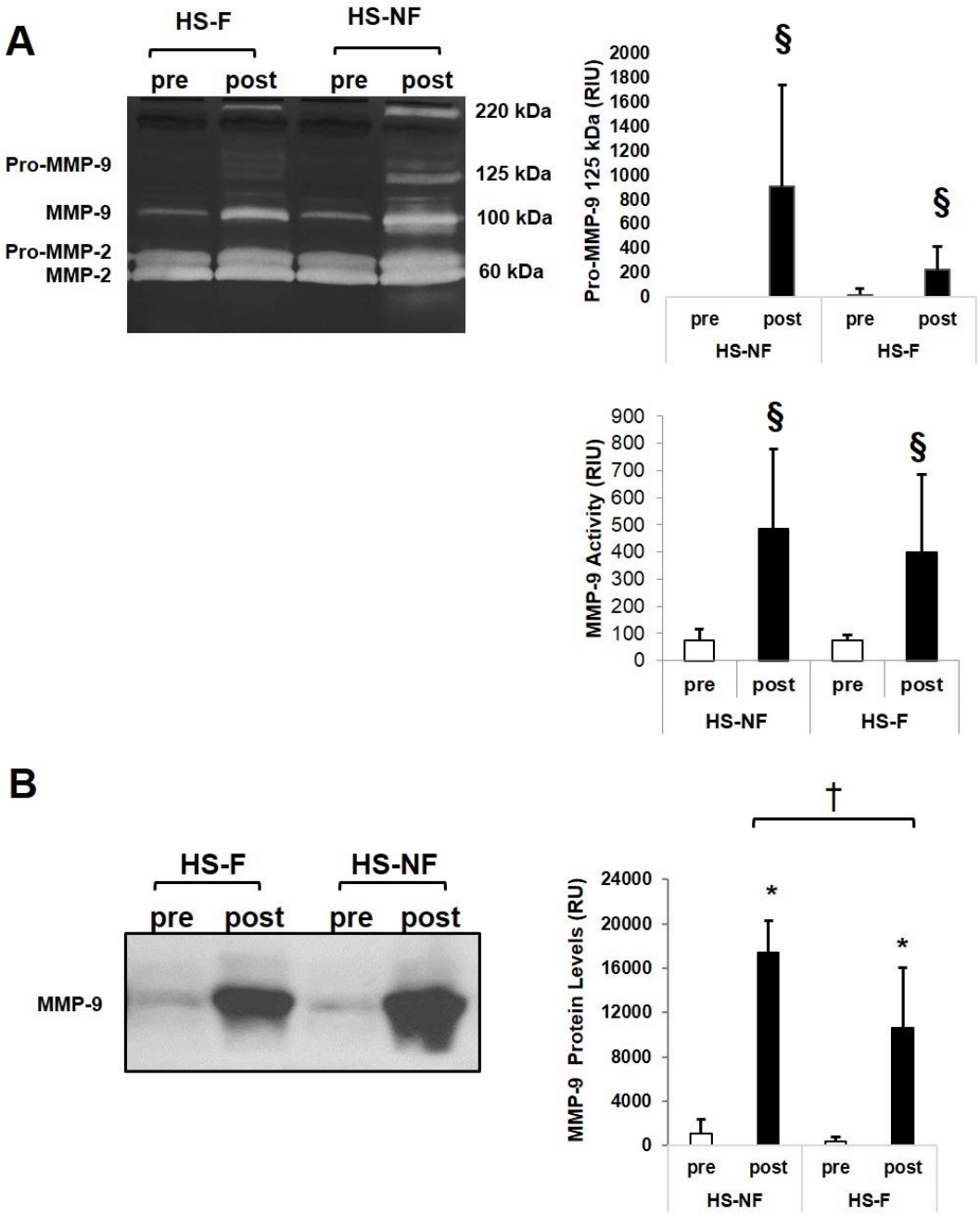

Figure 5.15 Plasma activity and protein levels of MMP-9. (A) The activity band corresponding to the MMP-9 dimer and active form of MMP-9 increased after shock as measured by gelatin gel zymography. **§**, $p<0.05$ by Mann Whitney test. (B) MMP-9 protein levels increased after hemorrhagic shock regardless of whether the intestine was flushed. *, $p<0.005$ by paired t-test between pre and post samples. †, $p<0.05$ by t-test between post-HS-F and post-HS-NF samples. Bar graphs show mean±SD. N=6 rats/group.

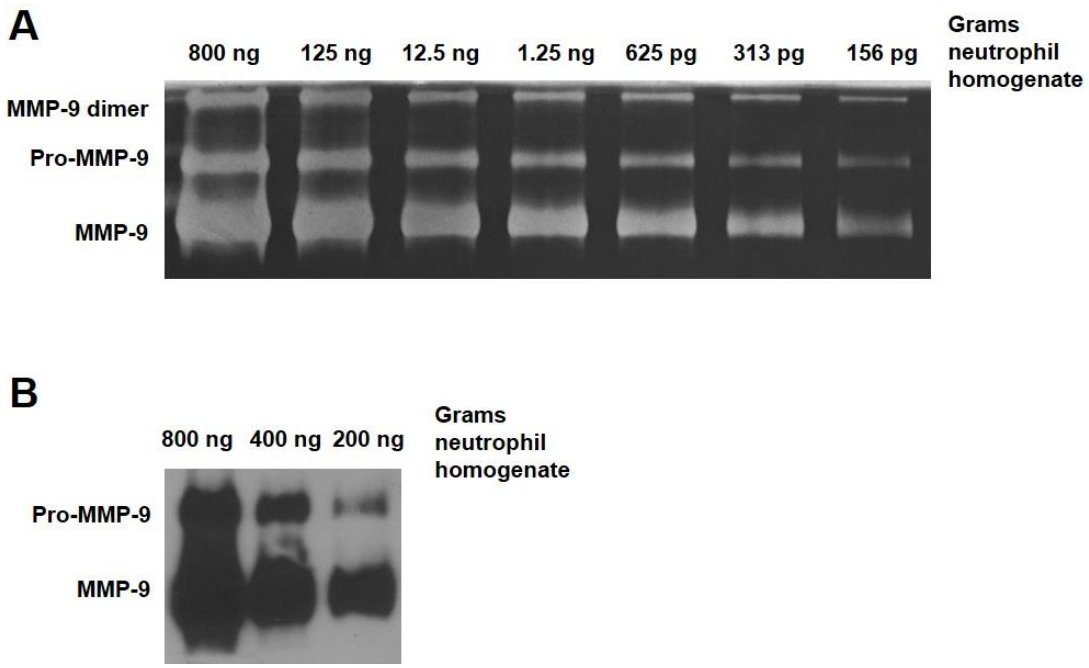

Figure 5.16 Neutrophil MMP-9 activity and levels. (A) Gelatinase activity of isolated neutrophils depicted three distinct bands for MMP-9, pro-MMP-9, and MMP-9 dimer at different dilutions. (B) MMP-9 bands were also detected by immunoblotting.

5.4.4. LUNG DAMAGE

Macroscopic bleeding into the lung tissue occurred in nearly all cases after hemorrhagic shock regardless of whether or not the intestine was flushed (Figure 5.17). Blind scoring of lung images did not serve to detect a significant difference between groups. Lung injury scores were 2.8±1.1 and 2.9±1.3, for the HS-F and HS-NF rats, respectively. Only one animal without a flushed intestine had a low lung injury. Histology of the sections indicates swelling of the alveoli (Figure 5.17).

Lung damage was also assessed by the amount of MPO activity in both the whole organ homogenate and the BALF fluid. In both flushed and no-flushed cases, there was an increase in MPO activity compared to the No-HS animals (Figure 5.18). BALF protein levels and MPO activity also increased following HS in both groups (Figure 5.18).

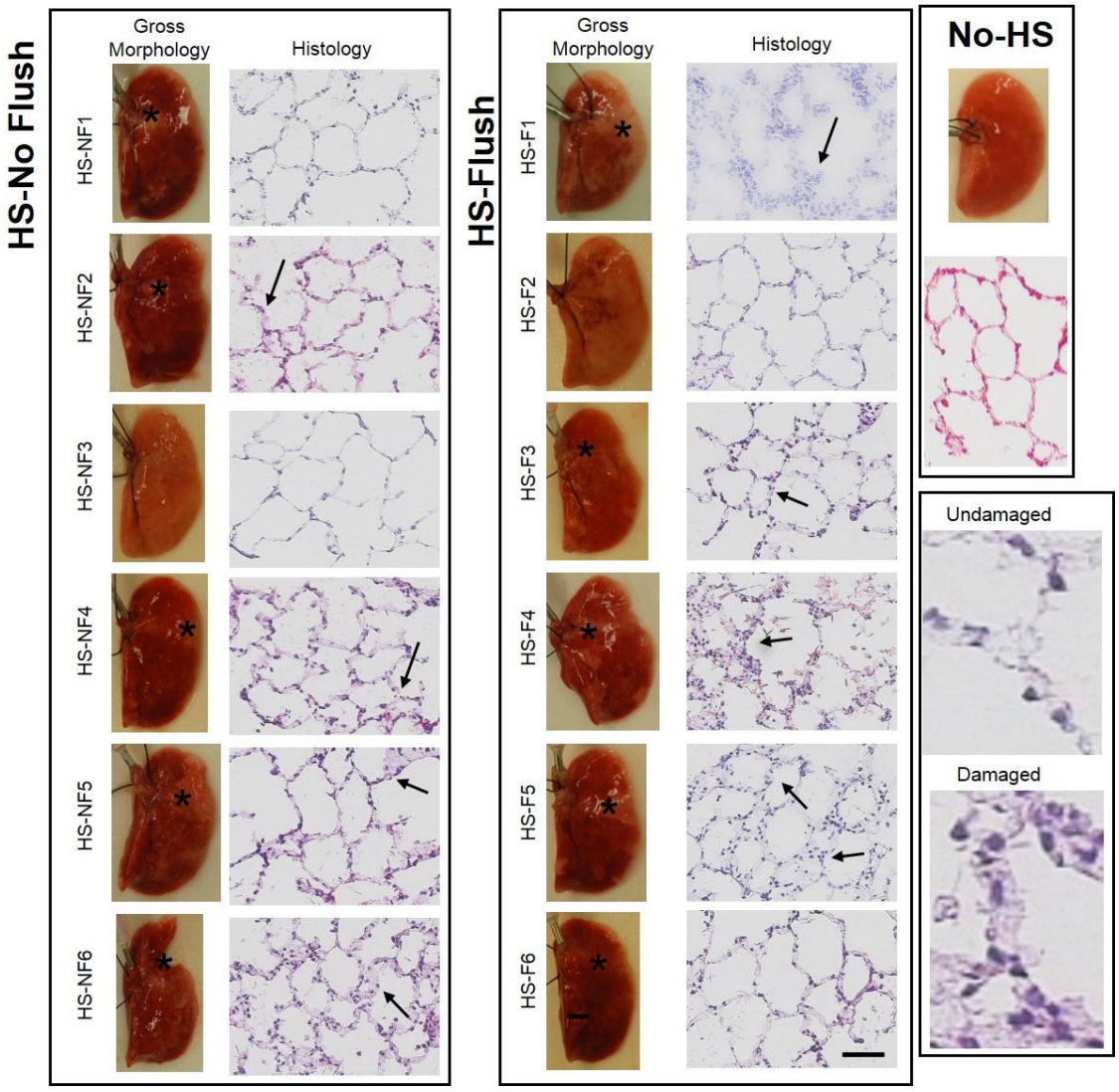

Figure 5.17 Gross morphology and lung histology. Lung damage in form of microhemorrhages was observed by gross morphology (see *). Histological sections of the most damaged lungs had visible swelling of the alveoli (arrows) and corresponding sample images magnified on the right. No-HS control exhibited no bleeding or swelling similar to HS-NF3.

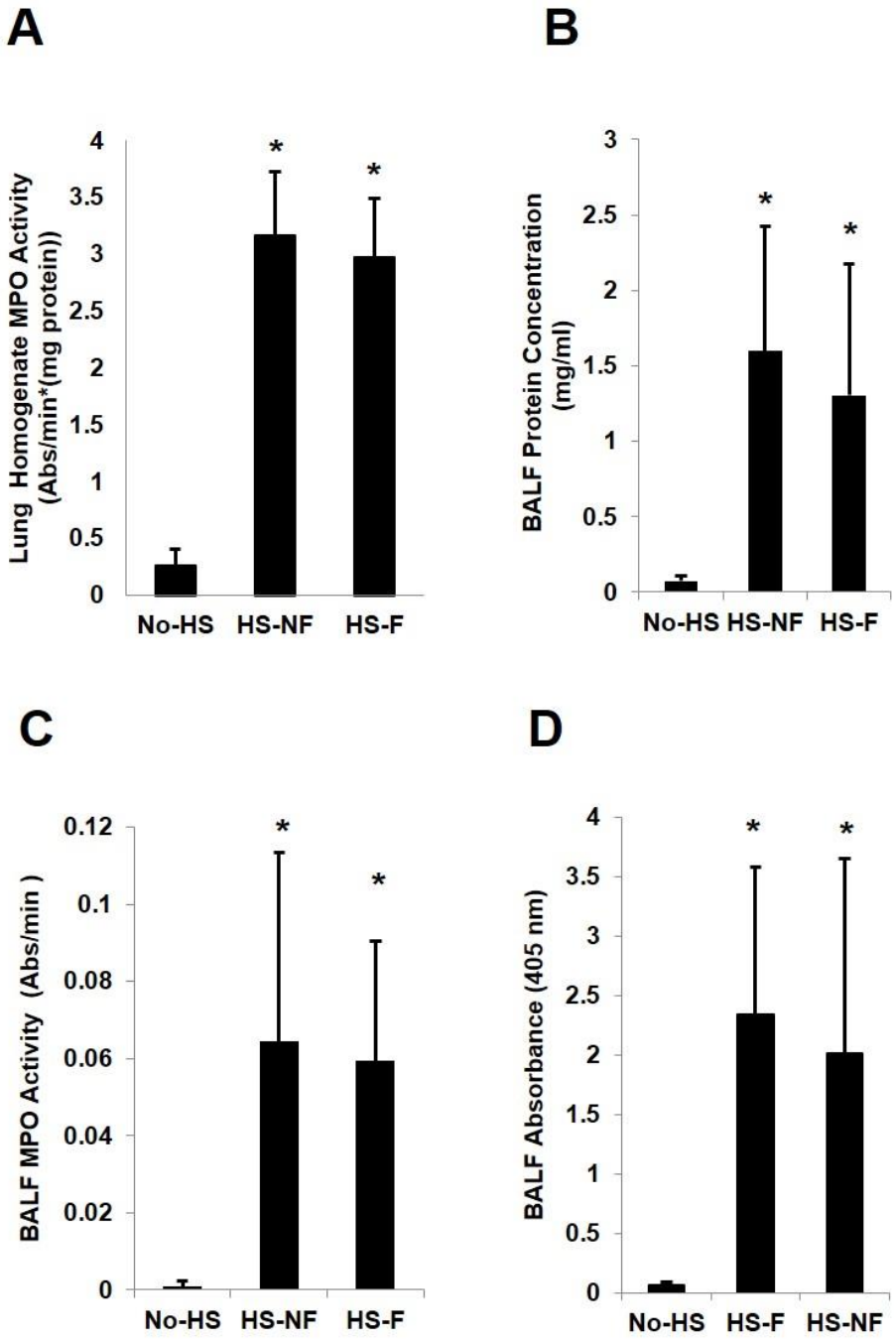

Figure 5.18 Lung injury parameters. (A) Lung MPO activity (B) BALF protein concentration, (C) BALF MPO activity, (D) BALF absorbance were all elevated after shock regardless of whether or not the intestine was flushed. *, $p<0.05$ by ANOVA followed by Tukey post-hoc. Bar graphs show mean± SD. N=6 rats/group.

5.4.5 Serine Protease Activity in the Intestine and Lung

In gelatin gel zymography, low molecular weight bands were found in the 20 kDa range (the same location as the serine protease band shown in the plasma in Figure 5.14B) of a flushed intestinal homogenate (Figure 5.19A). These bands were more intense in the HS-NF animals. Serine protease bands were also detected in lung homogenates in a similar pattern as the intestine (Figure 5.19B). The serine protease band densities were elevated in the lung homogenate of HS-NF animals and virtually absent in the No-HS and HS-F animals.

To verify that the low molecular weight bands were serine protease-derived, these bands were eliminated or reduced gels that were renatured and developed in either ANGD or TLCK (Figure 5.20A&B). Neither ANGD nor tranexamic acid reduced the gelatinase band intensities in the lung (Figure 5.20C).

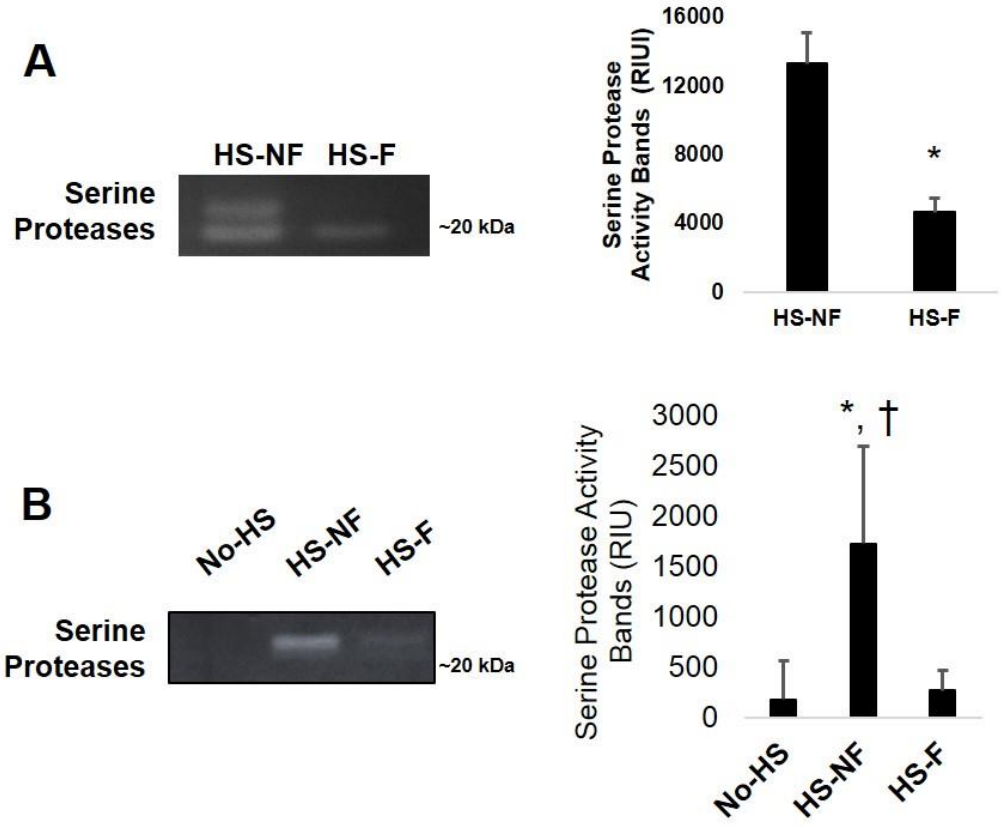

Figure 5.19 Serine protease bands detected in intestine and lung. (A) Serine protease activity bands in intestine are elevated in the homogenates of non-flushed intestines, although luminal content was removed prior to tissue processing. *, $p<0.05$ by t-test. (B) Serine protease activity bands were detected only in the lung homogenates of the intestines that were not flushed. *, $p<0.05$ compared to No-HS and †, $p<0.05$ compared to HS-F by ANOVA followed by Tukey post-hoc analysis. N=6 rats/group. Bar graphs show mean±SD.

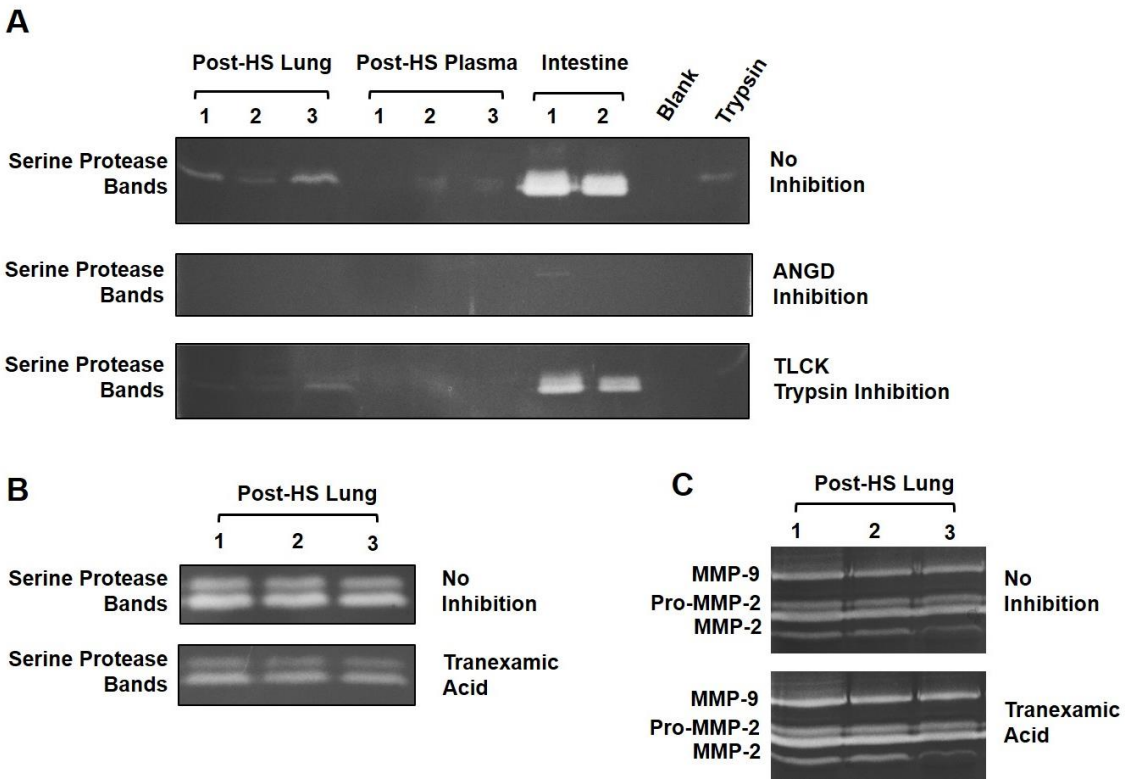

Figure 5.20 Serine protease activity inhibition during gelatin gel zymography. (A) Low molecular weight bands forming around 20 kDa were present in post-HS lung homogenate samples (20 µg protein/lane), plasma (0.5 µl/lane), and intestine homogenate (2 µg/lane). Renaturing and developing with ANGD eliminated all protease bands. Inhibition with the trypsin specific inhibitors reduced or eliminated the intensity in these bands. (B) Post-HS lung samples with serine protease bands were slightly reduced with 1 mM tranexamic acid renaturation but (C) unchanged in the gelatinase activities.

5.4.6 MMP Activity and Levels in the Lung

Active MMP-9 and pro-MMP-9 increased in both HS-F and HS-NF animals (Figure 5.21A). The active form of MMP-9 in the HS-NF animals was elevated compared to the HS-F animals. The protein levels as detected by immunoblotting were also elevated after HS (Figure 5.21B).

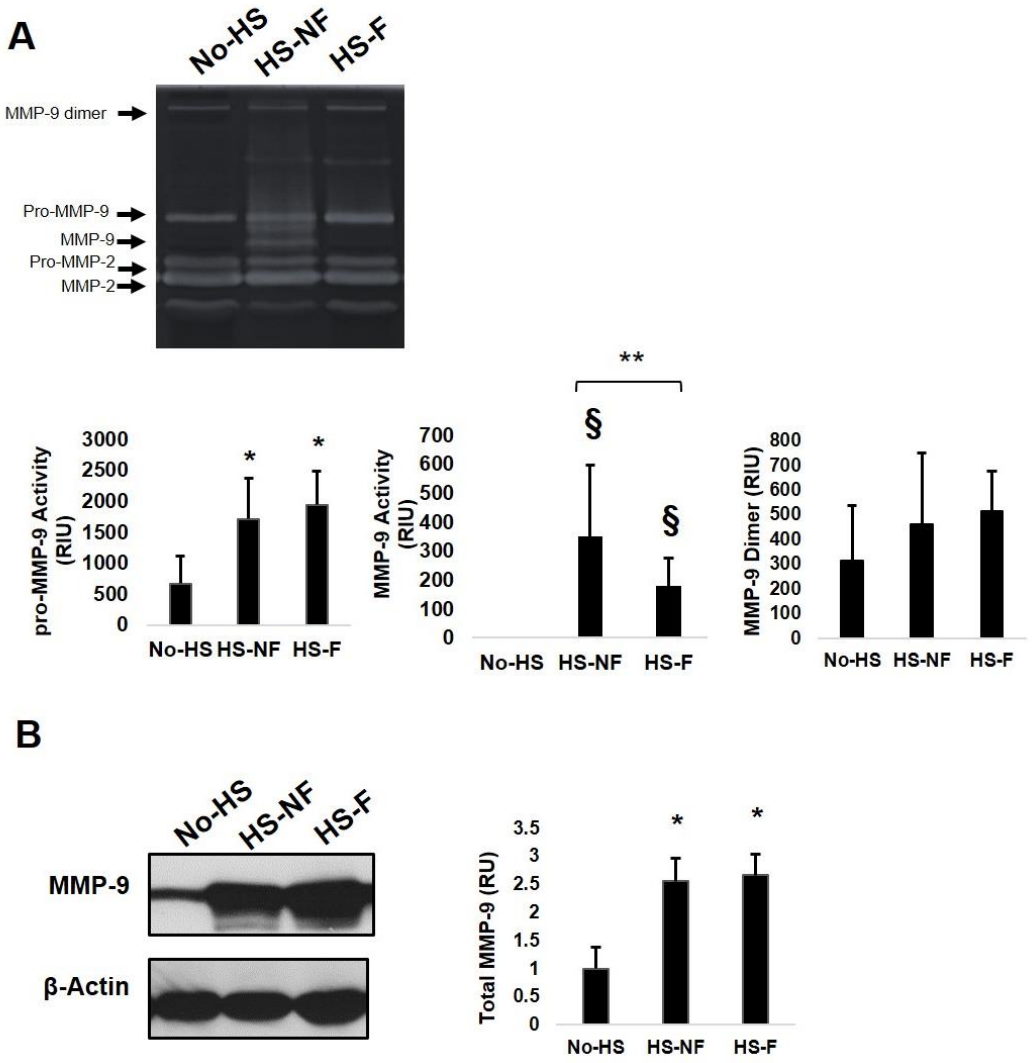

Figure 5.21 MMP-9 activity and levels in the lung. (A) The activity bands corresponding to both the pro- and active forms of MMP-9 increase after shock in both the HS-F and HS-NF cases, but there was no change in the MMP-9 dimer. (B) Protein levels of MMP-9 also increase after HS regardless of intestinal flush. *, $p<0.05$ compared to No-HS by ANOVA followed by Tukey post-hoc analysis. §, $p<0.05$ compared to No-HS and **, $p<0.05$ between HS-F and HS-NF by Mann Whitney test. Bar graphs show mean±SD. N=6 rats/group.

5.4.7 Endothelial Proteins in the Lung and Intestine

VE-cadherin was degraded in the lung after HS (Figure 5.22) regardless of intestinal flushing. E-cadherin, which appears in the epithelial and endothelial cells, was not significantly degraded after shock, but a lower molecular weight band (~135 kDa) increased after shock in both cases (Figure 5.22). The tight junction protein occludin decreased in the lung in both cases after hemorrhagic shock (Figure 5.22).

Both the mature and intermediate glycosylated forms of VEGFR-2 were decreased in the lung after HS (Figure 5.23). However, the VEGFR-2 and VEGFR-3 levels did not change in the intestine (Figure 5.24). The amount of VEGFR-2 in the intestine was low compared to the lung. In fact, VE-cadherin levels were hardly detectable by immunoblot in the intestine under these conditions.

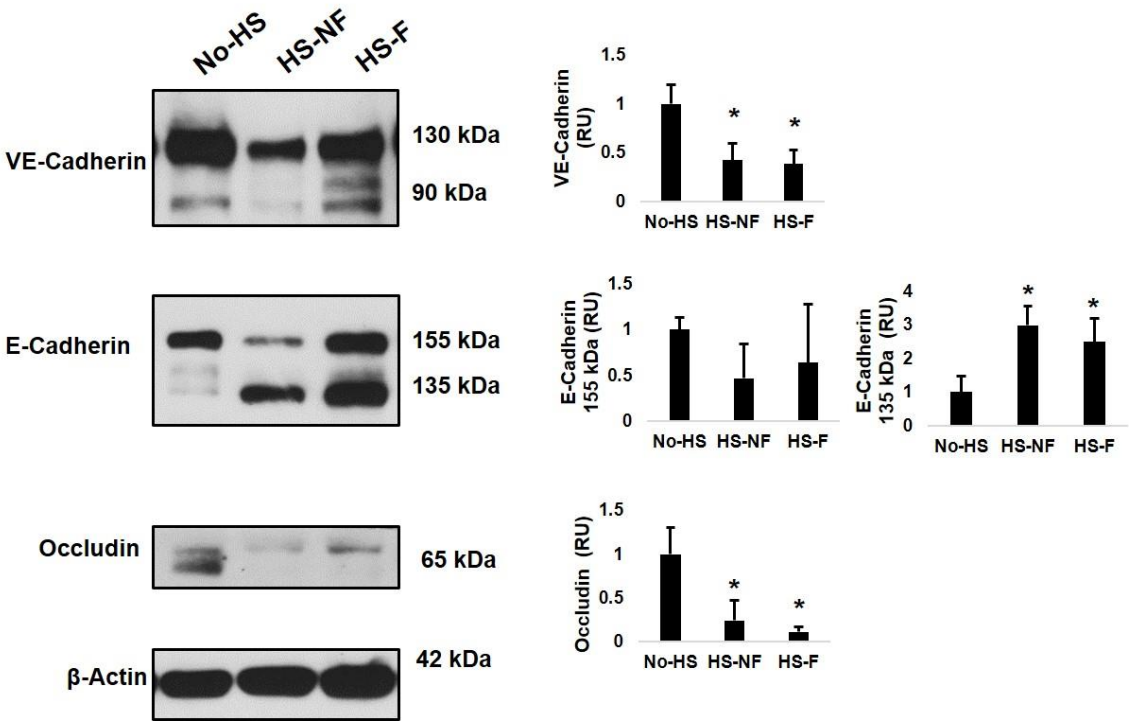

Figure 5.22 Adheren and tight junction proteins in the lung. VE-cadherin, E-cadherin, and occludin main isoforms all decrease following hemorrhagic shock. Band densities are normalized by β-actin bands and to No-HS levels. *, $p<0.05$ by ANOVA followed by Tukey post-hoc analysis. N=6 rats/group. Bar graphs show mean±SD.

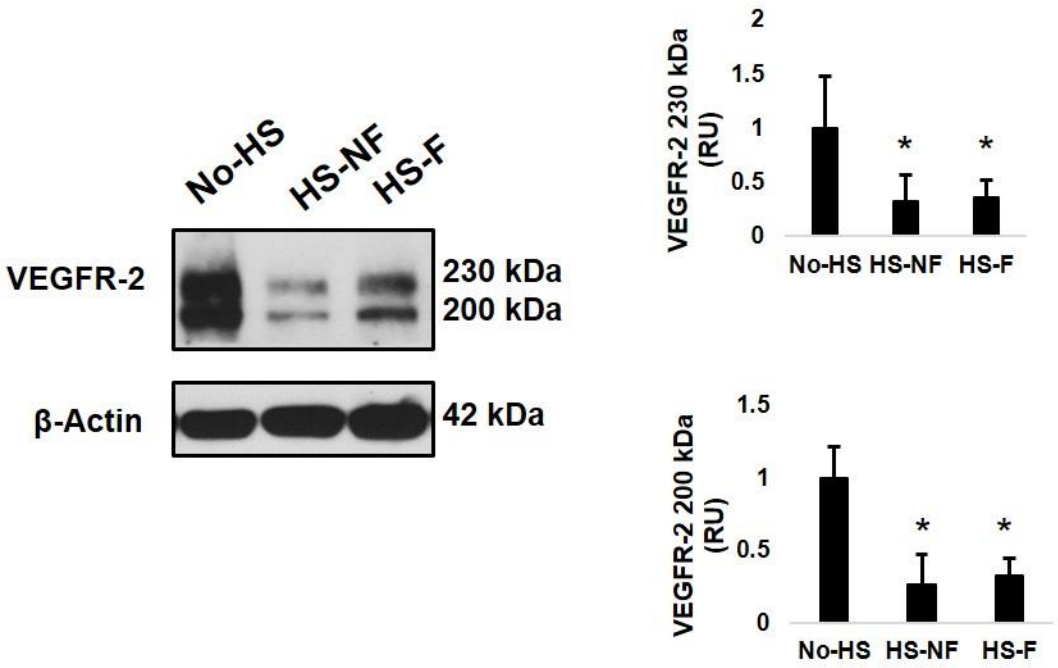

Figure 5.23 VEGFR-2 levels in lung. Both the 230 kDa mature and 200 kDa intermediate glycosylated forms of VEGFR-2 decreased after HS in the lung regardless of luminal contents. N=6 rats/group. *, $p<0.05$ by ANOVA followed by Tukey post-hoc analysis. Bar graphs show mean±SD.

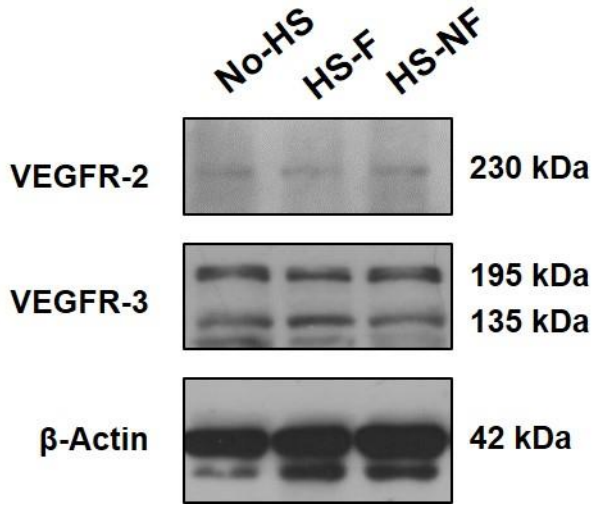

Figure 5.24 VEGFR-2 and VEGFR-3 levels in intestine. There was no change in VEGFR-2 or VEGFR-3 levels in the intestine after HS. N=6 rats/group.

5.5 Discussion

5.5.1 Summary

Intestinal damage on the macroscopic and molecular level is more severe if the animal are subject to hemorrhagic shock in the presence of its normal luminal contents (HS-NF group). Red cell escape and neutrophil accumulation positively correlated with proteolytic activity in intestinal homogenates. However, the presence of the intestine's luminal contents affected neither the levels of serine proteases in the plasma nor lung injury. Lung endothelial and epithelial proteins were degraded to the same extent in both groups even though HS-NF animals had greater lung proteolytic activity as measured by serine proteases and MMP-9 and greater MMP-9 levels in their plasma. The MAP of animals did not correlate with the degree of organ injury in the animals, indicating that degrading mechanisms may not be reflected by the animal's blood pressure.

5.5.2 Intestinal Injury Severity Increases if Luminal Contents are Present

Micrographs of the intestine after hemorrhagic shock show little physical destruction of the intestinal villi structure (Figure 5.10 and Figure 5.11) compared to that seen in SAO models [3,9-11]. The macroscopic hemorrhagic lesions in which red cells enter the intestinal wall and lumen are common after shock [12-14] and are only formed if the luminal contents are present (Figure 5.4 and 5.5). Furthermore, the strong correlation between intestinal wall hemorrhage and proteolytic activity of the intestinal

homogenate (Figure 5.7) suggests that the digestive proteases play a role in the formation of these vascular lesions.

Our group has shown previously that intestinal ischemia can result in transport of pancreatic proteases into the lamina propria [9,15]. For these enzymes to enter the intestinal wall (and subsequently for red blood cells to enter the intestinal lumen), the mucosal barrier must fail. Following HS, regardless of flushing, epithelial cells were present in the lumen (Figure 5.11) similar to previous reports, which observe epithelial shedding into the lumen after intestinal ischemia [10,16-18]. This suggests that even though the villi appear intact, openings in the barrier occur as epithelial cells are shed along with the attached mucin, providing exit pathways for pancreatic enzymes to enter the intestinal wall.

Since pancreatic proteases may promote epithelial barrier failure by cleaving adhesion proteins between the cells, we investigated whether epithelial junctional proteins were degraded after HS in the presence or absence of luminal content. The presence of luminal content did not affect the levels of the tight junctional protein occludin (Figure 5.13). However, the adheren junctional protein E-cadherin was degraded only in the non-flushed animals (Figure 5.13), which is consistent with previous reports from our group that E-cadherin degrades during intestinal ischemia, possibly by the digestive enzymes [9,15].

Pancreatic proteases are not the only proteases entering or activated in the intestinal wall during HS. No-HS and HS-NF animal intestines were homogenized with their luminal contents to determine the combined caseinolytic activity. The majority of the caseinolytic activity in a whole intestinal (wall plus lumen) homogenate is derived

from luminal pancreatic enzymes [19], which is expected to be similar between the two groups. However, the HS-NF animals exhibited higher levels of caseinolytic activity suggesting there may exist an additional source of proteases present in the HS-NF animals (Figure 5.5). Since MPO activity also increased in intestinal homogenates in the HS-NF animals (Figure 5.8) indicating neutrophil accumulation, neutrophil derived elastase or MMPs could be an additional source of proteolytic activity. Alternatively, pancreatic proteases may activate MMPs [20,21] or other proteases from their pro-forms or degrade inhibitors such as TIMPs yielding a net increase in protease activity. Studies using enteral treatment with the serine protease and lipase inhibitor ANGD have reduced microhemorrhages in the intestine and improved outcomes in experimental shock [3,6,7,22], which supports the hypothesis that digestive enzymes are responsible for the lesions. If the pancreatic enzymes enter the wall but are inactive, they would be unable to trigger a proteolytic activation cascade of MMPs (Figure 5.12 and Figure 5.15) or degrade epithelial proteins (Figure 5.13). However, it should be noted that ANGD is solubilized in a glucose solution, and glucose itself is sufficient to prevent the epithelial barrier from disintegrating during intestinal ischemia [23-25]. Failure of the epithelial barrier alone does not appear to be sufficient to cause hemorrhage since there were no hemorrhages in HS-F animals despite the lack of a metabolic energy source in the lumen of the intestine. Therefore, the most plausible explanation for the reduction in microhemorrhages is due to the absence of protease activity.

Development of microhemorrhage requires that the endothelial cells lining the blood vessels must fail. This could occur by a number of possible mechanisms. Pancreatic proteases may digest basement membrane and endothelial cell adhesion

proteins. Alternatively or in addition, the proteases may cleave extracellular matrix or dietary proteins into bioactive peptides that increase vessel leakage, or by cleaving fatty acid binding proteins, allow free fatty acids to dissolve the lipid membranes of the endothelial cells [26-28]. The actions of bioactive peptides or free fatty acids may also be pro-inflammatory [29-31] contributing to the neutrophil accumulation. Neutrophil elastase and neutrophil derived MMP-9 (Figure 5.16) can digest the endothelial basement membrane causing intestinal hemorrhage [32,33].

Since survival signaling could affect endothelial cell viability and thus permeability, we also examined protein levels of the endothelial growth receptors VEGFR-2 and VEGFR-3. Interestingly, despite the dense vascular network in the intestine, levels of the endothelial growth receptor VEGFR-2 were low and remained the same between the groups (Figure 5.24) while VEGFR-3 protein levels, associated more with lymphatic vessels, were more prevalent than VEGFR-2 (but also unchanged after shock) (Figure 5.24).

5.5.3 Serine Protease Transport Occurs before Shock, but Activity Increases only after Hemorrhagic Shock

The major exit routes of translocated luminal content from the intestine into the circulation can be directly via the portal venous circulation, the mesenteric lymph, or the peritoneal space and the lymphatics surrounding the peritoneum. Contrary to the previous model for hemorrhagic shock described in Chapter 3, the levels of trypsin and chymotrypsin as detected by immunoblotting were greater in plasma before and after

hemorrhagic shock in either HS-F or HS-NF animals (Figure 5.14A). This suggests an inherent difference between the two models (choice of anesthetic, rat strain, ischemic time, reperfusion time, and/or ischemic pressure). Since pancreatic proteases are present in all plasma samples before the onset of hemorrhagic shock, they may have already entered the circulation and were not cleared during the course of the experiment. However, the activity of low molecular weight bands formed by gelatin gel zymography always occur with greater intensity in post-HS plasma, regardless of the luminal contents (Figure 5.14B). The source of these enzymes could also be derived from the pancreas or unflushed regions of the intestine. Since these enzymes were inhibited when the zymography gels were incubated with ANGD or TLCK, they are of serine protease origin (Figure 20A&B).

Even though the luminal contents were only removed in the flushed group, the serine protease bands were detected by gelatin gel zymography in intestinal wall homogenates of both flushed and non-flushed intestines (Figure 5.19A), though to a greater extent in the non-flushed intestines. These proteases were only observed in lung tissue of the HS-NF group by gelatin gel zymography (Figure 5.19B). These pancreatic proteases in the lung could be transported through the mesenteric lymph and accumulate in the lung which is the first capillary bed encountered. Plasma proteins accumulate in the lung tissue after shock and serine proteases, composing a small fraction of the total plasma protein content, may contribute to the observed protease accumulation in the HS-NF lung tissues [34]. Since inhibition of these enzymes with ANGD and TLCK eliminated the bands, this suggests these are gut-derived pancreatic enzymes (Figure 5.20A&B) instead of MMPs or plasmin [35].

5.5.4 MMP-9 Accumulation in Tissues after Hemorrhagic Shock

In all animals, MMP-9 activity and levels increased in the plasma, which is consistent with the findings of Chapter 3. The protein levels in the plasma were elevated in groups without flushed intestine (Figure 5.15) suggesting that luminal contents have the ability to activate neutrophils and endothelial cells to increase secretion of MMP-9 into the plasma (Figure 5.16). The intestine's MMP-9 levels increased only in the HS-NF animals (Figure 5.12B) and may be due to increased neutrophil accumulation in the wall, an observation that is supported by the increased MPO activity (Figure 5.8). The MMP-9 protein accumulation in the intestine could also be caused by conversion of the dimer to the active form of MMP-9 (Figure 5.12A), although the activity levels did not increase as measured by gelatin gel zymography.

MMP-9 levels and activity also increased in the lung during hypotension in both the HS-F and HS-NF animals (Figure 5.21). The active form of MMP-9 was nearly doubled in the HS-NF group compared to the HS-F group (Figure 5.21A). The increase in MMP-9 activity may be due to activation by serine proteases transported into the lung (Figure 5.19B) [21]. Although there was more MMP-9 and serine protease activity in the lungs in the HS-NF animals, the BALF protein levels and MPO activity were elevated for both groups after hemorrhagic shock (Figure 5.18).

5.5.5 Protein Degradation in the Lung

Proteolytic degradation of both endothelial and epithelial proteins was observed in lung homogenates after hemorrhagic shock and did not differ between the HS-NF and HS-F groups. VE-cadherin, an adhesion protein expressed on lung endothelial cells [36], occludin, a tight junction protein present on both endothelial and epithelial cells in the lung, and both isoforms of the endothelial growth receptor VEGFR-2 were reduced after hemorrhagic shock in both groups (Figure 5.22 and 5.23). E-cadherin, another endothelial adhesion protein also decreased (non-significant) after shock, and there was a significant increase in a smaller molecular weight form of the protein suggesting cleavage by a protease (Figure 5.22). Neutrophils accumulate in the lung during shock (Figure 5.17) and could therefore contribute to the loss and/or cleavage of these proteins, as neutrophil elastase and MMPs have been documented to contribute to the destruction of cadherins [8,37], possibly as part of neutrophil transmigration. The loss of any or all of the proteins tested here could contribute to increased lung permeability. However, since all of these proteins were degraded regardless of the presence of luminal content, the mechanism is likely independent of the proteases present in the lumen of the intestine.

Alternatively, since we observed a slight reduction in the 155 kDa form of E-cadherin in the HS-NF animals compared to No-HS animals (Figure 5.22) and also detected serine protease bands by gelatin gel zymography in the lung homogenates of only HS-NF animals (Figure 5.19). Since E-cadherin was abolished in all the HS-NF *intestine* samples (Figure 5.13), the accumulation of serine proteases present in the lung may contribute to the enhanced degradation of lung E-cadherin.

5.5.6 LIMITATIONS

Although flushing the intestinal luminal contents is a useful experimental technique for determining which indices of organ damage are influenced by intestinal luminal factors during shock, it is clinically less feasible at the moment. Other limitations of this model include that while the jejunum and ileum regions were flushed, the duodenum and terminal ileum adjacent to the cecum contained luminal contents. Also, many of the same mediators that could originate from the intestine in the presence of luminal content can be generated in the ischemic pancreas [38] and would be unaffected by flushing the intestine. As with my other animal models, I chose not to control the food intake of the HS-NF animals, and the animals had variable amounts of food in different regions of the intestine and may explain some of the variability in the HS-NF group.

5.6 CONCLUSIONS

By investigating the outcome of hemorrhagic shock with or without luminal contents in the intestine, we observed an increase in intestinal damage in the presence of luminal contents. While the luminal contents increased the intestinal hemorrhage and protein degradation after hemorrhagic shock, reducing this damage by removing luminal content does not reduce the peripheral organ injury in the lung. Therefore, future studies need to investigate methods to prevent the escape of the luminal contents past the

epithelial barrier and alternative options to reduce lung injury following hemorrhagic shock.

Chapters 5, 6 and 7, in full, are currently being prepared for submission for publication entitled “Strategies to minimize organ injury by proteolytic enzymes in hemorrhagic shock” by Angelina E. Altshuler, Michael Richter, Jason Chou, Diana Li, Leena Kurre, Alexander H. Penn, and Geert W. Schmid-Schönbein. The dissertation author is the primary author of this manuscript.

5.7 REFERENCES

1. Ishimaru K, Mitsuoka H, Unno N, Inuzuka K, Nakamura S, Schmid-Schönbein GW. (2004) Pancreatic proteases and inflammatory mediators in peritoneal fluid during splanchnic arterial occlusion and reperfusion. Shock 22: 467-471.

2. Qin X, Sheth SU, Sharpe SM, Dong W, Lu Q, Xu D, Deitch EA. (2011) The mucus layer is critical in protecting against ischemia-reperfusion-mediated gut injury and in the restitution of gut barrier function. Shock 35: 275-281.

3. Mitsuoka H, Schmid-Schönbein GW. (2000) Mechanisms for blockade of in vivo activator production in the ischemic intestine and multi-organ failure. Shock 14: 522-527.

4. Mitsuoka H, Kistler EB, Schmid-Schönbein GW. (2000) Generation of in vivo activating factors in the ischemic intestine by pancreatic enzymes. Proc Natl Acad Sci U S A 97: 1772-1777.

5. Deitch EA, Shi HP, Lu Q, Feketeova E, Xu DZ. (2003) Serine proteases are involved in the pathogenesis of trauma-hemorrhagic shock-induced gut and lung injury. Shock 19: 452-456.

6. Doucet JJ, Hoyt DB, Coimbra R, Schmid-Schönbein GW, Junger WG, Paul LW, Loomis WH, Hugli TE. (2004) Inhibition of enteral enzymes by enteroclysis with nafamostat mesilate reduces neutrophil activation and transfusion requirements after hemorrhagic shock. J Trauma 56: 501-10; discussion 510-1.

7. DeLano FA, Hoyt DB, Schmid-Schönbein GW. (2013) Pancreatic digestive enzyme blockade in the intestine increases survival after experimental shock. Sci Transl Med 5: 169ra11.

8. Carden D, Xiao F, Moak C, Willis BH, Robinson-Jackson S, Alexander S. (1998) Neutrophil elastase promotes lung microvascular injury and proteolysis of endothelial cadherins. Am J Physiol 275: H385-92.

9. Chang M, Kistler EB, Schmid-Schönbein GW. (2012) Disruption of the mucosal barrier during gut ischemia allows entry of digestive enzymes into the intestinal wall. Shock 37: 297-305.

10. Ikeda H, Suzuki Y, Suzuki M, Koike M, Tamura J, Tong J, Nomura M, Itoh G. (1998) Apoptosis is a major mode of cell death caused by ischaemia and ischaemia/reperfusion injury to the rat intestinal epithelium. Gut 42: 530-537.

11. Grossmann J, Walther K, Artinger M, Rummele P, Woenckhaus M, Scholmerich J. (2002) Induction of apoptosis before shedding of human intestinal epithelial cells. Am J Gastroenterol 97: 1421-1428.

12. Chiu CJ, McArdle AH, Brown R, Scott HJ, Gurd FN. (1970) Intestinal mucosal lesion in low-flow states. I. A morphological, hemodynamic, and metabolic reappraisal. Arch Surg 101: 478-483.

13. Manohar M, Tyagi RP. (1973) Experimental intestinal ischemia shock in dogs. Am J Physiol 225: 887-892.

14. Haglund U, Hulten L, Ahren C, Lundgren O. (1975) Mucosal lesions in the human small intestine in shock. Gut 16: 979-984.

15. Chang M, Alsaigh T, Kistler EB, Schmid-Schönbein GW. (2012) Breakdown of mucin as barrier to digestive enzymes in the ischemic rat small intestine. PLoS One 7: e40087.

16. Vakonyi T, Wittmann T, Varro V. (1977) Effect of local circulatory arrest on the structure of the enterocytes of the isolated intestinal loop. Digestion 15: 295-302.

17. Robinson JW, Mirkovitch V, Winistorfer B, Saegesser F. (1981) Response of the intestinal mucosa to ischaemia. Gut 22: 512-527.

18. Bounous G, Cronin RF, Gurd FN. (1967) Dietary prevention of experimental shock lesions. Arch Surg 94: 46-60.

19. Penn AH, Hugli TE, Schmid-Schönbein GW. (2007) Pancreatic enzymes generate cytotoxic mediators in the intestine. Shock 27: 296-304.

20. Rosario HS, Waldo SW, Becker SA, Schmid-Schönbein GW. (2004) Pancreatic trypsin increases matrix metalloproteinase-9 accumulation and activation during acute intestinal ischemia-reperfusion in the rat. Am J Pathol 164: 1707-1716.

21. Duncan ME, Richardson JP, Murray GI, Melvin WT, Fothergill JE. (1998) Human matrix metalloproteinase-9: Activation by limited trypsin treatment and generation of monoclonal antibodies specific for the activated form. Eur J Biochem 258: 37-43.

22. Shi HP, Liu ZJ, Wen Y. (2004) Pancreatic enzymes in the gut contributing to lung injury after trauma/hemorrhagic shock. Chin J Traumatol 7: 36-41.

23. Kozar RA, Hu S, Hassoun HT, DeSoignie R, Moore FA. (2002) Specific intraluminal nutrients alter mucosal blood flow during gut ischemia/reperfusion. JPEN J Parenter Enteral Nutr 26: 226-229.

24. Chiu CJ, Scott HJ, Gurd FN. (1970) Intestinal mucosal lesion in low-flow states. II. the protective effect of intraluminal glucose as energy substrate. Arch Surg 101: 484-488.

25. Mirkovitch V, Menge H, Robinson JW. (1975) Protection of the intestinal mucosa during ischaemia by intraluminal perfusion. Res Exp Med (Berl) 166: 183-191.

26. Davis GE. (2010) Matricryptic sites control tissue injury responses in the cardiovascular system: Relationships to pattern recognition receptor regulated events. J Mol Cell Cardiol 48: 454-460.

27. Penn AH, Schmid-Schönbein GW. (2008) The intestine as source of cytotoxic mediators in shock: Free fatty acids and degradation of lipid-binding proteins. Am J Physiol Heart Circ Physiol 294: H1779-92.

28. Qin X, Dong W, Sharpe SM, Sheth SU, Palange DC, Rider T, Jandacek R, Tso P, Deitch EA. (2012) Role of lipase-generated free fatty acids in converting mesenteric lymph from a noncytotoxic to a cytotoxic fluid. Am J Physiol Gastrointest Liver Physiol 303: G969-78.

29. Badwey JA, Curnutte JT, Robinson JM, Berde CB, Karnovsky MJ, Karnovsky ML. (1984) Effects of free fatty acids on release of superoxide and on change of shape by human neutrophils. reversibility by albumin. J Biol Chem 259: 7870-7877.

30. Ferrante A, Goh D, Harvey DP, Robinson BS, Hii CS, Bates EJ, Hardy SJ, Johnson DW, Poulos A. (1994) Neutrophil migration inhibitory properties of polyunsaturated fatty acids. the role of fatty acid structure, metabolism, and possible second messenger systems. J Clin Invest 93: 1063-1070.

31. Penn AH, Altshuler AE, Small JW, Taylor SF, Dobkins KR, Schmid-Schönbein GW. (2012) Digested formula but not digested fresh human milk causes death of intestinal cells in vitro: Implications for necrotizing enterocolitis. Pediatr Res .

32. Allport JR, Lim YC, Shipley JM, Senior RM, Shapiro SD, Matsuyoshi N, Vestweber D, Luscinskas FW. (2002) Neutrophils from MMP-9- or neutrophil elastase-deficient mice show no defect in transendothelial migration under flow in vitro. J Leukoc Biol 71: 821-828.

33. Hu J, Van den Steen PE, Dillen C, Opdenakker G. (2005) Targeting neutrophil collagenase/matrix metalloproteinase-8 and gelatinase B/matrix metalloproteinase-9 with a peptidomimetic inhibitor protects against endotoxin shock. Biochem Pharmacol 70: 535-544.

34. Staub NC. (1981) Pulmonary edema due to increased microvascular permeability. Annu Rev Med 32: 291-312.

35. Frederiks WM, Mook OR. (2004) Metabolic mapping of proteinase activity with emphasis on in situ zymography of gelatinases: Review and protocols. J Histochem Cytochem 52: 711-722.

36. Shasby DM. (2007) Cell-cell adhesion in lung endothelium. Am J Physiol Lung Cell Mol Physiol 292: L593-607.

37. Navaratna D, McGuire PG, Menicucci G, Das A. (2007) Proteolytic degradation of VE-cadherin alters the blood-retinal barrier in diabetes. Diabetes 56: 2380-2387.

38. Kistler EB, Hugli TE, Schmid-Schönbein GW. (2000) The pancreas as a source of cardiovascular cell activating factors. Microcirculation 7: 183-192.

.

Chapter 6

Intervening with Intestinal Wall Breakdown during Hemorrhagic Shock

6.1 INTRODUCTION

The intestinal barrier is disrupted during ischemia, allowing luminal contents to leak into the wall of the intestine and penetrate into the periphery through the peritoneal space, circulation, or lymphatics [1,2]. The transport of luminal contents can be pro-inflammatory after hemorrhagic shock if they cross the mucosal barrier, causing a cascade of events including neutrophil accumulation and epithelial protein degradation [3-5].

The ideal solution to prevent luminal content from entering the wall of the intestine is to eliminate it completely from the lumen; however, this is difficult to accomplish in clinical situations. A more realistic approach is to prevent luminal contents from entering the wall of the intestine in the first place, which could even be achieved without blocking the digestive enzymes, as long as the mucosal barrier is intact. The intestinal barrier may be compromised by two major mechanisms. First, epithelial

shedding and apoptosis are accelerated during ischemia and can be prevented by enteral glucose treatment [6-11]. Second, the villi can be proteolytically degraded which can be ameliorated with tranexamic acid [5,12,13]. The majority of these studies using either enteral glucose or tranexamic acid administration only studied the outcome of the intestine and not the consequences of peripheral organ injury.

In Chapter 3, we found that even if we preserve the barrier with ANGD+glucose, there is still a rise in protease activity after hemorrhagic shock. One of the key observations from these studies is that MMP-9 activity increases after HS and could be responsible for the degradation of endothelial cell components that were discussed in Chapter 5. Inhibition of these enzymes reduces vascular injury in ischemia reperfusion models [14-18], but there has been little application to the model of hemorrhagic shock where the ischemia is global. If MMPs are inhibited, the peripheral injury may be reduced.

6.2 CHAPTER AIMS

In this chapter, I will test three different interventions to determine the underlying cause of peripheral organ injury. First, I will block MMPs by injecting doxycycline into the plasma and peritoneal space. Second, I will minimize gut barrier breakdown by enteral tranexamic acid treatment. Lastly, I will determine the effects glucose has on gut barrier breakdown and peripheral organ injury. From these studies, we will pinpoint which aspects of gut degradation (metabolic or proteolytic) are critical in protease

transport, peripheral protease activation, neutrophil accumulation, and protein degradation in peripheral organs.

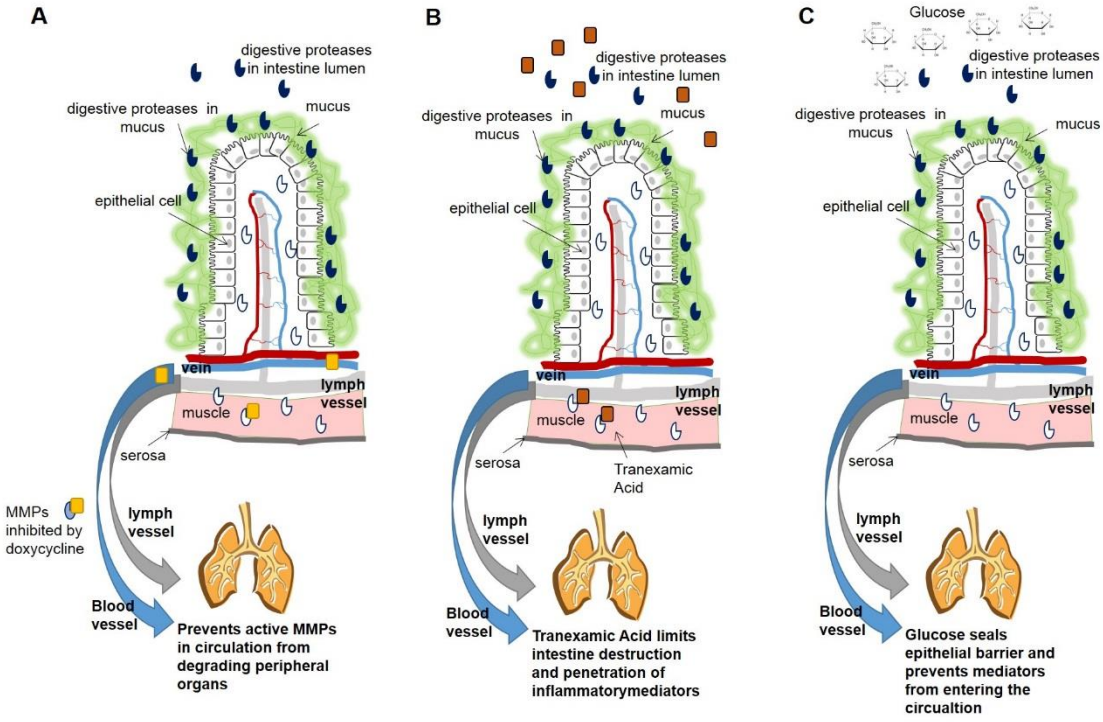

Figure 6.1 Working hypotheses. (A) Doxycycline prevents MMPs from degrading protein structures in the peripheral organs. (B) Tranexamic acid curtails protease digestion of the intestine hindering the generation of toxic gut-derived mediators. (C) Glucose prevents epithelial shedding and preserves the epithelial barrier so that inflammatory mediators do not exit the lumen of the intestine.

6.3 METHODS

6.3.1 ANIMALS

The animal protocol was reviewed and approved by the University of California, San Diego Institutional Animal Care and Use Committee. Male Sprague Dawley (body weight between 335±64 g [mean±SD], range; 230-448 g Harlan, Indianapolis, IN) were allowed food and water *ad libitum* prior to surgery. Rats were administered general anesthesia (xylazine, 4 mg/kg; ketamine 75 mg/kg IM) and euthanized by infusion of B-Euthanasia IV (120 mg/kg). Following general anesthesia, the animals were placed in the supine position before the femoral artery and vein were cannulated. Systolic, diastolic, heart rate, and mean arterial pressure (MAP) were recorded using LabChart (AD Instruments, Dunedin, New Zealand).

6.3.1.1 HEMORRHAGIC SHOCK PROCEDURE

Rats were randomly divided into the following groups: No-HS, Sham, HS+SAL, HS+DOX, HS+TA, or HS+GLUC (Table 6.1). No-HS animals were cannulated and immediately sacrificed for tissue collection.

In the other groups, rats were subjected to laparotomy and the intestine was exposed and a "*Before HS*" image was captured. Using a 5 ml syringe (Becton Dickinson), intraluminal treatments (Table 6.1) were warmed to 37 ºC in a water bath before injecting each treatment in two to three sites along the length of the intestine from

the jejunum to the ileum (10.9 ±1.7 ml; mean±SD). The intestine was never over-inflated. After injection, the intestine was carefully returned to the peritoneal cavity and the wound was covered with moist gauze and a piece of plastic wrap to keep the animal warm.

Table 6.1 Animal groups for single treatments.

	Intraluminal	IV	IP
No-HS	N/A	N/A	N/A
Sham	Saline	Saline	Saline
HS+SAL	Saline	Saline	Saline
HS+DOX	Saline	Doxycycline (5 mg/kg body weight)	Doxycycline (10 mg/kg body weight)
HS+TA	Tranexamic Acid (200 mM in saline)	Saline	Saline
HS+GLUC	Glucose (100 mg/ml in saline)	Saline	Saline

Doxycycline was prepared fresh for each animal as a stock solution (10 mg/ml) for both IP and IV injections following administration into the intestinal lumen. The total doxycycline or vehicle (saline) administration ranged between 0.35-0.70 ml and did not alter the starting pressure or final results. Sham animals were administered control treatments and monitored for a total of 5 hours (Table 6.1).

After treatments were administered, the animals were heparinized to minimize clotting inside catheters and the shed blood (1 U/ml IV assuming 6% blood volume per body weight) before onset of hemorrhage. MAP was reduced to 30 mmHg by drawing blood through the venous catheter (0.4 ml/min). The initial blood withdrawn (1 ml) was collected, centrifuged (1000 g, 5 min), and frozen at -80º C. The pressure was monitored and adjusted by withdrawal/return of blood over the 90-minute ischemia period. At the end of ischemia, the shed blood was returned to the animal plus 1 ml of saline (to replace

the collected blood). The animal remained anesthetized and was observed for 3 hours. Gross morphology images of the intestine were taken before and after shock.

At the end of the reperfusion period, post-hemorrhagic shock blood was collected through the arterial catheter and processed. Pieces of lung, liver, and intestine (jejunum; 10 cm from ligament of Treitz) were and embedded in O.C.T. (Tissue Tek) and snap frozen or frozen for homogenization.

6.3.1.2 BRONCHOALVEOLAR LAVAGE FLUID

BALF collection was carried as described in Section 5.3.1.2.

6.3.2 TISSUE HOMOGENIZATION

Tissues were homogenized as described in Section 5.3.3.

6.3.3 INTESTINAL HEMORRHAGE

Intestinal jejunum segments were processed as described in Section 5.3.3.

6.3.4 Enzyme and Protease Activity Measurements

6.3.4.1 Myeloperoxidase (MPO) Activity Assay

MPO activity was measured as described in Section 5.3.4.2.

6.3.4.2 MMP-1/9 Activity

To confirm the efficacy of doxycycline treatment, specific MMP 1/9 substrate was used to determine MMP-1/9 activity in pre- and post-HS plasma. In a 96 well plate, 1 µl of plasma was diluted in 9 µl MMP-1/9 digestion buffer (100 mmol NaCl, 23 mmol Tris HCl, 2.4 mmol $CaCl_2$, 5 µM $ZnCl_2$, 0.01% Brj 35, pH 7.6), 9 µl digestion buffer containing 1mM PMSF, or 1 mM PMSF and 0.05 mM EDTA to inhibit all MMP-1/9 activity. To these dilutions, 90 µl of 10 µM MMP-1/9 substrate was read every 5 minutes for 1 hour at 37 ºC. The results are presented as the change between the PMSF treated plasma and the PMSF plus EDTA rates of digestion of the fluorescent substrate.

6.3.4.3 Gelatin Gel Zymography

Lung and liver tissues were homogenized in PBS (pH 6.0) containing 0.5% HTAB (see Section 5.3.2). Protein concentration was determined using the BCA kit (ThermoScientific) before mixing each sample in a 1:1 ratio with loading dye (containing

SDS, but no reducing agent). 20 µg protein/lane of lung or liver homogenates were loaded. 0.5 µl of plasma was mixed with 2 µl loading dye and loaded into each lane.

Samples were separated by gel electrophoresis in 11% SDS-Page gelatin impregnated gels. Upon separation, gel proteins were renatured in 2.5% Triton-X 100 in water (4x, 15 min) before incubation at 37 ºC overnight in developing buffer (0.05 M Tris base, 0.2 M NaCl, 4 µM $ZnCl_2$, 5 mM $CaCl_2 \cdot 2H_2O$). Gels were then fixed and stained (50% methanol, 10% acetic acid, 40% water, and 0.25% Coomassie blue solution) for three hours. Gels were destained in water to achieve appropriate contrast before photographing and analyzing in ImageJ (http://rsb.info.nih.gov/ij/).

6.3.5 IMMUNOBLOTTING

Immunoblotting was performed as described in Section 5.3.6.

6.3.6 HISTOLOGY

Tissue histology was completed as described in Section 5.3.6.1 for mucin 2 and mucin 13 immunohistochemistry. TUNEL labeling was completed as described in Section 2.3.3.

6.3.7 Statistical Analysis

Results are presented as either mean±standard deviation (SD). Paired t-tests were completed for comparisons between groups for MAP during the reperfusion period and between pre- and post-shock plasma samples. Mann-Whitney tests were used for non-normally distributed means. ANOVA followed by Tukey post-hoc was used for comparisons of three or more normally distributed parametric variables. Statistical analysis was performed in OriginLabs (Northampton, MA).

6.4 Results

6.4.1 Hematological Parameters

To reach 30 mmHg, less blood was removed in the HS+TA and HS+GLUC groups (Figure 6.2). The average percent blood removed for all animals was 37.4±11.9% [mean±SD]. However, the maximum percent of the total blood removed during the 30 mmHg ischemic period for all HS animals was 54.2±8.3% [mean±SD]. The MAP pressure of HS+SAL animals was higher compared to untreated animals (HS-NF) (Figure 6.3). MAP of HS+SAL, HS+DOX and HS+GLUC animals began to decrease compared to the MAP at the start of reperfusion, but HS+TA animals remained unchanged throughout the reperfusion period (Figure 6.4).

The heart rate increased in the second and third hour of reperfusion in the HS+GLUC group and in the third hour of reperfusion in the HS+DOX group (Table 6.2).

There were no differences in heart rates between the groups during any of the time points among the HS groups (Table 6.2).

The pulse pressure of the HS+SAL group significantly decreased by the second hour of reperfusion (Table 6.3). The pulse pressure significantly began to drop by the third hour of reperfusion in all the HS groups compared to the first hour of reperfusion (Table 6.3).

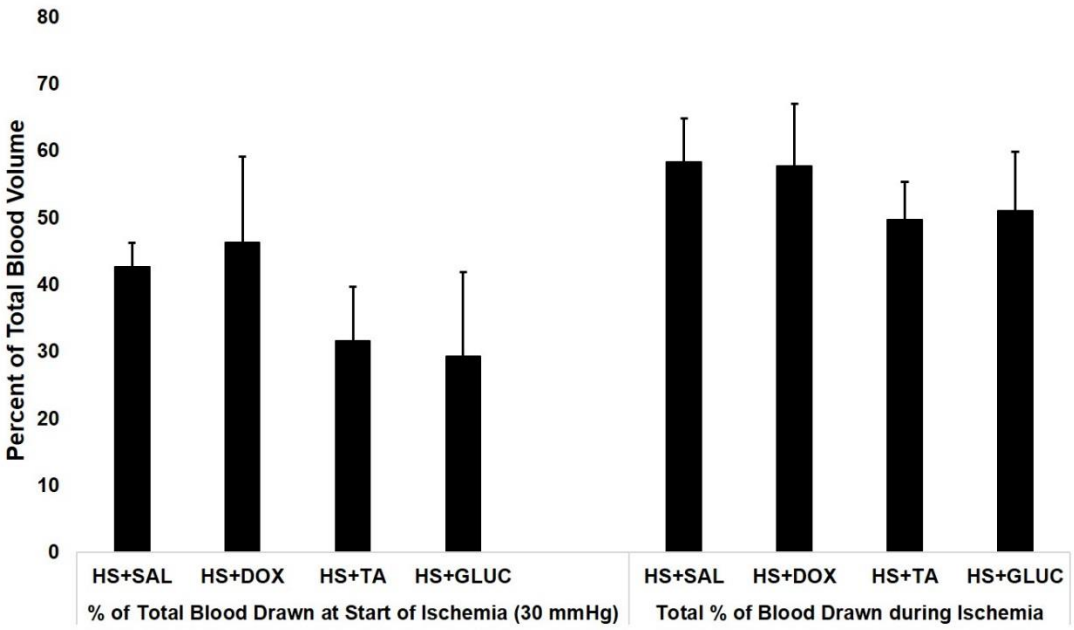

Figure 6.2 Blood drawn during ischemia. Percent blood volume removed to reach initial ischemia at 30 mmHg and total blood removed from the animal during ischemia. N=7 rats/group. Bar graphs represent mean ±SD.

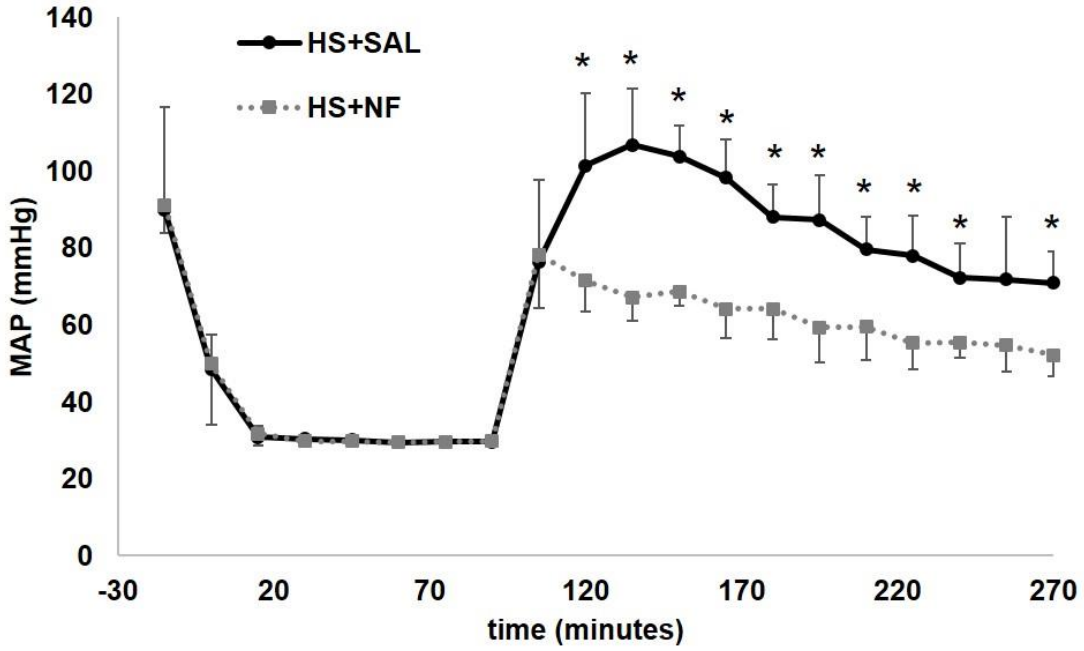

Figure 6.3 Mean arterial blood pressure history for HS+SAL and HS-NF animals. HS+SAL pressure traces remained elevated compared to HS-NF animals (described in Chapter 5) from initiation of reperfusion (105 min time point). *, $p<0.0005$ comparing the MAP of HS+SAL to HS-NF by t-test. Data are presented mean±SD. N=7 rats/group for HS+SAL and N=6 rats/group for HS-NF.

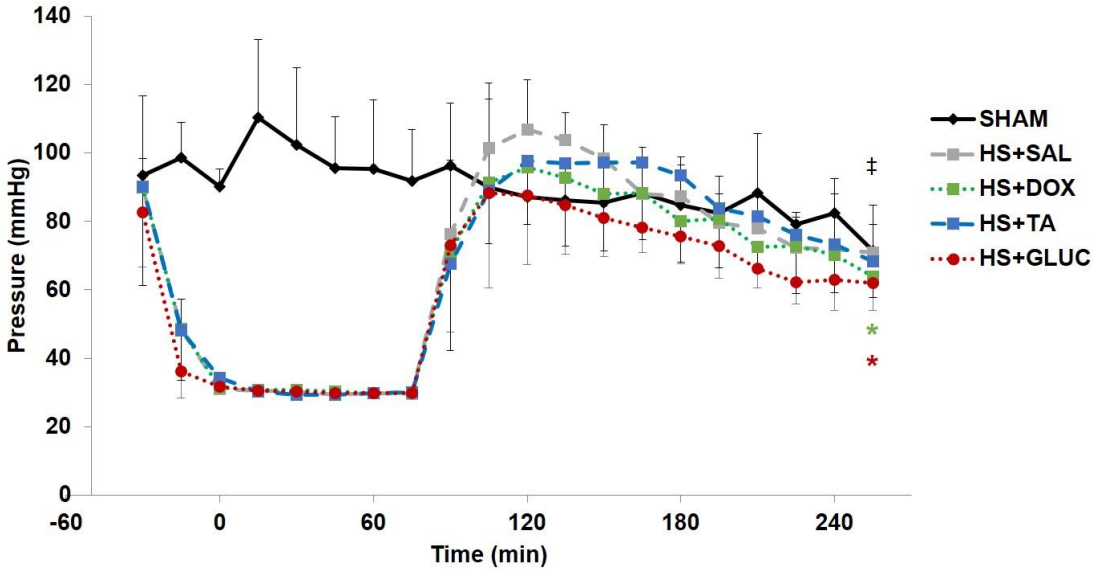

Figure 6.4 Mean arterial blood pressure traces. Pressure traces throughout observation of the animals during the duration of hemorrhagic shock. Pressures are reported as mean±SD. ‡, *, *, $p<0.05$ by paired t-test compared to the 105 minute MAP for HS+SAL, **HS+DOX**, and **HS+GLUC** respectively. N=7 rats/group for all groups except for Sham where N=5 rats/group. Data are presented as mean±SD.

Table 6.2 Hemorrhagic shock heart rates.

	Sham	HS+SAL	HS+DOX	HS+TA	HS+GLUC
Start	207±53	232±51	230±41	252±23	226±43
Blood Draw	242±39	156±30	152±14	172±17	165±39
Ischemia	234±30	158±43	177±41	181±28	174±29
Reperfusion	241±44	326±74	350±89	346±72	315±90
Hour 1	240±41	304±73	301±76	324±65	297±84
Hour 2	239±43	353±88	351±79	368±85	325±91*
Hour 3	243±49	306±68	365±101*	344±77	318±92*

Heart rates (beats/minute) are presented as mean±SD. *, $p<0.025$ by paired t-test compared to the heart rate of Hour 1. N=7 rats/group for all groups except for Sham where N=5 rats/group.

Table 6.3 Hemorrhagic shock pulse pressures.

	Sham	HS+SAL	HS+DOX	HS+TA	HS+GLUC
Start	45.0±5.9	37.8±5.6	49.1±12.8	42.4±7.0	38.0±10.8
Blood Draw	46.0±8.6	30.7±4.4	35.0±7.6	29.3±3.7	24.8±6.9
Ischemia	50.2±5.3	26.1±4.9	28.7±5.2	25.4±4.3	25.9±3.8
Reperfusion	44.2±4.4	41.6±5.5	42.7±9.0	41.9±4.8	42.7±2.0
Hour 1	45.5±4.8	55.6±10.7	50.9±14.9	51.0±5.1	52.9±6.6
Hour 2	43.6±4.4	43.5±6.0**	44.9±11.9	43.8±7.6	44.0±4.1
Hour 3	44.1±4.7	34.2±7.7**	33.2±4.5**	34.2±5.9**	32.9±6.8**

Pulse pressure (mmHg) is presented mean±SD. **, $p<0.01$ by paired t-test compared to Hour 1 Pulse Pressure. N=7 rats/group for all groups except for Sham where N=5 rats/group.

6.4.2 INTESTINAL DAMAGE

The rat intestines before hemorrhagic shock had a normal appearance without lesions or distension of the intestine (Figure 6.5). Sham animals had no visible damage to the intestine after 5 hours of observation (Figure 6.5). After shock in the HS+SAL and HS+GLUC animals tissue hemorrhage appeared primarily in the jejunum, but was attenuated with HS+DOX or HS+TA treatments (Figure 6.5). The sites where the tweezers were used to secure the intestine before the injections were subject to formation of small lesions.

There were no significant differences in the level of intestinal hemorrhage between the groups as measured by 405 nm absorbance of hemoglobin that had penetrated the intestinal wall (Figure 6.6). MPO activity of intestinal homogenates was elevated in all shock cases, but was statistically significant only in the HS+DOX group (Figure 6.7).

Cell death was prominent throughout the villi in the untreated HS+SAL case (Figure 6.8). The cell death, as measured by TUNEL labeling, was reduced by treatment in the HS+DOX, HS+TA, or HS+GLUC groups. Mucin 2 and mucin 13 density was distributed along the villi (Figure 6.9A&B), yet there was no change in the mucin 13 isoform levels in any of the groups following HS (Figure 6.9C).

Epithelial proteins occludin and E-cadherin in the intestine were not significantly reduced after HS (Figure 6.10). There was a significant elevation of the 135 kDa isoform of E-cadherin in the HS+DOX animals (Figure 6.10).

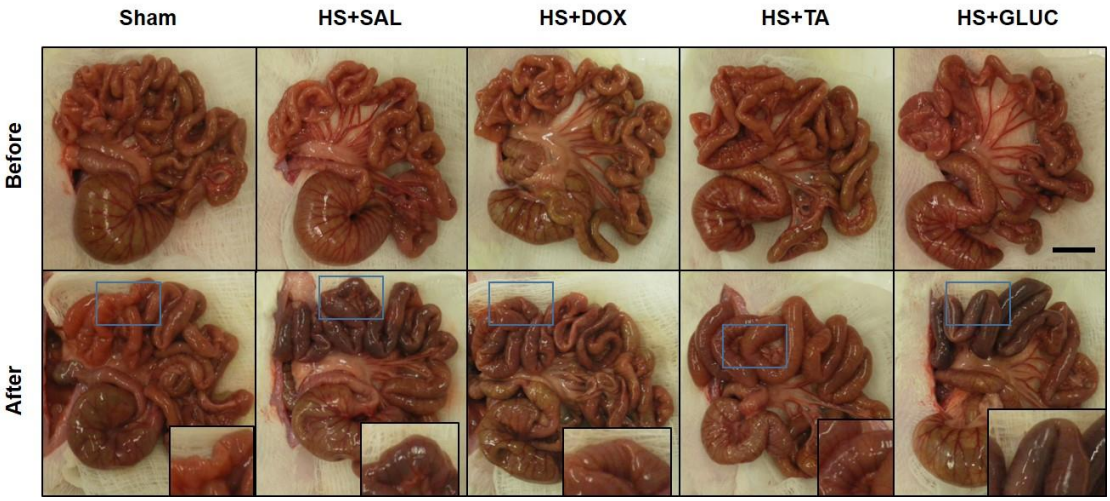

Figure 6.5 Macroscopic intestine images. Representative macroscopic images of the intestine before and after shock. The majority of hemorrhage occurs in the jejunum where the boxes are magnified. Scale corresponds to 1 cm.

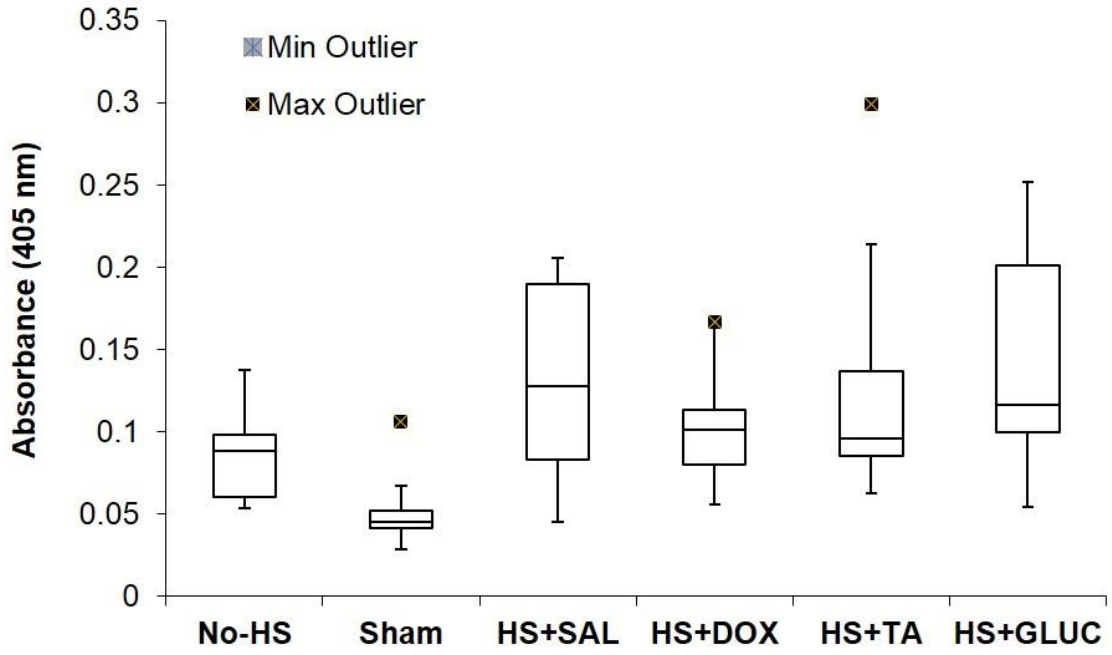

Figure 6.6 Hemoglobin absorbance in intestine homogenates. Absorbance of intestinal homogenates at 405 nm as a measure for hemoglobin penetration into the lumen of the intestine. N=7 rats/group except for the Sham group where N=5 rats/group. Box and whisker plots show the minimum and maximum data values. The central line is the median for the data and the lower and upper lines of the box correspond to the first and third quartiles respectively.

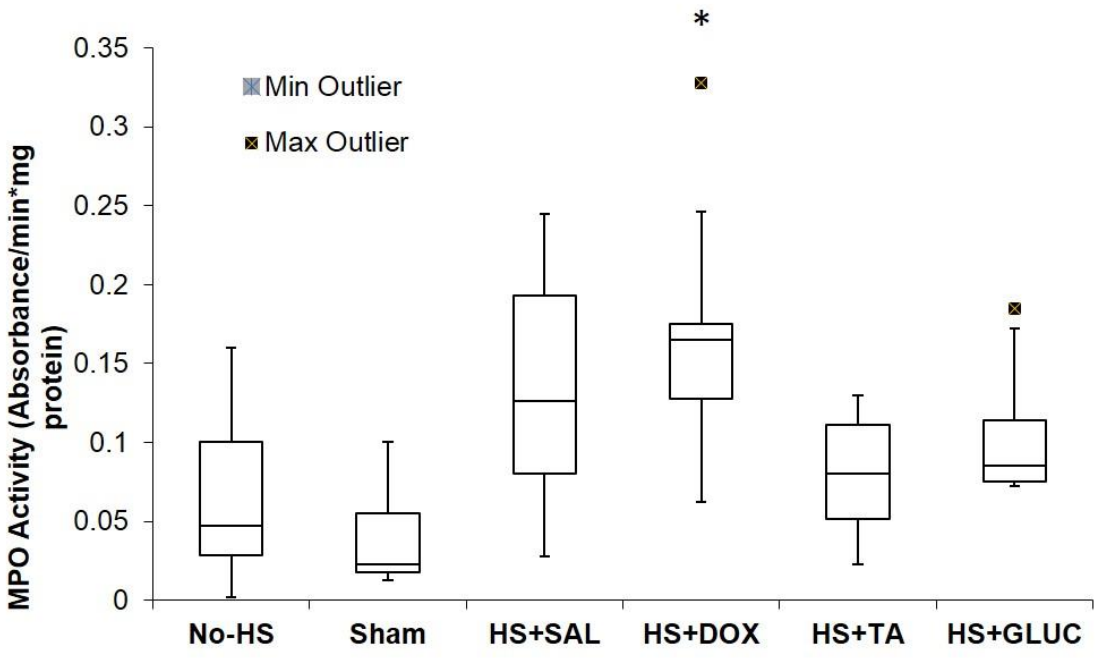

Figure 6.7 MPO activity in intestinal homogenates. MPO activity of intestinal homogenates as a measure for leukocyte infiltration. N=7 rats/group except for the Sham group where N=5 rats/group. *, $p<0.05$ by ANOVA followed by Tukey post-hoc analysis compared to No-HS.

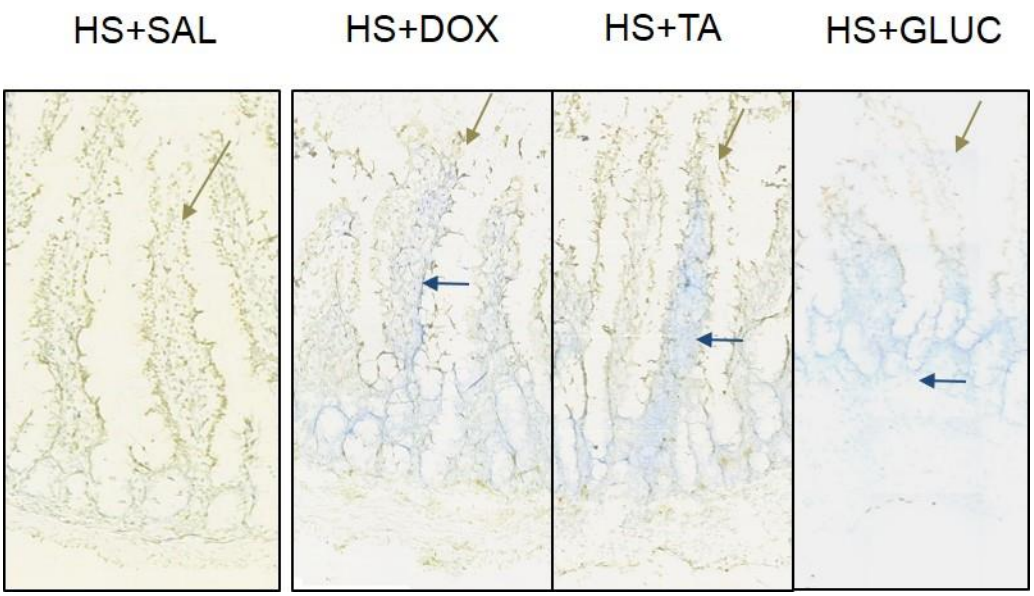

Figure 6.8 Apoptosis in intestinal villi. HS+SAL exhibited apoptosis throughout the villi and into the muscularis. Treatment with doxycycline, tranexamic acid, or glucose reduced the prominent apoptosis. **Brown** arrows show positive staining for cell death and **blue** arrows indicate regions without cell death, seen primarily in the crypts.

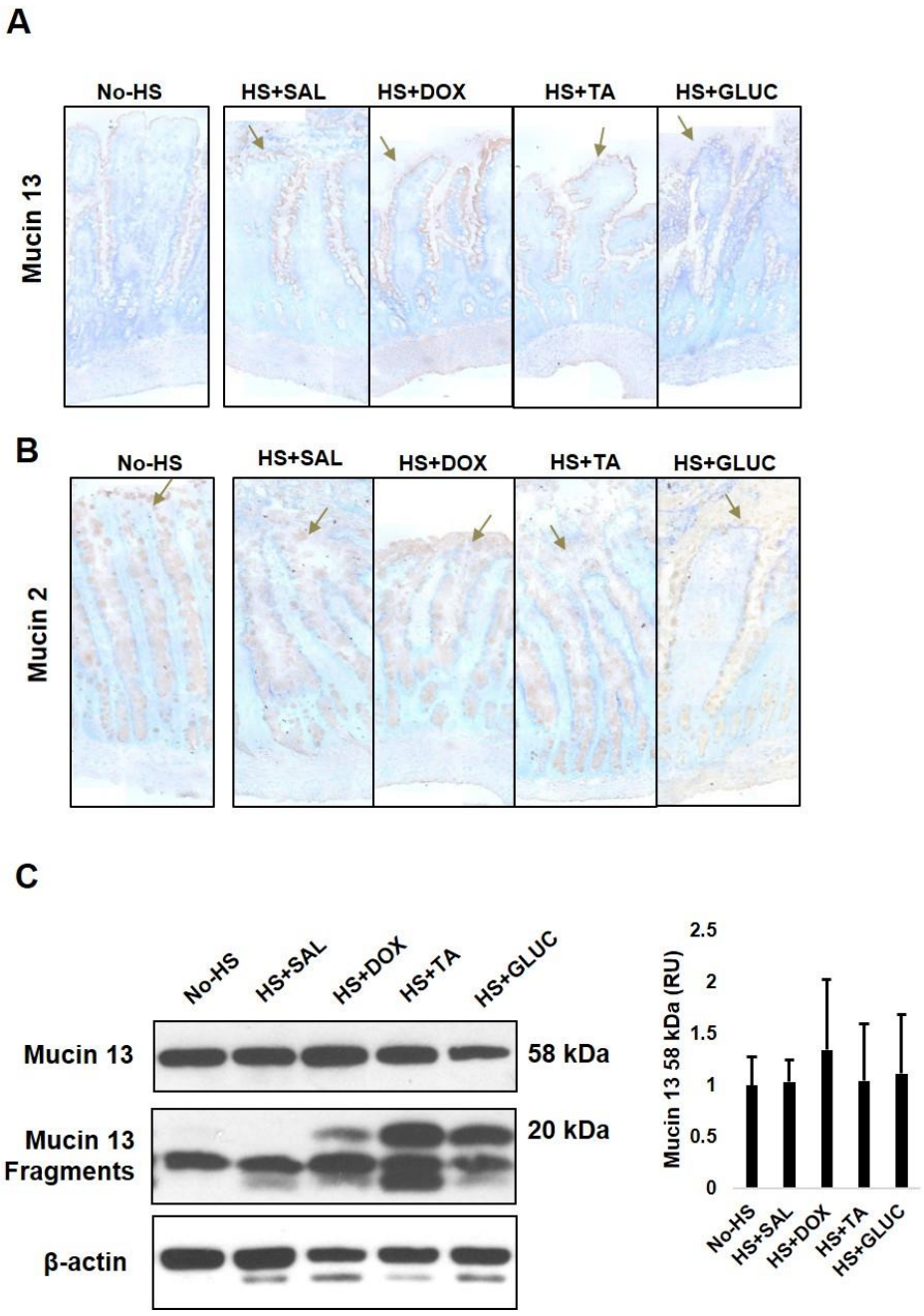

Figure 6.9 Mucin distribution and protein levels. Epithelial bound mucin 13 (A) and goblet cell derived mucin 2 (B) are present both before and after shock in the jejunum. Arrows indicate a positive staining for mucin 13 and mucin 2 on the epithelium as stained **brown** and counterstained nuclei in **blue**. (C) Immunoblot of epithelial mucin 13 shows that the levels of the core protein (58 kDa) do not significantly change between before and after HS, and there are mucin 13 fragments present in all cases both before and after shock. N=4 rats/group. Data are normalized to β-actin intensity. Bar graph shows mean±SD.

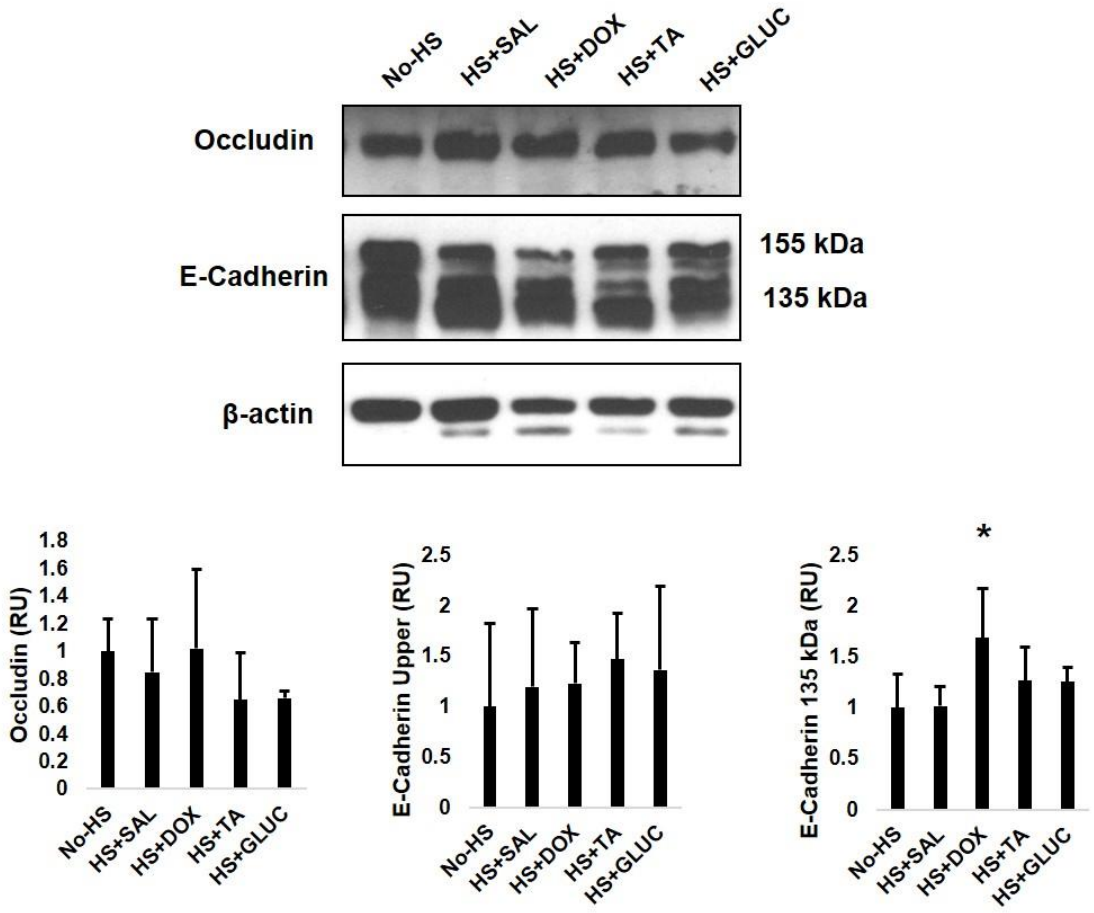

Figure 6.10 Epithelial proteins in the intestine. There were no significant changes in the tight junction protein occludin or the 155 kDa form of E-cadherin. HS+DOX treated animals had elevated levels of the 135 kDa E-cadherin isoform. *, $p<0.05$ by comparison of post-HS samples by ANOVA followed by Tukey post-hoc test. N=5 rats/group. Values are normalized to β-actin intensity. Bar graphs show mean±SD.

6.4.3 LUNG INJURY

The lung injury score as determined by gross morphology was significantly elevated between No-HS and HS+SAL animals (Table 6.4). The lung injury score was also elevated compared to the No-HS animals for HS+DOX and HS+TA (Table 6.4). However, the HS+GLUC group had a significant reduction in lung injury score compared to HS+SAL animals if one outlier was removed (Table 6.4). All HS groups had select animals that did not have severe lung injury, as determined by a low injury score of <1.

Table 6.4 Lung injury score.

No-HS	HS+SAL	HS+DOX	HS+TA	HS+GLUC
0.3±0.3	2.2±1.6*	1.9±1.3*	1.6±1.1*	0.5±0.5†

*, $p<0.05$ compared to No-HS and †, $p<0.05$ compared to HS+SAL by ANOVA followed by Tukey post-hoc correction, shown as mean±SD. There was one outlier from the HS+GLUC group that was excluded from statistical analysis which had a score of 3.

Despite the lower lung injury of the HS+GLUC animals, all HS animals exhibited a significant increase in MPO activity as a marker for neutrophil accumulation following HS (Figure 6.11). The BALF protein concentrations were non-significantly elevated after HS in all groups, though to a lesser extent with HS+GLUC treatment (Figure 6.12). The MPO activity in the BALF was also elevated in the case of shock (Figure 6.13) and was reflected by the increased red cell lysis in the BALF (Figure 6.14).

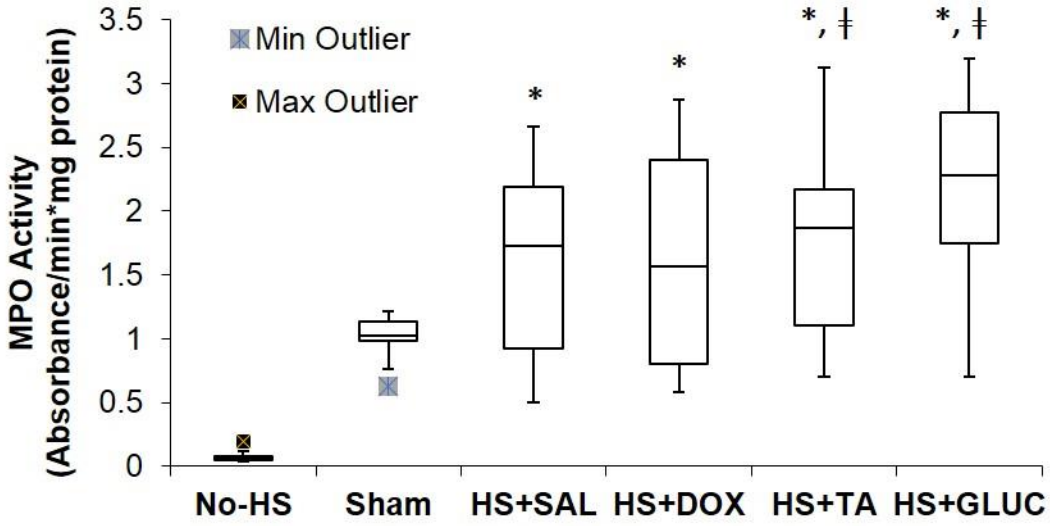

Figure 6.11 MPO activity in lung homogenates. MPO activity increased after HS regardless of the treatment. *, $p<0.05$ compared to No-HS. ǂ, $p<0.05$ compared to Sham by ANOVA followed by Tukey post hoc test. N=7 rats/group except for Sham where N=5 rats/group.

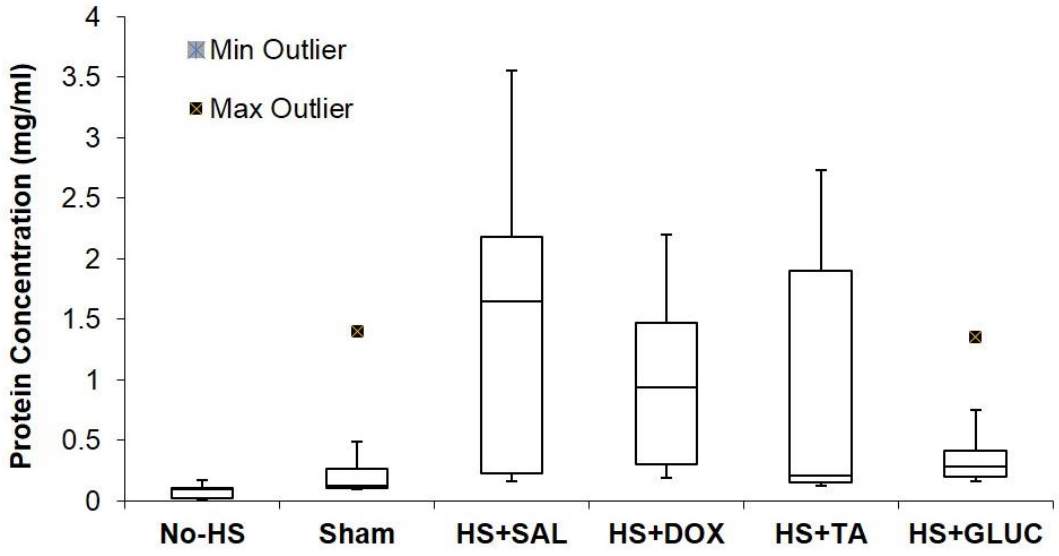

Figure 6.12 BALF protein concentration. BALF protein concentration increased non-significantly after shock. N=7 rats/group except for Sham where N=5 rats/group.

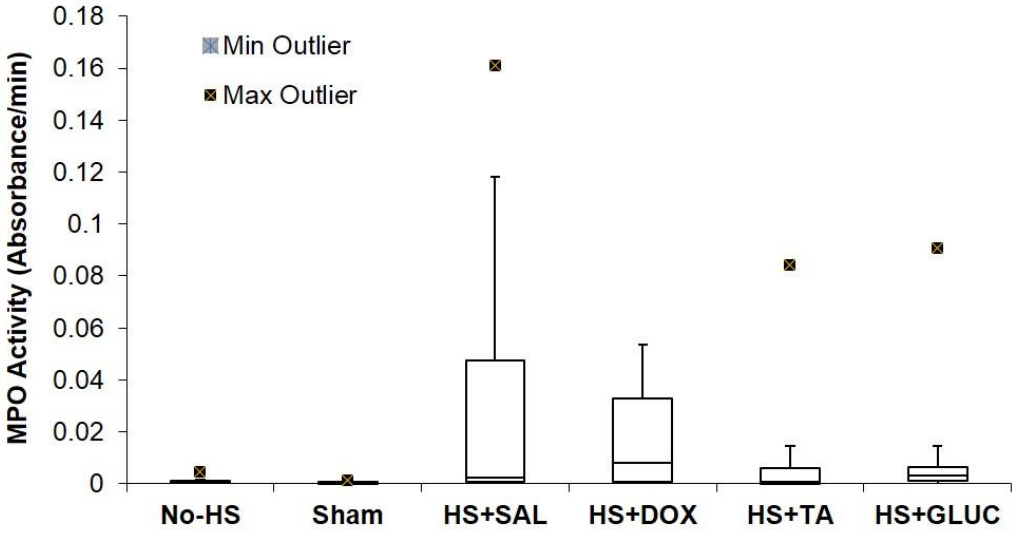

Figure 6.13 BALF MPO activity. MPO activity in the BALF increased with worsening condition in the lung, but there was great variability in these measurements. N=7 rats/group except for Sham where N=5 rats/group.

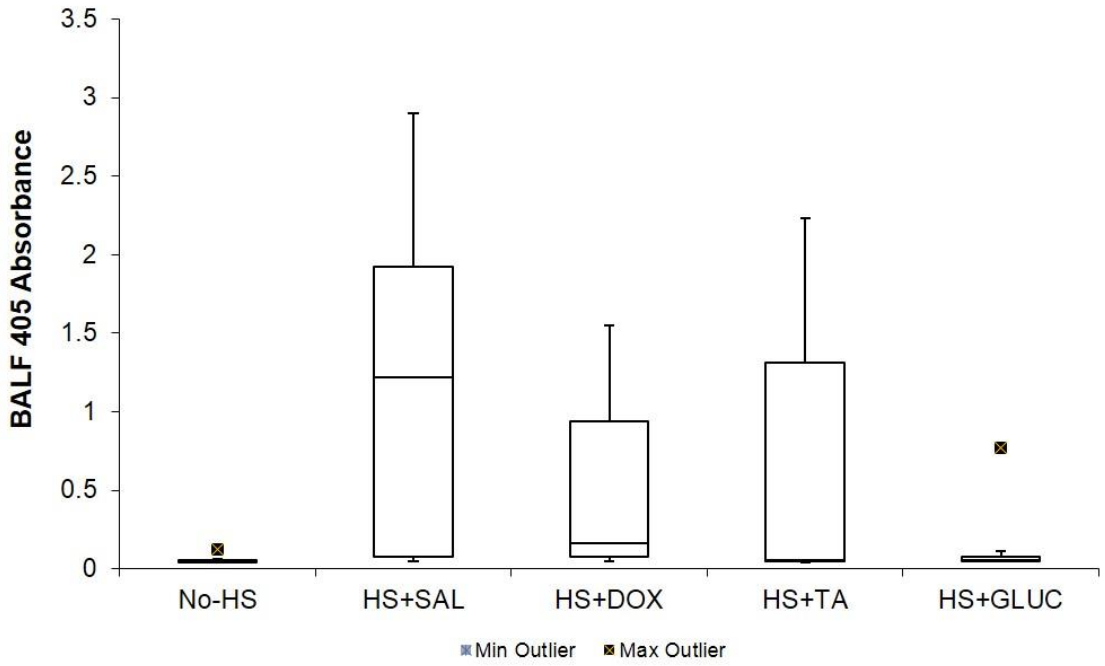

Figure 6.14 BALF hemoglobin absorbance. The hemorrhage into the BALF fluid was non-significantly increased in the post-HS cases. N=7 rats/group.

6.4.4 Plasma Protease Levels and Activities in Plasma

The pancreatic proteases trypsin and chymotrypsin were detected at equal levels between pre- and post-plasma samples and did not differ between treatments (Figure 6.15A). However, low molecular weight bands that appear around 20 kDa and disappear with ANGD or TLCK renaturation appeared significantly elevated after HS in all samples. These bands were significantly elevated with glucose treatment compared to HS+SAL animals (Figure 6.15B).

Since the electrophoresis process used to separate proteins during gelatin gel zymography removes protease inhibitors from their respective proteases, pre- and post-plasma samples were tested using a specific substrate for MMP-1/9. MMP-1/9 activity

was reduced by 85% in the HS+DOX animals compared to the HS+SAL animals. As expected, the other groups did not show any change in MMP-1/9 activity since they were not targeted at inhibiting MMPs.

Gelatin gel zymography, which separates non-covalently bound protease inhibitors from their respective proteases, revealed that plasma levels of MMP-9 and the neutrophil derived 125 kDa pro-MMP-9 isoform increased in all cases after HS (Figure 6.16A&B). There was a significant elevation in neutrophil pro-MMP-9 and MMP-9 activity in the HS+GLUC post-plasma samples compared to the HS+SAL post-plasma (Figure 6.16B). Additionally, the protein levels of MMP-9 as detected by immunoblotting were also elevated in all post-plasma samples regardless of treatment (Figure 6.17A). Despite the rise of MMP-9, its native inhibitor TIMP-1 did not change after HS (Figure 6.17B).

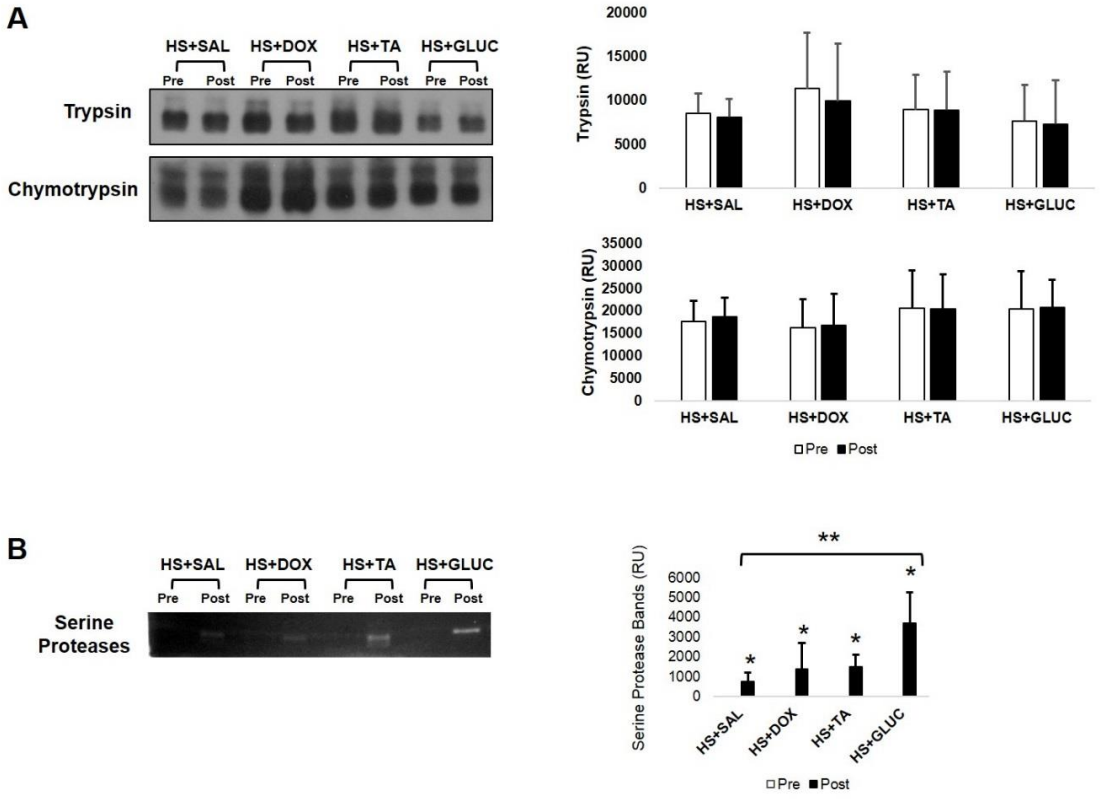

Figure 6.15 Trypsin and chymotrypsin activity in plasma. (A) Trypsin and chymotrypsin levels were unchanged from the pre-HS levels. N=5 rats/group. (B) Serine protease bands were identified by gelatin gel zymography. *, $p<0.05$ by Mann Whitney test. **, $p<0.05$ by ANOVA followed by Tukey post-hoc test. N=4 rats/group. Bar graphs show mean±SD.

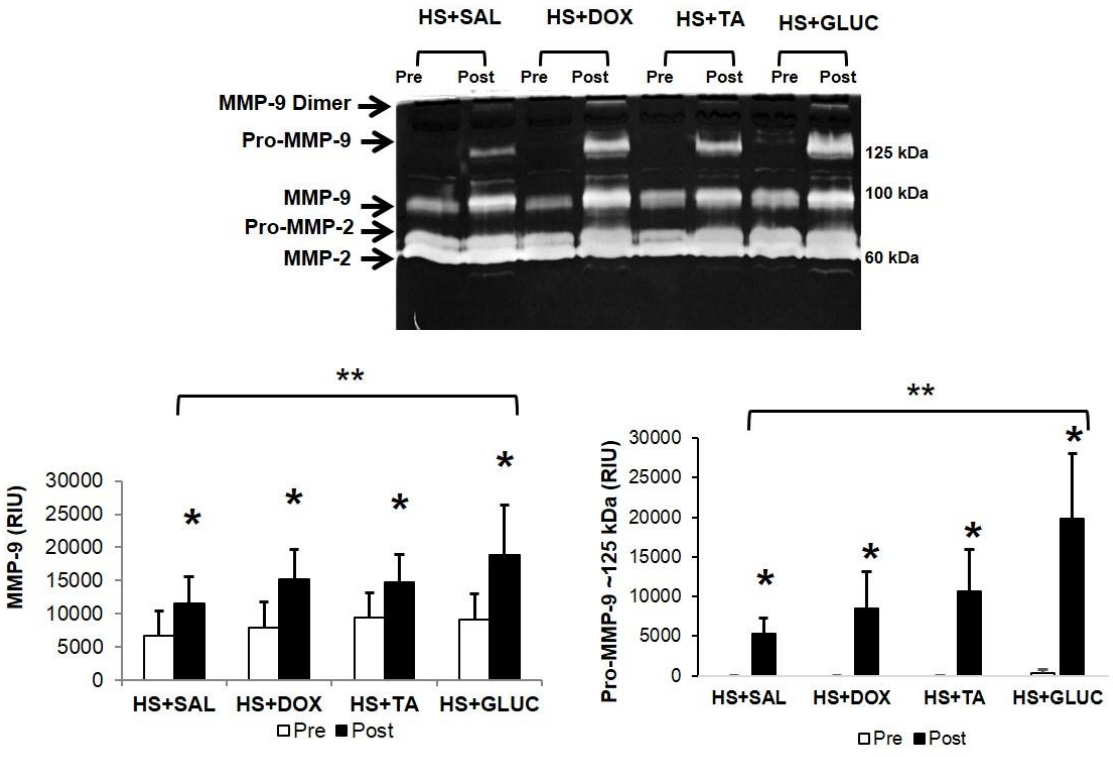

Figure 6.16 MMP activity in plasma. (A) MMP-9 activity and (B) The neutrophil pro-MMP-9 activities are elevated in the plasma by gelatin gel zymography. *, $p<0.05$ by paired t-test. **, $p<0.05$ by comparison of post-HS samples by ANOVA followed by Tukey post-hoc test. N=5 rats/group. Bar graphs show mean ±SD.

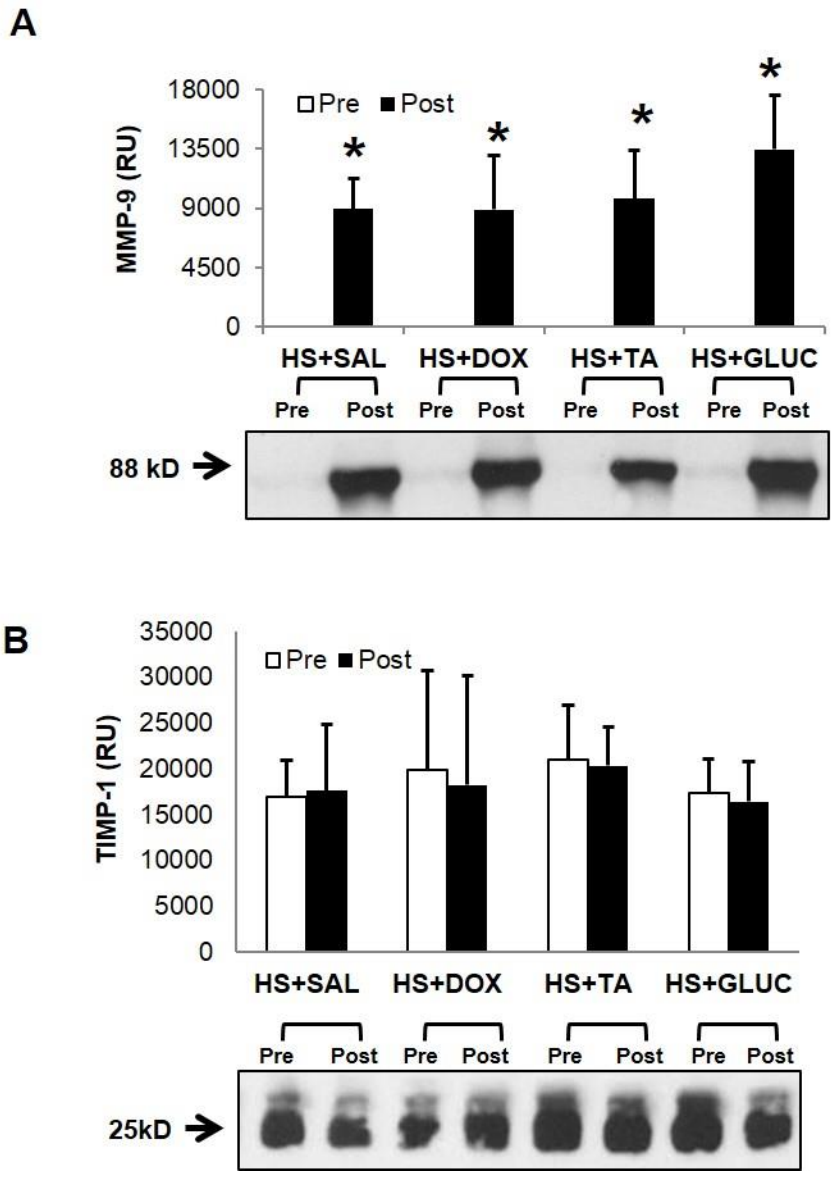

Figure 6.17 MMP-9 and TIMP-1 levels in plasma. (A) MMP-9 levels are elevated in the plasma by immunoblotting. Samples were reduced with β-mercaptoethanol so bands may consist of both dimer and MMP-9 levels. (B) TIMP-1 levels do not change. *, $p<0.05$ by paired t-test. N=5 rats/group. Bar graphs show mean±SD.

6.4.5 Protease Levels and Activities in Tissues

Low molecular weight bands corresponding to serine proteases were identified in lung tissue homogenate and were significantly elevated after HS in all cases (Figure 6.18A). These serine protease bands were even detected in select BALF samples at low levels (Figure 6.18B). Whole lung homogenates also had detectable trypsin levels (Figure 6.18C). The lung tissue homogenates exhibited elevated MMP-9 activities and levels after shock (Figure 6.19A). Since MMP-9 activity and levels consistently increased in the lung during shock, we measured TIMP-1 levels and found they were unchanged in the lung homogenate (Figure 6.19A). BALF also had elevated MMP activity in the more damaged lungs (Figure 6.19B). Localization of MMP-9 was observed primarily around blood vessels in cross sections of the lung tissue (Figure 6.19C).

The liver MMP-9 activities and levels were also elevated in all cases after HS (Figure 6.20). The TIMP-1 levels also remained unchanged in the liver between No-HS and after HS in all cases (Figure 6.20).

The intestine MMP-9 levels were non-significantly elevated after HS for all treatment groups. The TIMP-1 levels were also non-significantly elevated in intestinal homogenates after HS (Figure 6.21).

When equal amounts of protein were loaded into each well, MMP-9 levels of lung, liver, and intestine all were low in the No-HS control animals (Figure 6.22). After HS, MMP-9 levels increased the most in the lung relative to the liver or the intestine

(Figure 6.22). Reflecting back to the MMP-9 levels from neutrophils as seen in Chapter 5, it is likely that the increase in lung MMP-9 levels is caused by neutrophil entrapment.

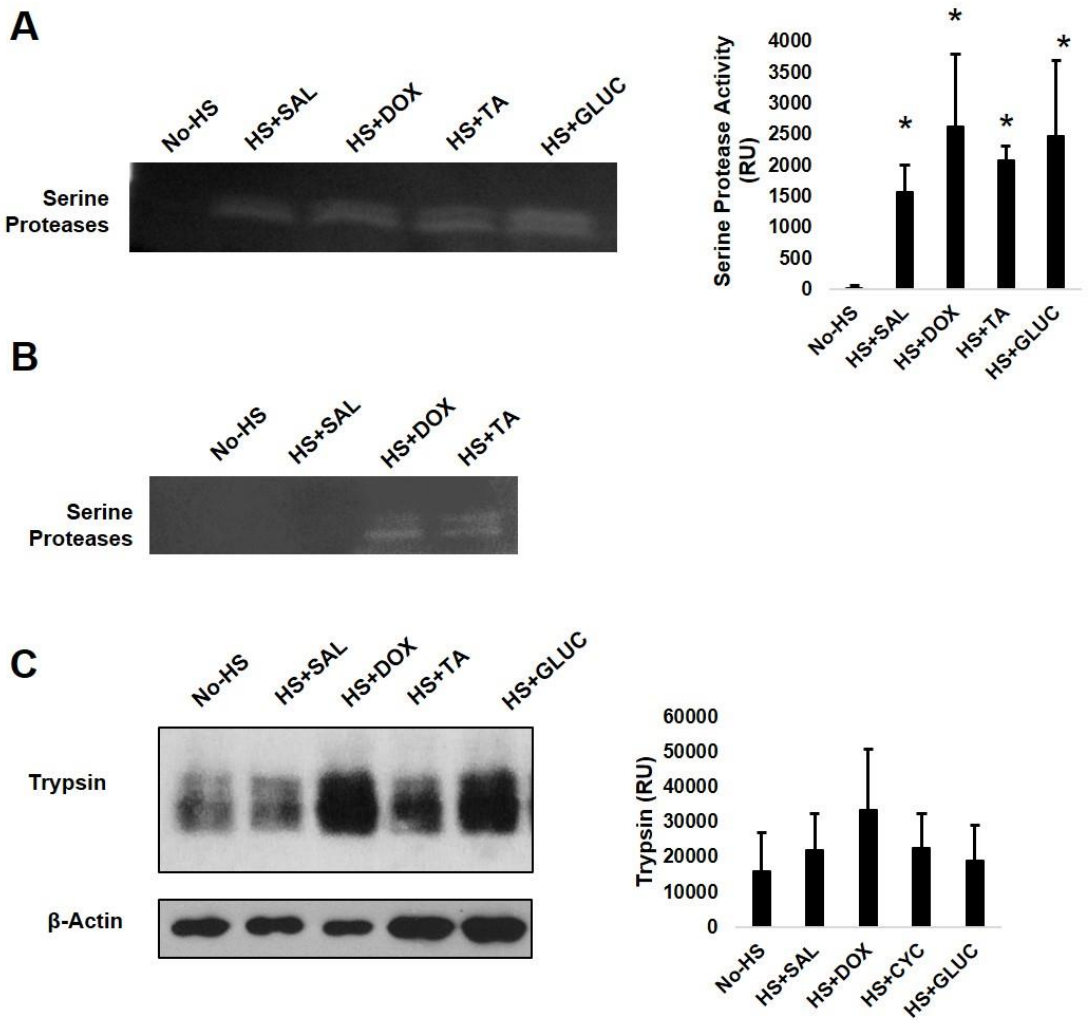

Figure 6.18 Serine proteases in lung homogenate. (A) Serine protease activity bands were elevated in all HS cases regardless of treatment. (B) These bands were also detected in some of the "worst" case BALF samples in low levels, but only in the HS+DOX and HS+TA cases and not HS+SAL or No-HS. (C) Trypsin levels in the lung were detected after HS. *, $p<0.05$ by comparison of post-HS samples by ANOVA followed by Tukey post-hoc test. N=4 rats/group. Bar graphs show mean±SD.

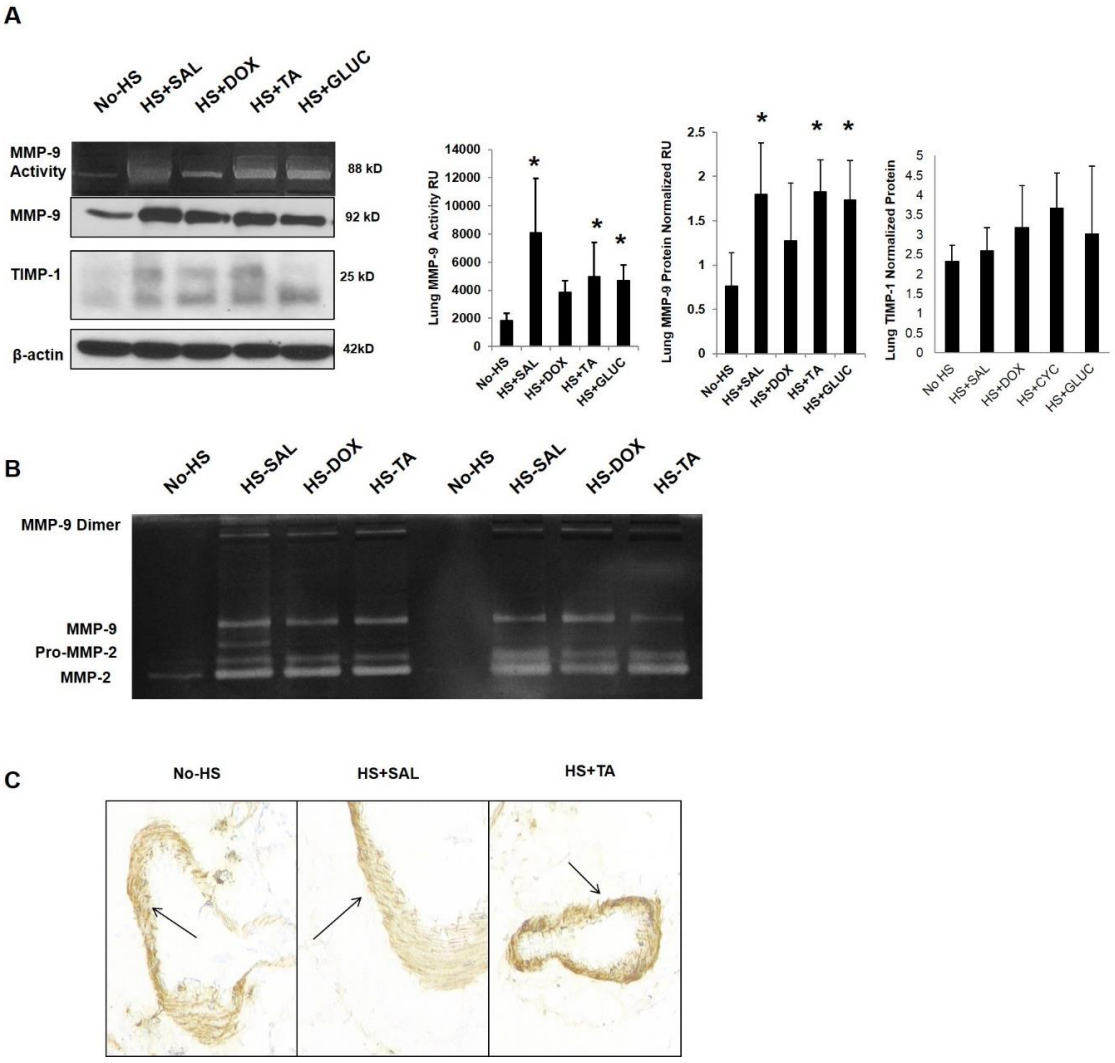

Figure 6.19 MMP-9 and TIMP-1 levels in the lung. (A) MMP-9 activity and protein levels increased in the HS+SAL, HS+TA, and HS+GLUC groups. (B) MMP activity was also detected in the BALF of highly damaged lungs. (C) Localization of MMP-9 to the vessels in the lung tissues. *, $p<0.05$ by comparison of post-HS samples by ANOVA followed by Tukey post-hoc test. N=5 rats/group. Immunoblot data are normalized to β-actin intensity. Bar graphs show mean±SD.

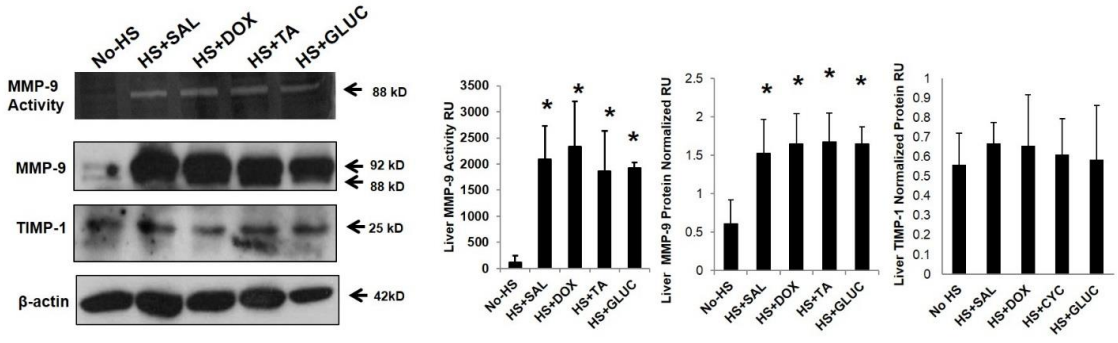

Figure 6.20 MMP-9 and TIMP-1 levels in the liver. MMP-9 activity and levels increased in the HS+SAL, HS+DOX, HS+TA, and HS+GLUC groups. *, $p<0.05$ by comparison of post-HS samples by ANOVA followed by Tukey post-hoc test. N=5 rats/group. Immunoblot data are normalized to β-actin intensity. Bar graphs show mean±SD.

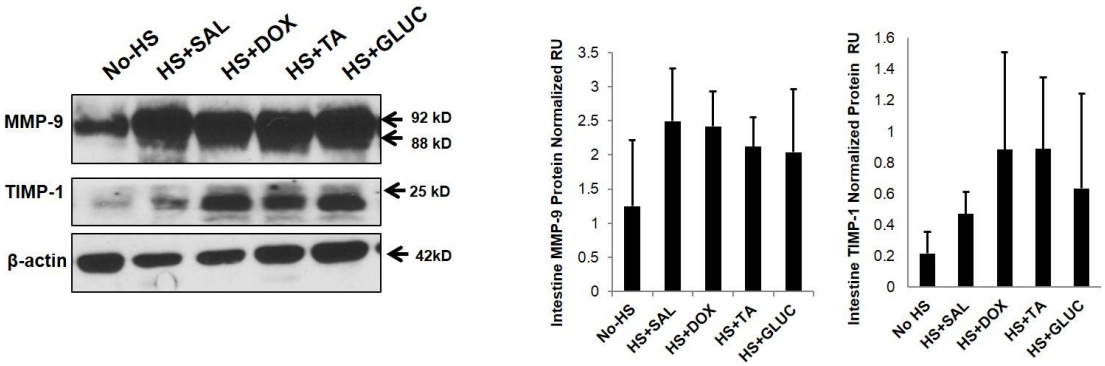

Figure 6.21 Intestine MMP-9 and TIMP-1 levels. The MMP-9 and TIMP-1 levels in intestinal homogenate were not statistically significant. *, $p<0.05$ by comparison of post-HS samples by ANOVA followed by Tukey post-hoc test. N=5 rats/group. Data are normalized to β-actin intensity. Bar graphs show mean±SD.

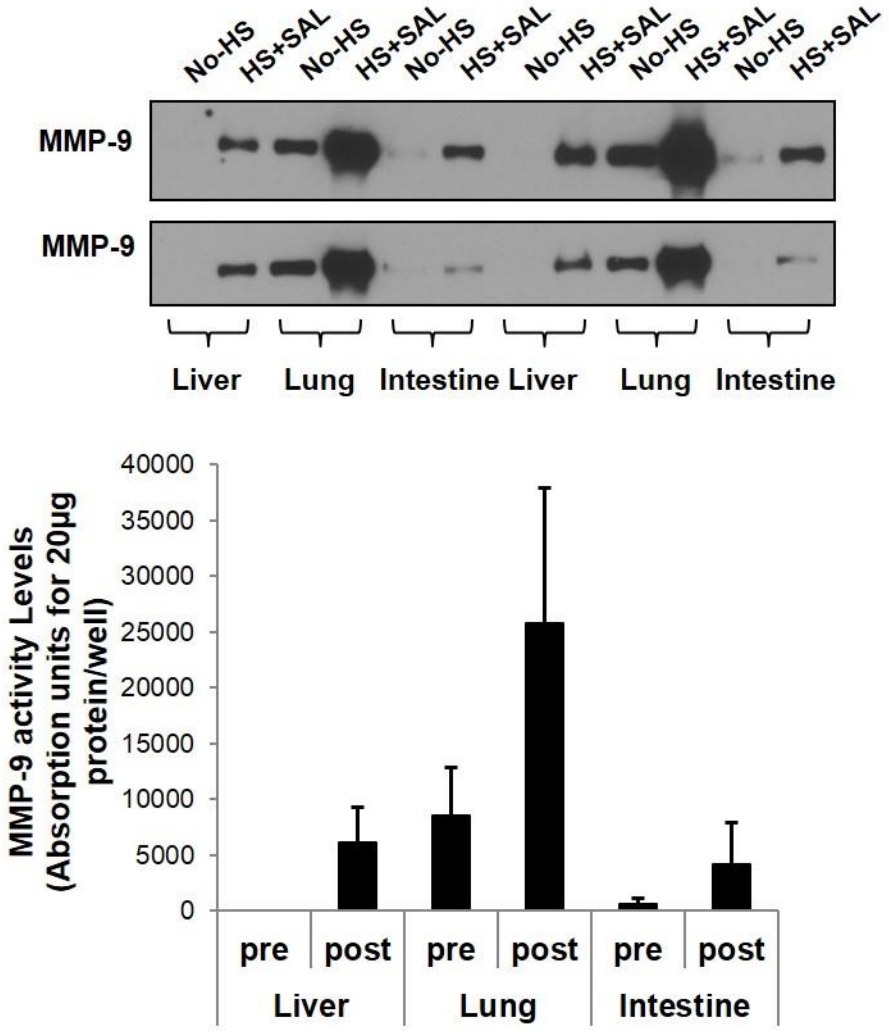

Figure 6.22 Comparative levels of MMP-9 in tissues. Equal loading of 20 µg protein/well depicted higher base levels in the lung with a greater increase after HS+SAL compared to either the liver or the intestine. Bar graphs show mean±SD.

6.4.6 Junctional Protein Degradation in Peripheral Organs

Occludin, the tight junction protein, label density did not change between the experimental groups (Figure 6.23A). Both VE-cadherin and the 155 kDa form of E-cadherin were reduced in the HS+SAL animals compared to the No-HS animals (Figure 6.23B). VE-Cadherin was also reduced in the HS+DOX and HS+TA cases, but not in the HS+GLUC group (Figure 6.23B). There was no change in the 135 kDa E-cadherin levels between the groups (Figure 6.23B).

In order to compare if cadherin degradation is a tissue specific event, we measured the VE-cadherin levels in the liver which were unchanged between the different groups (Figure 6.24).

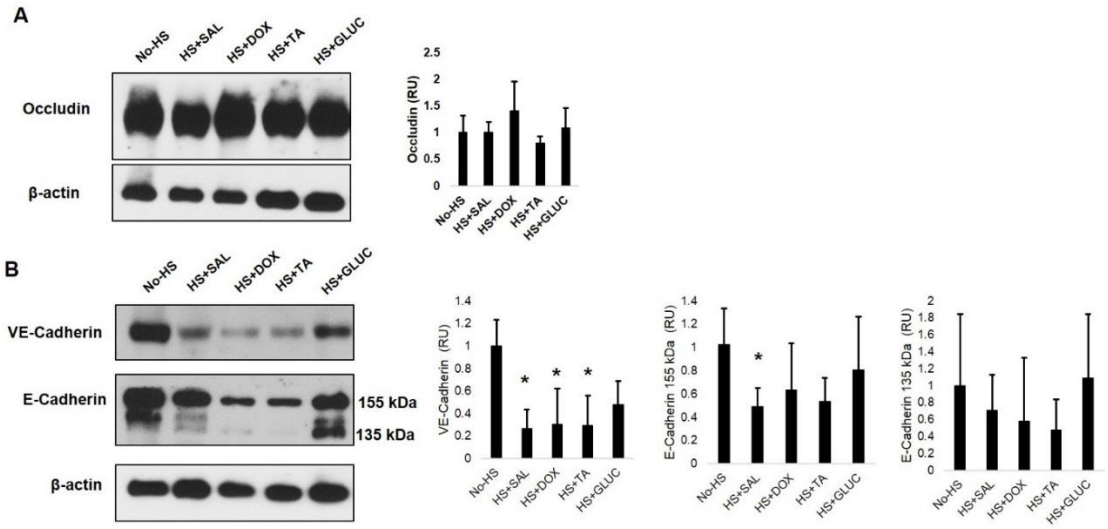

Figure 6.23 Lung junctional proteins. (A) The tight junction protein was not changed after HS regardless of the type of intervention. (B) VE-cadherin was significantly reduced for HS+SAL, HS+DOX, and HS+TA treatments, but E-cadherin levels were not statistically different. Measurements are expressed as relative units (RU) protein levels normalized to No-HS controls. *, $p<0.05$ by comparison of post-HS samples by ANOVA followed by Tukey post-hoc test. N=6 rats/group for No-HS and HS+SAL. N=7 rats/group for HS+DOX, HS+TA, and HS+GLUC. Data are normalized to β-actin intensity. Bar graphs show mean±SD.

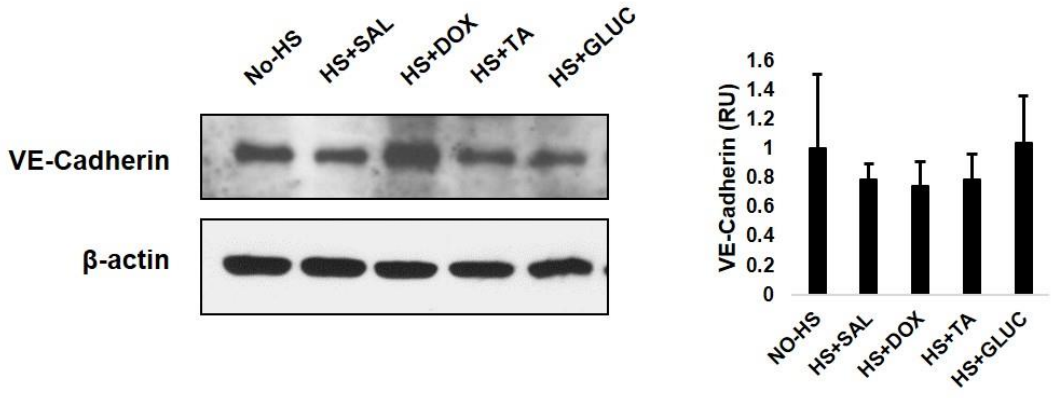

Figure 6.24 Liver VE-cadherin levels. The levels of VE-cadherin in the liver were unchanged after HS. Data are normalized to β-actin intensity. Bar graphs show mean±SD.

6.4.7 VEGFR-2 Degradation in Peripheral Organs

The mature form of VEGFR-2 (230 kDa) in the lung were diminished after HS in the HS+SAL, HS+DOX, and HS+GLUC groups, but preserved in the HS+TA animals (Figure 6.25A). The immature glycosylated form were also decreased after HS in the HS+SAL, HS+DOX, and HS+GLUC groups (Figure 6.25A). The VEGF levels in the lung tissue remained constant regardless of treatment (Figure 6.25A). VEGFR-2 levels were significantly decreased in the liver for all HS groups regardless of treatment, and the VEGF levels were unchanged between the groups (Figure 6.25B). VEGF levels in the plasma were elevated in every post-HS sample (Figure 6.25C).

Although VEGFR-2 levels decreased in the majority of the post-HS samples, the lung damage did not correlate with the preservation of VEGFR-2 after HS (Figure 6.26). There were cases in which the HS+SAL would have a low lung injury score <1 and very low levels of VEGFR-2.

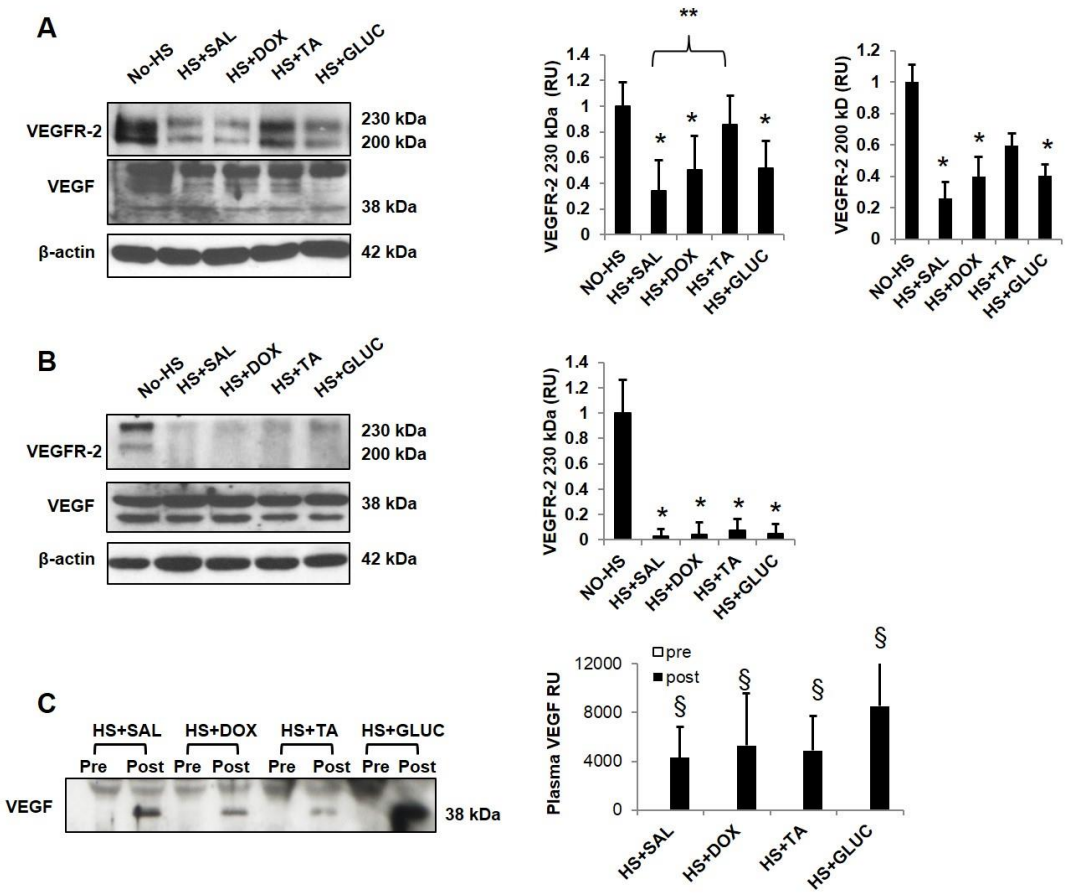

Figure 6.25 VEGFR-2 and VEGF levels in lung, liver, and plasma. (A) VEGFR-2 levels in the lung is significantly lowered after HS+SAL and recovered with HS+TA treatment. There was no change in the 38 kDa levels of VEGF. (B) VEGFR-2 levels in the liver were decreased after HS in all cases and there was no change in VEGF levels. (C) VEGF increased in the plasma in all groups. *, $p<0.05$ compared to No-HS and **, $p<0.05$ compared to HS+SAL by ANOVA followed by Tukey post-hoc. §, $p<0.05$ by paired t-test between pre and post samples. N=5 rats/group. Bar graphs show mean±SD.

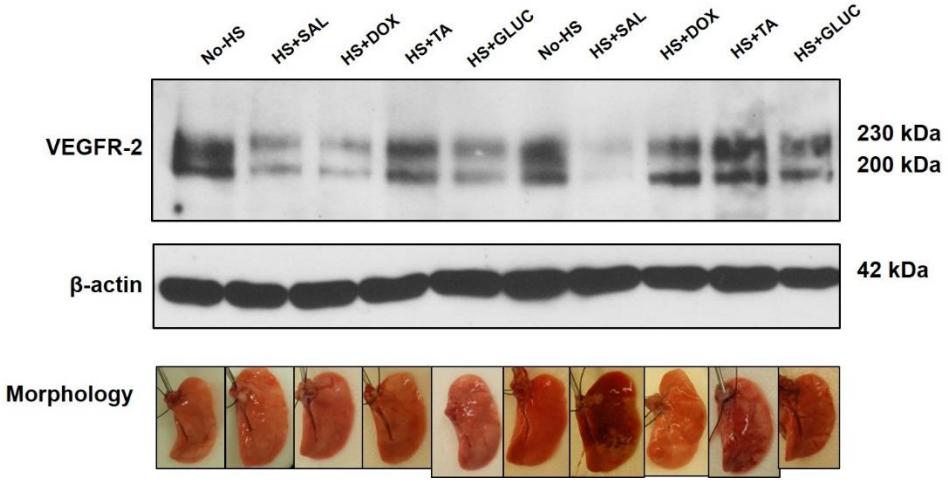

Figure 6.26 VEGFR-2 levels and lung damage. VEGFR-2 protein levels and lung damage do not correlate. HS+SAL to the left indicates an example of a low lung injury score and degradation of VEGFR-2 receptor.

6.5 Discussion

6.5.1 Summary

Even the animals given saline to the lumen of the intestine before the onset of HS improved blood pressure compared to no intervention against HS (HS-NF animals). Metabolic support by glucose reduced bleeding into the BALF, BALF protein levels, and MPO activity in the BALF, but did not reduce the MPO activity in whole lung homogenate or prevent lesion formation in the jejunum of the intestine. While the intestinal gross morphology was improved by HS+TA and HS+DOX interventions, serine protease bands formed in the lung homogenate and plasma samples after all interventions. Pancreatic trypsin was detected after shock in lung samples regardless of the intestine's condition. While global protease inhibition with doxycycline reduced the plasma MMP activity and MMP-9 levels in the lung, it was unable to prevent protein degradation in the lung. Tranexamic acid treatment effectively prevented VEGFR-2 degradation in the lung. All groups had elevated levels of circulating VEGF after HS. In summary, single interventions were able to stabilize the blood pressure, protect the intestine, and reduce some protein degradation; however, peripheral organ inflammation was not attenuated at the termination of the experiment.

6.5.2 Resuscitation by Enteral Treatment Reduces Organ Injury following HS

Oral resuscitation following shock has been demonstrated to be an effective method to improve the outcome of shock victims [19]. Even injection of saline improves the outcome following HS by providing an additional fluid source that may contain oxygen for epithelial cells [9]. When comparing the blood pressure of HS-NF animals to HS+SAL animals, the addition of an average of 10.9 ml of saline to the intestine before HS was sufficient to increase the pressure during the 3 hour reperfusion period (Figure 6.3). There were some improvements with saline treatment alone in other parameters aside from pressure. Lung damage as measured by gross morphology, BALF protein concentration, and BALF MPO activity was not as severe compared with the animals in the HS-NF group from Chapter 5. The elevation of blood pressure could initially help the animal, but at later hours of reperfusion the animal may enter the same state as the HS-NF animals and with time, proteins in the lung such as occludin may degrade.

6.5.3 Intestinal Damage is Reduced but Not Eliminated with TA or Doxycycline Treatments

Unlike the experiments in Chapter 5 in which the luminal contents were removed, the native luminal contents remained in the intestine at the start of these experiments to test whether we could prevent the contents from crossing the barrier. While the gross morphology of the intestine was improved with either doxycycline or tranexamic acid

treatment, there was still neutrophil accumulation and some hemorrhage into the lumen. These lesions primarily occurred in the jejunum regions (Figure 6.5). The neutrophils could be attracted to the luminal contents in the intestine and cause their accumulation. The hemorrhage in the jejunum was the worst with glucose, possibility suggesting glucose solution alone could be pro-inflammatory. The concentration of glucose we used was double the concentration used in previous models, and further experimentation needs to be conducted to determine an optimal glucose concentration [7,13].

6.5.4 Relationship between Intestinal Damage and Lung Damage

The only HS group that showed a significant reduction in lung injury was the HS+GLUC group compared with the HS+SAL (Table 6.4). Even though the lungs lacked the characteristic microhemorrhages seen in the other HS groups, the MPO activity of lung homogenates remained elevated (Figure 6.11) in the HS+GLUC group. This infers that the ANGD portion of the ANGD+glucose treatment given to the animals in Chapter 3 (Figure 3.2) was responsible for reducing the neutrophil infiltration in the lungs following HS. ANGD and neutrophil elastase inhibitors have been shown to reduce neutrophil infiltration into the organs [20-23]. This evidence suggests that inhibiting serine proteases in the periphery may be a requirement to prevent neutrophil extravasation.

However, in every HS+GLUC animal, there were severe lesions in the jejunum (Figure 6.5), even though the MPO activity in the intestinal homogenates (Figure 6.7) and MMP-9 levels (Figure 6.21) were non-significantly elevated. The blood flow to the

jejunum has been observed to increase in the presence of glucose followed by ischemia/reperfusion injury [24]. These observations suggest that neutrophils potentially accumulate to a greater degree in the intestine where there is increased perfusion. During the low flow state, neutrophils accumulate in the microcirculation [25,26], and the presence of luminal content may attract neutrophils to the intestine to a greater degree. The animals that received glucose had elevated MMP-9 activity in the plasma (Figure 6.16) which suggests that the pharmacological concentration of glucose that was administered to the intestine before HS may be causing more cells (neutrophils, endothelial cells) to secrete MMP-9.

6.5.5 Intestinal Cell Death

While the villi were not destroyed in this model of hemorrhagic shock, there was extensive cell death even into the crypts of the intestinal villi as seen in cross sections of the jejunum (Figure 6.8). The inability for the crypts to regenerate new epithelial cells is associated with a poor outcome after shock [8,27]. Like the previous findings in the HS-F and HS-NF animals from Chapter 5, mucin 13 bound to epithelial cells was unchanged which indicates that even though cells in the villi become TUNEL-positive, the mucus layer is still intact (Figure 6.9).

In Chapter 2, we observed that the intestine was preserved with glucose in a model of complete intestinal ischemia. Since hemorrhagic shock is less severe, any of the interventions tested reduced the apoptosis in the crypt region of the villi (Figure 6.8) and could be beneficial in improving the survival of the animal.

6.5.6 Epithelial Protein Degradation

In these animals, there were no changes in the occludin or E-cadherin levels (Figure 6.10). Unlike the results in the previous chapter where the HS-NF animals showed complete destruction of E-cadherin in the presence of luminal content, the lack of E-cadherin destruction suggests that there was insufficient protease concentration in these samples reflecting the HS-F cases. Alternatively, the fluid injections into the lumen of the intestine may be diluting the proteases so that their concentration becomes insufficient to destroy E-cadherin [28].

6.5.7 Doxycycline Did not Prevent Protein Degradation

While pre-treating the rats before HS with doxycycline did reduce the plasma protease activities, it moderately improved the intestinal gross morphology appearance and reduced lung microhemorrhages (Figure 6.5 and Table 6.4). However, there was a lack of protection in protein degradation of VE-cadherin in the lung. In previous reports that used doxycycline as an MMP inhibitor at comparable concentrations, they documented improvement in vascular injury in organs such as the brain, lung, and kidney [29-32]. The lack of protection we see in the lung after doxycycline intervention suggests that in hemorrhagic shock, lung injury may be occurring by multiple mechanisms. Alternatively, the ischemic conditions could be causing the pericytes or other proteases beneath the surface of the endothelial cells to degrade the junctional endothelial proteins from the basal side of the vessel [33]. Since MMPs secreted beneath

the surface of the endothelial cells would not interface with the doxycycline after IV administration, the inhibitory efforts may potentially not target the exact MMPs that cause degradation of the wall structure.

As seen in all HS groups, there was a significant increase in MPO activity in the lung homogenates (Figure 6.11) which indicates neutrophil and monocyte accumulation in the tissue. These cells do not only secrete MMP-9 to excavate past the endothelial layer, but they may also secrete elastase, which was not blocked with any of our interventions. Therefore, the neutrophils may in part be contributing to the damage of cadherins [34]. Alternatively, the secretion of MMPs may be directed at the immediate adhesion area beneath the adhered neutrophil, and there would not be enough time for the doxycycline to inhibit the newly secreted MMPs. Hemorrhage from the lung microvessels likely does not require complete destruction of the entire vessel, but rather small holes are sufficient to allow red cells and plasma to escape into the alveolar space. MMP-9 localization occurs primarily in the immediate vicinity of the blood vessels (Figure 6.19C).

6.5.8 Transport of Pancreatic Proteases into the Periphery

Since the lung is often associated with gut damage, mediators coming from the gut could also be transported through the mesenteric lymph fluid (Figure 3.8). Even before HS, trypsin and chymotrypsin were present in the plasma (Figure 6.15A). However, the activity of serine proteases increased after HS in the plasma (Figure 6.15B), the lung (Figure 6.18A), and even the BALF (Figure 6.18B). Since these intestines had

native luminal contents inside their lumen, the proteases could be derived from either the intestine's lumen or the pancreas and then accumulate in the lung, which is the first microvascular bed they encounter during venous return. Glucose treatment which best preserved the epithelial barrier in the current experimental groups had the greatest increase in plasma protease activity (Figure 6.15B), suggesting that glucose is encouraging the transport of serine proteases into the circulation by preserving the intestinal microvascular and lymphatic network.

6.5.9 Protease Activity in the Periphery Does Not Correspond to Receptor Damage

Despite identifying a global increase in MMP-9 activity in every compartment after HS, this did not affect VE-cadherin degradation. In the liver, there was no change in VE-cadherin (Figure 6.24) despite the rise in MMP-9 activity (Figure 6.20). In the lung, there was an increase in MMP-9 and serine protease activity (Figure 6.18 and Figure 6.19) in all groups but no degradation of E-cadherin and partial reduction of VE-cadherin (Figure 6.23). Even though the MMPs are present, they may not be responsible for cleavage of cadherins. Additionally, serine proteases entering into the BALF could contribute in part to the generation of blood leakage into the alveolar space (Figure 6.19C). The tight junction protein occludin still may be protected from proteolytic degradation in the lung and intestine at the time of tissue collection in the current experiments (Figure 6.10 and Figure 6.23). Alternatively, occludin can be degraded if the lung enters apoptosis [35] which may have occurred in the HS-F and HS-NF models,

but not in the animals which received at least saline as an intervention against hemorrhagic shock.

6.5.10 VEGFR-2 AND THE RELATIONSHIP BETWEEN MMP-9 AND CIRCULATING VEGF

After HS, there was a decrease in VEGFR-2 receptor density in both the liver and lung in HS+SAL animals (Figure 6.25). However, the liver VEGFR-2 levels decreased in all groups whereas the lung VEGFR-2 levels were preserved in the HS+TA group (Figure 6.25) indicating the receptor degradation is tissue-specific at the three hour time point after HS. Since the entire animal is ischemic for 90 minutes during the model, tranexamic acid in the gut could be penetrating into the periphery and protecting the surface levels of the VEGFR-2 receptor from degradation. Previously, intestinal ischemia alone was not sufficient to reduce VEGFR-2 levels in the lung which suggests that the global ischemia is necessary to decrease lung VEGFR-2 levels [36]. Since hemorrhagic shock is associated with global ischemia, tranexamic acid may be inhibiting proteases in the plasma such as plasmin, which may cause the VEGFR-2 damage. Surprisingly, VEGFR-2 levels even decreased in lungs that had a low lung injury score in HS+GLUC or HS+SAL animals (Figure 6.26) suggesting that lung injury and VEGFR-2 levels are potentially not correlated.

Although VEGF levels in the tissues were unchanged after HS, there was a significant release of soluble VEGF into the circulation, especially in the HS+GLUC group (Figure 6.25). The HS+GLUC group also had the greatest increase in MMP-9 release into the plasma (Figure 6.16). Since TIMP-1 levels remained unchanged in the

circulation (Figure 6.16), the unchecked upregulation of MMP-9 may be responsible for the degradation of the extracellular matrix and VEGF release from the tissue into the circulation [37]. MMP-9 can also post-process VEGF to different isoforms [38]. While the mechanisms in tissue repair are often associated with angiogenic responses to hypoxic conditions, it may be possible that the release of VEGF after ischemia is an early response to stimulate the endothelial cells to repair damaged vessels. However, since the etiology of shock is very complex and VEGFR-2 may be cleaved or internalized upon binding to the ligand VEGF, the cells may be unable to synthesize new VEGFR-2. The lack of VEGFR-2 receptors and the increase in VEGF ligand may cause an imbalance in the signaling cascade and future work should investigate both the signaling and functional responses in endothelial cells following ischemia/reperfusion injury. In support of tranexamic acid treatment, survival increases drastically after HS if animals are given enteral tranexamic acid, and thus the preservation of VEGFR-2 could contribute to the positive outcome documented from this treatment [13].

6.5.11 LIMITATIONS

The major weakness derived from single time point experiments is the fact that kinetics of receptor degradation and restoration over longer periods of time following shock are not well understood. Even though the intestines of the HS+SAL group were damaged, extending the reperfusion observation to longer time points may be sufficient to achieve similar degradation of lung proteins compared to the HS-NF animals. In the current experiments, we chose to not flush the luminal contents, so the non-homogeneous

distribution of food along the intestine may be explained by this innate characteristic of the gut. Finally, we chose to pre-treat the animals, which may realistically be an option only for patients anticipating intestinal ischemia during elective surgery. Therefore, more thorough studies should investigate these parameters after some time elapses between the initial insult and the treatment.

6.6 CONCLUSIONS

These studies demonstrate that even saline in the lumen of the intestinal can help to maintain central blood pressure and reduce the severity of intestine and lung damage after HS. Doxycycline administration reduces the MMP activity in the plasma and some intestinal damage, but is relatively ineffective at preventing protein degradation in the lung. Enteral tranexamic acid treatment also helps to preserve the gut and the VEGFR-2 receptor in the lung. Glucose protects tissue lesions to form in the lung, but not neutrophil accumulation. Each of these treatments has select advantages. The next step is to study combinations of these particular treatments and whether they may provide enhanced protection of the gut and peripheral organs following hemorrhagic shock.

Chapters 5, 6 and 7, in full, are currently being prepared for submission for publication entitled “Strategies to minimize organ injury by proteolytic enzymes in hemorrhagic shock” by Angelina E. Altshuler, Michael Richter, Jason Chou, Diana Li, Leena Kurre, Alex H. Penn, and Geert W. Schmid-Schönbein. The dissertation author is the primary author of this manuscript.

6.7 REFERENCES

1. Ishimaru K, Mitsuoka H, Unno N, Inuzuka K, Nakamura S, Schmid-Schönbein GW. (2004) Pancreatic proteases and inflammatory mediators in peritoneal fluid during splanchnic arterial occlusion and reperfusion. Shock 22: 467-471.

2. Magnotti LJ, Upperman JS, Xu DZ, Lu Q, Deitch EA. (1998) Gut-derived mesenteric lymph but not portal blood increases endothelial cell permeability and promotes lung injury after hemorrhagic shock. Ann Surg 228: 518-527.

3. Deitch EA. (2010) Gut lymph and lymphatics: A source of factors leading to organ injury and dysfunction. Ann N Y Acad Sci 1207 Suppl 1: E103-11.

4. Qin X, Sheth SU, Sharpe SM, Dong W, Lu Q, Xu D, Deitch EA. (2011) The mucus layer is critical in protecting against ischemia-reperfusion-mediated gut injury and in the restitution of gut barrier function. Shock 35: 275-281.

5. Chang M, Kistler EB, Schmid-Schönbein GW. (2012) Disruption of the mucosal barrier during gut ischemia allows entry of digestive enzymes into the intestinal wall. Shock 37: 297-305.

6. Vakonyi T, Wittmann T, Varro V. (1977) Effect of local circulatory arrest on the structure of the enterocytes of the isolated intestinal loop. Digestion 15: 295-302.

7. Chiu CJ, Scott HJ, Gurd FN. (1970) Intestinal mucosal lesion in low-flow states. II. the protective effect of intraluminal glucose as energy substrate. Arch Surg 101: 484-488.

8. Robinson JW, Mirkovitch V. (1972) The recovery of function and microcirculation in small intestinal loops following ischaemia. Gut 13: 784-789.

9. Mirkovitch V, Menge H, Robinson JW. (1975) Protection of the intestinal mucosa during ischaemia by intraluminal perfusion. Res Exp Med (Berl) 166: 183-191.

10. Robinson JW, Mirkovitch V. (1977) The roles on intraluminal oxygen and glucose in the protection of the rat intestinal mucosa from the effects of ischaemia. Biomedicine 27: 60-62.

11. Flynn WJ,Jr, Gosche JR, Garrison RN. (1992) Intestinal blood flow is restored with glutamine or glucose suffusion after hemorrhage. J Surg Res 52: 499-504.

12. Chang M, Alsaigh T, Kistler EB, Schmid-Schönbein GW. (2012) Breakdown of mucin as barrier to digestive enzymes in the ischemic rat small intestine. PLoS One 7: e40087.

13. DeLano FA, Hoyt DB, Schmid-Schönbein GW. (2013) Pancreatic digestive enzyme blockade in the intestine increases survival after experimental shock. Sci Transl Med 5: 169ra11.

14. Caron A, Desrosiers RR, Beliveau R. (2005) Ischemia injury alters endothelial cell properties of kidney cortex: Stimulation of MMP-9. Exp Cell Res 310: 105-116.

15. van der Kaaij NP, Kluin J, Haitsma JJ, den Bakker MA, Lambrecht BN, Lachmann B, de Bruin RW, Bogers AJ. (2008) Ischemia of the lung causes extensive long-term pulmonary injury: An experimental study. Respir Res 9: 28.

16. Waldow T, Witt W, Buzin A, Ulmer A, Matschke K. (2009) Prevention of ischemia/reperfusion-induced accumulation of matrix metalloproteinases in rat lung by preconditioning with nitric oxide. J Surg Res 152: 198-208.

17. Chen W, Hartman R, Ayer R, Marcantonio S, Kamper J, Tang J, Zhang JH. (2009) Matrix metalloproteinases inhibition provides neuroprotection against hypoxia-ischemia in the developing brain. J Neurochem 111: 726-736.

18. Kunugi S, Shimizu A, Kuwahara N, Du X, Takahashi M, Terasaki Y, Fujita E, Mii A, Nagasaka S, Akimoto T, Masuda Y, Fukuda Y. (2010) Inhibition of matrix metalloproteinases reduces ischemia-reperfusion acute kidney injury. Lab Invest .

19. Kramer GC, Michell MW, Oliveira H, Brown TL, Herndon D, Baker RD, Muller M. (2010) Oral and enteral resuscitation of burn shock the historical record and implications for mass casualty care. Eplasty 10: e56.

20. Mitsuoka H, Schmid-Schönbein GW. (2000) Mechanisms for blockade of in vivo activator production in the ischemic intestine and multi-organ failure. Shock 14: 522-527.

21. Doucet JJ, Hoyt DB, Coimbra R, Schmid-Schönbein GW, Junger WG, Paul LW, Loomis WH, Hugli TE. (2004) Inhibition of enteral enzymes by enteroclysis with nafamostat mesilate reduces neutrophil activation and transfusion requirements after hemorrhagic shock. J Trauma 56: 501-10; discussion 510-1.

22. Toda Y, Takahashi T, Maeshima K, Shimizu H, Inoue K, Morimatsu H, Omori E, Takeuchi M, Akagi R, Morita K. (2007) A neutrophil elastase inhibitor, sivelestat, ameliorates lung injury after hemorrhagic shock in rats. Int J Mol Med 19: 237-243.

23. Kotake Y, Yamamoto M, Matsumoto M, Morisaki H, Takeda J. (2005) Sivelestat, a neutrophil elastase inhibitor, attenuates neutrophil priming after hepatoenteric ischemia in rabbits. Shock 23: 156-160.

24. Kozar RA, Hu S, Hassoun HT, DeSoignie R, Moore FA. (2002) Specific intraluminal nutrients alter mucosal blood flow during gut ischemia/reperfusion. JPEN J Parenter Enteral Nutr 26: 226-229.

25. Moore RM, Bertone AL, Bailey MQ, Muir WW, Beard WL. (1994) Neutrophil accumulation in the large colon of horses during low-flow ischemia and reperfusion. Am J Vet Res 55: 1454-1463.

26. Ratliff NB, Wilson JW, Mikat E, Hackel DB, Graham TC. (1971) The lung in hemorrhagic shock. IV. the role of neutrophilic polymorphonuclear leukocytes. Am J Pathol 65: 325-334.

27. Sukhotnik I, Helou H, Mogilner J, Lurie M, Bernsteyn A, Coran AG, Shiloni E. (2005) Oral arginine improves intestinal recovery following ischemia-reperfusion injury in rat. Pediatr Surg Int 21: 191-196.

28. Bounous G. (1967) Role of the intestinal contents in the pathophysiology of acute intestinal ischemia. Am J Surg 114: 368-375.

29. Hanemaaijer R, Visser H, Koolwijk P, Sorsa T, Salo T, Golub LM, van Hinsbergh VW. (1998) Inhibition of MMP synthesis by doxycycline and chemically modified tetracyclines (CMTs) in human endothelial cells. Adv Dent Res 12: 114-118.

30. Reyes R, Guo M, Swann K, Shetgeri SU, Sprague SM, Jimenez DF, Barone CM, Ding Y. (2009) Role of tumor necrosis factor-alpha and matrix metalloproteinase-9 in blood-brain barrier disruption after peripheral thermal injury in rats. J Neurosurg 110: 1218-1226.

31. Ihtiyar E, Yasar NF, Erkasap N, Koken T, Tosun M, Oner S, Erkasap S. (2011) Effects of doxycycline on renal ischemia reperfusion injury induced by abdominal compartment syndrome. J Surg Res 167: 113-120.

32. Palei AC, Zaneti RA, Fortuna GM, Gerlach RF, Tanus-Santos JE. (2005) Hemodynamic benefits of matrix metalloproteinase-9 inhibition by doxycycline during experimental acute pulmonary embolism. Angiology 56: 611-617.

33. Chantrain CF, Henriet P, Jodele S, Emonard H, Feron O, Courtoy PJ, DeClerck YA, Marbaix E. (2006) Mechanisms of pericyte recruitment in tumour angiogenesis: A new role for metalloproteinases. Eur J Cancer 42: 310-318.

34. Carden D, Xiao F, Moak C, Willis BH, Robinson-Jackson S, Alexander S. (1998) Neutrophil elastase promotes lung microvascular injury and proteolysis of endothelial cadherins. Am J Physiol 275: H385-92.

35. Bojarski C, Weiske J, Schoneberg T, Schroder W, Mankertz J, Schulzke JD, Florian P, Fromm M, Tauber R, Huber O. (2004) The specific fates of tight junction proteins in apoptotic epithelial cells. J Cell Sci 117: 2097-2107.

36. Mura M, Han B, Andrade CF, Seth R, Hwang D, Waddell TK, Keshavjee S, Liu M. (2006) The early responses of VEGF and its receptors during acute lung injury: Implication of VEGF in alveolar epithelial cell survival. Crit Care 10: R130.

37. Hollborn M, Stathopoulos C, Steffen A, Wiedemann P, Kohen L, Bringmann A. (2007) Positive feedback regulation between MMP-9 and VEGF in human RPE cells. Invest Ophthalmol Vis Sci 48: 4360-4367.

38. Lee S, Jilani SM, Nikolova GV, Carpizo D, Iruela-Arispe ML. (2005) Processing of VEGF-A by matrix metalloproteinases regulates bioavailability and vascular patterning in tumors. J Cell Biol 169: 681-691.

Chapter 7

Application of Combination Interventions to Attenuate Intestinal Wall Breakdown and Distant Organ Injury

7.1 Introduction

The system-wide multiple organ failure that occurs after hemorrhagic shock is not limited to one mechanism caused by the gut, but may be caused by a multitude of factors including reduction of nutrient supply, cell and tissue failure, barrier breakdown, release of inflammatory mediators, cell activation, and activation of several enzyme systems [1-7]. While some of these outcomes are connected, multiple strategies may be required to reduce the extent of organ failure following hemorrhagic shock.

Aside from the luminal pancreatic enzymes, there appear to be two protease systems involved in the degradation of the mucosal barrier of the intestine during the pathogenesis of shock. In Chapter 2, we explored the benefits that tranexamic acid provided to prevent gut barrier breakdown. Furthermore, we observed an even better

protection of the gut if both tranexamic acid and glucose were given simultaneously. We know that if the gut barrier is preserved, the escape of inflammatory mediators into the circulation is reduced and neutrophil activation is attenuated [8-10].

However, proteases in the circulation can also contribute to the demise of tissue and surface receptors as seen in Chapter 4-6. If we can reduce peripheral damage in addition to hindering gut barrier breakdown, we may increase the protection of the animal from injury after shock.

7.2 Chapter Aims

In previous chapters, I studied how single treatments targeting three different mechanisms can partially improve the outcome of specific parameters after hemorrhagic shock. The aim of this chapter is to study peripheral organ injury following hemorrhagic shock if the animal is pre-treated with two or three interventions simultaneously. I will combine the following treatments: MMP inhibition in the circulation, tranexamic acid protection in the gut and/or metabolic support with glucose in the gut. I hypothesize that combining several interventions will more effectively preserve the gut barrier, reduce the transport of inflammatory mediators, and improve receptor density in peripheral organs (Figure 7.1).

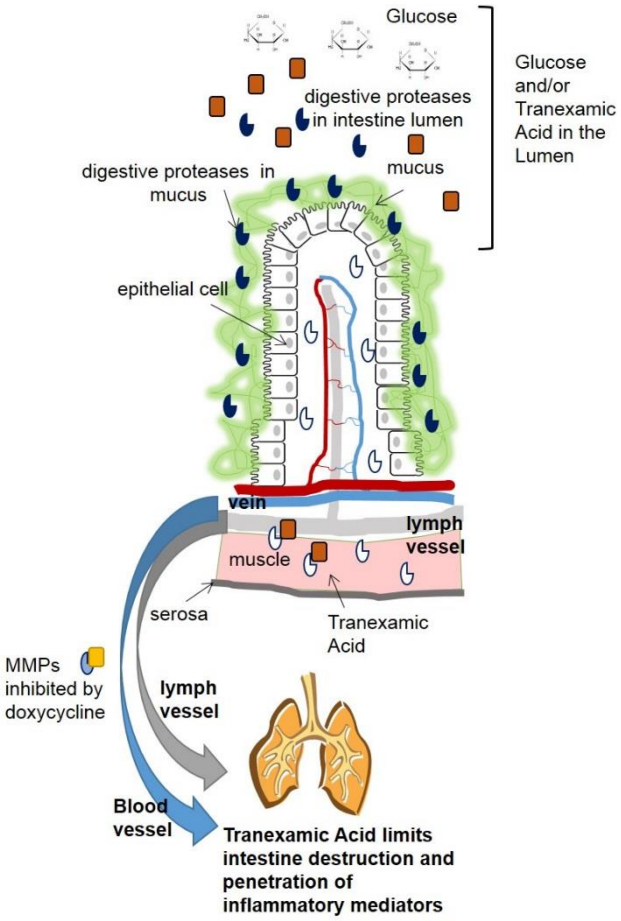

Figure 7.1 Hypothesis summary. If multiple interventions are simultaneously administered to the animal before the onset of shock, the gut barrier will be better preserved and receptor damage in the periphery is reduced.

7.3 METHODS

The animal protocol was reviewed and approved by the University of California, San Diego Institutional Animal Care and Use Committee. Male Sprague Dawley (body weight between 322±51 g [mean±SD], range; 233-385 g Harlan, Indianapolis, IN) were allowed food and water *ad libitum* prior to surgery. Rats were administered general anesthesia (xylazine, 4 mg/kg; ketamine 75 mg/kg IM) and euthanized by infusion of B-Euthanasia IV (120 mg/kg). Following general anesthesia, the femoral artery and vein were cannulated. Systolic, diastolic, heart rate, and mean arterial pressure (MAP) were recorded using LabChart (AD Instruments, Dunedin, New Zealand).

7.3.1 ANIMALS

7.3.1.1 HEMORRHAGIC SHOCK PROCEDURE

In this chapter, we will combine the interventions previously described in Section 7.3.1.1. The treatments administered to the animals are described in Table 7.1.

Table 7.1 Multiple treatments for hemorrhagic shock.

	Intraluminal	IV	IP
HS+DOX+TA	Tranexamic Acid (200 mM)	Doxycycline (5 mg/kg body weight)	Doxycycline (10 mg/kg body weight)
HS+DOX+GLUC	Glucose (100 mg/ml in saline)	Doxycycline (5 mg/kg body weight)	Doxycycline (10 mg/kg body weight)
HS+TA+GLUC	Glucose (100 mg/ml in saline) Tranexamic Acid (200 mM in saline)	Saline	Saline
HS+DOX+TA+GLUC	Glucose (100 mg/ml in saline) Tranexamic Acid (200 mM in saline)	Doxycycline (5 mg/kg body weight)	Doxycycline (10 mg/kg body weight)

7.3.1.2 BRONCHOALVEOLAR LAVAGE FLUID

BALF collection was performed as described in Section 5.3.1.2.

7.3.2 TISSUE HOMOGENIZATION

Tissues were homogenized as described in Section 5.3.3.

7.3.3 INTESTINAL HEMORRHAGE

Intestinal jejunum segments were processed as described in Section 5.3.3.

7.3.4 Enzyme and Protease Activity Measurements

7.3.4.1 Myeloperoxidase (MPO) Activity Assay

MPO activity was performed as described in Section 5.3.4.1.

7.3.4.2 Gelatin Gel Zymography

Gelatin gel zymography was performed as described in Section 6.3.4.3.

7.3.5 Immunoblotting

Immunoblotting was performed as described in Section 5.3.6.

7.3.6 Lung Histology

Tissue histology was completed as described in Section 5.3.6.1.

7.3.7 Statistical Analysis

Results are presented as either mean±standard deviation (SD). Paired t-tests were completed for comparisons between groups for MAP during the reperfusion period and between pre- and post-shock plasma samples. Mann-Whitney tests were used for non-

normally distributed means. ANOVA followed by Tukey post-hoc was done for comparisons of three or more. Statistical analysis was performed in OriginLabs software.

7.4 RESULTS

7.4.1 HEMATOLOGICAL PARAMETERS

Rats had comparable amounts of blood withdrawn in order to achieve a 30 mmHg pressure and maintain it during ischemia (Figure 7.2). It should be noted that during the ischemic period, the majority of rats did not decompensate as severely as untreated shock (HS-F, HS-NF, or HS+SAL). The MAP of all the treated animals was greater than the HS-NF animals during reperfusion (Figure 7.3). If the final reperfusion period for HS-NF, HS+SAL, and HS+DOX+TA+GLUC are fit with linear curves, the HS-NF and HS+SAL fit a linear trend with strong correlation, but the HS+DOX+TA+GLUC group did not (Figure 7.4). The HS-NF and HS+SAL had negative slopes indicating the decrease in pressure that would ultimately end in death.

The heart rates of the animals were not significantly different between the different periods of reperfusion (Table 7.2). The pulse pressure of the rats began to drop by the second hour of reperfusion in the HS+DOX+GLUC and HS+TA+GLUC groups and was significantly decreased in all groups by the third hour (Table 7.3).

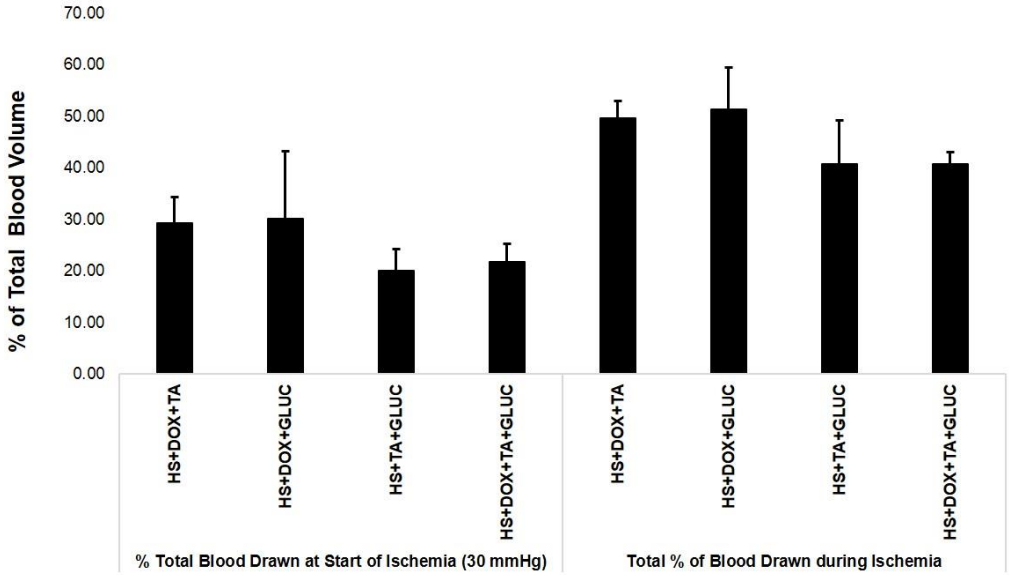

Figure 7.2 Blood volume withdrawal during ischemia. Percent blood volume removed to reach initial ischemia at 30 mmHg and total blood removed from the animal during ischemia. N=4 rats/group. Bar graphs represent mean±SD.

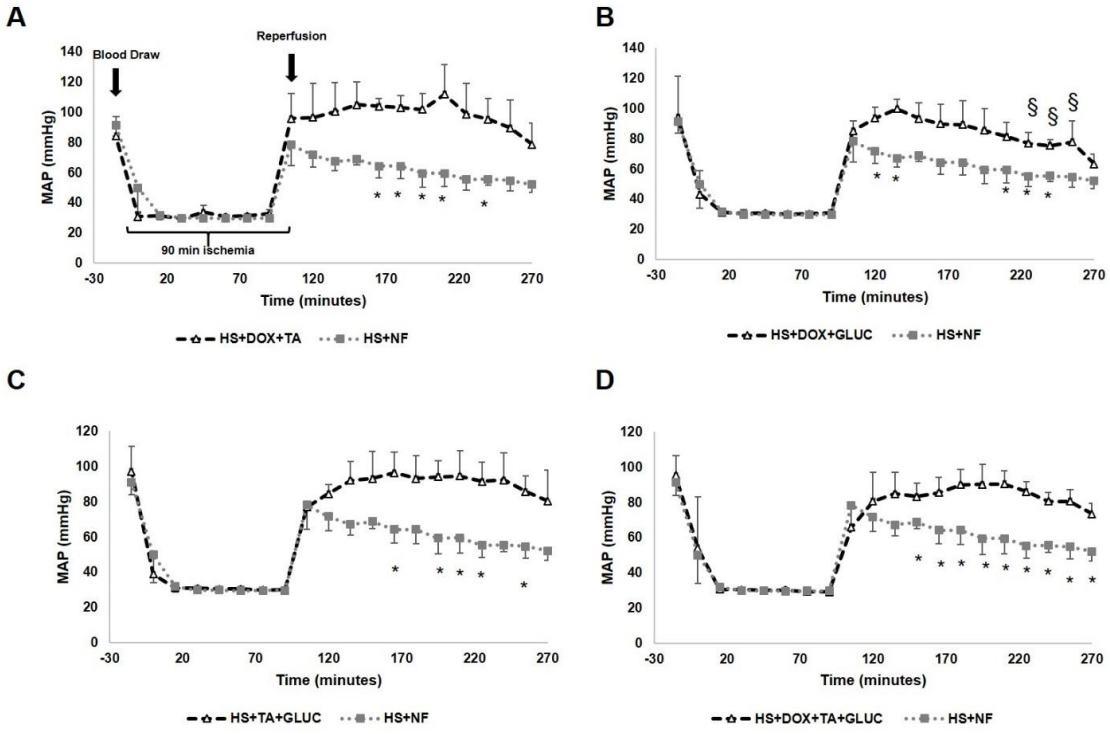

Figure 7.3 Pressure traces with multiple treatments. Pressure traces plotted with HS-NF and. *, $p<0.05$ compared to the MAP of HS-NF at each time point for (A) HS+DOX+TA, (B) HS+DOX+GLUC, (C) HS+TA+GLUC, or (D) HS+DOX+TA+GLUC. §, $p<0.05$ compared to the MAP at the 105 min time point within each treated groups. N=6 rats/group for HS-NF and N=4 rats/group for all other groups. Data are presented as mean±SD.

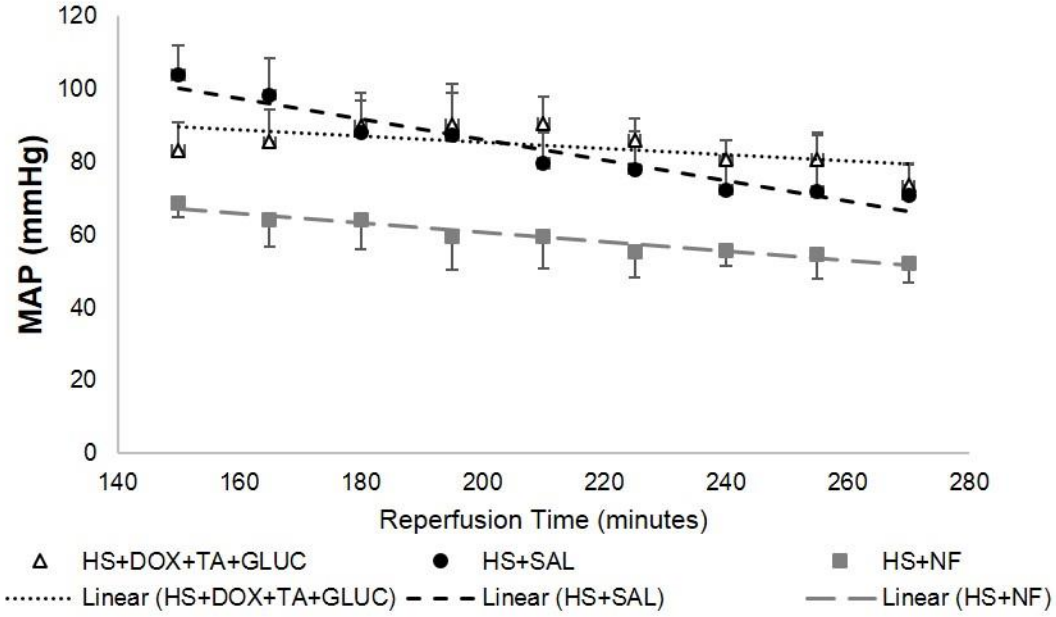

Figure 7.4 Reperfusion period of HS-NF, HS+SAL and HS+DOX+TA+GLUC. The last two hours of reperfusion were fit with a linear curve. The linear approximations were for HS+DOX+TA+GLUC ($y = -0.085x + 102.25$; $R^2 = 0.3847$), for HS+SAL ($y = -0.2803x + 142.19$; $R^2 = 0.9332$) and for HS-NF ($y = -0.1294x + 86.472$; $R^2 = 0.9408$). N=6 rats/group for HS-NF, N=7 rats/group for HS+SAL, and N=4 rats/group for HS+DOX+TA+GLUC.

Table 7.2 Hemorrhagic shock heart rates.

	HS+DOX+TA	HS+DOX+GLUC	HS+TA+GLUC	HS+DOX+TA+GLUC
Start	190±18	195±9	217±10	217±21
Blood Draw	142±8	153±24	182±28	166±13
Ischemia	154±33	165±34	188±29	213±24
Reperfusion	250±25	251±22	244±8	293±24
Hour 1	258±32	240±21	249±18	289±20
Hour 2	265±41	262±27*	247±11*	297±24
Hour 3	235±13	250±20*	238±7*	292±28

Heart rates (beats/minute) are presented as mean±SD. *, $p<0.025$ by paired t-test compared to the heart rate of Hour 1. N=4 rats/group.

Table 7.3 Hemorrhagic shock pulse pressures.

	HS+DOX+TA	HS+DOX+GLUC	HS+TA+GLUC	HS+DOX+TA+GLUC
Start	44.8±4.1	43.9±4.2	43.2±4.0	43.7±3.1
Blood Draw	36.6±7.3	32.5±6.9	27.9±6.6	25.8±4.7
Ischemia	32.3±6.8	35.6±1.0	34.7±4.6	29.8±6.8
Reperfusion	46.0±2.8	50.9±2.5	52.9±3.1	54.5±17.2
Hour 1	53.3±2.7	62.7±1.8	59.1±4.4	60.1±14.7
Hour 2	47.5±2.4	52.1±2.6*	54.1±2.6*	57.1±19.4
Hour 3	40.5±3.3*	41.0±6.1*	47.6±3.5*	47.4±16.4*

Pulse pressure (mmHg) are presented as mean±SD. *, $p<0.01$ by paired t-test compared to Hour 1 pulse pressure. N=4 rats/group.

7.4.2 INTESTINAL DAMAGE

Before the onset of hemorrhagic shock, all intestines appeared healthy without evidence of microhemorrhages or distention. After shock, especially with treatments containing tranexamic acid, the intestine also appeared without symptoms after hemorrhagic shock (Figure 7.5). If glucose and tranexamic acid were injected into the lumen of the intestine, not all fluid was absorbed at the end of these current experiments, unlike the animals treated with saline alone, where all the fluid was absorbed after HS. At the end of the reperfusion period, peristaltic movements were observed in the majority of cases. Although gross morphology improved after shock, the absorbance of the tissue homogenate was not significantly elevated in all groups (Figure 7.6). The MPO activity of intestinal homogenates resembled the No-HS group for HS+DOX+TA treated animals, but remained unchanged among the other groups (Figure 7.7). MMP-9 levels in the intestine were elevated after HS, though not significantly compared to No-HS (Figure 7.8).

Epithelial junctional proteins were compared against the HS-F or HS-NF animals for the multi-treated groups and we found that for the case of E-cadherin, these proteins resembled the HS-NF animals which were significantly reduced in the three isoforms (Figure 7.9). The tight junction protein occludin did not change between groups (Figure 7.9).

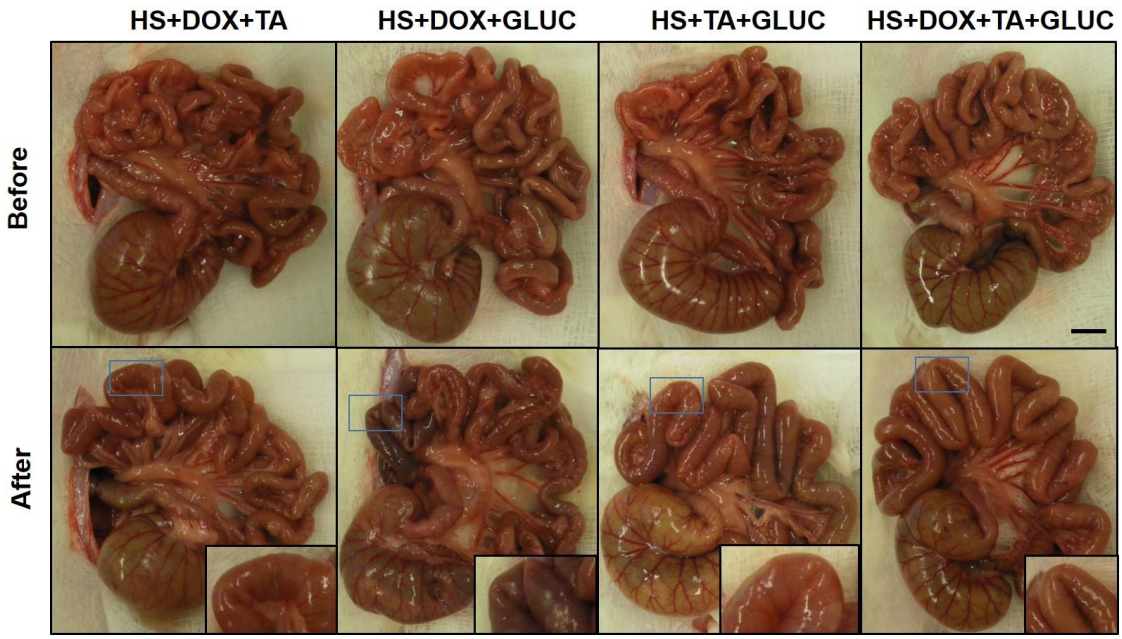

Figure 7.5 Gross morphology of intestines before and after HS. The gross morphology of the intestine was improved the best when tranexamic acid was part of the treatment. Blue boxes are zoomed in the lower left corner. Length bar equals 1 cm.

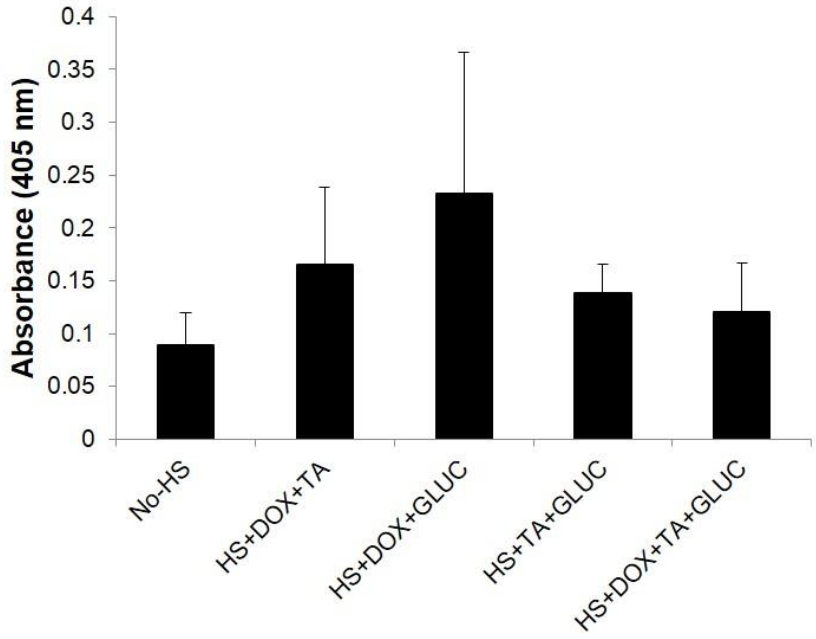

Figure 7.6 Hemorrhage into the intestine. Light absorbance values in intestinal homogenates at 405 nm due to hemoglobin accumulation. N=6 rats/group for No-HS. N=4 rats/group for all other treatments. Data are presented as mean±SD.

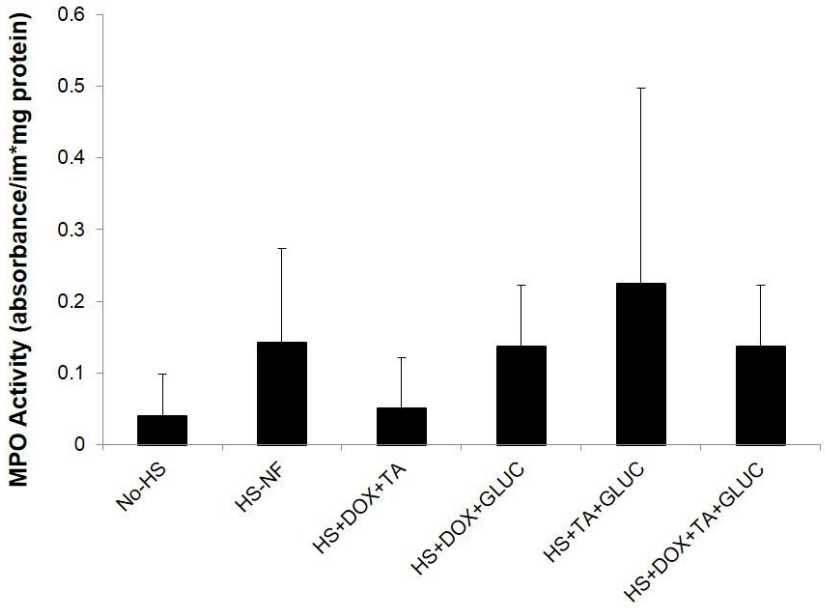

Figure 7.7 MPO activity in the intestine. MPO activity in intestinal homogenates (containing luminal content). N=6 rats/group for No-HS and HS-NF and N=4 rats/group for all other groups. Data are presented as mean±SD.

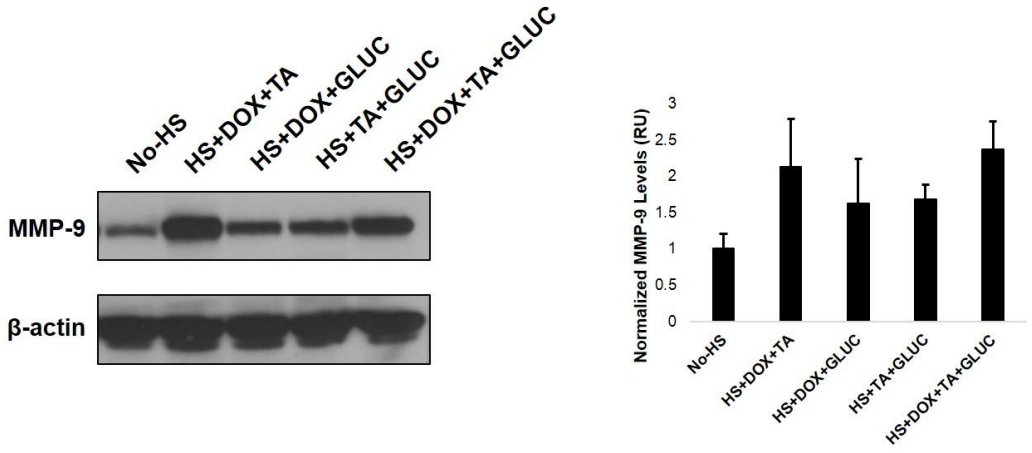

Figure 7.8 MMP-9 protein levels in the intestine. MMP-9 levels in the intestinal wall homogenates increased after HS regardless of treatment. N=4 rats/group. Bar graph depicts mean±SD.

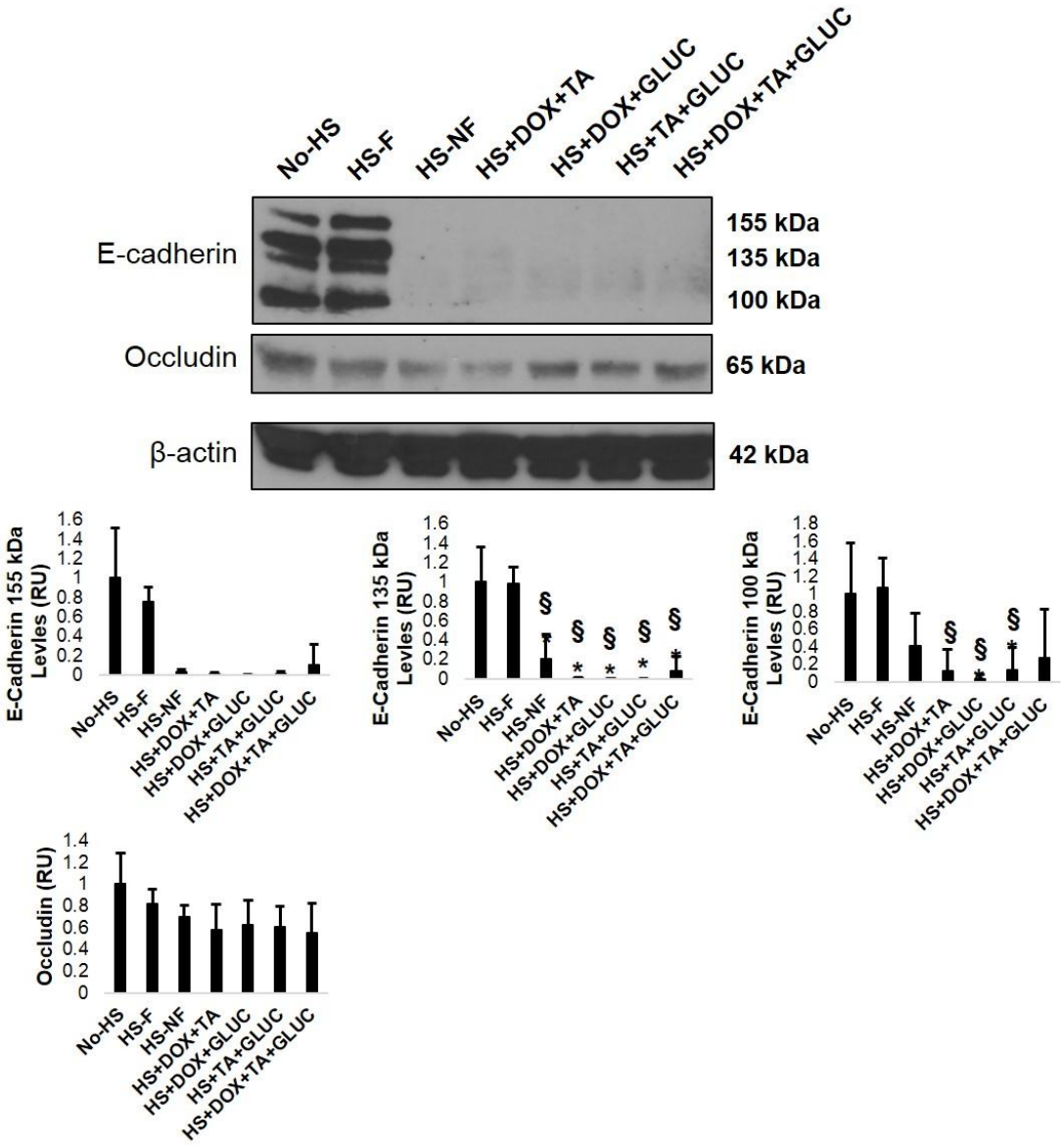

Figure 7.9 Epithelial junctional protein levels. E-cadherin was decreased in the cases that contained the native luminal contents for the 100, 135, and 155 kDa isoforms. *, $p<0.05$ compared to No-HS and §, $p<0.05$ compared to HS-F by ANOVA followed by Tukey post-hoc test. N=4 rats/group. Bar graphs indicate mean±SD.

7.4.3 Protease Activity and Levels in Plasma

In order to determine if the interventions had an effect on the transport of serine proteases, we detected the protease activities by gelatin zymography. The low molecular weight bands that were confirmed to be of serine protease origin were also seen in the plasma after HS in all treatment groups (Figure 7.10).

The neutrophil derived pro-form of MMP-9 increased in the HS+TA+GLUC and the HS+DOX+TA+GLUC groups (Figure 7.11A and B). Active MMP-9 was increased after HS in all groups and there was no change in pro-MMP-9 levels (Figure 7.11A and B). Immunoblotting the non-reduced protein samples confirmed the three protease forms: MMP-9, pro-MMP-9 derived from neutrophils, and MMP-9 dimer (Figure 7.11C).

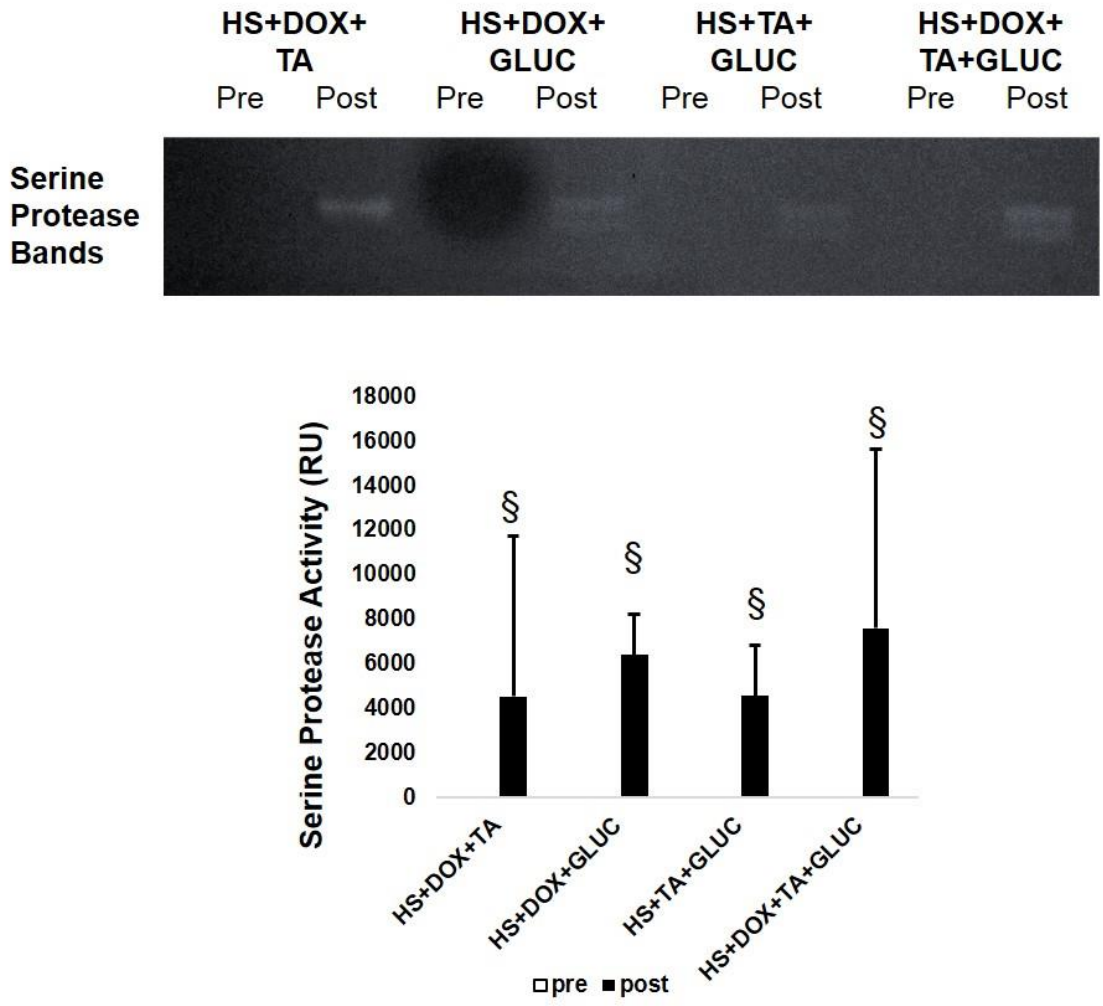

Figure 7.10 Serine protease bands in plasma. Serine protease bands formed in plasma only after HS regardless of treatment. N=4 rats/group. §, $p<0.05$ by Mann Whitney test. Bar graphs are presented as mean±SD.

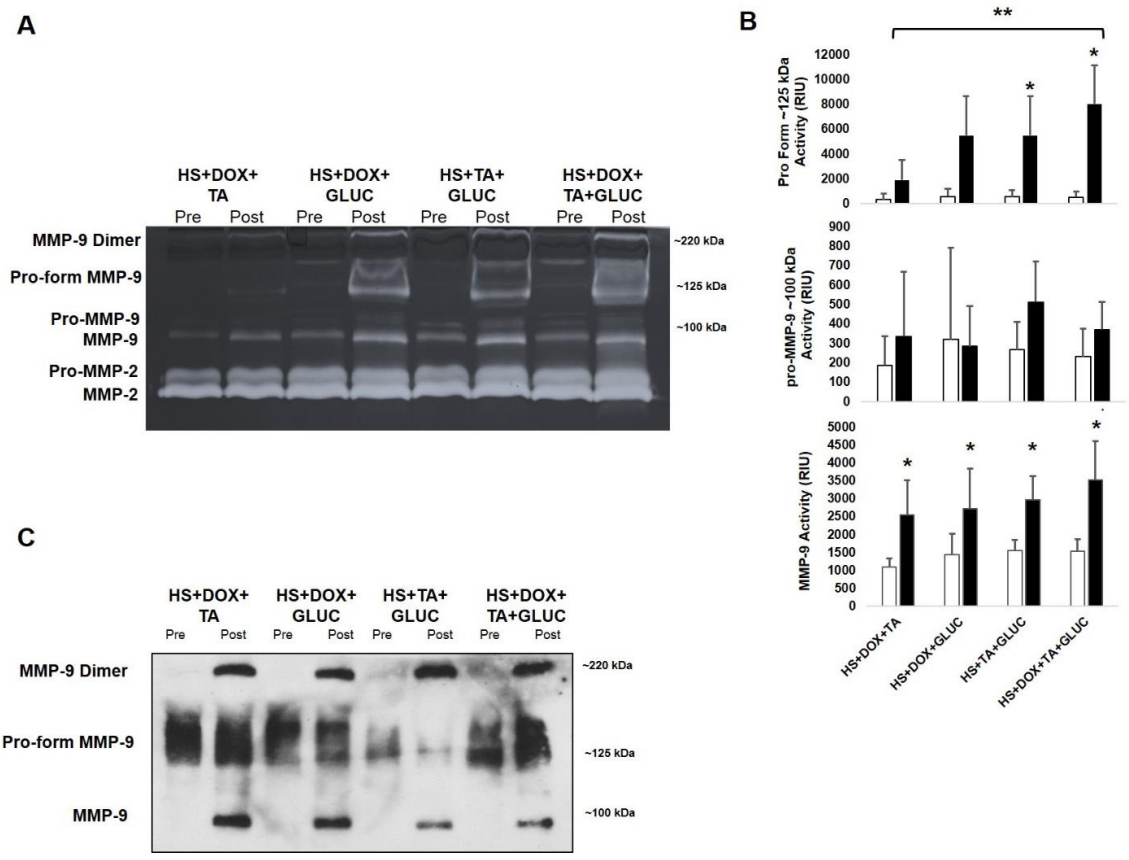

Figure 7.11 MMP-9 activity in plasma. (A) Gelatin gel zymography showed neutrophil derived pro-MMP-9 (150 kDa) and MMP-9 active enzymes were significantly elevated (B) after HS. *, $p<0.05$ by paired t-test. **, $p<0.05$ by ANOVA followed by Tukey post hoc. (C) Immunoblotting for MMP-9 without reducing samples showed three distinct forms of MMP-9 in the plasma that appear as MMP-9 dimer (220 kDa), a neutrophil pro-form of MMP-9 (125 kDa), and an active form of MMP-9. N=4 rats/group. Bar graphs are presented as mean±SD.

7.4.4. LUNG DAMAGE

Macroscopic bleeding in the lung occurred in nearly all cases regardless of treatment (Figure 7.12), and there were no significant differences in the lung injury score when blindly assessed (Table 7.4). The MPO activity of lung homogenates was elevated compared to No-HS animals in all cases (Figure 7.13). The protein concentration in the BALF was significantly elevated in the HS+TA+GLUC and HS+DOX+TA+GLUC groups (Figure 7.14). MPO activity in the BALF was not significantly reduced in the HS+TA+GLUC group, but elevated in all other groups (Figure 7.15). The absorbance of hemoglobin in the BALF was significantly elevated in the HS+TA+GLUC and HS+DOX+TA+GLUC animals (Figure 7.16).

Table 7.4 Lung injury score.

HS+DOX+GLUC	HS+DOX+TA	HS+TA+GLUC	HS+DOX+TA+GLUC
2.1±1.3	2.1±1.5	2.3±1.4	2.6±1.0

Lung injury score ranging between 0 (lowest) and 5 (maximum). Data shown as mean±SD.

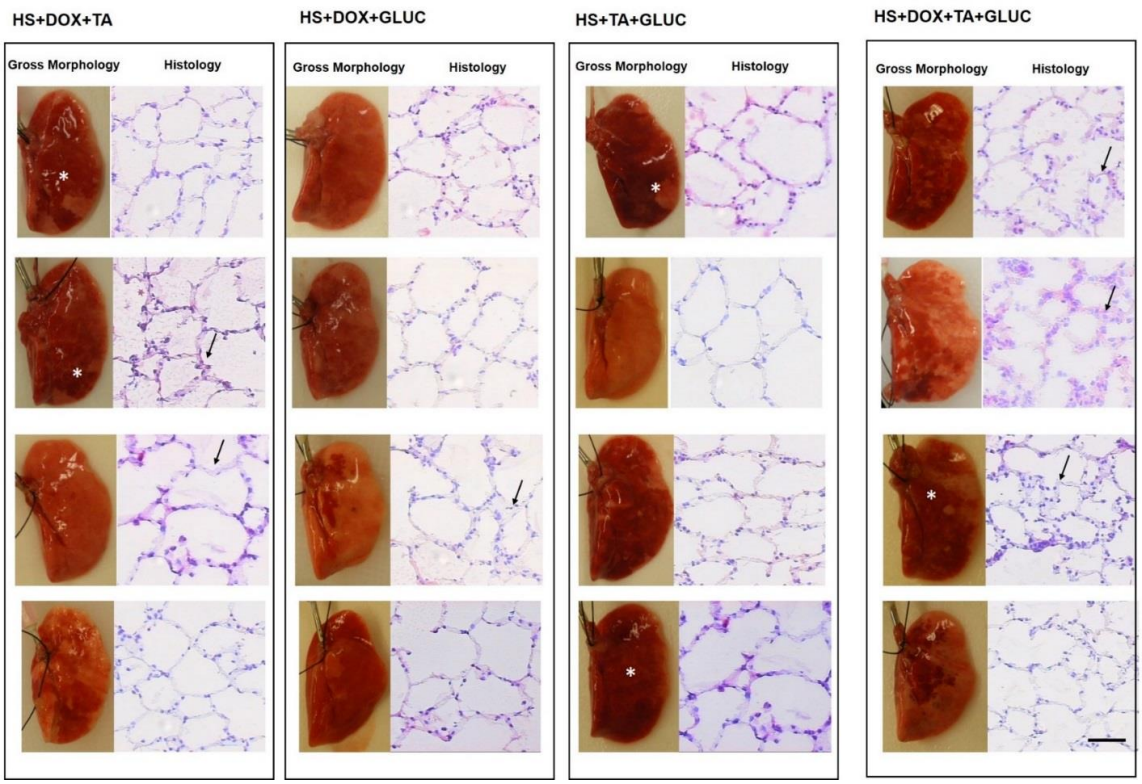

Figure 7.12 Lung gross morphology and histological sections. Severe lung damage in the form of macroscopic lesions was observed in all groups (white star). Arrows indicate swelling of the alveoli. Length bar equals 30 μm.

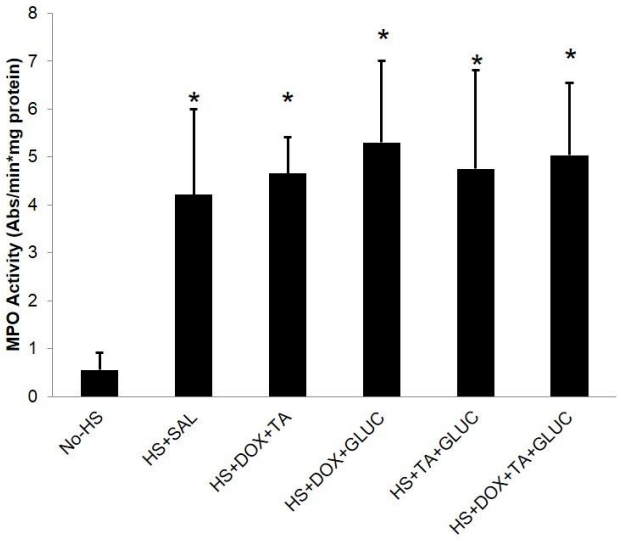

Figure 7.13 MPO activity in lung homogenates. MPO activity of lung homogenates was elevated in all cases after HS. *, $p<0.05$ by ANOVA followed by Tukey post-hoc. N=4 rats/group. Bar graph is presented as mean±SD.

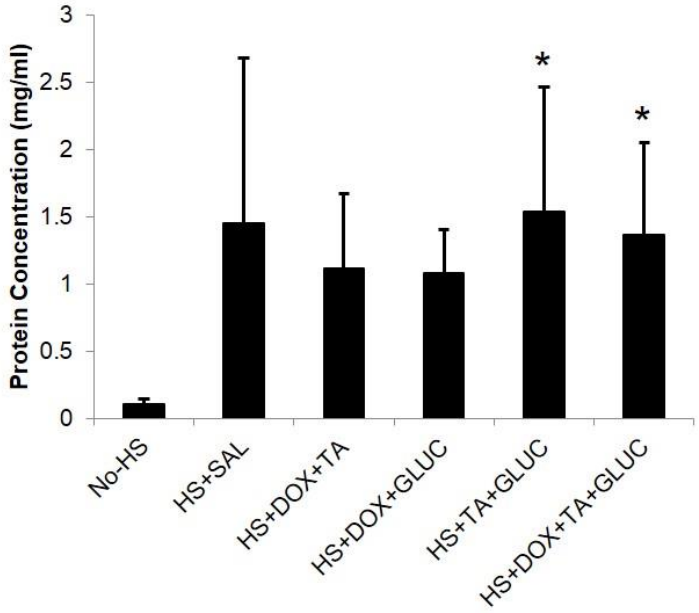

Figure 7.14 Protein concentration in the BALF. The protein concentration of the BALF was only significantly elevated in the HS+TA+GLUC and HS+DOX+TA+GLUC groups. N=4 rats/group. *, $p<0.05$ by ANOVA followed by Tukey post-hoc. Bar graph is presented as mean±SD.

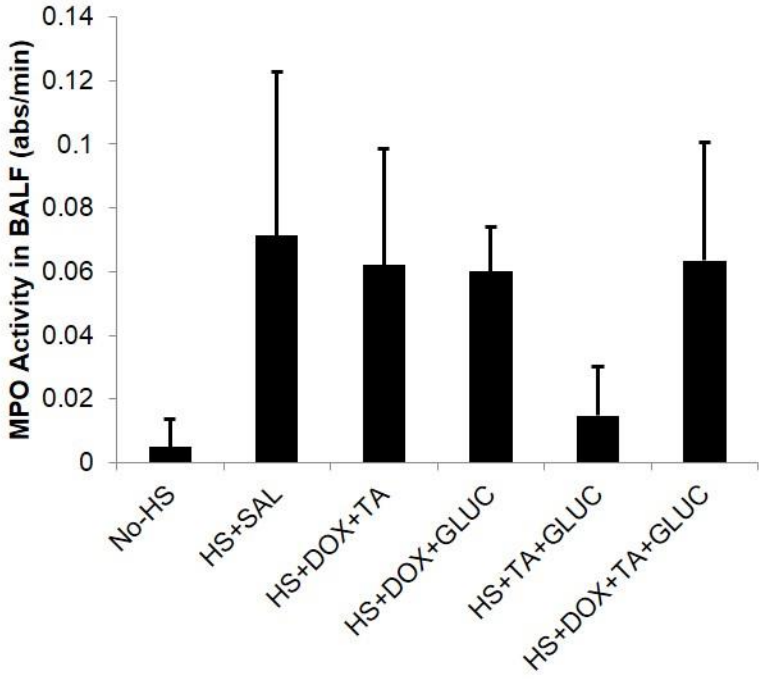

Figure 7.15 MPO activity in BALF. MPO activity in the BALF was unchanged between the different treatment groups. N=4 rats/group. Bar graph shows mean±SD.

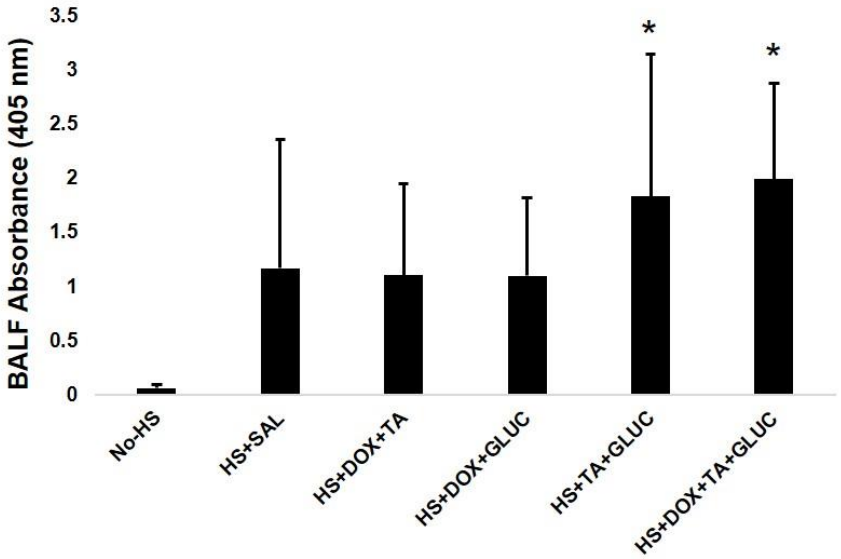

Figure 7.16 BALF hemoglobin absorbance. The absorbance of hemoglobin was significantly elevated in the BALF of HS+TA+GLUC and HS+DOX+TA+GLUC treated animals. N=4 rats/group. *, $p<0.05$ by ANOVA followed by Tukey post-hoc. Bar graph is presented as mean±SD.

7.4.5 Serine Protease Activity in the Lung

As previously documented, low molecular weight bands appeared with greater intensity during gelatin gel zymography of lung homogenates after HS in all cases (Figure 7.17A). Trypsin appeared in all lung homogenates as detected by immunoblotting after HS (Figure 7.17B).

MMP-9 and MMP-9 dimer activity in the lung homogenates as detected by gelatin gel zymography were not significantly increased (Figure 7.18A). However, the protein levels of MMP-9 were elevated in the lung in all cases (Figure 7.18B).

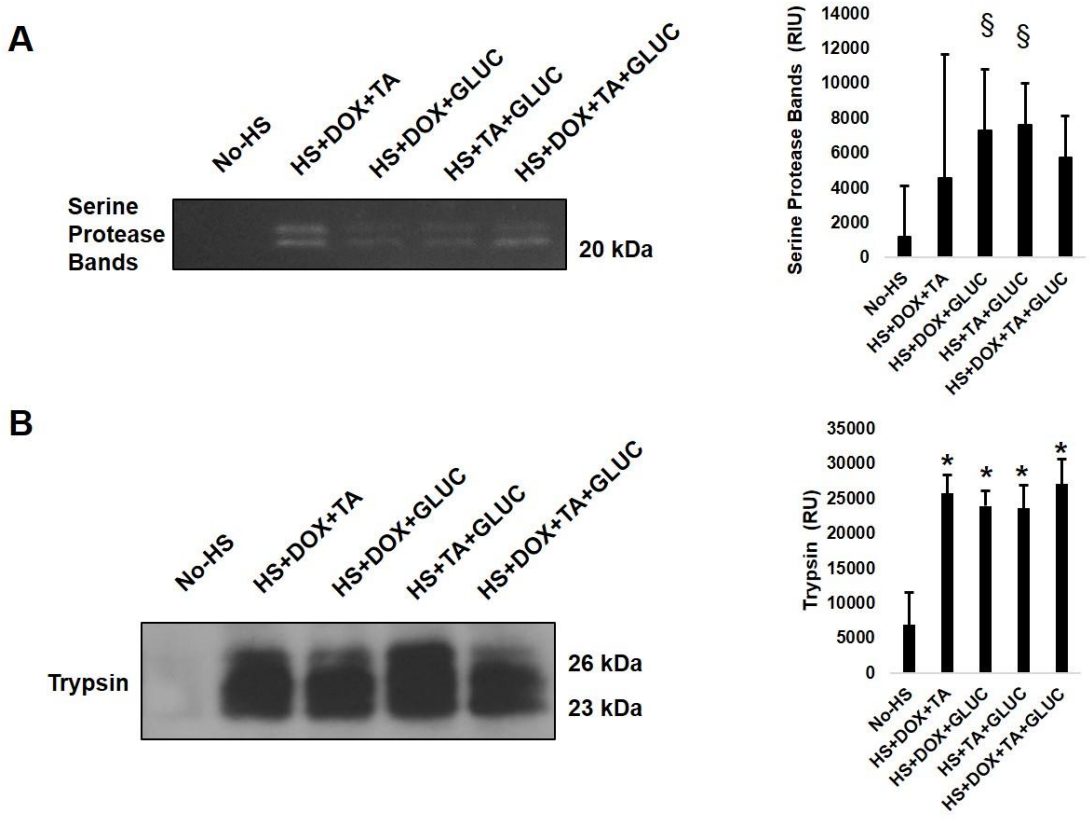

Figure 7.17 Lung serine protease levels. (A) Low molecular weight serine protease bands appeared in the lung homogenate in all cases after HS. (B) Trypsin was detected by immunoblotting and significantly elevated in all lung homogenates after HS. §, $p<0.01$ by Mann Whitney test. *, $p<0.05$ by ANOVA followed by Tukey post-hoc test. N=4 rats/group except No-HS where N=6 rats/group. Bar graphs are presented as mean±SD.

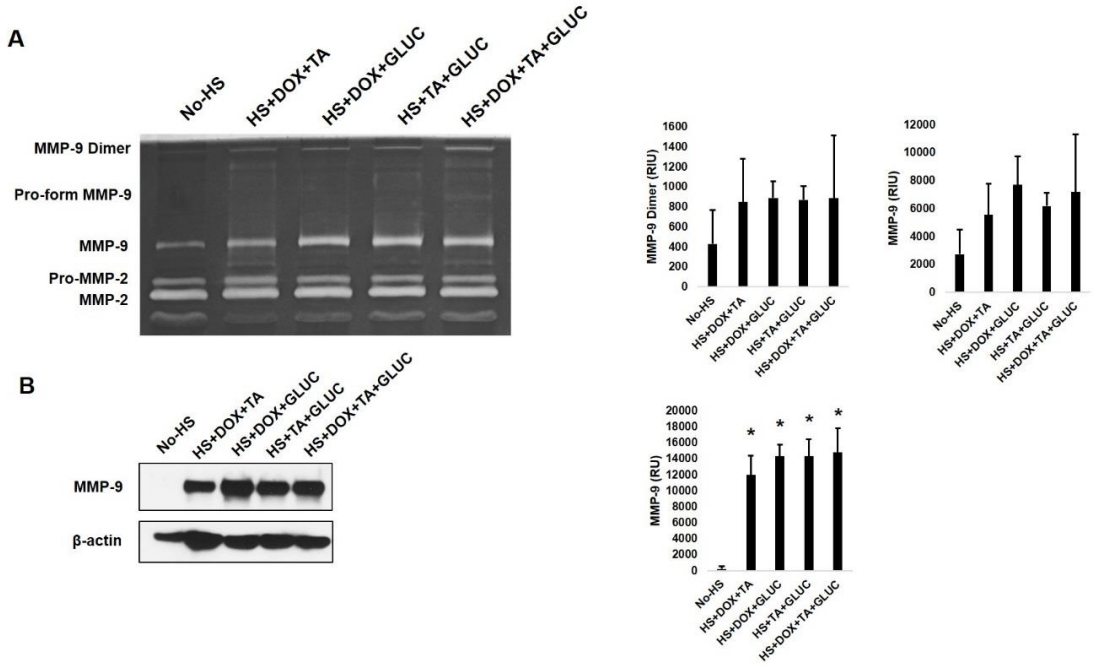

Figure 7.18 MMP levels in lung homogenate. (A) MMP-9 and MMP-9 dimer activity were non-significantly elevated in all HS groups. (B) MMP-9 protein levels were elevated in the lung homogenate. *, $p<0.05$ by ANOVA followed by Tukey post-hoc test. N=4 rats/group except No-HS where N=6 rats/group. Bar graphs are presented as mean±SD.

7.4.6 Lung Endothelial Protein Damage

The tight junction protein occludin was significantly decreased in HS-NF lungs, but not restored with the different treatments (Figure 7.19A). Like we saw in Chapter 4, HS-NF animals had reduced VE-cadherin and E-cadherin, but they were not significantly reduced in the treated HS cases (Figure 7.19B).

The 230 kDa mature form of VEGFR-2 in the lung was significantly reduced in the HS-NF and HS+DOX+TA+GLUC animals (Figure 7.20). The intermediate glycosylated form was reduced in all cases after HS except for HS+TA+GLUC (Figure 7.20).

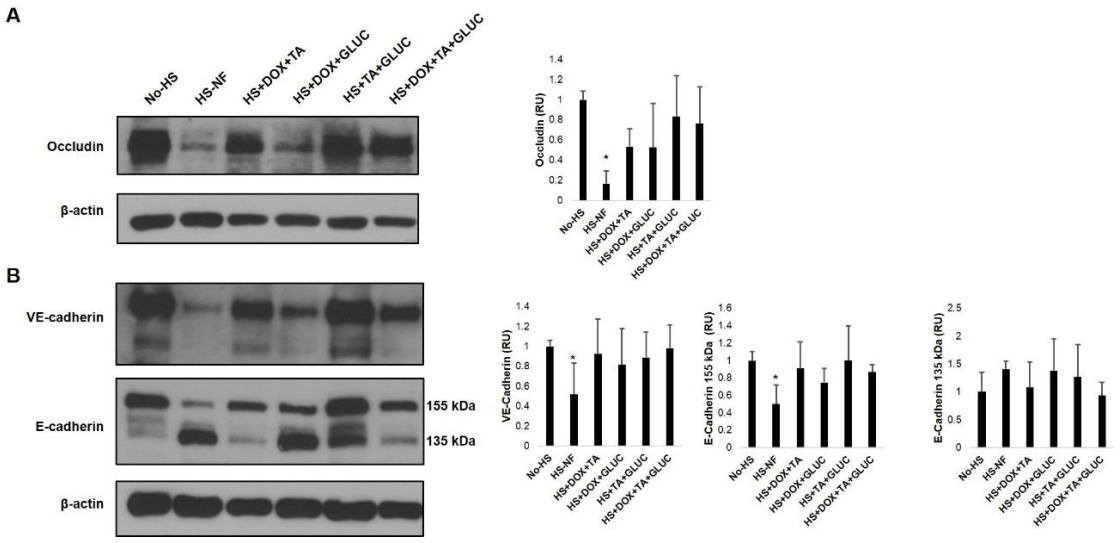

Figure 7.19 Lung endothelial cell junctional protein levels. (A) The lung tight junction protein occludin was significantly reduced in the HS-NF animals. (B) Both VE-cadherin and E-cadherin were reduced in the HS-NF animals. *, $p<0.05$ by ANOVA followed by Tukey post-hoc test. N=4 rats/group. Bar graphs are presented as mean±SD.

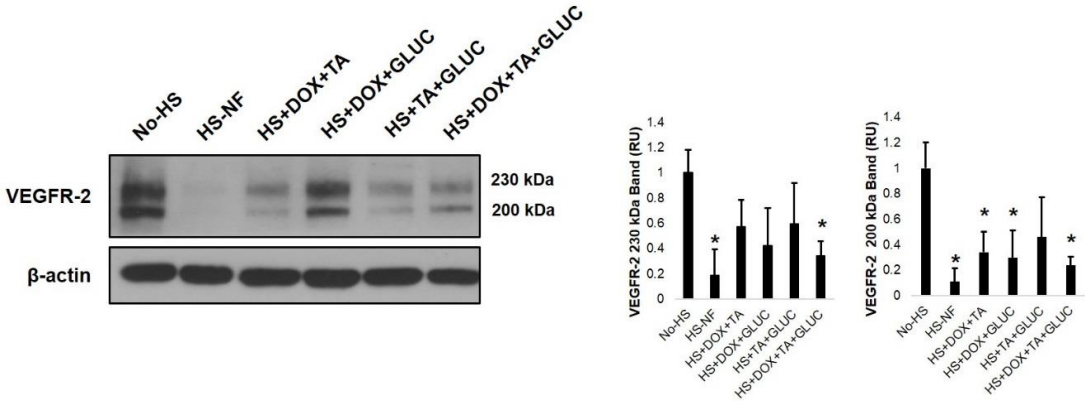

Figure 7.20 Lung VEGFR-2 protein levels. The 230 kDa band of VEGFR-2 in the lung was significantly decreased in the HS-NF and HS+DOX+TA+GLUC groups compared to the No-HS animals. The 200 kDa band was decreased compared to the No-HS levels for all groups except HS+TA+GLUC. *, $p<0.05$ by ANOVA followed by Tukey post-hoc test. N=4 rats/group. Bar graphs are presented as mean±SD.

7.5 Discussion

7.5.1 Summary

The combination of multiple treatments targeted to reduce intestinal degradation served to improve the gross morphology of the gut and provided the animals with hemodynamic stability during the reperfusion period. However, no E-cadherin preservation was achieved in the intestine. Neutrophils continued to accumulate in the lung and intestine as determined by MPO activity. Serine proteases still formed after HS in plasma and lung homogenate samples regardless of the treatments. Trypsin was detected in lung homogenate after HS in all treated animals, and lung injury was not attenuated by any of the interventions as measured by blind scoring. Despite the damage observed in the lungs, the protein degradation in the lungs was not as severe for occludin, VEGFR-2, VE-cadherin, and E-cadherin compared to untreated animals.

7.5.2 Gut Protection by Combination Treatments

Preservation of the gut by both internal and external methods may be the hallmark of preventing entry into irreversible shock. While each intervention was strategically targeted at a slightly different mechanism to preserve intestinal structure, the combination did not reduce lung injury. All combination except HS+DOX+GLUC improved the appearance of the gut and preserved the peristaltic motion at the end of the reperfusion

period. Observing a functional intestine suggests that the gut was not irreversibly injured during the ischemic period and able to return to normal.

The only group that had consistent hemorrhage was the HS+DOX+GLUC group where microhemorrhages formed in the jejunum region in a pattern similar to the HS+GLUC alone group (Figure 6.5). This suggests that the hemorrhages in the intestine occur regardless of doxycycline treatment; indicating that MMP inhibition alone may not prevent the hemorrhages. If we recall the intestine tissues in the HS-F animals, the HS+DOX+TA resembled this group the best (Figure 5.4 and Figure 7.3). This indicates that the TA provided protection similar to a flushed lumen, or alternatively, the digestive enzymes were not able to destroy the underlying microvessels that cause microhemorrhages. Using doxycycline and tranexamic acid to prevent intestinal wall breakdown suggests that the barrier has to fail first before digestive enzymes can transport across and contribute to intestinal injury. Even though the HS+DOX+TA preserved the intestine, there still was neutrophil accumulation and increased MMP-9 levels in this group (Figure 7.6 and Figure 7.8).

Although the preservation of the gut was improved using HS+DOX+TA, HS+TA+GLUC, or HS+DOX+TA+GLUC combinations, E-cadherin degradation continued to occur in a pattern similar to the HS-NF animals (Figure 7.9). In both experiments, the luminal contents were present which suggests that luminal digestive enzymes are likely responsible for digesting epithelial-derived E-cadherin.

7.5.3 Transport of Serine Proteases to the Systemic Circulation

Despite the benefits of gut barrier protection, the transport of pancreatic serine proteases from the gut into the plasma and lung still occurred (Figure 7.10 and Figure 7.17). These bands appeared more pronounced compared to the HS+SAL animals seen in Chapter 3 and Chapter 6 (Figure 3.6 and Figure 6.15). In the treated animals with ANGD, these bands also appeared with greater intensity (Figure 3.6). Even though we protected the gut by four major interventions, the protease transport into the lung tissue continued unless the luminal contents were removed (Figure 5.18B). Therefore, the pancreatic proteases may have traveled through the mesenteric lymph (Figure 3.8) and became entrapped in the lung during shock (Figure 3.9, Figure 5.19, Figure 6.18, and Figure 7.16). Since we observed that the trypsin appearance in the lung was elevated in non-flushed animals that received treatment, it is possible that the treatments prevented destruction of lymphatic vessels so that lymph fluid continued during the reperfusion phase transporting digestive enzymes. During shock, the lung accumulates proteins. Since the pancreatic proteases appear in the circulation even before the onset of hemorrhagic shock and the levels do not change (Figure 5.14A and Figure 6.15), the lack of synthesis of pancreatic protease inhibitors may give rise to the observed increase in activity. The fact that these serine proteases are even identified in BALF (Figure 6.19B) suggests that they enter across the endothelial barrier with the plasma into the alveolar space, and the proteases may even contribute to the breakdown of the lung.

7.5.4 Lung Damage Still Occurs with Multiple Gut Treatments

The lung damage after HS occurred regardless of the interventions, and even to a greater extent than single interventions alone, such as HS+GLUC (Table 6.4). When the gut was protected, the neutrophils that normally might reside in the intestinal tissue following ischemic injury may not have been attracted to the same degree and accumulated elsewhere. This could cause a greater percentage of the neutrophil population to reside in the lung and other organs. Even if the neutrophils accumulate in organs such as the lung, they may not necessarily be activated and secrete MPO into the BALF (Figure 6.13 and Figure 7.15).

Microhemorrhages occurred even when animals were treated with the multiple combined interventions. This suggests that other factors may be contributing to their activation, including release of cell-activating factors from the pancreas [9]. Additionally, the low flow state alone could be the major contributor for neutrophil accumulation in the lung [11] and the secretion of proteases could be stimulated by an alternative mechanism, potentially related to the intestinal barrier.

The interventions discussed in both this Chapter and Chapter 5 were not targeted at blocking digestive enzymes, but rather tested methods to preserve the barrier by preventing luminal contents from crossing into the intestinal wall tissue. Despite the known efficacy of glucose and tranexamic acid in the gut, these treatments were unable to prevent neutrophil accumulation to the same degree in organs distant from the gut as the serine protease and lipase inhibitor ANGD. Both our group and others have observed that ANGD was able to reduce peripheral organ inflammation (Figure 3.2) [10,12,13].

ANGD in the gut can act in multiple ways. It can prevent digestive enzymes from destroying the intestinal wall and generating bioactive molecules. Since ANGD can block lipase, fewer free fatty acids would be generated in the gut and therefore decrease their likelihood for pro-inflammatory signaling [2,14-16].

Finally, if ANGD escapes via the lymph or portal venous circulation into the central circulation, it may inhibit neutrophil elastase. Neutrophil elastase has been attributed to lung injury and can be prevented by inhibiting the elastase activity [17-20]. However, in pilot studies where we used sivelestat, an elastase inhibitor, in addition to the three treatments that protected the intestine and stabilized the pressure, lung microhemorrhages still formed. We further explored if aprotinin, another serine protease inhibitor, could reduce the microhemorrhages in the lung and were also unsuccessful. Our inability to attenuate the microhemorrhages may be due to this hemorrhagic shock model being more extreme compared to previous models or the choice of ketamine as the anesthetic. Since there are many insults to the lung in hemorrhagic shock, including toxic lymph fluid, bacteria and their byproducts, free fatty acids, protease activation, and/or neutrophil accumulation, overcoming all of the potential mediators is a challenge in extreme hypotension [21]. Since ANGD could not be tested with glucose in this model due to the parasympathetic effects combined with ketamine/xylazine (3/3 animals died during ischemia) [22], we can only postulate based on Chapter 3 and previous work that ANGD may prevent lung hemorrhage in this model [10,12,23].

7.5.5 Lung Protein Degradation Is Attenuated with Gut Interventions

Despite the increase in traditional mediators like MPO activity, BALF protein concentration, and MMP-9 activity being just as severe as the animals in the HS-F and HS-NF cases, the degradation of key endothelial proteins was attenuated in the lung of treated animals in both this Chapter and Chapter 5 (Figure 6.23, Figure 6.25, Figure 7.19, and Figure 7.20). Even fluid resuscitation by enteral administration of saline improved occludin breakdown in the lung (Figure 5.21, Figure 6.23). Proteins like lung VE-cadherin and E-cadherin were improved more effectively with multiple inhibitor treatments than with single inhibitors (Figure 6.23 and Figure 7.19).

Lastly, the functional receptor VEGFR-2 density in the lung decreased after HS and was only restored in tranexamic acid treated intestines (Figure 6.25). The ability for cells to restore functional receptors may be important in the repair process after ischemic injury. In survival studies with tranexamic acid and ANGD+glucose, the animals that lived were able to restore normal physiological functions such as eating [24]. Our evidence suggests that proteolytic breakdown is a key process that is responsible in the progression of irreversible shock. However, not all proteins may be of significant importance, but if cells lack receptors necessary for survival, like VEGFR-2, then the subsequent repair processes may be impaired.

7.6 CONCLUSIONS

Although multiple interventions helped alleviate intestinal damage, entrapped neutrophils still appeared to contribute to lung injury in HS. Although glucose and tranexamic acid in combination were effective at preserving the gut barrier during ischemia as seen in Chapter 2, transport of pancreatic enzymes from the gut into the periphery and peripheral protease activation continued to occur. From these studies we learn that even though we preserve the gut barrier, we cannot completely attenuate lung inflammation without the presence of a serine protease and lipase inhibitor like ANGD. Therefore, inhibition of serine proteases and lipases in the lumen may still provide potential benefits, in addition to both glucose and tranexamic acid to prevent the initial gut barrier injury.

Chapters 5, 6 and 7, in full, are currently being prepared for submission for publication entitled "Strategies to minimize organ injury by proteolytic enzymes in hemorrhagic shock" by Angelina E. Altshuler, Michael Richter, Jason Chou, Diana Li, Leena Kurre, Alexander H. Penn, and Geert W. Schmid-Schönbein. The dissertation author is the primary author of this manuscript.

7.7 REFERENCES

1. Ishimaru K, Mitsuoka H, Unno N, Inuzuka K, Nakamura S, Schmid-Schönbein GW. (2004) Pancreatic proteases and inflammatory mediators in peritoneal fluid during splanchnic arterial occlusion and reperfusion. Shock 22: 467-471.

2. Penn AH, Schmid-Schönbein GW. (2008) The intestine as source of cytotoxic mediators in shock: Free fatty acids and degradation of lipid-binding proteins. Am J Physiol Heart Circ Physiol 294: H1779-92.

3. Waldo SW, Rosario HS, Penn AH, Schmid-Schönbein GW. (2003) Pancreatic digestive enzymes are potent generators of mediators for leukocyte activation and mortality. Shock 20: 138-143.

4. Sato H, Kasai K, Tanaka T, Kita T, Tanaka N. (2008) Role of tumor necrosis factor-alpha and interleukin-1beta on lung dysfunction following hemorrhagic shock in rats. Med Sci Monit 14: BR79-87.

5. van Meurs M, Wulfert FM, Knol AJ, De Haes A, Houwertjes M, Aarts LP, Molema G. (2008) Early organ-specific endothelial activation during hemorrhagic shock and resuscitation. Shock 29: 291-299.

6. Senthil M, Brown M, Xu DZ, Lu Q, Feketeova E, Deitch EA. (2006) Gut-lymph hypothesis of systemic inflammatory response syndrome/multiple-organ dysfunction syndrome: Validating studies in a porcine model. J Trauma 60: 958-65; discussion 965-7.

7. Haglund U. (1993) Systemic mediators released from the gut in critical illness. Crit Care Med 21: S15-8.

8. Shi HP, Liu ZJ, Wen Y. (2004) Pancreatic enzymes in the gut contributing to lung injury after trauma/hemorrhagic shock. Chin J Traumatol 7: 36-41.

9. Kistler EB, Hugli TE, Schmid-Schönbein GW. (2000) The pancreas as a source of cardiovascular cell activating factors. Microcirculation 7: 183-192.

10. Doucet JJ, Hoyt DB, Coimbra R, Schmid-Schönbein GW, Junger WG, Paul LW, Loomis WH, Hugli TE. (2004) Inhibition of enteral enzymes by enteroclysis with nafamostat mesilate reduces neutrophil activation and transfusion requirements after hemorrhagic shock. J Trauma 56: 501-10; discussion 510-1.

11. Ratliff NB, Wilson JW, Mikat E, Hackel DB, Graham TC. (1971) The lung in hemorrhagic shock. IV. the role of neutrophilic polymorphonuclear leukocytes. Am J Pathol 65: 325-334.

12. Deitch EA, Shi HP, Lu Q, Feketeova E, Xu DZ. (2003) Serine proteases are involved in the pathogenesis of trauma-hemorrhagic shock-induced gut and lung injury. Shock 19: 452-456.

13. Mitsuoka H, Schmid-Schönbein GW. (2000) Mechanisms for blockade of in vivo activator production in the ischemic intestine and multi-organ failure. Shock 14: 522-527.

14. Qin X, Dong W, Sharpe SM, Sheth SU, Palange DC, Rider T, Jandacek R, Tso P, Deitch EA. (2012) Role of lipase-generated free fatty acids in converting mesenteric lymph from a noncytotoxic to a cytotoxic fluid. Am J Physiol Gastrointest Liver Physiol 303: G969-78.

15. Tao W, Miao QB, Zhu YB, Shu YS. (2012) Inhaled neutrophil elastase inhibitor reduces oleic acid-induced acute lung injury in rats. Pulm Pharmacol Ther 25: 99-103.

16. Soto-Guzman A, Navarro-Tito N, Castro-Sanchez L, Martinez-Orozco R, Salazar EP. (2010) Oleic acid promotes MMP-9 secretion and invasion in breast cancer cells. Clin Exp Metastasis 27: 505-515.

17. Toda Y, Takahashi T, Maeshima K, Shimizu H, Inoue K, Morimatsu H, Omori E, Takeuchi M, Akagi R, Morita K. (2007) A neutrophil elastase inhibitor, sivelestat, ameliorates lung injury after hemorrhagic shock in rats. Int J Mol Med 19: 237-243.

18. Wakayama F, Fukuda I, Suzuki Y, Kondo N. (2007) Neutrophil elastase inhibitor, sivelestat, attenuates acute lung injury after cardiopulmonary bypass in the rabbit endotoxemia model. Ann Thorac Surg 83: 153-160.

19. Ishikawa N, Oda M, Kawaguchi M, Tsunezuka Y, Watanabe G. (2003) The effects of a specific neutrophil elastase inhibitor (ONO-5046) in pulmonary ischemia-reperfusion injury. Transpl Int 16: 341-346.

20. Tomizawa N, Ohwada S, Ohya T, Takeyoshi I, Ogawa T, Kawashima Y, Adachi M, Morishita Y. (1999) The effects of a neutrophil elastase inhibitor (ONO-5046.na) and neutrophil depletion using a granulotrap (G-1) column on lung reperfusion injury in dogs. J Heart Lung Transplant 18: 637-645.

21. Matute-Bello G, Frevert CW, Martin TR. (2008) Animal models of acute lung injury. Am J Physiol Lung Cell Mol Physiol 295: L379-99.

22. Penn AH, Schmid-Schönbein GW. (2011) Severe intestinal ischemia can trigger cardiovascular collapse and sudden death via a parasympathetic mechanism. Shock 36: 251-262.

23. Harada N, Okajima K, Kushimoto S. (1999) Gabexate mesilate, a synthetic protease inhibitor, reduces ischemia/reperfusion injury of rat liver by inhibiting leukocyte activation. Crit Care Med 27: 1958-1964.

24. DeLano FA, Hoyt DB, Schmid-Schönbein GW. (2013) Pancreatic digestive enzyme blockade in the intestine increases survival after experimental shock. Sci Transl Med 5: 169ra11.

Chapter 8

Conclusions and Future Directions

In this thesis, I have investigated the role of degrading proteases both from the gut and the peripheral tissues in the progression of shock and multiple organ failure. I determined the contribution of proteases to intestinal breakdown, transport, and organ injury. A common feature is that protease activities appear to be a unifying theme in the degradation of tissues and pathophysiology of shock.

Our model for analyzing the intestinal barrier during severe ischemia in the absence of luminal contents has brought to light inhomogeneous protease activities and barrier properties between the ileum and jejunum regions. Future studies should continue to study the regional differences in the intestine. We demonstrate that the intestinal barrier is destroyed by two major mechanisms. First, the epithelial barrier is disrupted during ischemia and can be preserved if glucose is present in the lumen of the intestine as a metabolic source of energy for epithelial cells. A second barrier beneath the epithelium can be degraded during ischemia by MMPs preexisting in the intestinal tissue. If the epithelial layer is preserved, key proteins like mucin 13 and occludin are protected during ischemia. Future work could explore exactly which extracellular matrix proteins are degraded beneath the epithelial layer by MMPs during intestinal ischemia.

In the clinically relevant case of hemorrhagic shock with ischemia/reperfusion injury in the entire animal, we have identified major routes via the blood, peritoneal fluid, and lymph fluid for the escape of digestive enzymes from the lumen of the intestine into the periphery. In all cases after hemorrhagic shock, the activities of serine proteases increase which can lead to activation of other proteases and degradation of surface receptors. Serine proteases from the lumen of the intestine accumulate in the lung tissue and enter into the BALF after hemorrhagic shock.

Since complete removal of luminal contents by flushing the intestine prior to shock greatly reduces intestinal damage, but not lung damage, we focused our therapies towards preserving the gut barrier especially in the presence of luminal contents. Although tranexamic acid alone or in combination with other interventions prevented intestinal damage to levels comparable to the protection seen after flushing luminal contents, the lung still had neutrophil accumulation, yet there was reduced destruction of receptors like VEGFR-2. However, the serine protease and lipase inhibitor ANDG was effective at preventing neutrophil accumulation in peripheral organs, but not at preserving lung junctional proteins such as VE-cadherin. We also identified peripheral MMPs as potential candidates for lung damage and protein degradation. MMP inhibition in the plasma only partially reduced organ damage, but did not prevent endothelial protein degradation. These studies have uniquely identified that the progression of shock involves multiple proteases that when blocked, improve the outcome of the animal. Also, other extracellular proteins could be studied beyond the candidate junctional proteins and receptors studied in this thesis. Not only have the mechanisms of organ injury been clarified, clinical solutions can be advanced based on the outcomes of this work.

For the future, several studies need to investigate the roles and function of these interventions. First, VEGFR-2 levels in the lung and liver decrease while VEGF levels increase in the plasma after HS. Since tranexamic acid was able to prevent breakdown of this protein in the lung, it suggests that either a proteases is directly responsible for the destruction of this receptor, or tranexamic acid is inhibiting other pathways that prevent its degradation. VEGFR-2 regulates endothelial permeability and survival, functional studies characterizing the signaling and binding capabilities should be investigated as this may be important for the survival of animals after shock.

I identified neutrophils as a source of MMP-9 in the tissues and plasma. I also pinpointed the intestine as the source for serine proteases that accumulate in the lung after HS. In this thesis, we have developed support for two main classes of proteases to target: pancreatic enzymes in the lumen and proteases in the tissues. Optimization of concentrations, delivery routes, and types of interventions for inhibiting degrading enzymes resulting in the most effective shock therapy are important future experiments.

The kinetics of tissue repair should also be investigated at later time points after shock than investigated in these studies. One of the limitations of this model is that I only reperfused the animal for three hours after ischemia. At later time points, cells may or may not be able to synthesize new proteins. The repair process may be critical for understanding the recovery of animals after hemorrhagic shock.

Finally, since proteases or their byproducts are important in the progression of shock, there is a potential for development of clinical diagnostics to determine the severity of shock in patients based on byproducts of proteases. Proteases may be damaging organs and causing them to fail, which may not be immediately reflected by

the status of the patient. Therefore, developing early markers applicable in patients could be a critical step to determine a patient's severity of shock. This approach could be accomplished by either measuring protease activity, soluble receptors, or other protease degradation byproducts. Since there are no clinical solutions or preventive approaches for shock patients, methods to improve both detection and treatment options would constitute significant advancements in the field of critical care.